Investigating Drugs that Enhance Imatinib Uptake and Factors which Contribute to the Functional Activity of OCT-1 CML Cells

Jueqiong WANG

The Melissa White Laboratory
Department of Haematology
Centre for Cancer Biology
SA Pathology (IMVS)
Adelaide, Australia

&

Faculty of Health Sciences
Department of Medicine
The University of Adelaide
Adelaide, Australia

A thesis submitted to the University of Adelaide
in candidature for the degree of Doctor of Philosophy
November 2012

TABLE OF CONTENTS

List of Figures and Tables

ABBREVIATIONS

15d-PGJ2	15-deoxy-Δ12,14-PGJ2
ABCB1/ABCG2	ATP binding cassette (ABC) transporter proteins B1 and G2
ABL	Abelson kinase
ACD	Anticoagulent Citrate Dextrose Solution Formula A
AP	Accelerated phase
ATP	Adenosine triphosphate
BC	Blast crisis
BCR	Breakpoint cluster region
BCR-ABL	Breakpoint cluster region-Ableson kinase fusion transcript/protein
BM	Bone marrow
BSA	Bovine serum albumin
C	Celcius
CCyR	Complete cytogenetic response
CD	Cluster of differentiation
cDNA	Complementary deoxyribonucleic acid
CHIP	Microarray chip
CHR	Complete haematologic response
CMAP	Connectivity map
CML	Chronic myeloid leukaemia
CMR	Complete molecular response
COX-1/2	Cyclooxygenase-1/2
CP	Chronic phase
Crkl	Crk-like protein
DDI	Drug-drug interaction
DEPC	Diethyl pyrocarbonate
DMSO	Dimethyl sulphoxide
DNA	Deoxyribonucleic acid
dNTPs	Deoxynucleotide triphosphates
DTT	Dithiothreitol
EDTA	Ethylene diamine tetraacetate
ERK	Extracelullar signal-regulated kinase
FBS	Foetal Bovine Serum
FC	Fold change
FITC	Fluorescein isothiocyanate
GAPDH	Glyceraldehyde 3-phosphate dehydrogenase
GUSB	Beta-glucuronidase
HBSS	Hanks Balanced Salt Solution

HCL	Hierarchical Clustering
IC50	50% inhibitory concentration
IFN-α	Interferon alpha
IgG	Immunoglobulin G
IRIS	International randomised study of interferon versus STI571
IUR	Intracellular uptake and retention
kD	Kilo Dalton
L	Litre
M	Molar
MACS	Magnetically activated cell sorting
MAPK	Mitogen activating protein Kinase
MCyR	Major cytogenetic response
mM	Milli Molar (10-3 Molar)
MMR	Major molecular response
MNC	Mononuclear cells
mRNA	Messenger ribonucleic acid
NF-κB	Nuclear factor of kappa light polypeptide gene enhancer in B-cells
ng	Nano gram (10^{-9} gram)
nM	Nano molar (10^{-9} Molar)
NSAIDs	Non-steroidal anti-inflammatory drugs
OA	OCT-1 activity
OAT-1	Organic anion transporter-1
OCT-1	Organic cation transporter 1
PB	Peripheral blood
PBS	Phosphate Buffered Saline
PCR	Polymerase chain reaction
p-Crkl	Phosphorylated Crk-like protein
PE	Phycoerythrin
PGE2	Prostaglandin E2
Ph	Philadelphia chromosome
PI3K	Phosphatidylinositol3 kinase
PPARγ	Peroxisome Proliferator Agonist Receptor
PTGS	Prostaglandin-endoperoxide synthase (COX)
p-**value**	Probability value
PVDF	Polyvinylidene fluoride
RANKL	Receptor activator of nuclear factor kappa-b ligand
RNA	Ribonucleic acid
ROC	Receiver operating characteristic
RPMI	Roswell Park Memorial Institute (media)

RQ-PCR	Real-time quantitative polymerase chain reaction
SDS-PAGE	Sodium dodecyl sulphate-polyacrylamide
SEM	Standard error of the mean
STI571	Signal transduction inhibitor 571 (imatinib)
TBP	TATA-binding protein
TBS	Tris buffered saline
TBST	Tris buffered saline with 0.1% Tween20
TKI	Tyrosine kinase inhibitor
TWC	Total white cells
U	Units
v/v	Volume per volume
vs.	versus
w/v	Weight per unit volume
µg	Micro gram (10^{-6} gram)
µM	Micro molar (10^{-6} molar)

PUBLICATIONS

Manuscripts

Wang J, Hughes TP, Kok CH, Saunders VA, Frede A, Groot-Obbink K, et al. Contrasting effects of diclofenac and ibuprofen on active imatinib uptake into leukaemic cells. British Journal of Cancer. 2012;106(11):1772-8 **Impact Factor 5.04**

Conference Abstracts

Wang J, Hughes TP, Kok CH, White DL, et al. Screening Potential OCT-1 Activity Enhancers may Improve the Outcome of Imatinib Therapy in CML. *New Directions in Leukaemia Research*, March 2010. Sunshine Coast, Australia. Poster Presentation.

Wang J, Hughes TP, Kok CH, White DL, et al. PPARγ ligands modulate OCT-1 activity in BCR-ABL+ cell lines and primary CML cells. *Postgraduate Research Conference in the Faculty of Health Sciences,* August 2011. Adelaide, Australia. Poster Presentation.

Wang J, Hughes TP, Kok CH, White DL, et al. PPARγ ligands modulate functional OCT-1 activity in a cell-lineage dependent way. *Haematology Society of Australia and New Zealand Annual Meeting*, October 2011. Sydney, Australia. Oral Presentation

Wang J, Hughes TP, Kok CH, White DL, et al. Non-Steroidal Anti-Inflammatory Drugs and imatinib; drug interactions that may impact efficacy. *American Society of Haematology Annual Meeting*, December 2011. San Diego, USA. Poster Presentation

Wang J, Hughes TP, Kok CH, White DL, et al. Dissecting the mechanism of OCT-1 Activity enhancement by diclofenac in CML cells. *New Directions in Leukaemia Research*, March 2012. Sunshine Coast, Australia. Poster Presentation.

Wang J, Hughes TP, Kok CH, White DL, et al. Manipulation to Enhance the Functional Activity of OCT-1 Influx Pump to Increase the Intracellular Concentration of Imatinib in Target Cells. *Postgraduate Research Conference in the Faculty of Health Sciences,* August 2012. Adelaide, Australia. Poster Presentation.

SCHOLARSHIPS & AWARDS

Poster Prize, Postgraduate Research Conference in the Faculty of Health Sciences. 2011.

For the abstract entitled "PPARγ ligands modulate OCT-1 activity in BCR-ABL+ cell lines and primary CML cells", Adelaide, August 2011.

Poster Prize, Postgraduate Research Conference in the Faculty of Health Sciences. 2012.

For the abstract entitled "Manipulation to Enhance the Functional Activity of OCT-1 Influx Pump to Increase the Intracellular Concentration of Imatinib in Target Cells", Adelaide, August 2011.

Non-member Travel Grant, Haematology Society of Australia and New Zealand Annual Meeting, 2011.

For the abstract entitled "PPARγ ligands modulate functional OCT-1 activity in a cell-lineage dependent way", Sydney, October 2011.

PhD Scholarship, The Chinese Scholarship Council-the University of Adelaide Joint Scholarship. 2008-2012.

To provide support for the educational and professional development of Chinese researchers and other professionals undertaking a PhD in the University of Adelaide.

ACKNOWLEDGEMENTS

It is my great honor to study as a PhD candidate in the Melissa White Laboratory. Doing a PhD is a very challenging journey especially for an oversea student with English as a second language like me. Without the help and support from a large number of individuals, I would not be able to finish my research work and fulfill the whole procedure.

I would like to thank my fantastic supervisors, Professor Timothy P Hughes, Associate Professor Deborah L White and Associate Professor Richard D'Andrea for their generous help throughout my PhD candidature. Their patience, encouragement, and their understanding are essential for all of my achievements. Without their extremely rapid feedback, I would not be able to finish the thesis writing in such a short period.

I would like to thank Dr. Chung Hoow Kok for selflessly sharing his bioinformatics knowledge and laboratory techniques with me. Thanks to the entire lab team, from whom I have learnt a lot of valuable skills. Whenever I need help in the lab, I know they will be there for me. Thanks also go to all the students, past and present. The friendship established in our PhD student office is such a unique one that I would never ever forget. Also, I must thank Carine and Verity, who spent their precious time helping me with most tedious grammar mistakes in my writing and also gave me numerous constructive comments for my thesis.

I would like to thank my parents and my family members for their endless support as well as their understandings. I am also so lucky to have good friends who would listen to my complaints and help me regain my confidence. There is no doubt that it is the courage rooting from my family and friends that keeps me moving forward.

Lastly, my deepest thanks to my dear Ting XIA. Four years ago, it was you who helped me make the decision to study abroad, for which I have never felt regret. With your company, my days in Adelaide were much more colourful. Thank you for all the joy you have brought into my life.

ABSTRACT

In CML cells, the functional OCT-1 activity (OA) in mononuclear cells (MNC) from *de novo* chronic myeloid leukaemia patients in chronic phrase (CP-CML) is significantly associated with imatinib-mediated *in vitro* tyrosine kinase inhibition and is a strong indicator of imatinib response.

Here we identified candidate drugs as potential OA enhancers using Connectivity Map analysis (CMAP). Their effects on OA were extensively validated in CML cell lines and patient samples, together with 12 NSAIDs and 11 commonly prescribed drugs. A significant enhancement of OA was observed after the treatment with diclofenac. Importantly this increase in OA translated to a significant increase in BCR-ABL kinase inhibition. Additionally, the long-term co-administration of diclofenac sensitized CML cells to imatinib on cell proliferation. In CML patients' mononuclear (MNC) samples, diclofenac significantly increased OA especially in patients with low OA. In contrast, ibuprofen significantly decreased the OA in CML cell lines and primary samples. This effect on OA also translated into a reduction in BCR-ABL kinase inhibition and an increase in cell growth in the presence of imatinib. Unlike diclofenac, the inhibitory effect of ibuprofen is also observed in normal cells most likely in an independent manner from OCT-1 protein.

The enhancement of OA by diclofenac could be eliminated in the presence of Actinomycin D (a transcription inhibitor), indicating that diclofenac regulated OA at a transcriptional level. However, the expression of *SLC22A1* (*OCT-1*) remained unchanged after treatment with diclofenac. Since diclofenac is an inhibitor for cyclooxygenase-2 (COX-2), the potential involvement of COX-2 in OA regulation was investigated. The plasma concentration of 15-deoxy-Δ12,14-PGJ2 (15d-PGJ2), a

prostaglandin product by COX-2, was significantly associated with OA in CP-CML. Given 15d-PGJ2 is a potent agonist for peroxisome proliferator-activated receptor γ (PPARγ) and diclofenac is also a known PPARγ ligand, whether PPARγ had a role in OA regulation was then investigated. Significant increase in OA in KU812 cells was observed after treatment with PPARγ antagonist GW9962, while treatment with PPARγ agonists (GW1929, troglitazone, or rosiglitazone) significantly decreased OA. In addition, there was a significant negative association between OA and the PPARγ transcriptional activity in CP-CML MNC collected at diagnosis. Further identification of the key factor contributing to high PPARγ activation in patients with low OA may provide better understanding of intrinsic OA interpatient variability, as well as the clinical and biological relevance of PPARγ in CML.

DECLARATION

This thesis contains no material which has been accepted for the award of any other degree or diploma in any university or other tertiary institution and, to the best of my knowledge and belief, contains no material previously published or written by another person, except where due reference has been made in the text.

I give consent to this copy of my thesis when deposited in the University Library, being made available for loan and photocopying, subject to the provisions of the Copyright Act 1968.

The author acknowledges that copyright of published work contained within this thesis (as listed below) resides with the copyright holder(s) of those works.

Wang J *et al*. British Journal of Cancer. 2012. (Appendix A)

I also give permission for the digital version of my thesis to be made available on the web, via the University's digital research repository, the Library catalogue, the Australasian Digital Theses Program (ADTP) and also through web search engines, unless permission has been granted by the University to restrict access for a period of time.

Jueqiong Wang

November 2012

CHAPTER I
Introduction

1.1. Chronic myeloid leukaemia

1.1.1. Clinical features of CML

Chronic myeloid leukaemia (CML) is a cancer of hematopoietic progenitors characterized by increased and deregulated growth of predominantly myeloid cells in the bone marrow and the accumulation of these cells in the blood (1). CML represents about 15-20% of all cases of adult leukemia in Western populations. Approximately 20-40% of patients are asymptomatic at diagnosis, with an elevated white blood cell count. Other common symptoms of CML include fatigue, weight loss, sweating, anemia, and splenomegaly (2). The typical complete blood count of CML patients shows an increase in cells of the myeloid lineage, with basophils and eosinophils universally increased. As the first malignancy to be linked to a clear genetic abnormality, CML is diagnosed by detecting the Philadelphia chromosome with techniques such as routine cytogenetics, fluorescent *in situ* hybridization, or PCR for the *BCR-ABL* fusion gene (2). Although occurring in all age groups, CML most commonly affects the middle-aged and elderly with an annual incidence of 0.001% (3). CML is classically defined in three phases based on clinical characteristics and laboratory findings. The majority of patients (approximately 90%) with CML are in the chronic phase (CP) at the time of diagnosis, during which patients are usually asymptomatic or have only mild symptoms. The duration of chronic phase is highly variable. With cytoreductive treatment, chronic phase usually lasts between 4 to 6 years. In the absence of effective treatment, the disease then transforms to an accelerated phase (AP) lasting an average of 12 months. The terminal phase of CML is blast crisis (BC), which clinically behaves like an acute leukemia with rapid progression and short survival (4). When given early, effective drug treatment can usually stop the progression of CML. However, some patients may have already

developed AP-CML or BC-CML by the time of diagnosis or within month of diagnosis and these patients are harder to manage with standard drug therapy. Furthermore, for some CP-CML patients on treatment, disease transformation is highly probable due to an additional accumulation of chromosomal and molecular abnormalities (4).

1.1.2. Pathophysiology of CML

CML is a clonal myelo-proliferative disease characterized by the presence of the Philadelphia (Ph) chromosome which was first discovered and described in 1960 (5). This specific chromosomal abnormality arises from a reciprocal translocation between the Abelson (*ABL*) tyrosine kinase gene on chromosome 9 and the break point cluster (*BCR*) gene on chromosome 22 (Figure 1.1A) (6, 7). Present in more than 95% of CML patients, the Ph chromosome results in the chimeric oncogene *BCR-ABL* which in turn encodes a hybrid 210 kDa protein, BCR-ABL (the molecular weight of the protein can range from 185 to 230 kDa, depending on the precise location of the breakpoint, Figure 1.1B) (8). The constitutive tyrosine kinase activity of BCR-ABL alone has been demonstrated to be essential and sufficient to cause the clinical CML features (9, 10). Several experimental systems have been used to investigate CML pathogenesis and progression. After the transduction of a retroviral vector containing *BCR-ABL*, human cord blood CD34$^+$ cells exhibited less adhesion, enhanced migration, improved cell survival in cytokine depleted media and increased numbers of granulocyte-macrophage colony-forming units (GM-CFU) (11). Similar evidence has also been demonstrated by various *in vivo* models. Mice transplanted with *BCR-ABL*-positive hematopoietic cells developed either CML features (including elevated leukocyte count, splenomegaly and an accumulation of immature myeloid cells in the spleen, liver and bone marrow (9)), or an acute leukemia phenotype (12). Additionally, in a transgenic *BCR-ABL* tetracycline-regulated mouse model, CML features disappeared when *BCR-ABL* expression was turned off (13).
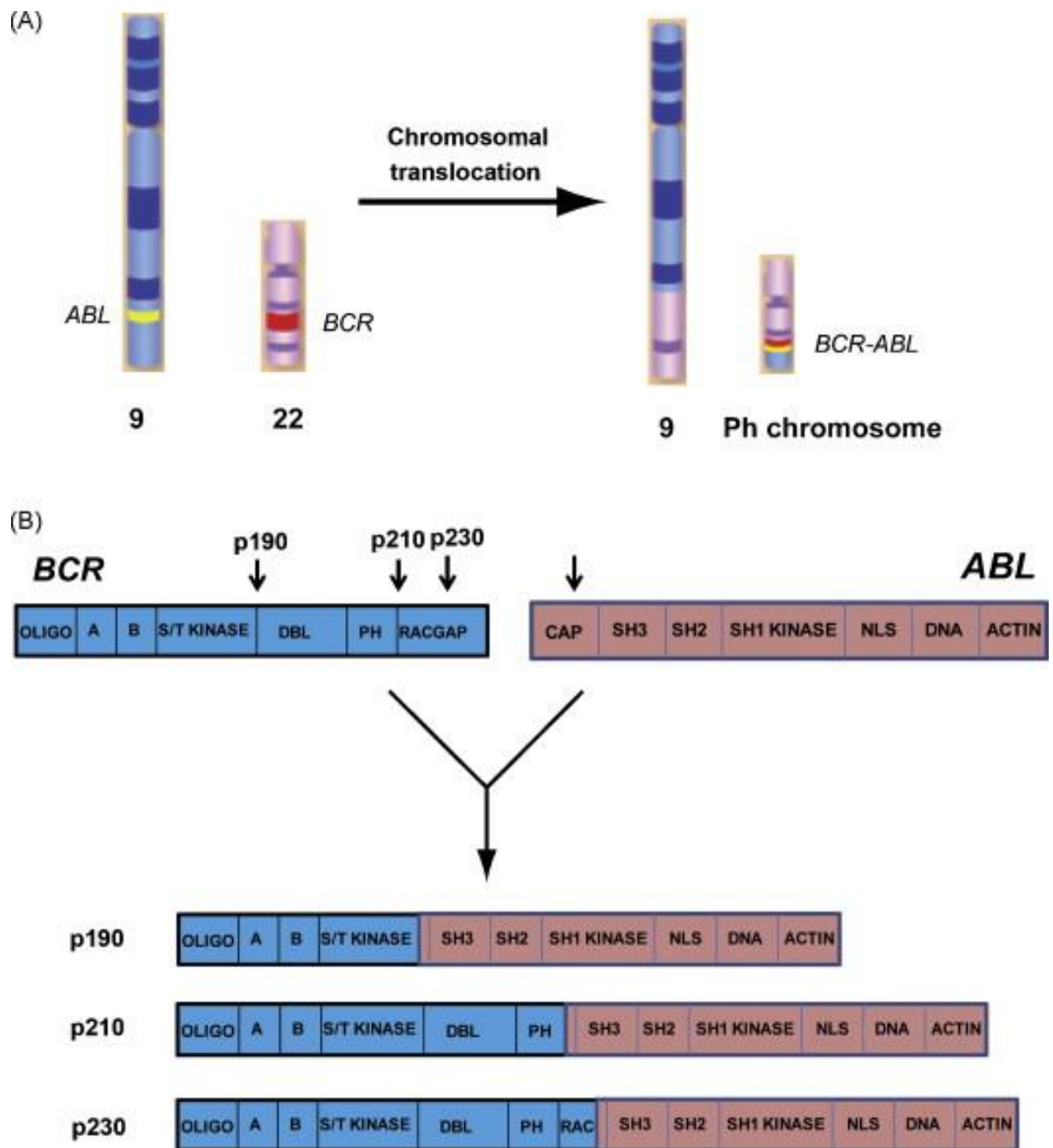
Figure 1.1   The Philadelphia Chromosome and BCR-ABL oncogenes

(A) The Philadelphia Chromosome arises from the reciprocal translocation between the long arms of chromosomes 9 and 22. **(B)** Varies breakpoint locations on the *ABL* and *BCR* gene result in chimeric protein products (p190, p210, p230) with variable molecular weights. (Figure from Sullivan et al. 2010)

The presence of BCR-ABL stimulates various signal transduction pathways, including the activation of the Ras, Jak/Stat and PI3-kinase pathways (Figure 1.2) (14-16). Activation of these pathways leads to enhanced cell proliferation, reduced apoptosis, increased cell adhesion and cytokine-independent survival (17-19). With the formation of multimeric complexes between BCR-ABL and components of the PI3-kinase pathway, BCR-ABL positive cells continually exhibit a proliferative and survival advantage over normal cells (20). Furthermore, BCR-ABL makes the cells more susceptible to further genetic abnormalities development by inhibiting DNA repair and causing genomic instability (21). Clinical observations and experimental studies have indicated that the genomic instability induced by BCR-ABL may lead to further mutations and/or chromosomal translocations. This phenomenon normally occurs in patients transitioning from chronic phase of CML to more aggressive disease phases, AP and terminal BC (22). In addition, mutations caused by this genomic instability are also a main contributor towards resistance to the targeted therapies of tyrosine kinase inhibitors (TKIs) (23).

1.2.   CML therapies in Pre-TKI era

During the first half of the 20th century, the treatments for CML patients were limited and ineffective. Early choices of therapy included the use of arsenic, radiotherapy and splenic irradiation, all of which only provided symptom control without survival benefit. The use of the cytoreductive agent, busulfan to treat CML, began in 1953. Busulfan targets mainly the haematopoietic cells, particularly those of the granulocytic lineage. Thus, treatment resulted in more efficient control of CML and remained the front-line treatment for nearly two decades (24). Hydroxyurea, an inhibitor of ribonucleotide reductase, was later used to alleviate CML symptoms and achieved a moderate improvement of median survival rates over busulfan, with reduced toxicity (25, 26).
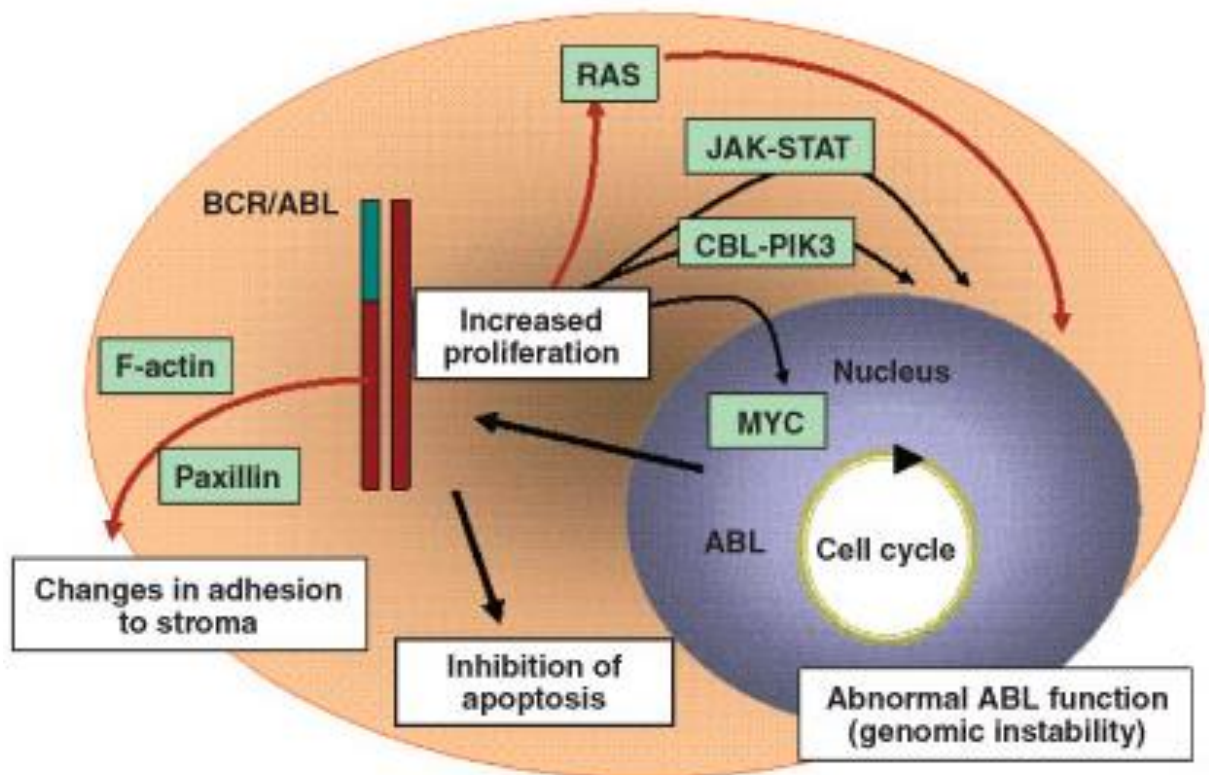
Figure 1.2   BCR-ABL signal transduction pathways

This schematic outlines the major signal transduction pathways activated by BCR-ABL tyrosine kinase, including the PI3-kinase, Ras/Raf and Jak/Stat pathways. Interruptions of these pathway result in uncontrolled cell proliferation and reduced apoptosis. (Figure from Jabbour et al. 2007)

However, these drugs could neither induce lasting cytogenetic responses nor prevent progression to BC-CML. Unlike these two chemotherapeutic drugs, interferon-alpha (IFN-α) treatment was the first agent that induced complete cytogenetic remissions (CCyR, 0% Philadelphia-chromosome positive) in CML patients (27). Randomized controlled trials showed that 6-year survival for patients on IFN-α therapy was superior to chemotherapeutics (50% vs 29% with either busulfan or hydroxyurea) (28). However, IFN-α treatment could only induce durable cytogenetic remissions in a small minority of patients while the majority of patients eventually progressed to BC (29).

In the pre-TKI era, allogeneic stem cell transplant (allo-SCT) was the front-line treatment of choice for CML patients without significant comorbidities and mostly to those younger than 60 years. Presently, it is still considered the only consistent curative treatment for CML (30). The observation in the late 1970s that the Ph chromosome often disappeared after transplantation of bone marrow from identical twins established the curative potential of transplantation for CML (31). Elucidated by this pioneer study and many studies in the early 1980s, allo-SCT provided another treatment of choice for young CML patients with available human leukocyte antigen (HLA)-identical donor (32-35). Even for those patients with advanced-stage CML, allo-SCT was sometimes an effective treatment. A large clinical study demonstrated that CP patients treated with allo-SCT achieved a 70% survival rate at 10 years. In addition, using FISH and RQ-PCR to detect minimal residual disease, long-term follow up study showed that many patients remained BCR-ABL negative many years after transplantation (36). Furthermore, patients remained in remission for years after allo-SCT, even if low levels of BCR-ABL transcript were detected (37). However, the outcome of transplant in more aggressive CML cases still requires improvement. The results of allo-SCT in AP-CML and BC-CML were significantly worse than those in

CP-CML due to the increased chances of recurrence and treatment-related mortality (38).

Despite the durable responses, transplantation is associated with high rates of morbidity and mortality. Since CML most commonly occurs in the middle-aged and elderly, the majority of patients are not eligible for the myeloablative transplant due to considerable toxicity. So far, many different approaches have been tested to overcome this limitation, including T-cell–depleted transplants (39, 40), autologous transplants (41-44), and reduced-intensity conditioning (45, 46). Unfortunately, these less intensive methods are normally associated with increased rates of graft failure and disease relapse, most likely due to the lack of the "graft versus leukaemia" effect. Therefore, the most common treatment before the TKI era was firstly allo-SCT for eligible patients, or otherwise, IFN-α therapy.

1.3.   CML therapies in the era of tyrosine kinase inhibitors

As mentioned in Section 1.1.2, the constitutively active tyrosine kinase BCR-ABL was identified as the key pathophysiology mechanism causing CML. This unique tyrosine kinase was exploited for targeted therapy with the development of the first successful tyrosine kinase inhibitor, imatinib (47). Imatinib has become a hallmark for successful cancer therapy based on a rational treatment approach.

1.3.1.   First generation TKI: imatinib

Imatinib mesylate (STI571/Gleevec, Novartis) is a 2-phenylaminopyrimidine compound and is a competitive inhibitor of the BCR-ABL tyrosine kinase(48). Identified by high throughput screening of a chemical database, imatinib was regarded as a successful example of structure-based drug design. By binding at the adenosine tri-phosphate (ATP)-binding site, imatinib stabilizes the BCR-ABL tyrosine kinase in the inactive conformation, and thus prevents ATP hydrolysis and

phosphorylation of substrates (Figure 1.3) (49). Additional effects of imatinib include the inhibition of the normal ABL protein, Arg (ABL-related gene) protein (50), stem cell factor receptor (Kit) (51), the macrophage colony stimulating factor receptor, c-fms (52), and platelet derived growth factor receptor α and β (PDGFRα and PDGFRβ) tyrosine kinases (51).

Shortly after the development of imatinib, its preclinical efficacy was intensively investigated in patient-derived BCR-ABL expressing cells and then in a mouse model expressing BCR-ABL positive cells (53). In the phase I trial with an initial cohort of 83 patients, imatinib was well tolerated and had significant anti-leukemic activity. A clear dose-response was observed and 400 mg/day was selected as an effective dose (47). More than 1,000 patients were then enrolled in several clinical efficacy (phase II) studies conducted for each disease phase of CML (CP, AP, and BC). Similar or greater efficacy of imatinib was reported in these later studies. Accumulated experience demonstrated the cytogenetic response benefit of early imatinib initiation; but also confirmed that responses in more aggressive disease phases (AP/BC) were more difficult to achieve and less durable than in the CP (54-56).

In the phase III, randomized, open-label International Randomized Study of Interferon versus STI571 (IRIS) trial, 1106 CP-CML patients at diagnosis were recruited and randomized to 400mg imatinib daily or IFN-α plus low dose cytarabine (57). The results clearly demonstrated the superiority of imatinib over IFN-αplus low-dose cytarabine for CP-CML in haematological and cytogenetic responses. By 18 months, 76.2% of patients treated with imatinib achieved CCyR while only 14.5% of IFN-αtreated patients achieved the same landmark. In addition, 96.7% of patients in the imatinib group did not progress to AP or BC, while 91.5% in the IFN-α group did not progress. Due to the obvious superiority of imatinib therapy, a considerable proportion of IFN-α group was switched to the imatinib arm. Based on the efficacy
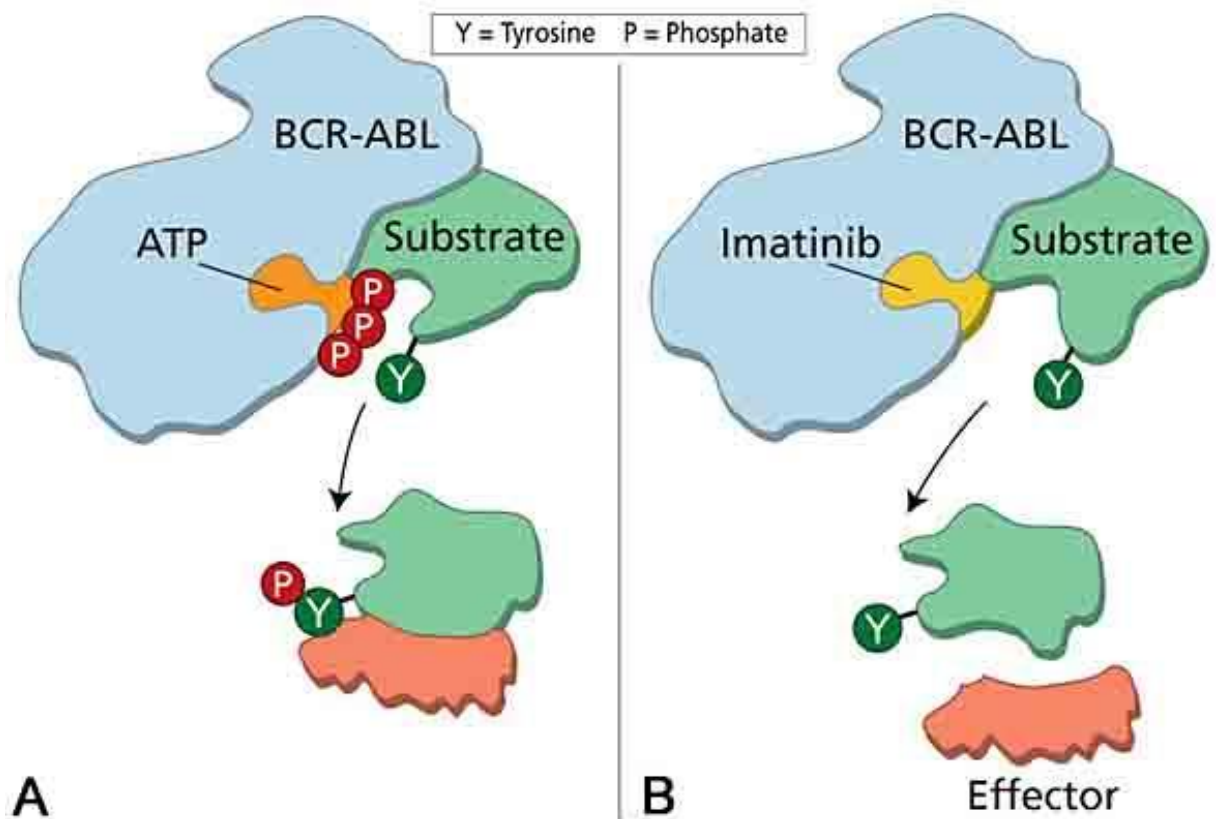
Figure 1.3   Mechanism of imatinib

Imatinib competitively binds into the ATP binding pocket in the BCR-ABL protein. This binding prevents ATP from binding and phosphorylating adaptor proteins, thereby inhibiting the downstream signaling pathways. **(A)** BCR-ABL activity in the absence of imatinib. **(B)** Imatinib binds BCR-ABL in the ATP binding pocket of the kinase domain. (Figure from Goldman et al. 2001)

observed in these studies, imatinib was approved by the United States Food and Drug Administration (FDA) firstly for the treatment of patients who had failed IFN-α in 2001 and subsequently for newly diagnosed patients in 2003. Imatinib then became widely used as first-line therapy for CP-CML patients.

Subsequent updates of the IRIS study at five years follow-up confirmed that patients in the imatinib arm maintained their haematological and cytogenetic responses, had low progression rates to AP or BC, and excellent survival outcomes (58). 87% of patients treated with imatinib achieved CCyR and 93% of patients did not progress to AP or BC. Furthermore, a remarkable 89% overall survival in the imatinib group surpassed all the previous IFN-based regimens. There was no survival difference compared to the IFN-α arm in the IRIS trial due to the high level of cross-over of patients to imatinib arm. At 8 years of follow-up, the response to imatinib had been maintained. The estimated overall survival rate at 8 years was 85% (93% when only CML-related deaths and deaths before stem cell transplantation were considered) (59).

The other important finding of the IRIS study was the significant association between the degree of reduction of BCR-ABL transcript levels and the long-term clinical outcome (60, 61). Of those patients who achieved CCyR at 12 months in the imatinib arm, 57% had a 3-log reduction in BCR-ABL transcript levels (major molecular response, MMR). The achievement of MMR at 12 months was associated with a complete freedom of progression to AP/BC at 24 months (60). Analysis of the 7-year update revealed similar result. Patients who achieved MMR by 18 months had durable responses, with no progression to AP/BC at 7 years. The probability of loss of CCyR by 7 years for patients who had achieved MMR by 18 months was significantly lower compared to those who achieved CCyR but not MMR (3% versus 26%) (61).

1.3.2. *Resistance to imatinib*

Despite the promising efficacy of imatinib in treating CML, there is a significant group of patients who do not respond adequately to imatinib. For this cohort of patients, the risk of relapse or progression is unacceptably high by current standards. As imatinib is given orally, variations in cytochrome p450 isoenzyme 4A (CYP3A4) concentrations and the plasma-protein binding has been investigated as potential mechanism of imatinib resistance. Other mechanisms include intracellular drug concentration, increased expression of BCR-ABL, mutations in the ABL-kinase domain, and the development of alternative pathways of signal transduction (Figure 1.4). Resistance to imatinib can be divided into primary, in which patients exhibit lack of efficacy from the start of therapy, and secondary (also referred to as "acquired resistance") which is defined as the loss of recovery benchmarks while on treatment.

1.3.2.1. *Primary resistance to imatinib*

Primary resistance occurs when a newly diagnosed patient fails to achieve satisfactory response to drug, i.e., a major cytogenetic response (MCyR, less than 35% Ph-positive marrow metaphases) by 6 months, a CCyR by 12 months, or a MMR by 18 months (62). In the phase III IRIS study with imatinib, around 2% of patients failed to achieve a haematological response, and 8–13% failed to achieve a major or complete cytogenetic response (63).

Primary resistance to imatinib is thought to be conferred by the inadequate inhibition of the kinase activity of BCR-ABL. Thus the 50% inhibitory concentration for imatinib ($IC50^{imatinib}$) was developed to evaluate BCR-ABL inactivation by imatinib *in vitro* (64). $IC50^{imatinib}$ is calculated by assessing the *in vitro* phosphorylation status of the adaptor protein Crkl (CT10 regulator of kinase-like), a known downstream substrate of BCR-ABL. The $IC50^{imatinib}$ value is defined as the concentration of imatinib required to reduce p-Crkl by 50% *in vitro*. $IC50^{imatinib}$ has been shown to be highly predictive of a
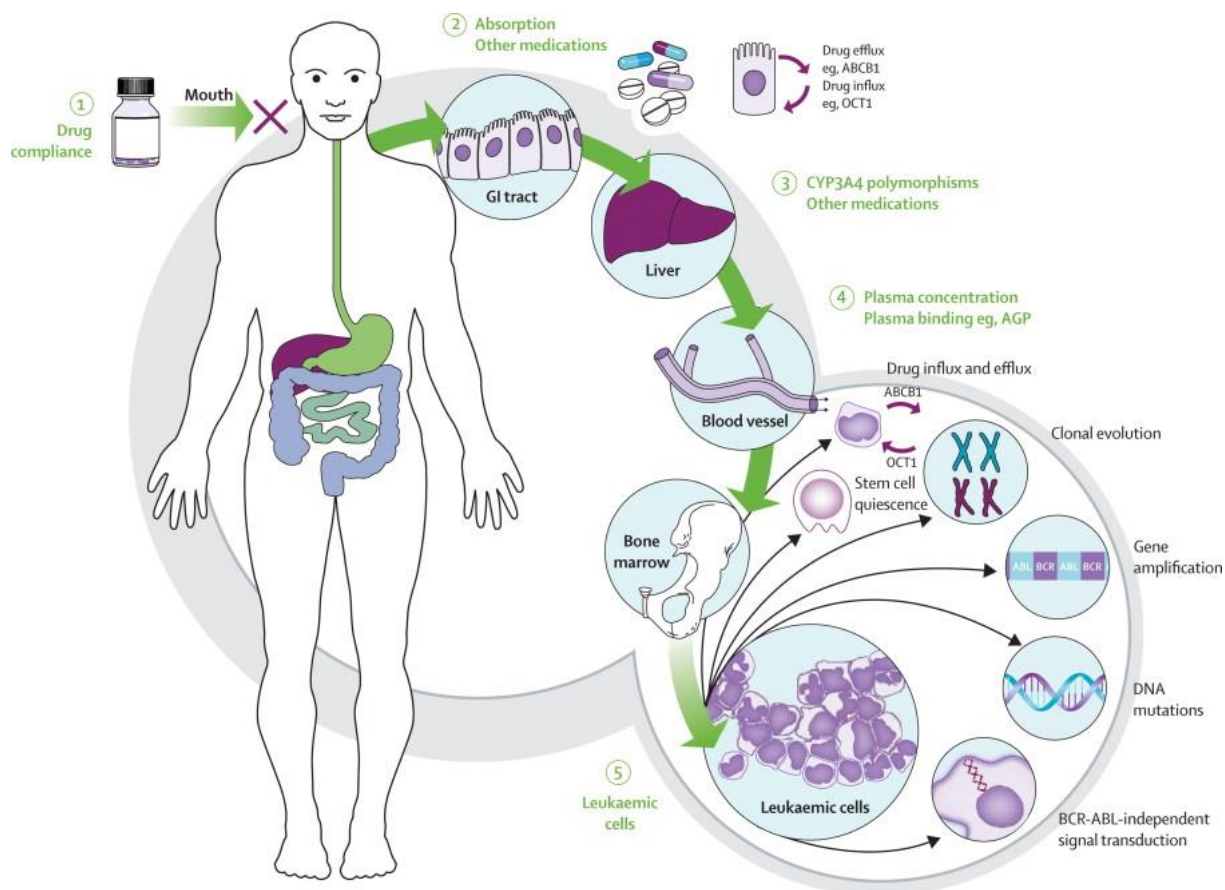
Figure 1.4   Mechanisms of imatinib resistance

Resistance to imatinib is likely to be a multifactorial process. Given orally, imatinib is therefore subject to variations in gastrointestinal absorption and first-pass metabolism, as well as: plasma-protein binding, cellular drug influx and drug efflux, enzymatic inactivation, changes in expression or mutations of the target molecule, defects in apoptosis, and the development of alternative pathways of signal transduction. (Figure from Apperley. 2007)

patient's subsequent molecular response (65). A significantly higher proportion of patients with a low IC50^{imatinib} (high intrinsic sensitivity to imatinib-induced kinase inhibition) achieve MMR by 12 months when compared with those patients with high IC50^{imatinib}. In addition, a 50% reduction in p-Crkl *in vivo* measurement by day 28 of imatinib treatment provides a strong predictor for achievement of MMR by 24 months (65). The degree of BCR-ABL kinase inhibition achieved in patients is highly variable and is a critical determinant of response to imatinib therapy. By measuring the intracellular concentration of imatinib, the intracellular uptake and retention (IUR) of imatinib significantly correlates with the extent of imatinib-induced BCR-ABL kinase inhibition (66). Patients with a lower intracellular concentration of imatinib (low IUR) achieved poorer kinase inhibition (high IC50) compared to those with higher IUR. This result indicates that a low intracellular concentration of imatinib may be a major contributor for the primary resistance to imatinib. The primary resistance may be caused by up-regulation of imatinib-export proteins (such as ABCB1 and ABCG2) and down-regulation of the human organic cation transporter SLC22A1 (as known as organic cation transporter 1, OCT-1), which has been identified as the influx transporter for imatinib. The transporters responsible for imatinib influx and efflux will be described in the Section 1.4.

1.3.2.2. Secondary/acquired resistance to imatinib

Secondary/acquired resistance is defined as the failure of a patient on treatment to maintain the response initially achieved. In the IRIS trial, the proportion of patients with any progression event in CP taking imatinib was 18% at the 5-year follow-up (58). The rates of resistance and relapse were dramatically higher in patients with advanced disease: 75% or more in AP and 95% in BC patients. Acquired resistance to imatinib is commonly attributed to the emergence of point mutations in the ABL kinase domain of the BCR-ABL fusion protein, which largely abrogates drug affinity.

The first mutation identified in resistant patients was the exchange of threonine for isoleucine at amino acid 315 (T315I) located at the imatinib binding site (49, 67). Since then, more than 50 different mutations have been described (68, 69), with variable biochemical impact on imatinib sensitivity (70). Secondary TKI resistance has also been linked with increased expression of BCR-ABL (67, 71, 72). Duplication or amplification of the BCR-ABL oncoprotein leads to ineffective kinase inhibition at pharmacologically achievable TKI concentrations (73). Other proposed mechanisms of imatinib resistance include changes in drug efflux transporters (such as ABCB1 and ABCG2) that result in low intracellular drug concentrations (74, 75). In addition, there are accumulating instances/examples of BCR-ABL-independent mechanisms conferring resistance to imatinib, such as a constitutive activity of the PI3K/AKT pathway (76) or over-expression of Src kinases (77, 78).

1.3.3.   Second generation TKIs: dasatinib and nilonitib

Despite the excellent efficacy of imatinib treatment, there are still a number of patients exhibiting sub-optimal response to therapy as a result of either primary or secondary resistance. Furthermore, imatinib has been found to be less effective when treating patients in AP/BC. Therefore, second generation rationally designed TKIs were developed to circumvent the imatinib resistant mutation, namely nilotinib (AMN107, Tasigna®; Novartis Pharmaceuticals) and dasatinib (BMS-354825, Sprycel®; Bristol-Myers Squibb) (Figure 1.5).

Based on thorough analysis of the ABL–imatinib complex to increase binding affinity, nilotinib was rationally designed to have improved efficacy. Compared with imatinib, nilotinib exhibits more selective and a more potent interaction (10-50 times) with the ATP binding site of ABL, resulting in further inhibition of proliferation in BCR-ABL positive cells (79, 80). Furthermore, nilotinib is effective in blocking BCR-ABL carrying point mutations that confer resistance to imatinib, except for the T315I, Y253H,
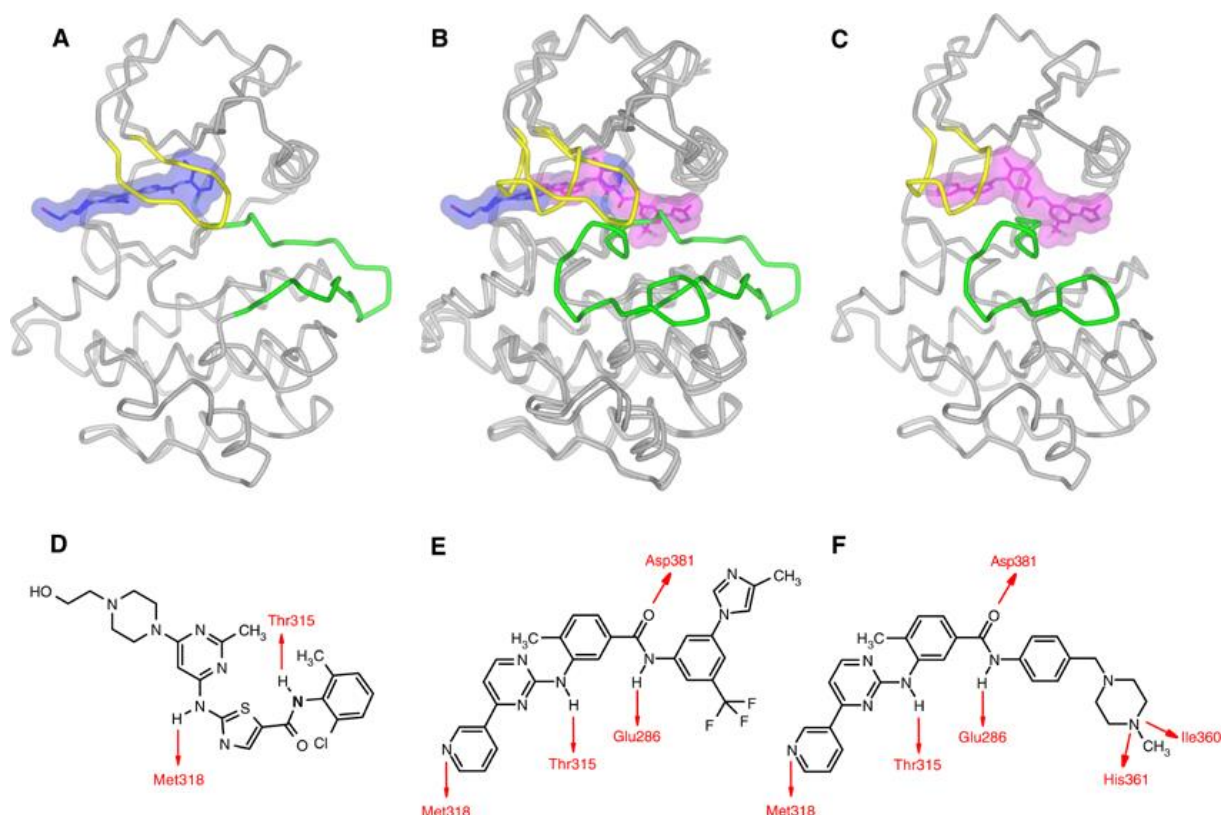
Figure 1.5   Mechanism of action of nilotinib and dasatinib

Structures of Abl kinase (**A**) in the active and (**C**) inactive states, with dasatinib (blue) docked and nilotinib (magenta) as bound in the crystal structure, respectively. The differing conformations of the glycine-rich or P-loop (yellow) and the activation loop (green) are induced or stabilized by the different binding modes of the two inhibitors. (**B**) shows a superposition of the two distinct conformations, emphasizing how dasatinib and nilotinib occupy different parts of the cleft between the N- (upper) and C-terminal (lower) lobes of the kinase. The corresponding aspects of the molecular structures of (D) dasatinib and (E) nilotinib are depicted, with their respective H-bond interactions with the Abl kinase domain indicated in red, in comparison to imatinib (F). (Figure from Weisberg et al. 2006)

and F359V/C mutations (81, 82). In phase I studies for nilotinib, promising results in imatinib-resistant CP-CML patients have been observed, but not for BC patients (83). In subsequent phase II studies, 48% CP and 29% AP patients achieved MCyR when treated by 400 mg nilotinib twice daily (84, 85). In patients with prior sub-optimal response to imatinib, nilotinib has demonstrated rapid and durable responses (86, 87). The phase III trial Evaluating Nilotinib Efficacy and Safety in Clinical Trials-Newly Diagnosed Patients (ENESTnd) compared therapy regimens of nilotinib (300 or 400 mg twice daily) with imatinib (400 mg once daily). Both nilotinib dosage arms achieved significantly higher MMR and CCyR than the imatinib arm (88). Encouraged by these results, the approval of nilotinib for newly diagnosed CML patients was granted by the FDA in 2010 (89).

While nilotinib is a more selective ABL inhibitor, dasatinib is a dual src-kinase inhibitor, effective against the ABL kinase and the Sarcoma (Src) family of tyrosine kinases. Dasatinib binds to both ABL and the Src kinase in the ATP-binding site with high affinity, inducing a 300 times greater ABL inhibition potency than imatinib (90). In addition, c-KIT, PDGFR-α/β, and the ephrin receptor kinases are also targeted by dasatinib (91). Another unique characteristic of dasatinib is that it can bind both the inactive and active forms of BCR-ABL, leading to a more complete tyrosine kinase inhibition (90). Importantly, dasatinib is active against most imatinib resistant mutations, with the exception being the T315I and F317 mutation (92, 93). The phase II trials for Src/ABL Tyrosine kinase inhibition Activity Research Trials of dasatinib (START) revealed that dasatinib demonstrated a promising response rate and high rate of progression-free survival in CP (94). Similar to experiences with nilotinib, impressive responses were observed in AP and BC, but much less durable than those in CP (95). Dasatinib induces notable haematological and cytogenetic responses in CP after failure of imatinib therapy (94). To evaluate the outcome of dasatinib in a *de*

novo CML cohort, the Dasatinib versus Imatinib Study in Treatment-Naïve CP-CML Patients (DASISION) trial was conducted comparing dasatinib at 100 mg daily versus imatinib 400 mg daily. The advantage demonstrated in the DASISION trial (regarding MMR and CCyR for dasatinib over imatinib) led to the regulatory approval of dasatinib for newly diagnosed CP-CML patients in October 2010.

With higher binding-affinity for ABL kinase and the ability to target many imatinib resistant mutations (except T315I, which is resistant to all three TKIs), nilotinib and dasatinib offer alternative therapies to patients who harbour imatinib resistant mutations or have a poor response to imatinib.

1.3.4. Third generation TKI: ponatinib

Ponatinib (AP24534, Ariad) is currently the most advanced third-generation inhibitor of BCR-ABL (96). The unique characteristic of ponatinib is its ability to bind T315I-mutated BCR-ABL molecule, as well as wild-type BCR-ABL. In addition, it binds a large number of other TKI-resistant BCR-ABL mutants (97). In addition to its "pan-BCR-ABL" binding, ponatinib also inhibits other kinases including FLT3, FGFR, VEGFR, c-Kit, and PDGFR (98, 99).

In a phase I study of patients with refractory CML and hematologic malignancies, ponatinib induced McyR in 46% of chronic-phase patients resistant to second-line tyrosine kinase inhibitors. The most impressive responses were in patients with the T315I mutation. All 7 evaluable T315I CP-CML patients had complete haematologic response (CHR) and 4 of them achieved CCyR (100). Currently ponatinib is being tested in a global, single-arm phase II clinical trial (Ponatinib Ph+ ALL and CML Evaluation, PACE) including patients in all disease phases of CML and Ph+ ALL. The randomized phase 3 trial of ponatinib (Evaluation of Ponatinib versus Imatinib in Chronic Myeloid Leukaemia, EPIC) was just initiated to investigate the efficacy of

ponatinib as a front-line therapy for *de novo* CML patients in comparison to imatinib based on evaluation of the primary endpoint of major molecular response (MMR) at 12 months. The trial is expected to complete patient enrolment by the end of 2013.

1.3.5. *Transplantation in the era of TKIs*

Shortly after peaking in the late 1990s, the number of CML patients undergoing allo-SCT decreased after the approval of imatinib by the FDA (38, 101), especially in CP-CML patients (102). The current rationale for considering allo-SCT includes failure or intolerance of all available TKIs, development of TKI-resistant mutations such as T315I, or progression to AP/BP CML.

For all the TKIs currently approved, patient outcomes are less durable in AP and BC. Although the outcome after transplantation for these patients is suboptimal (38), allo-SCT still remains the only curative therapy in advanced-phase CML. For patients who harbour the T315I mutation, early allo-SCT is recommended due to the lack of effectiveness of the three currently available TKIs (103). Clinical data suggests that the results of transplantation for patients with T315I are better than that achieved by non-transplant strategies (103-105). However, this advice may change when third generation of TKI ponatinib becomes clinically available.

Another notable change for the allo-SCT procedure is that the majority of transplant patients are usually initiated with TKI treatment. Several groups have reported that treatment with imatinib pre-transplant is safe and is not associated with increased transplant-related mortality (106-109). In recent years, second-generation TKIs have also been reported to be safe to use prior to allo-SCT (110, 111).

Patients undergoing transplantation still remain a challenging group, as long-term disease control remains suboptimal. The role of allo-SCT in the management of CML

will require continual evaluation as the third-generation TKI, ponatinib, may provide a promising alternative therapy for T315I mutated patients (112).

1.4. Drug transporters for imatinib

1.4.1. Efflux transporters: ABCB1 and ABCG2

Imatinib has been show to interact with the ATP-Binding Cassette (ABC) subfamily B member 1 (ABCB1; formerly known as P-glycoprotein or MDR1) (113-115) and subfamily G member 2 (ABCG2; formerly known as the breast cancer resistance protein or BCRP) (116, 117). Both ABCB1 and ABCG2 are expressed in a variety of organs, including the liver, intestines, kidneys, placenta, and at the blood-brain barrier (51, 118-121). To determine their roles in acquired imatinib resistance, these two efflux transporters have been intensively investigated using ABCB1/ABCG2 over-expressing cell lines or mice models. There is currently conjecture regarding how imatinib interacts with ABCB1 and ABCG2, and whether imatinib acts as a substrate (74, 122-124), an inhibitor (125-127) or both. There is a growing consensus that the inhibitory effect of imatinib on ABC transporters is dose dependent, and only occurs at higher concentrations (116, 117, 123). However, no significant effect on the intracellular concentration of imatinib was observed when primary CML patient mononuclear cells (MNC) were co-incubated with imatinib and the ABCB1 inhibitor PSC833. Similar negative results were observed when patients' peripheral blood (PB) MNC were treated with imatinib and the ABCG2 inhibitor, fumitremorgin C (66).

1.4.2. Influx transporters for imatinib: OCT-1

Imatinib is weakly cationic at a physiological pH. The organic cation transporters (OCTs, belong to the SLC22 family) are responsible for the absorption, elimination and distribution of cationic drugs and other xenobiotics *in vivo* (128, 129). There are four known members of the OCT family, named OCT-1, OCT-2, OCT-3 and OCT-6.

The impact of these OCT transporters on the intracellular concentration of imatinib were determined using a series of specific OCT inhibitors (130). In the leukemia cell line CCRF-CEM and its drug-resistant subline VBL100, the intracellular concentration of radio-labeled imatinib was significantly reduced in the presence of the inhibitors prazosin (OCT-1 & OCT-3), procainamide (OCT-1 & OCT-2), verapamil (OCT-1 & ABCB1) and amantadine (OCT-1 & OCT-2). When subsequently incubated with the specific OCT-2 inhibitor (N-methylnicotinamide) and OCT-3 inhibitor (corticosterone), no significantly change was found on the uptake of imatinib. Therefore, OCT-1, rather than family members 2 or 3, was suggested as the likely influx transporter for imatinib.

First identified in 1994, OCT-1 is a polyspecific transporter primarily located in the liver (131, 132). It is also expressed in the large and small intestine, stomach, lungs, kidneys and heart (129). OCT-1 is predicted to have 12 transmembrane domains and binding pockets with partially overlapping interaction domains for different substrates and inhibitors (Figure 1.6) (129). The transport of imatinib by OCT-1 was also demonstrated in primary CML samples by the intracellular uptake and retention (IUR) assay (66). In the presence of prazosin, the IUR of CML-MNC was significantly reduced compared with the control. More importantly, the IUR was decreased by prazosin to the same level as the IUR observed when the assay was performed at 4°C, where all the ATP-dependent transporters cease functioning. This result provides further evidence that OCT-1 is the predominant active transporter for imatinib in CML PB-MNCs.

The uptake of the second generation TKIs were also assessed to determine whether OCT-1 was also responsible for the transport of nilotinib (66) and dasatinib (133, 134). As OCT-1 inhibitors did not decrease the drugs uptake, neither nilotinib nor dasatinib was thought to be transported by OCT-1 in CML cells.

ORGANIC CATION TRANSPORTER 1 (SLC22A1)
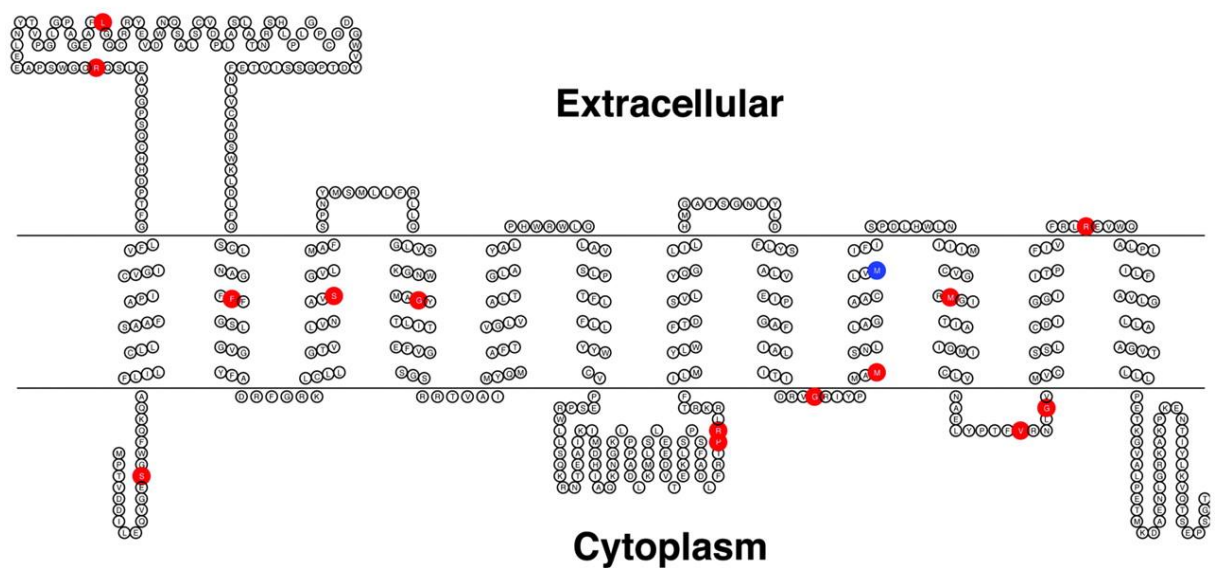
Figure 1.6 Secondary structure and alignment of OCT1 with coding region SNPs

The current model of membrane topology for OCT-1contains 12 transmembrane domains. The protein has a large intracellular and extracellular loop. Nonsynonymous amino acid changes are shown in red, and amino acid deletion is shown in blue. (Figure from Shu et al. 2003)

1.4.2.1. OCT-1 transcript levels and polymorphism

As the intracellular concentration of imatinib is a key contributor to primary imatinib-resistance, a number of studies have been conducted to investigate the mechanism underlying the differences in imatinib uptake among patients. In a study using OCT-1 over-expressed KCL22 cells, the uptake of imatinib was significantly increased compared with the parental line (135). Encouraged by this result, several groups have investigated the feasibility of using OCT-1 expression levels as a clinical determinant of the response to imatinib in CML (135, 136). It has been reported that a high OCT-1 transcript level at diagnosis is significantly associated with rates of MMR by 24 months (137) and by 6 years of imatinib treatment (138). However, no difference was observed when comparing the OCT-1 transcript levels at diagnosis of patients who did and did not achieve CCyR by 12 months of imatinib therapy (139). Furthermore, dividing patients into low and high OCT-1 expression groups was not predictive of MMR, complete molecular response (CMR), event-free survival, or mutation development (62, 140), suggesting that the level of OCT-1 mRNA alone is insufficient to predict response and progression. Therefore, whether OCT-1 transcript levels could be established as a reliable method to determine patient response to imatinib therapy still remains in contention.

Another possible explanation for the inter-patient variability in levels of imatinib uptake is non-synonymous, single-nucleotide polymorphisms (SNPs). In a recent study the G401S (rs34130495) SNP was showed to be significantly associated with a higher rate of MMR in a cohort of 132 CML patients treated with imatinib in chronic phase (141). However, it is very unlikely that this SNP is responsible for the MMR observed in CP-CML patients treated with imatinib, as the frequency of this SNP is low, at 0.045. Furthermore, a similar study by our group performed with 136 newly diagnosed

CP-CML patients revealed no association between the presence of OCT-1 SNPs and molecular response to imatinib (142).

1.4.2.2. OCT-1 activity

In addition to transcript levels and polymorphisms, it is possible that the OCT-1 protein level and functionality are important factors in determining imatinib IUR. However, as there is no current effective antibody for this protein, protein levels have been difficult to interrogate. An assay was therefore developed to directly assess the functional OCT-1 activity (OA) (66). OA was measured in pre-therapy PB-MNC from CP-CML patients by calculating the difference in IUR of ^{14}C-imatinib with and without the potent inhibitor of OCT-1, prazosin. The OA of CP-CML patients at diagnosis correlates significantly with their IC50^{imatinib} (62), indicating that OA is a mediator of sensitivity to imatinib. Furthermore, OA has been shown to be associated with molecular response to imatinib therapy. Patients with a higher OA (above the median) achieved significantly higher rate of molecular response than those with low OCT-1 activity (below the median) by 24 months of therapy (140). As shown in Figure 1.7A and Figure 1.7B, further analysis with a follow-up of 5 years indicated a strong link between high OA and better rates of MMR (89% versus 55%) and CMR (59% versus 31%) (140). In addition, a low OA was associated with a significantly lower overall and event-free survival rate, as well as a higher kinase domain mutation rate. Taken together, OCT-1 activity is a strong indicator of molecular response and long term outcome of imatinib therapy in *de novo* CML patients.

1.5. Drug interactions with imatinib via transporters

As previously described, imatinib acts as a substrate of the drug transporters *ABCB1*, *ABCG2* and OCT-1. A standard regimen can therefore result in very different intracellular imatinib concentration profiles from one patient to another, thus leading to
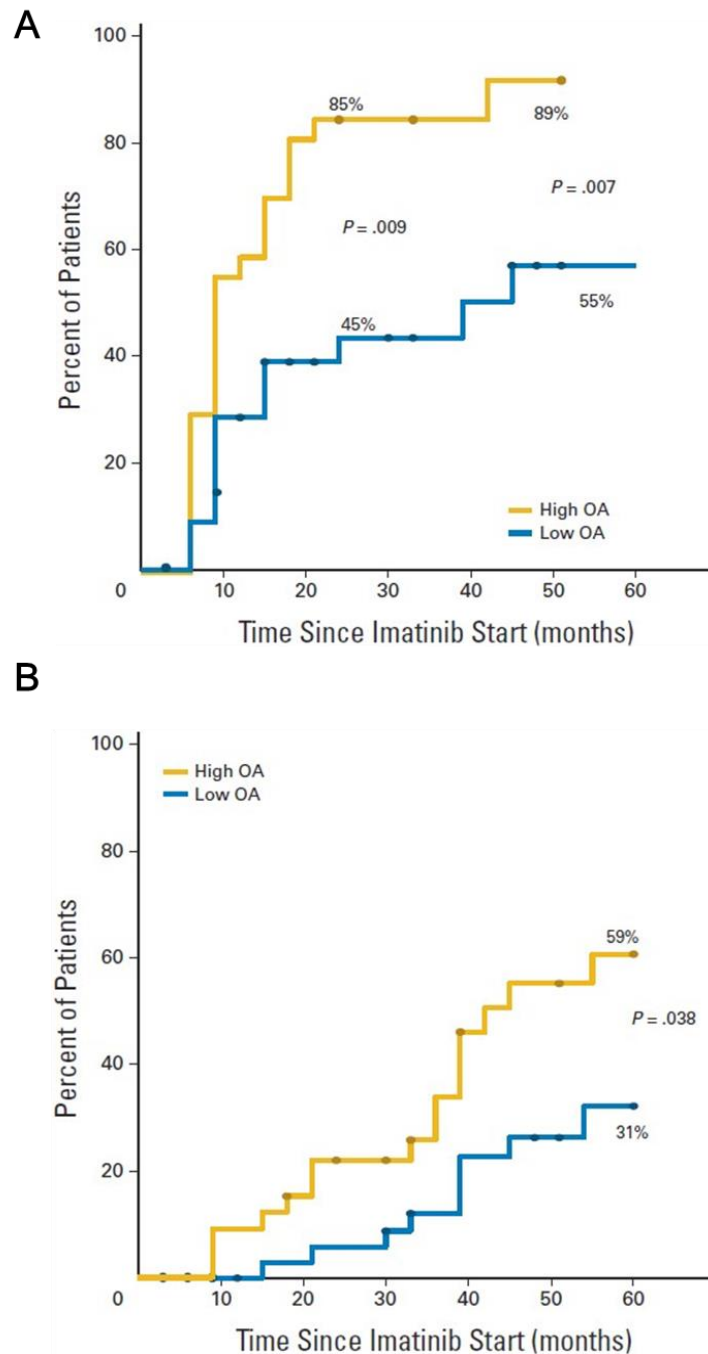
Figure 1.7   OCT-1 activity is associated with molecular response to imatinib therapy

The percentage of patients achieving (**A**) major molecular response (MMR) and (**B**) complete molecular response (CMR) on the basis of low and high OCT-1 activity groups. Kaplan-Meier curves demonstrate that a significantly greater proportion of patients who had high OCT-1 activity achieve MMR and CMR by 5 years when compared with patients who had low OCT-1 activity. (Figure from White et al. 2010)

variable intracellular drug exposure and tyrosine kinase inhibition (143, 144). Pharmacologic interactions between imatinib and drugs concomitantly prescribed to patients have been investigated to maximize therapeutic benefit of imatinib for CML patients.

It has been demonstrated *in vitro* that elacridar (ABCB1 inhibitor) and pantoprazole (ABCG2 inhibitor) inhibit the efflux of imatinib in ABCG2 over-expressing MDCKII cells (145). In addition, co-administration of these efflux-transporter inhibitors significantly reduced the clearance of intravenous imatinib in wild-type mice. More importantly, co-administration of pantoprazole significantly increased the brain penetration of imatinib administered orally in wild-type mice. Accumulating evidence indicates that ABCB1 inhibitors (such as verapamil, erythromycin, clarithromycin, ciclosporin, ketoconazole, fluconazole, and itraconazole) can increase intracellular concentrations of imatinib by inhibiting the efflux by ABCB1 and might therefore enhance the tyrosine inhibition (146-148).

There are relatively few studies investigating drug interactions with imatinib and OCT-1. The known inhibitors of OCT-1, quinidine, ranitidine, or midazolam, have been suggested to decrease the intracellular exposure of target cancer cells to imatinib (148). Other inhibitors of OCT-1 include metformin, amiodarone, levofloxacin, ganciclovir, valganciclovir, saquinavir, indinavir, lamivudine, and chloroquine. However, all these studies are limited because they have used a genetically engineered cell line model. There is currently limited knowledge of OA enhancers and their potential clinical benefits.

1.6. Hypothesis and aims

Imatinib mesylate is a rationally designed inhibitor of BCR-ABL. It has resulted in significantly better clinical outcomes, with higher response rates and a longer overall

survival time compared with the previous standard treatment. Despite excellent overall responses in the majority of CP-CML patients, primary and secondary resistance to imatinib remain an inevitable clinical challenge. The function of the influx protein OCT-1 (OCT-1 activity, OA) has been shown to be a strong predictor of molecular response and long-term outcome to imatinib therapy. However, little is known about the interaction between imatinib and other drugs via OCT-1. By identifying drugs that can enhance OA, the intracellular concentration of imatinib and the degree of kinase inhibition can be increased in CML cell-lines and patients' samples with low OCT-1 activity. This could potentially translate to an improved molecular response to imatinib *in vivo* and more effective depletion of primitive leukaemia progenitors than standard imatinib administration, leading to a substantial clinical benefit. More detailed study of the mechanism of action of OCT-1 enhancers will also provide a better understanding of OCT-1 regulation, and therefore a launching point for new strategies in overcoming resistance and suboptimal response to imatinib.

This thesis therefore addresses the following aims:

- To identify candidate drugs that can increase OCT-1 functional activity in BCR-ABL positive cell-lines.

- To validate the effect of candidate drugs by *in vitro* tyrosine inhibitory assay (IC50^{imatinib}) and cell viability assay.

- To validate the effect of candidate drugs on OA using primary patient samples.

- To investigate the mechanism of OCT-1 regulation by the OA enhancers.

CHAPTER II
Materials and Methods

2.1. Commonly used reagents

Table 2.1 Suppliers of commonly used reagents

Reagent	Supplier	Catalogue Number
Acrylamide/Bis solution 40%	Bio Rad	161-0148
Bovine Serum Albumin (BSA)	Sigma-Aldrich	A2153
Chloroform	Merck	100776B
Complete (Protease inhibiter cocktail Tablets)	Roche	4693116001
Diethyl pyrocarbonate (DEPC) H_2O	MP Biomedicals	821739
Dimethyl sulphoxide (DMSO)	Merck	K39661852
ECF substrate Attaphos	GE Healthcare	PRN 5785
Ethanol	Merck	4.10230.2511
Ethylenediaminetetraacetic acid (EDTA)	APS	180-500G
Foetal Bovine Serum (FBS)	JRH Biosciences	12003-500M
Glycogen	Roche	901393
Hanks Buffered Saline Solution (Hanks)	Sigma-Aldrich	H9394
HEPES 1M	Sigma-Aldrich	H0887
L-glutamine 200mM	SAFC Biosciences	59202C
Lymphoprep	Axis Shield	1114547
MACS beads CD14	Miltenyi Biotech	130-050-201
MACS beads CD15	Miltenyi Biotech	130-046-601
Methanol	Chem Supply	MA004-P
Microscint-20 scintillation fluid	Perkin Elmer	6013621
Pefabloc (protease inhibiter)	Roche	11429868001
Penicillin / Streptomycin	Sigma-Aldrich	P4458
Phosphate Buffered Saline (PBS)	SAFC Biosciences	59331C

PhosSTOP (phosphatase inhibitor cocktail Tablets)	Roche	4906845001
Prazosin Hydrochloride	Sigma-Aldrich	P7791
PVDF (Western blot membrane)	GE Healthcare	PRN 303F
RPMI-1640 Medium w/o L-glutamine	Sigma-Aldrich	R0883
RT² SYBR® Green qPCR Mastermix	Supermix SA Biosciences	PA-012-24
Sodium Chloride (NaCl)	Ajax Finechem	1128
Tris	Merck	1.08382.0500
Trizol Reagent	Invitrogen	15596-018
Trypan Blue Solution (0.4%)	Sigma-Aldrich	T8154
Tween20	Sigma-Aldrich	P9416
Western Blocking Reagent	Roche	11921673001

Table 2.2   Suppliers of antibodies

Reagent	Supplier	Catalogue Number
β-actin (N-21) Antibody	Santa Cruz	sc-130656
Crk-L (C-20) Antibody	Santa Cruz	sc-319
Lamin B1 Antibody	Cell Signalling	9087
PPARγ (H-100) Antibody	Santa Cruz	sc-7196
FITC Mouse Anti-Human CD15	BD Biosciences	555401
FITC Mouse Anti-Human IgM	BD Biosciences	555782
GAPDH (14C10) rabbit mAb	Cell Signalling	2118
goat anti-rabbit IgG-AP	Santa Cruz	SC-2007
PE Mouse Anti-Human CD11b/Mac-1	BD Biosciences	555388
PE Mouse Anti-Human CD14	BD Biosciences	347497
PE Mouse IgG1, κ Isotype Control	BD Biosciences	555749
PE Mouse IgG2b κ Isotype Control	BD Biosciences	555743

2.2.   Solutions, buffers and media

2.2.1.   *Cell culture media*

500 mL RPMI 1640 Medium

5 mL L-Glutamine (200 mM)

5 mL Penicillin 5000 µg/mL / Streptomycin Sulphate 5000 µg/mL

50 mL Foetal Bovine Serum (FBS) (10%)

The medium was stored at 4°C and preheated to 37°C prior to use.

2.2.2.   *Complete (25x stock)*

one Complete Tablet

2 mL Milli-Q H_2O

The stock was stored at -20°C.

2.2.3.   *Flow cytometry fixative (FACS Fix)*

500 mL PBS

5 mL 40% w/v Formaldehyde

10 g D-glucose

0.1 g NaN_3 sodium azide

The media was stored at 4°C.

2.2.4.   *Hanks balanced salt solution (HBSS)*

10 mM HEPES 1 M was added prior to use.

2.2.5.   *Freeze Mix*

70% HBSS

20% FBS

10% DMSO

The media was made fresh on the day of use and chilled on ice prior to use.

2.2.6. Laemmli's buffer

50 mM Tris-HCl, pH 6.8

10% glycerol

2% sodium dodecyl sulfate SDS

5% β-mercaptoethanol

0.1% bromophenol blue

1 mM NaVanadate

10 mM NaFluoride

The buffer was stored in 1 mL aliquots at -20°C, thawed at room temperature (15–25°C) or briefly in 100°C heating block before use.

2.2.7. 1 x Red Cell Lysis buffer:

0.144 M NH_4Cl = 7.7g

0.01 M NH_4HCO_3 = 0.795g

1 L sterile MilliQ water

The buffer was sterilised and stored at room temperature.

2.2.8. MACS buffer

500 mL PBS

2.5 g BSA

0.37 g EDTA (2 mM)

The buffer was sterilised using a 0.2 µm bottle top filter and stored at 4°C.

2.2.9. TBS

20 mM Tris-HCl, pH 7.5

150 mM NaCl

2.2.10. TBST

20 mM Tris-HCl, pH 7.5

150 mM NaCl

0.1% Tween20

2.2.11. Membrane blocking solution (2.5%)

12.5 g Western Blocking Reagent

500 mL TBS

The solution was stored at 4°C.

2.2.12. Pefabloc stock solutions

Used at 2 mM from 100 mM stock

100 mM stock = 25 mg/mL Milli-Q H_2O

The stock was stored at -20°C.

2.2.13. PhosSTOP (10x stock)

one PhosSTOP Tablet

1 mL Milli-Q H_2O

The stock was stored at -20°C.

2.2.14. Prazosin hydrochloride

Used at 100 µM from 10 mM stock

10 mM stock = 4.2 mg/mL methanol

2.2.15. RIPA Buffer

50 mM Tris-HCl, pH 7.4

1% NP-40

0.25% Na-deoxycholate

150 mM NaCl

2 mM Pefabloc

1x Complete Cocktail

1x PhosSTOP

The solution (without protease and phosphatase inhibitors) was stored at 2–8°C. Pefabloc, Complete Cocktail and PhosSTOP were added to the solution immediately before use.

2.2.16. SDS-Polyacrylamide Gel

	Resolving gel (12%)	Stacking gel (5%)
Milli-Q H_2O	12.9 mL	6 mL
40% Acrylamide	9 mL	1.26 mL
1.50 M Tris-HCl	7.50 mL	2.52 mL
10% SDS	300 µL	100 µL
10% APS	300 µL	100 µL
TEMED	18 µL	10 µL

2.2.17. 2xSDS load buffer

0.125 M   TrisHCL pH 6.8

4% SDS

20%   glycerol

10%   β-mercaptoethanol

0.05%   bromophenol blue

The buffer was stored in 1 mL aliquots at -20°C, thawed at room temperature or briefly in 100°C heating block before use.

2.2.18. Thaw solution

500 mL HBSS

25 mL 5% FBS

25 mL 5% Anticoagulent Citrate Dextrose Solution Formula A (ACD)

5 mL 1 M HEPES

The solution (without ACD) was stored at 4°C. ACD was added and the solution was pre-heated to 37°C prior to use.

2.2.19. Tyrosine kinase inhibitors

2.2.19.1.   Imatinib mesylate

Imatinib (imatinib mesylate; Glivec) was kindly provided by Novartis Pharmaceuticals (Basel, Switzerland). Stock solutions were prepared at 10 mM with distilled water, sterile filtered and stored at -70°C.

2.2.19.2.   100 µM ^{14}C-Imatinib mixture (50%)

29.5 µL ^{14}C-imatinib (1695.72 µM, specific activity 3.394 MBq/mg)

5 µL 10mM imatinib

966 µL RPMI medium

The solution was made fresh on the day of use.

2.2.20. White cell fluid

2 mL Glacial acetic acid

98 mL Milli-Q H_2O

Few crystals of Methyl Violet

The solution was filtered using a 0.2 µm bottle top filter, and stored at room temperature.

2.3. Cell lines

2.3.1. K562

The continuous cell line K562 was established by Lozzio and Lozzio (149) from the pleural effusion of a 53-year-old female with CML in terminal blast crisis. Cells were obtained from the American Type Culture Collection (Manassas, America).

2.3.2. KU812

The KU812 cell line was established from the peripheral blood of a 38-year-old male with CML in blast crisis (150). Cells were obtained from the American Type Culture Collection (Manassas, America).

2.3.3. HL60

The HL60 cell line was established from a 36-year-old female patient with acute promyelocytic leukemia (151). Cells were obtained from the American Type Culture Collection (Manassas, America).

2.3.4. HeLa

The HeLa cell line was derived from a 31-year-old female with Henrietta Lacks, a patient with cervical cancer (152). Cells were obtained from the American Type Culture Collection (Manassas, America).

2.4. Primary cells from CML patients or healthy donors

The primary samples used in this study were collected from chronic phase chronic myeloid leukaemia (CP-CML) patients enrolled in the TIDEL II study. TIDEL II is a multi-centre, single arm prospective Phase II trial in which *de novo* CP-CML adult patients are treated with 600mg/day imatinib upfront and are dose escalated to imatinib 400mg twice daily or switched to nilotinib 400mg twice daily for either intolerance or failure to meet pre-defined early molecular markers of sub-optimal response (BCR-ABL RQ-PCR of 10%, 1% and 0.1% international scale at 3, 6 and 12 months, respectively). All peripheral blood (PB) samples from CML patients at diagnosis or normal donors were collected with informed consent in accordance with the Institutional Ethics approved protocols and with reference to the Declaration of Helsinki.

2.5. General techniques

2.5.1. Bradford protein assay

Working reagent A′ was prepared by adding 20 µL of reagent S provided with the DC protein assay kit (Bio-Rad, Hercules, America) to every millilitre of reagent A (provided with the kit). A protein standard was prepared by making 7 dilutions of protein standard (BSA) from 0 µg/uL to 2 µg/uL. A 5 µL aliquot of standard or samples was dispensed in duplicate into opaque 96-well flat bottomed microplate (PerkinElmer, Waltham, America), while 5 µL of H_2O was added in blank wells. Then 25 µL of reagent A′ was added into each well, followed by adding 200 µL of reagent B. The plate was covered and incubated at room temperature for 15 minutes before the absorbance was measured on a spectrophotometer at 595 nm wavelength. The assay was repeated if the R value for the standard curve was less than 0.8 or if any sample well generated absorbance greater than the highest standard.

2.5.2. *Cell counts and cell viability determination*

Cells were gently agitated to ensure even suspension throughout media. In a laminar flow cabinet, a 1-2 mL aliquot was taken in 2 mL microcentrifuge tube (Eppendorf, North Ryde, Australia). A 10 µL aliquot of cells was then mixed with 10 µL Trypan Blue (Sigma-Aldrich, Castle Hill, Australia), and 10 µL of this mixture was loaded onto a haemocytometer counting chamber (Neubauer Improved, Assistant, Germany) and live cell concentration calculated accordingly. For primary samples from CML patients or healthy donors, cell concentration was determined by diluting the cell suspension in white cell fluid (WCF) and cell viability was assessed by diluting samples with trypan blue solution.

2.5.3. *Cryopreservation of cells*

Cells were cryopreserved in a "Freeze Mix" of 70% HBSS, 20% FBS and 10% DMSO as detailed in Section 2.2. Cells were pelleted, resuspended in chilled Freeze Mix at 2×10^6 cells/mL (for primary samples 1×10^7 cells/mL), and transferred quickly to 1.5 mL cryoampoules (Nalgene, Rochester, America) before being cryopreserved using a "Mr. Frosty" container (Nalgene, Scoresby, Australia) for a minimum of 4 hours at -70°C. Cryoampoules were finally stored in liquid nitrogen (-196°C).

2.5.4. *Tissue culture*

All tissue culture was performed in a Class two "biohazard" laminar flow cabinet (Gelman Sciences, Lane Cove, Australia). Cell lines were maintained at a cell density between 1.5×10^5 and 1.2×10^6 cells/mL, depending on the rate of proliferation, in 25 cm^2 or 75 cm^2 tissue culture flasks (Greiner, Frickenhausen, Germany). Culture media was RPMI (Sigma-Aldrich, Castle Hill, Australia) supplemented with penicillin/streptomycin (Sigma-Aldrich, Castle Hill, Australia), L-glutamine (SAFC Bioscience, Lenexa, America) and FBS (Trace Biosciences, Sydney, Australia) as detailed in Section 2.2.1. Cell cultures were kept in a 37°C/5% CO_2 incubator (Sanyo,

Osaka, Japan). Cell cultures were checked every second day for contamination, counted and seeded at the above concentrations with fresh media (warmed to 37°C prior to use).

2.5.5. Thawing cells

1.5 mL cryoampoules were removed from liquid nitrogen and thawed rapidly in a 37°C water bath. In a laminar flow cabinet, cells were transferred to a 60-mL polypropylene tube (BD Biosciences, North Ryde, Australia). Approximately 30 mL warmed culture media was added drop-wise, with constant mixing. A further 20 mL media was added with constant mixing. Cells were then pelleted at 1200 rpm for 10mins, and the supernatant was discarded. Cells were again resuspended in 50mL warmed culture media (as above). Cells were again pelleted and 40 mL of the supernatant discarded. Cells were resuspended in the remaining 10mL, counted and seeded in 25 cm^2 tissue culture flasks (Greiner, Frickenhausen, Germany).

2.5.6. Lymphoprep isolation of mononuclear cells (MNC)

40-60 mL of peripheral blood from CML patients at diagnosis or normal donors was collected into Lithium Heparin tubes. A white cell count was performed using white cell fluid with a 10 µL aliquot of sample. A maximum of 1x10^8 cells (maximum of 15 mL) were transferred into a 60-mL polypropylene tube. The blood volume was brought to 35 mL using HBBS and underlain with 15 mL of lymphoprep. Tubes were then centrifuged at 1,200 rpm for 30 minutes with no brake. The interface containing the mononuclear cells (MNC) was then transferred to a new 60-mL polypropylene tube and washed once in HBBS buffer followed by a white cell count.

2.6. Specialised techniques

2.6.1. *Imatinib intracellular uptake and retention (IUR) assay*

The IUR assay was performed as previously described [66]. In brief, 200,000 viable cells (cell lines or cryopreserved and subsequently thawed primary patient PB MNC at diagnosis) were incubated for 2 hours at 37°C/5% CO_2 in 2 mL of RPMI + 10% FCS media in the presence or absence of 2 µM ^{14}C-labelled imatinib. After incubation, cells were pelleted at 6,800 rpm for 5 minutes, then at 13,000 rpm for 30 seconds. A 20 µL aliquot of supernatant from each tube was dispensed into an opaque 96-well flat bottomed microplate (PerkinElmer, Waltham, MA, America) with appropriate wells containing 100 µL of Microscint-20 scintillation fluid. The remaining supernatant was then carefully aspirated from the tubes and 50 µL of Microscint-20 scintillation fluid was added. The tubes were vortexed and centrifuged for 15 seconds at 13,000rpm. The lysed cells were then transferred to the 96 well-plate with wells containing 50 µL of Microscint-20 scintillation fluid. The plate was covered with an adhesive plastic seal and was counted on a Top Count Microplate Beta scintillation counter (Perkin Elmer) as counts per minute (Cpm). All assays were performed in triplicate and repeated if the assay demonstrated non-concordance.

The IUR of ^{14}C-labelled imatinib was then calculated as ng imatinib/200,000 cells using the formula as below:

$$\frac{(Cpm\,cells\ background)}{[(Cpm\,cells\ background) + (Cpm\,S/N\ background)]} \times ng\,of\ ^{14}C\text{ - TKI added}$$

The OCT-1 inhibitor prazosin was added at 100 µM in the media and incubated with cells for 2 hours. The OCT-1 activity was calculated as the difference between the IUR values with or without prazosin. In IUR assays with primary patient material, the

OA was scored as 0 ng/200,000 cells when IUR values in the presence of prazosin were equal or higher than the values in the absence of prazosin.

2.6.2.   Western blot for phosphorylated Crkl (p-Crkl) and IC50

Western blot assays for p-Crkl were performed as previously described (64). Briefly, 2×10^5 BCR-ABL positive cells were incubated for 2 hours at 37°C with concentrations of imatinib ranging from 0 µM to 200 µM in 60-mL polypropylene tubes. Following incubation, cells were washed once with cold phosphate-buffered saline (PBS) and pelleted by centrifugation for 5 minutes at 6,500 rpm. Then cells were placed into a 1.5 mL tube and lysed in 20 µL of Laemmli's buffer by boiling for 12 minutes. Lysates were clarified by centrifugation and stored at –20°C. Cell lysates were resolved on a 12% sodium dodecyl sulphate-polyacrylamide (SDS-PAGE) gel and the protein was electrophoretically transferred to a polyvinylidenefluoride (PVDF) membrane (GE Healthcare, Pittsburgh, America). Following 1 hour blocking at room temperature with 1% membrane blocking agent (Roche, Sydney, NSW, Australia), the membrane was probed for 2 hours at room temperature   with 1:500 anti-Crkl antibody (Santa Cruz Biotechnology, Santa Cruz, America) in 2.5% membrane blocking solution. The membrane was rinsed twice in 1xTBST buffer, and then washed 3x5 minutes with 1xTBST buffer. The membrane was then incubated with 1:2000 goat anti-rabbit IgG secondary antibody (alkaline-phosphatase conjugated) (Santa Cruz Biotechnology, Santa Cruz, America) in 2.5% blocking solution for 1 hour at room temperature. The membrane was then rinsed twice in 1xTBST buffer, washed 3x5 minutes in 1xTBST buffer and then 2x5 minutes in 1xTBS buffer. Bound antibodies were detected with ECF substrate (GE Healthcare, Pittsburgh, America) by Typhoon FLA 9000 FluorImager (GE Healthcare, Pittsburgh, America). Non-phophorylated and phosphorylated Crkl bands were then quantified using ImageQuant software 5.2 (Molecular Dynamics Inc., Sunnyvale, America) and phosphorylated Crkl (p-Crkl) was

determined as a % of the total Crkl protein. IC50 values were determined as the dose of drug required to reduce levels of p-Crkl by 50%.

2.6.3. Real time quantitative PCR (RQ-PCR)

2.6.3.1. RNA extraction

$1x10^6$-$1x10^7$ cells were pelleted in an RNase-free polypropylene centrifuge tube and membranes disrupted in 1 mL of Trizol reagent. The tube containing the homogenate was incubated at room temperature for 5 min. A 200 µL aliquot of chloroform was added to the tube containing the homogenate. The tube was then shaken vigorously for 15 seconds and incubated at room temperature for 2-3 minutes. Then the tubes were centrifuged at 12,000g for 15 minutes at 4°C. The upper aqueous phase was transferred to a new collection tube and mixed thoroughly with approximately 1.5 volumes (usually 750 µL) of 100% ethanol by pipetting several times. The sample, including any precipitate that may have formed, was pipetted into an RNeasy Mini spin column in a 2 mL collection tube (supplied with the RNeasy Mini kit, QIAGEN, Venlo, Netherlands). The spin column together with the collection tube were centrifuged at ≥8000 x g (≥10,000 rpm) for 15 seconds at room temperature. The flow-through was discarded. A 700 µL aliquot of buffer RWT was added to the RNeasy Mini spin column. The spin column together with the collection tube were centrifuged at ≥8000 x g (≥10,000 rpm) for 15 seconds at room temperature and the flow-through was discarded. The spin column together with the collection tube was washed twice by 500 µL buffer RPE by centrifugation and the flow-through was discarded. The RNeasy Mini spin column membrane was dried by another centrifugation at ≥8000 x g (≥10,000 rpm) for 2 minutes at room temperature. The RNeasy Mini spin column was transferred to a new 1.5 mL collection tube. Approximately 30–50 µL RNase-free water was added directly onto the RNeasy Mini spin column membrane. The spin column together with the collection tube were

centrifuged for 1 minute at ≥8000 x g (≥10,000 rpm) to elute the RNA. RNA was quantified using a NanoDrop Spectrophotometer (Thermo scientific, Melbourne, Australia) and samples were stored at -70°C for later use.

2.6.3.2. cDNA synthesis

Template RNA was thawed on ice. gDNA Wipeout Buffer, quantiscript Reverse transcriptase, quantiscript RT Buffer, RT Primer Mix, and RNase-free water (supplied with the QuantiTect Rev. Transcription Kit, QIAGEN, Venlo, Netherlands) were thawed on bench at room temperature. The genomic DNA elimination reaction was prepared on ice as indicated in Table 2.3.

Table 2.3   Genomic DNA elimination reaction components

Component	Volume/reaction
gDNA Wipeout Buffer, 7x	2 µL
Template RNA	Variable (up to 1 µg)
RNase-free water	Variable
Total volume	14 µL

The Genomic DNA elimination reaction was incubated for 2 minutes at 42°C and immediately placed on ice.   The reverse-transcription master mix was prepared on ice as described in Table 2.4.

Table 2.4   Reverse-transcription reaction components

Component	Volume/reaction (µL)
Quantiscript Reverse Transcriptase	1
Quantiscript RT Buffer, 5x	4
RT Primer Mix	1
Total volume	6

The reverse-transcription master mix (6 µL) was pipetted into each tube containing template RNA from the entire genomic DNA elimination reaction (total volume was 20 µL). The sample was then mixed and incubated for 15 minutes at 42°C, followed by 3 minutes at 95°C to inactivate Quantiscript Reverse Transcriptase. A 20 µL aliquot of RNase-free water was further added to dilute the cDNA and the cNDA was stored at -20°C for later use.

2.6.3.3. RQ-PCR for mRNA expression

RQ-PCR for target genes mRNA expression was performed using the SYBR Green ROX mix (2 x concentrated) (Qiagen, Venlo, Netherlands). Primers (see Supplementary Table 1) were diluted to a working stock of 100 ng/µL in DEPC water.

For each primer set to be tested PCR master mix was prepared fresh as indicated in Table 2.5.

Table 2.5   Preparation of PCR Master Mix

Reagent	per sample (µL)
SYBR Green ROX mix 2x	5
Forward primer 100 ng/µL	0.5
Reverse primer 100 ng/µL	0.5
DEPC water	2

An 8 µL aliquot of appropriate Master Mix was added to 0.1 mL PCR tube (Corbett Life Science, Mortlake, Australia) in cold rack. One microliter of RankL standard cDNA was added to RANKL tubes. Two microlitres DEPC water or cell line cDNA were added to the allocated tubes. All samples were run in triplicate. The PCR tubes were then loaded into a 72 well Rotor-Gene 6000 PCR cycler machine (Corbett Research, Cambridgeshire, UK) with the following profile settings:

Hold 1 @ 50°C, 2 minutes

Hold 2 @ 95°C, 15 minutes

Cycling (40 repeats)

Step 1 @ 95°C, hold 15 seconds

Step 2 @ 60°C, hold 26 seconds

Step 3 @ 72°C, hold 10 seconds, acquiring to Cycling A (Sybr)

Hold 3 @ 72°C, 30 seconds

Melt: Ramp from 72°C – 99°C, increasing by 1°C each step. Wait for 15 seconds on first step, then 5 seconds for each step afterwards

After completion of the run, results were analysed using the Rotor-Gene 6000 series software 1.7 (Corbett Life Science, Mortlake, Australia) and a standard curve previously generated was used for analysis each time. The expression of target genes was calculated as a percentage of reference gene expression.

2.6.4. Gene expression profiling analysis

The Affymetrix GeneChip® Human gene 1.0 ST array was performed at Adelaide Microarray Facility. RNA samples from cells were prepared using a miRNeasy Mini kit from QIAGEN (as described in Section 2.6.3). The array data was normalised with robust multichip array (RMA) as implemented in the Aroma.Affymetrix package. The quality control was assessed using NUSE plot as implemented in the Aroma.Affymetrix package. The analysis was performed using R statistical software. The heat maps were created using Hierarchical Clustering (HCL) by Multiple Experiment Viewer 4.8 to reflect gene expression values in different conditions. A fold change (FC) greater than 1.5 (log base 2 of 1.5=0.59) was used as a criterion for selecting genes of interest. The linear model for microarray analysis (LIMMA) package was used to generate the *p*-value from the moderated t-stats. Genes with FC>1.5 and *p*-value<0.05 were considered genes of interest. The Chromatin-immunoprecipitation sequencing studies were analysed by ChEA (ChIP

Enrichment Analysis) (153) which is a web-based interactive application to identify transcription factors of interest direct target genes within that enriched in gene-sets/potential candidate genes.

2.6.5. *Enzyme immunoassays for prostaglandin E2 (PGE2)*

ELISA assays for PGE2 plasma levels were performed using the PGE2 EIA kit (R&D Systems, Minneapolis, America). In brief, plasma was collected from *de novo* CML PB samples or healthy donor PB samples, using EDTA as an anticoagulant, by centrifugation for 15 minutes at 1000 x g and was stored at -70°C. When conducting the assay, plasma samples were thawed to room temperature and a 2-fold dilution was performed with the Calibrator Diluent RD5-39 (provided with the PGE2 EIA kit). PGE2 standard (ranging from 39 to 2,500 pg/mL), wash buffer and substrate solution were prepared following the manufacturer's instructions and warmed to room temperature.

A 100 µL aliquot of standard or samples was dispensed into each well on the 96-well PGE2 assay plate provided in the kit. Calibrator Diluent RD5-39 was added into the zero standard wells and non-specific binding (NSB) wells. A 50 µL aliquot of primary antibody solution was added into each well except NSB wells. The plate was covered with the adhesive strip provided and incubated for 1 hour at room temperature on a horizontal orbital microplate shaker (IKA Labortecknik, Staufen, Germany) at 500 rpm. The PGE2 conjugate (50 µL) was then dispensed into each well. The plate was sealed and incubated for another 2 hours at room temperature on the shaker. After incubation, each well on the plate was washed 3 times with 400 µL wash buffer. A 200 µL aliquot of substrate solution was then added to all wells and the plate was incubated in darkness for 30 minutes at room temperature. After incubation, 50 µL stop solution was added and the absorbance was read on a spectrophotometer

(Bio-Tec Instruments Inc., Burlington, America) within 30 minutes at 450 nm with a reference wavelength of 540 nm.

2.6.6. Enzyme immunoassays for 15-deoxy-Δ12,14-PGJ2 (15d-PGJ2)

The ELISA assay for 15d-PGJ2 plasma levels were performed using the 15d-PGJ2 EIA kit (ENZO Life Sciences, Farmingdale, America). Plasma was prepared as described in Section 2.6.5. Before the assay, plasma samples were thawed to room temperature and a 2-fold dilution were performed with assay buffer (provided with the PGE2 EIA kit). The 15d-PGJ2 standard (range from 195 to 200,000 pg/mL), wash solution and 15d-PGJ2 conjugate were prepared following the manufacturer's instructions and warmed to room temperature.

A 100 µL aliquot of standard or samples was added to allocated wells on the 96-well assay plate provided with the kit. A 100 µL aliquot of assay buffer was dispensed into the NSB and zero standard wells. Primary antibody solution and blue conjugate was then added to wells, except the total activity (TA) and blank wells. The plate was covered with an adhesive strip and incubated for 2 hours at room temperature on a horizontal orbital microplate shaker (IKA Labortecknik, Staufen, Germany) at 500 rpm. After incubation, each well on the plate was washed 4 times with 300 µL wash solution. A 5 µL aliquot light blue conjugate (1:10 dilution) was added to the TA wells. After the addition of 200 uL pNpp Substrate Solution to each well, the plate was incubated in darkness for 30 minutes at 37ºC. Fifty microlitres of stop solution was added after incubation and the absorbance was read on a spectrophotometer (Bio-Tec Instruments Inc., Burlington, America) within 30 minutes at 405 nm with a reference wavelength of 570 nm.

2.6.7. *Western blotting for protein of interests*

2.6.7.1. *Lysate preparation with modified RIPA Lysis Buffer*

Approximately 2×10^6 cells were washed once with cold PBS and pelleted by centrifugation for 5 minutes at 6,500 rpm. Then cells were placed into a 1.5 mL microcentrifuge tube and lysed in 40 µL of ice-cold modified RIPA lysis buffer by incubating on ice for 30 minutes. The precipitate was pelleted in a microcentrifuge at full speed for 10 minutes. The supernatant was gently transferred into a fresh tube kept on ice. A Bradford protein assay was carried out to determine protein concentrations (described in Section 2.5.1). The protein concentration was calculated from the standard curve (generated from absorbance readings of the BSA standards). The 2x SDS load buffer was added to lysate at 1x concentration and boiled for 5 minutes at 95°C. The lysate was stored at -20°C and boiled for 4 minutes before use.

2.6.7.2. *Western blotting*

Cell lysates were resolved on a 10% SDS-PAGE gel and the protein was electrophoretically transferred to PVDF. Following 1 hour blocking at room temperature with 5% blocking agent, the membrane was probed for primary antibodies at 4°C overnight. The primary antibodies were prepared as per Table 2.6 for each antibody to be tested.

Table 2.6   Primary antibodies for western blot

antibody	source	molecular weight (kDa)	buffer	dilution
β-actin	rabbit	43	5% skim milk	1:1000
Lamin B1	rabbit	68	5% BSA	1:1000
PPARγ	rabbit	54, 57	5% skim milk	1:1000
GAPDH	rabbit	37	5% BSA	1:1000

After incubation, the membrane was rinsed, incubated with secondary antibody and scanned as described in Section 2.6.2. Protein bands were analysed using ImageQuant TL 1D software version 7.0 (GE Healthcare, Pittsburgh, America) with GAPDH as loading control bands to quantify the protein amounts in each lane.

2.6.8. *Preparation of nuclear extract and cytoplasmic fraction*

The buffers were prepared immediately before use with the reagents provided in the Nuclear Extraction Kit (Active Motif, Carlsbad, America) as described in Table 2.7. The volume of the reagents was adjusted accordingly as the cell number varied. Buffers and tubes needed were placed on ice before beginning assay.

An aliquot of 2×10^7 cells was collected and washed with 16.0 mL ice-cold PBS/Phosphatase Inhibitors. The cells were pelleted by centrifugation for 5 minutes at 500 rpm in a centrifuge pre-cooled at $4^{\circ}C$. The supernatant was discarded and the cell pellet was gently resuspended in 1.0 mL 1X Hypotonic buffer. The suspension was

Table 2.7 Buffers and reagents for nuclear extract preparation

Reagents to Prepare	Components	2×10^7 cells
PBS/Phosphatase Inhibitors	Distilled water	13.6 mL
	10 x PBS	1.6 mL
	Phosphatase inhibitors	0.8 mL
1X Hypotonic Buffer	Distilled water	0.9 mL
	10X Hypotonic Buffer	100.0 µL
Complete Lysis Buffer	Lysis Buffer AM1	89.0 µL
	10 mM DTT	10.0 µL
	Protease Inhibitor Cocktail	1.0 µL

transferred to a pre-chilled 1.7-mL microcentrifuge tube and incubated for 15 minutes on ice. Approximately 25 µL Detergent was added and the tube was vortexed thoroughly for 10 seconds at highest setting. The precipitate was pelleted for 30

seconds at 14,000 x g in a microcentrifuge pre-cooled at 4ºC. The supernatant (cytoplasmic fraction) was carefully removed and transferred into a new pre-chilled microcentrifuge tube. The nuclear pellet was resuspended in 50 µL Complete Lysis Buffer by pipetting up and down and the tube was vortexed thoroughly for 10 seconds at highest setting. The suspension was incubated for 30 minutes on ice on a rocking platform set at 150 rpm. The tube was vortexed for 30 seconds at highest setting after the incubation and the precipitate was pelleted for 10 minutes at 14,000 x g in a microcentrifuge pre-cooled at 4ºC. The supernatant (nuclear fraction) was transferred into a pre-chilled microcentrifuge tube. A Bradford protein assay was carried out (as described in Section 2.5.1) before the nuclear extraction and the cytoplasmic fraction was stored at –80ºC.

2.6.9. *Peroxisome proliferator agonist receptor γ transcription factor assay*

The buffers were prepared immediately before use with the reagents provided in the Peroxisome Proliferator Agonist Receptor γ (PPARγ) Transcription Factor Assay Kit (Active Motif, Carlsbad, America) as described in Table 2.8.

Table 2.8   Buffers and reagents for PPARγ Transcription Factor Assay

Reagents to prepare	Components	For 96 wells
Complete Lysis Buffer	DTT (1M)	1.2 µL
	Protease Inhibitor Cocktail	10.8 µL
	Lysis Buffer AM1	1.068 mL
Complete Binding Buffer	Herring sperm DNA	43.2 µL
	Binding Buffer AM6	4.277 mL
1x Wash Buffer	Distilled water	194.4 mL
	10X Wash Buffer AM2	21.6 mL
1x Antibody Binding Buffer	Distilled water	19.44 mL
	10X Ab Binding Buffer AM2	2.16 mL

A 40 μL aliquot of complete binding buffer was dispensed into each well on the 96-well PPARγ assay plate provided in the kit. For positive control wells, 5 μg of the provided nuclear extract diluted in 10 μL of complete lysis buffer was added while 10 μL complete lysis buffer was added into the blank wells. Five microgram nuclear extraction samples diluted in 10 μL complete lysis buffer were then added in to the sample wells. The plate was sealed with the provided adhesive cover and incubated for 1 hour at room temperature with mild agitation (100 rpm on a rocking platform). After incubation, each well on the plate was washed 3 times with 200 μL 1x wash buffer. A 100 μL aliquot of diluted PPARγ antibody (1:1000 dilution in 1x antibody binding buffer) was then added to all wells being used. The plate was sealed and incubated for 1 hour at room temperature without agitation, followed by washing 3 times with 200 μL 1x wash buffer. After washes, 100 μL diluted anti-mouse HRP-conjugated antibody (1:1000 dilution in 1x antibody binding buffer) was added and the plate was incubated for 1 hour at room temperature without agitation, followed by washing 4 times with 200 μL 1x wash buffer. Then 100 μL developing solution (warmed to room temperature before use) was dispensed into all wells being used and the plate was incubated for 5-10 minutes at room temperature protected from direct light. A 100 μL aliquot of stop solution was added and the absorbance was read on a spectrophotometer (Bio-Tec Instruments Inc., Burlington, America) within 5 minutes at 450 nm with a reference wavelength of 655 nm.

2.6.10. CD14$^+$ and CD15$^+$ cells isolation

2.6.10.1. Isolation of leukocytes from red blood cell layer

After removing MNC from the 60-mL polypropylene tube (as described in Section 2.5.6), a thin layer of leukocytes in between the lymphoprep and the red blood cells pellets was collected with a sterile pasteur pipette. To lyse the red cells, no more than

20 mL of sample was poured into a 60-mL polypropylene tube. The volume was brought to 50 mL using red cell lysis buffer. Following mix on rolling-mixer for 10 mins, the leukocytes were pelleted at 3000 g for 10 mins. The supernatant containing lysed red cells were carefully aspirated. The pellet was then resuspended in HBSS+Hepes buffer followed by a white cell count.

2.6.10.2. Magnetic cell sorting (MACS)

Approximately 1 x 10^7 MNC were suspended in 80 µL MACS buffer together with 20 µL CD14$^+$ MicroBeads to magnetically label the cells. CD15$^+$ MicroBeads were used to magnetically label the leukocyte from red blood cell layer. The suspension was incubated at 4°C for up to 30 minutes. After incubation, cells were washed with 2 mL MACS buffer and resuspended in 500 µL MACS buffer. The suspension was passed through yellow pre-separation filters into an ice-cold 15-mL polycarbonate tube on ice. The sample tubes together with empty 15-mL polycarbonate tubes (for negative fraction) and empty 10-mL polypropylene collection tubes were loaded in pre-cooled tube rack. The tube rack along with running buffer and wash buffer were placed in AutoMACS pro machine (Miltenyi Biotec GmbH, Bergisch Gladbach, Germany) and a positive selection was performed. A white cell count in white cell fluid and a cell viability calculation with trypan blue solution was performed after the separation.

2.6.10.3. Preparation of aliquots of CD14$^+$ and CD15$^+$ cells for further analysis

After Magnetic separation, aliquots of cell suspension were processed for different assays as follows:

- 3×10^4 cells in 100 µL HBSS for morphological evaluation (described in Section 2.6.10.4).

- 2×10^5-3x10^5 cells in 200 µL HBSS for immunofluorescent evaluation (described in Section 2.6.10.5).

- 2×10^7 cells in ice-cold PBS for PPARγ activity assay (described in Section 2.6.9).

2.6.10.4. *Morphological evaluation*

Samples for Morphological evaluation were prepared by suspending 3×10^4 cells in 100 µL HBSS. The labelled microscope slides, together with a two-hole filter card and a sample chamber, were placed into appropriate slots in the cytospin. Cell suspension was then loaded in each sample chamber and spun at 800 rpm for 5 minutes. The filter card and the sample chamber were gently removed from microscope slides without damaging the fresh cytospin. Each slide was examined under the microscope to be sure that the cells had adhered properly. The slides were placed in a laminar flow cabinet overnight and Wright's staining was conducted within two days.

2.6.10.5. *Flow cytometric analysis of surface markers expression*

Approximately 1×10^5 cells (for isotype control) or 2×10^5-3×10^5 cells (for experimental samples) were transferred to 5 mL round-bottom polypropylene tubes and suspended in approximately 500 µL of HBSS. Phycoerythrin (PE) or Fluorescein isothiocyanate (FITC) conjugated antibodies were added to tubes as indicated in Table 2.9.

The cells were incubated for a period of 40 minutes on ice in the dark. Cells were then washed twice with HBSS and re-suspended in 200 µL cold FACS fixative. Samples were protected from light and refrigerated until analysis on a Cytomics FC 500 Series flow cytometer (Beckman Coulter, Fullerton, America). Control tubes stained with isotype control were used to define the gates for positive and negative expression. Cell populations were analysed based on their forward and side light scattering properties (indicating cell size and granularity, respectively) and the fluorescence intensity of PE or FITC fluorochromes. The fluorescence intensity was examined using FCS express version 4 software (De Novo Software, Los Angeles, America).

Table 2.9   Volumes and conditions for MACS staining

Antibody	Volume	Specificity
IgG2bκ PE	5 µL (for 1×10^5 cells)	Isotype control
IgM FITC	5 µL (for 1×10^5 cells)	Isotype control
CD11b PE	20 µL (for up to 1×10^6 cells)	activated lymphocytes, monocytes, granulocytes and NK cells
CD14 PE	20 µL (for up to 1×10^6 cells)	strongly expressed on most monocytes and macrophages and weakly on neutrophils and some myeloid dendritic cells
CD15 FITC	20 µL (for up to 1×10^6 cells)	neutrophils, eosinophils, and monoblastoid precursor cells of the myeloid lineage but not on basophils and lymphocytes

2.7.   Statistics

Figures were generated using GraphPad Prism 5.01 © software (GraphPad Software Inc. San Diego, USA). All statistical analyses were performed using GraphPad Prism 5.01 © software (GraphPad Software Inc. San Diego, USA). Normality tests were performed using a Kolmogorov-Smirnov test. The Mann-Whitney Rank Sum or the Student's t-test was used to determine differences between experimental groups. Where the data sets passed the normality and equal variance tests a Student's t-test was applied to determine statistical differences between experimental groups. Where the data failed the normality and equal variance tests a Mann-Whitney Rank Sum was used. Correlations were performed using the Pearson Product Moment or Spearman Rank Order as appropriate, depending on the data distribution. Differences were deemed statistically significant when probability value (*p*-value) was less than 0.05.

CHAPTER III
Identification and Validation of OCT-1 Activity Enhancers by Bioinformatics and Experimental Approaches

3.1.   Introduction

Imatinib mesylate is currently used as first-line treatment for chronic phase chronic myeloid leukaemia (CP-CML) (57, 61, 154). The human organic cation transporter-1 (OCT-1) has been identified as the major transporter responsible for imatinib uptake in CML cells (130). A functional assay was developed to assess the amount of active imatinib uptake by using the potent OCT-1 inhibitor prazosin to measure the OCT-1 functional activity (OA) in mononuclear cells (MNC) from untreated *de novo* CP-CML patients (65). OA is significantly associated with imatinib-mediated *in vitro* tyrosine kinase inhibition (64). A significant correlation was observed between OA and the molecular response to imatinib treatment at both 24 months (65) and at 5 years (140). Thus, the functional activity of the OCT-1 protein is a strong predictor of imatinib response in *de novo* CML patients.

It has been demonstrated that in some patients the negative impact of a low OA may be partially overcome by escalating imatinib dosage where tolerated (155). In a phase 2 study, all adult patients with newly diagnosed CML commenced imatinib at 600 mg per day. The dose was increased to 800 mg/d if a patient failed to achieve any of the following landmarkers: CHR by 3 months; MCyR by 6 months; CCyR by 9 months; or 4-log reduction in BCR-ABL compared with standardized baseline by 12 months. The results showed that patients with high OA achieved excellent molecular response regardless of dose, whereas the response of patients with low OA was highly dose dependent. In the high OA cohort, no significant difference in molecular response was observed between the patients who received increased dose of imatinib (from 600 mg to 800 mg per day) and the patients who failed to dose increase. In contrast, patients with a low OA performed equally well as those patients with high activity when they are dose increased to 800 mg/day. Those with low OA who did not dose increase had

significantly inferior molecular responses at 24 months (156). However, clinical experience has demonstrated that increasing imatinib dose is related to higher rates of adverse events and may lead to dosage interruptions or cessation (157). This increasing imatinib dosage may only benefit the approximately 60% of patients who are able to tolerate this increased regimen without unacceptable toxicity (155). Second generation TKI's (nilotinib and dasatinib), which are not substrates of OCT-1 (130, 158), may provide a therapeutic alternative for patients with low OA. However, imatinib has an excellent long-term safety profile. In addition, there will be significant cost advantage of using imatinib with the generic version entering the clinic after the expiration of the current patent. Therefore, it would be of great clinical value to develop a therapeutic intervention to allow those patients to continue on safe dose of imatinib treatment.

Several commonly prescribed drugs have been identified as substrates or inhibitors of OCT-1, thus, the contribution of OCT-1 to drug-drug interactions (DDI) has been reported recently in several pharmacokinetic studies (159, 160). Most of these studies used cell lines stably expressing OCT-1, with 1-methyl-4-phenylpyridinium (MPP$^+$) and metformin as test compounds. In MDCKII-OCT-1 cells, OCT-1 mediated MPP$^+$ and metformin uptake were inhibited by oral anti-diabetic drugs, rosiglitazone and repaglinide (161). Antiretroviral drugs for HIV treatment and cardiovascular drugs have been found to inhibit OCT-1 mediated MPP$^+$ uptake in transformed HEK293 cells expressing OCT-1 and in primary hepatocytes (162, 163). Although there is accumulating evidence regarding OCT-1 mediated DDI, few studies have investigated the effect of DDI on imatinib uptake via OCT-1. Minematsu *et al.* (164) reported the selective and potent inhibitory effect of imatinib on ^{14}C-metformin uptake using HEK293 cells stably expressing OCT-1. However, the DDI involving imatinib and OCT-1 in CML cells has not been fully assessed to date.

Non-steroidal anti-inflammatory drugs (NSAIDs) are a class of structurally diverse drugs which effectively inhibit cyclooxygenases (COX), also known as prostaglandin-endoperoxide synthases (PTGS) (165). NSAIDs are commonly used for treatment of arthritic conditions and different types and severities of inflammation. There has been abundant evidence of DDI between NSAIDs and other co-administrated drugs, which may prolong the drug plasma elimination and lead to various side effects such as liver damage (166), kidney dysfunction (167), and aggravation of cardiovascular diseases (168). Recently, several studies suggested that the transporter responsible for the renal uptake and secretion for NSAIDs is the human organic anion transporter-1 (OAT-1) (169-171). At clinically relevant concentrations, NSAIDs efficiently inhibit hOAT-1 mediated transport of adefovir in a cell line stably expressing hOAT-1 (172). Although it has been reported that NSAIDs are not substrates of OCT transporters (173), NSAIDs such as diclofenac, ibuprofen, indomethacin and sulindac have been demonstrated to significantly inhibit OCT-1 mediated TEA uptake at the concentration of 0.5 mM in transfected Schneider 2 cells expressing hOCT-1 (173). Since about one-quarter to one-half of CML patients on imatinib develop musculoskeletal complaints (muscle cramps, myalgia, arthralgia) which are often managed with NSAIDs (154), it is of particular relevance to investigate the effect of NSAIDs on imatinib uptake. In addition to NSAIDs, several other drugs (i.e., amiloride hydrochloride, atrovastatin, simvastatin, domperidone, frusemide) with a relatively negligible toxicity profile are commonly used by CML patients. Determining whether these drugs may interfere with active imatinib influx in BCR-ABL-positive cells is potentially of significant value for clinical practice.

The rich resource of microarray datasets that have been available for public access had made it possible to use these gene expression profiles to identify drugs that are associated with gene expression. For instance, the Connectivity Map (CMAP) (174,

175) is a collection of genome-wide transcriptional profiling data from cultured human tumour cells (AML-HL60, prostate cancer-PC3, breast cancer-MCF7, and melanoma-SKMEL5) treated with small molecules. It has been widely used to identify potential drugs for targeted cancer therapies (176-179). The CMAP links human disease phenotype with drugs via comparison of gene expression profiles with a large bank of drug expression profiling experiments, facilitating prediction of links between drugs and expression. 1309 compounds have been arrayed in the latest public CMAP release (Build 2), which makes CMAP a powerful tool for predicting DDI that can be tested with experimental approaches (179). Successful experiences of using this application include identification of specific compounds as potential treatment for acute lymphoid leukaemia and solid tumours (176-178).

This chapter aims to identify potential OA enhancers by utilizing the CMAP (174). Systematic functional analysis including radio-labelled intracellular uptake and retention (IUR) assay, OA and IC50^{imatinib} assays were performed to investigate the use of pharmacological intervention to induce higher levels of OA and therefore higher levels of kinase inhibition in leukemic cells.

3.2. Methods

3.2.1. Selection of candidate drugs as functional OA enhancers

Connectivity Map version 2 (http://www.broad.mit.edu/cmap) was used to explore the candidate compounds as functional OA enhancers. The imatinib influx transporter OCT-1 (*SLC22A1*) was defined as the key gene of interest for increased expression. As the CMAP requires input of up- and down-regulated probes, imatinib efflux transporter genes *ABCB1* and *ABCG2* (as described in Chapter 1) were selected as probes for which a decreased expression level was required. Small molecules or drugs with low toxicity selected from CMAP analysis were then prioritised for testing

as potent OA enhancers for further validation. To fully investigate the possible combination therapy strategy, 12 NSAIDs and 11 clinically applicable drugs (Table 3.1 and Table 3.2) with negligible toxicity profile were selected for this study. The effects on imatinib uptake via OCT-1 in CML cells of these compounds were then investigated using the IUR assay.

3.2.2. Drugs preparation

Imatinib mesylate, ^{14}C-imatinib, together with the OCT-1 inhibitor prazosin were prepared as described in Section 2.2. All the compounds were dissolved as per manufacturer's instructions. For those drugs dissolved in DMSO or ethanol, vehicle control was used and the final concentration of the solvents ranged from 0.14-0.25% (v/v). The concentrations of compounds used in this study were selected according to the concentrations reported to be the maximum plasma concentrations after therapeutic dosing. For those of which the optimal concentrations were unknown, the concentrations commonly chosen in high-throughput cell-based small-molecule screens were used (Table 3.1 and Table 3.2).

3.2.3. Validation of functional OA enhancer candidates

The IUR assay was performed over a 2-hour period, and was expressed as ng of imatinib per 200,000 cells (Section 2.6.1). The candidate OA enhancers and the potent inhibitor of OCT-1, prazosin were added to the IUR assay simultaneously with radio-labelled imatinib. The OA was determined by calculating the difference of the IUR with or without 100 μM prazosin. The IC50 assay was performed to further investigate the effects of OA enhancer candidates on the extent of BCR-ABL kinase activity inhibition (Section 2.6.2). The effects of OA enhancer candidates were determined by comparing the IC50 in the presence and absence of compounds in cell lines and primary patients' material. Trypan blue exclusion assays were conducted to

Table 3.1   NSAID agents selected in this study

Relative selectivity on COX	Compound	COX-2 selectivity IC50 COX-1/COX-2*	Concentration (µM)	Solvent
Non-specific	diflunisal	0.84	16	DMSO
	fenbufen	N/A	16	Ethanol
	fenoprofen	0.68	7	Ethanol
	flufenamic acid	N/A	8	Ethanol
COX-1 inhibitors	ibuprofen	0.22	145	Ethanol
	indomethacin	0.01	11	Ethanol
	naproxen	0.33	16	Ethanol
COX-2 inhibitors	diclofenac	2.33	10	Water
	celecoxib	6.36	10	DMSO
	rofecoxib	37.25	10	DMSO
	paracetamol	4.41	26	Water
	sulindac	1.66	11	Ethanol

For those drugs dissolved in DMSO or ethanol, the final concentration of the solvents ranged from 0.7-1.6‰ (v/v). *, data from Mitchell et al. 1993 and Hinz et al. 2008)

Table 3.2   Clinically applicable drugs selected in this study

Drug	Concentration used	Solvent
amiloride	13 uM	Water
Atrovastatin	200 nM	DMSO
Bupropion	14 uM	Water
Citalopram	1 uM	DMSO
Domperidone	7 uM	DMSO
Frusemide	12 uM	DMSO
Hydrochlorothiazide	13 uM	Ethanol
IFN-α	15 IU/ml	Water
Lansoprazole	11 uM	Ethanol
Pantoprazole	14.4 uM	Water
Simvastatin	10 uM	Ethanol

For those drugs dissolved in DMSO or ethanol, the final concentration of the solvents ranged from 0.02-1.3‰ (v/v).

assess the effects of OA enhancer candidates on the number of viable cells in the presence of imatinib for 72 hours (as indicated in Section 2.5.2). To assess the effect of candidates on OA in CML primary samples, MNC were isolated from the PB of CP-CML patients at diagnosis using lymphoprep density gradient separation (Section 2.5.6) and IUR assays were performed with either frozen or fresh CML MNCs.

3.3. Results

3.3.1. The Connectivity Map (CMAP) as a tool to select candidate drugs as functional OA enhancers

The Connectivity map (CMAP), together with its biomedical web-based application, have been described in Section3.2 as a tool for gene-drug connection analysis. CMAP (build 02) (http://www.broad.mit.edu/cmap) was used to identify compounds that were predicted to selectively increase expression of imatinib influx transporter OCT-1 (*SLC22A1*) and decrease imatinib efflux transporters *ABCB1* and *ABCG2.* The human Affymetrix HGU-133A probe-set IDs for these up- and down-regulated genes were then uploaded to the Connectivity Map version 2.

The query result output in CMAP consists of two parts, detailed result and permuted result. For the detailed result (Figure 3.1), the up and down scores represent the absolute enrichment of the up- and down-regulated probes in a given instance. A high positive score indicates that the corresponding compound induced the expression of the probes, while a high negative score indicates the repressed expression of the probes by the corresponding treatment. Each of the drug-treated instances was ranked by the connectivity score, which is a relative value generated with the Kolmogorov-Smirnov statistic by combining the up and down score of query probe sets (*SLC22A1, ABCB1* and *ABCG2*). As each compound is tested in several instants, in the permuted result CMAP subsequently determines the enrichment score of the

rank	batch	cmap name	dose	cell	score	up	down	istance_id
1	1086	IC-86621	1 µM	MCF7	1	0.982	-0.83	7513

1086 - IC-86621 1 µM MCF7

up tags

jump to down tags

probe_id	rank	score	amplitude
207201_s_at	398	0.982	0.62

down tags

jump to up tags

probe_id	rank	score	amplitude
209735_at	18488	-0.496	-0.24
209993_at	19807	-0.222	-0.34
209994_s_at	21177	0.05	-0.52
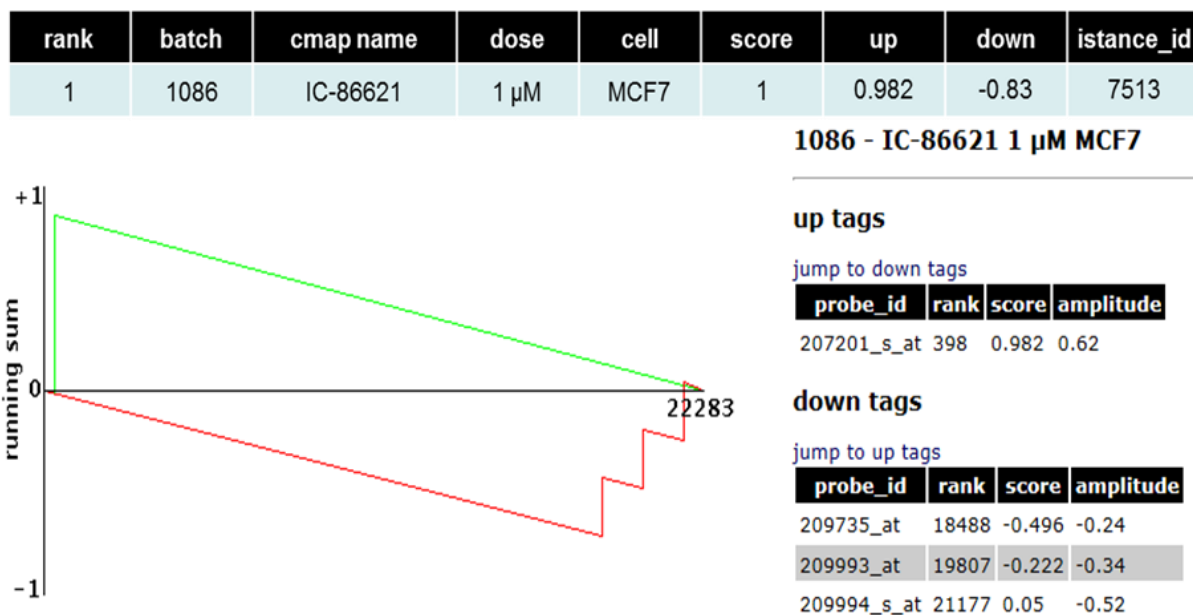
Figure 3.1   Detailed results for one instance in Connectivity Map

In detailed result the summary table displays the condition of each instance, the connectivity score, the up and down score. In the plots, up regulated genes and down regulated genes are represented by the green and red lines, respectively. The maximum deviation on the y-axis for each line defines the up score / down score, which is a function of the position of the query genes in the list of all probe sets in the feature set ordered by the extent of their differential expression in the selected instance, represented by the x-axis. The location of a gene is appreciated by an up-tick in the trajectory of the colored lines. Note that the up score and down score are absolute measures, unlike connectivity score, which is a relative value.

When MCF7 cells were treated with 1 µM IC-86621, the up tags (*SLC22A1*) are nearer the top of the rank ordered list of probe sets and the down tags (*ABCB1* and *ABCG2*) are nearer the bottom of the ordered list of probe sets. Correspondingly, the up score and down score for the signature in the instance represented is approximately +0.982 and -0.83, respectively. By combining the up and down score, the connectivity score for this instance is 1.

instance set for each compound, and a permutation *p*-value for that enrichment score is then determined using Kolmogorov-Smirnov test statistics (174). As the aim of this study is to increase imatinib uptake by via OCT-1, the absolute expression level of the up-tag gene (*SLC22A1*) was considered as a priority criteria for enhancer selection. Other criteria included positive connectivity score (in the detailed result), positive enrichment score for the instance set (in the permutated result), and the permutation *p*-value. Due to only 3 probes being used as input, a less stringent *p*-value ($p<0.1$) was used.

As shown in Figure 3.2A, there were 404 compounds with fold change of *SLC22A1* ranked in top 500 instances after removing repetitive compounds in the whole instance set. Twenty-five compounds were identified as being significantly associated with the *SLC22A1*, *ABCB1* and *ABCG2* signatures based on the criteria as described above ($p<0.1$, connectivity score mean>0 and enrichment score>0, Figure 3.2B). Table 3.3 shows all the 25 potential drugs or compounds ranked on *p*-value.

Among the 25 potential candidates from this CMAP analysis, 16 compounds were excluded due to either considerable toxicity or impracticability for clinical treatment. The remaining 8 compounds with less toxicity were selected for further validation. The CMAP interface provides a bar-plot and summary Table displaying enrichment of the user-provided gene-set to each of the drug profiles across 1309 compounds. Bar plots for each of the OA enhancer candidates are shown in Figure 3.3. Table 3.4 shows all the information of the drug preparation with the concentrations determined from the Connectivity Map.

Figure 3.2   Summary of Connectivity Map Compounds identified with different criteria to enhance OCT-1 activity

A: Flow chat shows the methods used to select potential OA enhancers from CMAP based on the positive connectivity score, permutation *p*-value<0.1 and positive enrichment score cut-off. **B:** Venn diagram showing compounds selected from Connectivity Map with different criteria. Among 404 compounds with fold change of *SLC22A1* ranked in top 500 instances, 25 compounds were identified when all the criteria applied.
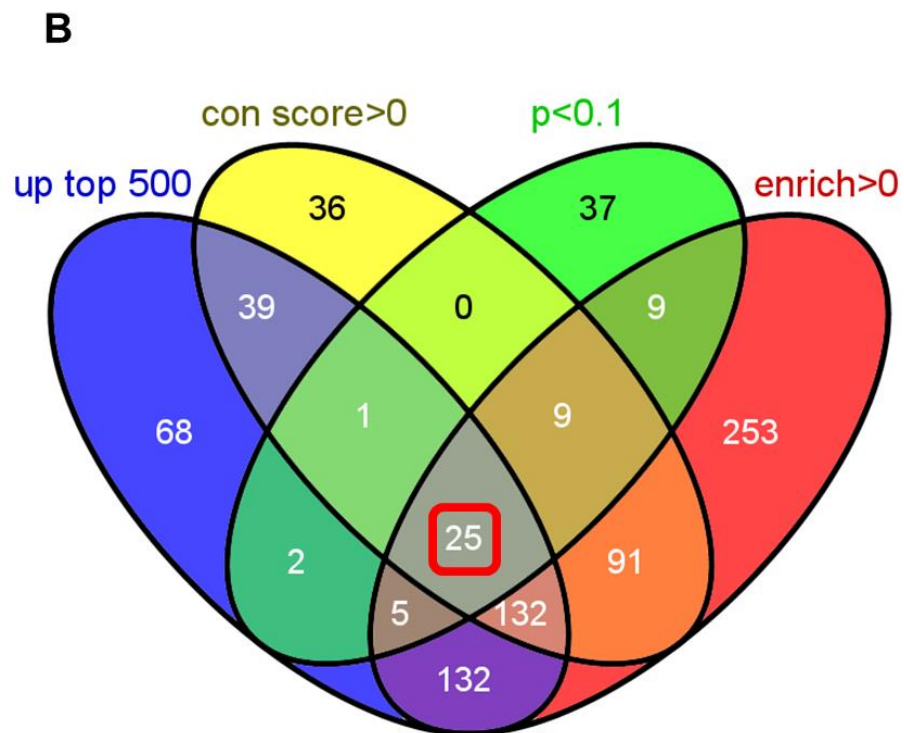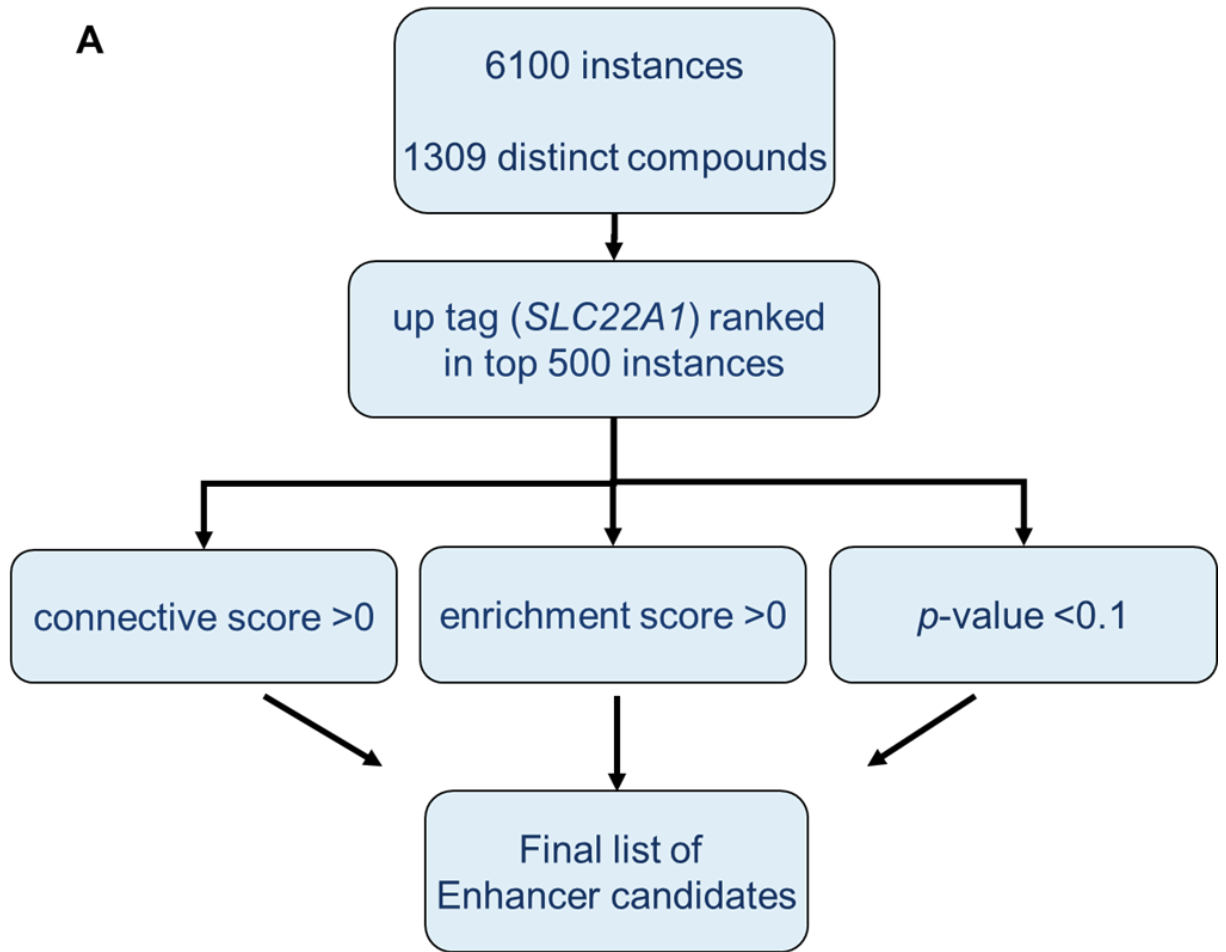
Table 3.3 Top 25 Connectivity Map compounds identified using an input signature weighted to OCT-1 as the primary up-regulated gene

rank	CMAP name	mean	enrichment	*p*-value
1	tracazolate	0.60	0.82	0.002
3	flunixin	0.53	0.74	0.003
4	benzthiazide	0.49	0.76	0.006
7	paromomycin	0.39	0.74	0.008
10	nadide	0.60	0.74	0.009
12	fluticasone	0.34	0.74	0.009
13	labetalol	0.36	0.74	0.009
17	iocetamic acid	0.58	0.72	0.013
19	sulfadimethoxine	0.55	0.65	0.014
23	gelsemine	0.42	0.70	0.018
30	procyclidine	0.58	0.68	0.025
31	IC-86621	0.63	0.67	0.025
33	difenidol	0.45	0.76	0.029
35	Prestwick-674	0.40	0.55	0.032
37	demeclocycline	0.34	0.54	0.037
45	etidronic acid	0.36	0.64	0.043
51	meclofenoxate	0.48	0.52	0.049
52	levcycloserine	0.31	0.62	0.050
61	PHA-00851261E	0.33	0.44	0.062
65	sulfametoxydiazine	0.48	0.61	0.063
66	suxibuzone	0.52	0.60	0.065
71	N-acetylmuramic acid	0.49	0.60	0.070
73	betonicine	0.48	0.49	0.078
76	PHA-00745360	0.21	0.42	0.081
87	etamsylate	0.32	0.57	0.094

Compounds or drugs were selected based on positive mean connectivity score and positive enrichment score cut-off and *p*-value<0.1. The compounds were ranked by p-value. Mean indicates the connectivity score for correlation with the query gene-expression (OCT-1 as up-regulated gene, ABCB1 and ABCG2 as down-regulated genes).
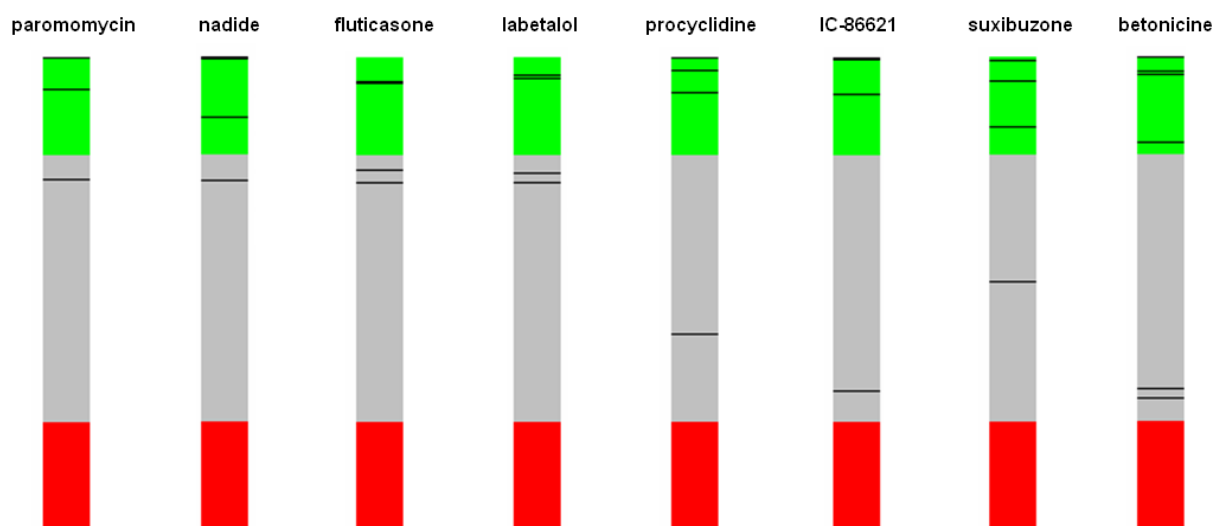
Figure 3.3   Bar plot for eight candidate drugs selected from Connectivity Map

After meeting all the selection criteria, 16 compounds were excluded due to either considerable toxicity or impracticability for clinical treatment. The remaining 8 compounds with less toxicity were selected for further validation. The bar-plot consists of three sections labelled by different colours (red - positive correlation to the input signature, grey – no correlation, and green - negative correlation). The black lines distributed in the bar-plot represented the enrichment of each compound associated with genes signature inquired.

Table 3.4   Candidate compounds selected from CMAP

Reagent	Concentration used (uM)	Solvents
Procyclidine	12	Ethanol
Fluticasone	8	DMSO
Paromomycin	6	Water
IC-86621	1	DMSO
Nadide	16	Water
Suxibuzone	9	Ethanol
Labetalol	11	Water
Betonicine	25	Ethanol

The concentration of each drug was determined from the Connectivity Map. For those drugs dissolved in DMSO or ethanol, the final concentration of the solvents ranged from 0.1-2.5‰ (v/v).

3.3.2. Experimental validation of OCT-1 enhancer candidates with IUR assay

As described in Section 3.2.1, 31 OA enhancer candidates were divided into three groups (Group I: 8 compounds selected from CMAP, Group II: 12 NSAIDs, Group III: 12 clinically applicable drugs with negligible toxicity profile). All the candidate drugs were prepared as per the manufacturer's instructions. Their effects on OA were determined using the IUR assay in BCR-ABL positive cells.

3.3.3. Effects of CMAP candidates on IUR and OA in K562 cell lines

The IUR of 2 µM imatinib and OA in K562 cells were determined with or without 8 CMAP compounds over a 2-hour period. As indicated in Figure 3.4A, the average of IUR in K562 cells was 24.7 ng/200,000 cells (range 19.1-28.2) and remained unchanged after 2-hour incubation with most of the CMAP candidates tested (7 out of 8). The IUR of imatinib in the presence of paromomycin was significantly increased to 28.4 ng/200,000 cells (range 25.1-29.7, p=0.005). The addition of prazosin reduced the IUR of imatinib in K562 cells to 13.8 ng/200,000 cells (range 10.7-17.8) and remained the same level after the treatment with all CMAP candidates (p>0.05). Assessment of OA revealed similar trends to IUR (Figure 3.4B), where the incubation of paromomycin resulted in the highest OA with a fold change of 1.32 compared with the untreated control (average OA increased from 10.5 to 13.4 ng/200,000 cells, p=0.019). No significant changes were observed in OA in K562 cells after the incubation of the other 7 CMAP candidates. Notably, as the genome-wide expression profiles in CMAP were generated using cell lines treated with small molecules for 6 hours (174, 175), pro-longed incubation (6 hours) was also applied to all CMAP candidate compounds. Similar results to the 2 hours experiments were observed in K562 cells where only paromomycin increased the IUR of imatinib and OCT-1.
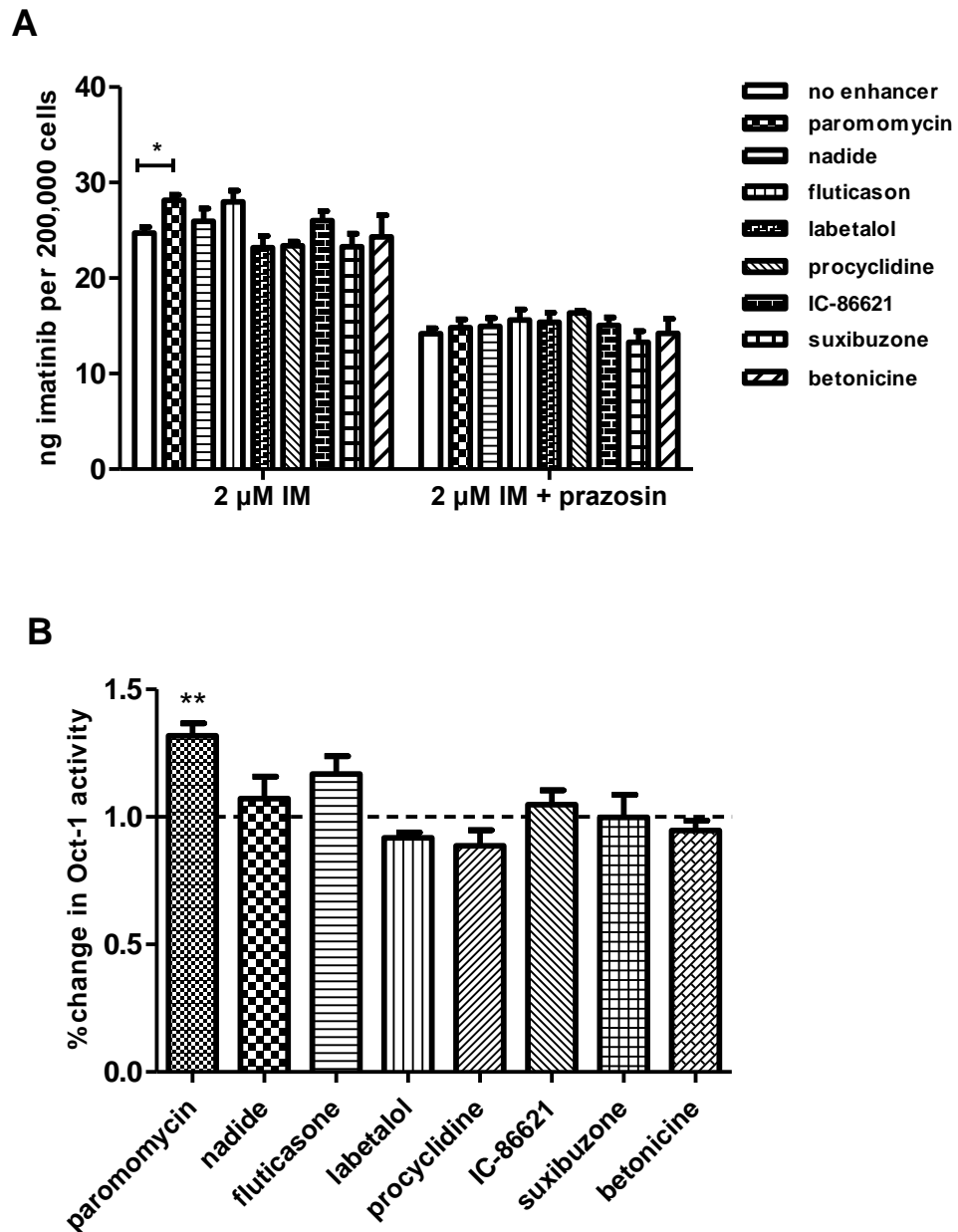
Figure 3.4 Intracellular uptake of imatinib and OCT-1 activity in K562 cells in the absence or presence of CMAP candidates

The IUR of 2 μM imatinib (**A**) and OCT-1 activity (**B**) in K562 cells was determined with or without 8 CMAP compounds over a 2-hour period. The error bars represent the standard deviation of the mean (n≥3). *, $p<0.05$; **, $p<0.001$

3.3.4. Effects of NSAIDs on IUR of imatinib and OA in K562 cell lines

These studies were recently published in British Journal of Cancer with myself as first author (180) and this paper is included as an Appendix. Briefly, the IUR of imatinib and OA in K562 cells were measured in the absence or presence of 12 NSAIDs over a 2-hour period. To determine whether these drugs have any common effect on IUR or OA, the NSAIDs were further divided into 3 groups (non-specific COX inhibitors, COX-1 inhibitors and COX-2 inhibitors) based on their specific inhibition towards COX. Diverse effects of the NSAIDs on IUR were observed, however, there was no consistent effect on IUR shared by drugs with a similar pharmacological profile. Although the majority of NSAIDs selected (9 of 12) failed to induce any significant change in IUR, the average IUR of imatinib in K562 cells increased from 25.7 ng/200,000 cells to 29.35 ng/200,000 cells after treatment with diclofenac (p=0.0123). Similar change was also observed when K562 cells were incubated with fenbufen (average IUR increased from 24.4 to 27.5 ng/200,000 cells, p=0.0306). Surprisingly, the average IUR dropped from 25.43 ng/200,000 cells to 18.57 ng/200,000 cells (p=0.0046) in the presence of ibuprofen. The addition of prazosin reduced the IUR to the same level for all the scenarios (average 13.6 ng/200,000 cells). Assessment of OA (Figure 3.5) revealed similar trends to IUR where a significant increase in OA was observed in K562 cells treated with either fenbufen (average OA increased from 10.8 to 12.9, average fold change of 1.33, p=0.006) or diclofenac (average OA increased from 11.4 to 14.2, average fold change of 1.27, p=0.007). In contrast, the OA was significantly reduced in the presence of ibuprofen (average OA increased from 11.95 to 5.63, 48% of vehicle control, p<0.001), which is in agreement with the IUR data.
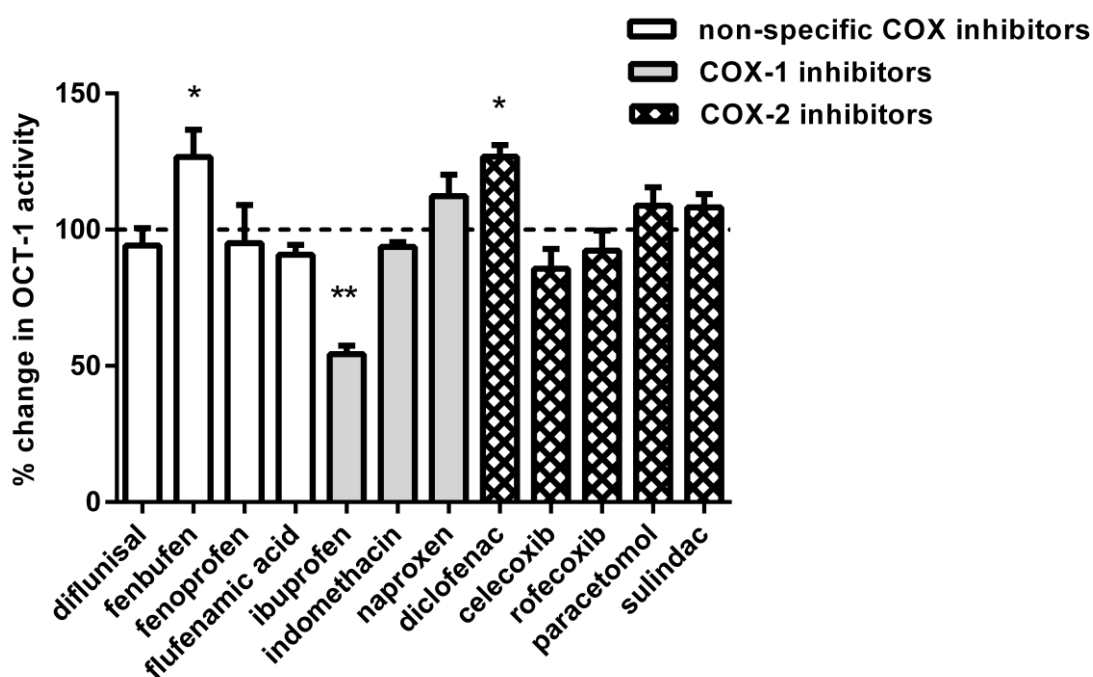
Figure 3.5   OCT-1 activity in K562 cells in the absence or presence of NSAIDs

OCT-1 activity in K562 cells was assessed with or without 12 NSAIDs over a 2-hour period. Results (mean±SEM) are expressed as percentage of own solvent control, which was set at a value of 100% (n≥3). *, $p<0.05$; **, $p<0.001$

3.3.5. Effects of clinically applicable drugs on IUR of imatinib and OA in K562 cell lines

The IUR of imatinib and OA in K562 cells were also assessed after 2 hours treatment with 11 clinically applicable drugs. Despite the variable pharmacological activity of these drugs, none of them showed any significant effect on the IUR in K562 cells (average 24.5 ng/200,000 cells, range 19.5-29.8, $p>0.05$). In the presence of prazosin the IUR of imatinib of K562 cells was decreased to a similar level (average 14.0 ng/200,000 cells, range 12.6-15.7). Thus, the OA for K562 cells treated with 11 drugs remained unchanged compared with un-treated cells ($p>0.05$, Figure 3.6).

3.3.6. Effects of clinically applicable drugs on IUR and OA in KU812 cell lines

To examine whether the effects of the OA regulators were consistent in other CML cell lines, the IUR of imatinib and OA were assessed in KU812 cells in the presence or absence of paromomycin, diclofenac, fenbufen and ibuprofen. The average imatinib IUR in KU812 cells was 26.2 ng/200,000 cells (range 18.3-30.37) which was reduced to 15.9 ng/200,000 cells (range 12.0-18.51) in the presence of prazosin (Figure 3.7A). The KU812 cells displayed a similar OA value to that of the K562 cells (average 10.34, range 5.2-14.8). Consistent with the result observed in K562 cells, the IUR of imatinib in KU812 cells was significantly increased after treatment with diclofenac (29.8 ng/200,000 cells, range 20.0-38.1, $p<0.0001$) and decreased to 20.0 ng/200,000 cells (range 13.8-23.9, $p<0.0001$) in the presence of ibuprofen. However, unlike in K562 cells, no significant changes of IUR were observed in KU812 cells when incubated with paromomycin (24.6 ng/200,000 cells, range 19.3-30.2, $p=0.14$) and fenbufen (25.1 ng/200,000 cells, range 19.3-28.8, $p=0.07$). With the addition of prazosin, the IUR was reduced to a similar level in all groups, except in ibuprofen-treated cells, where a slight but significant decrease of IUR was observed in the presence of prazosin (average 13.86 ng/200,000 cells vs 15.89 ng/200,000 cells, $p<0.0001$).
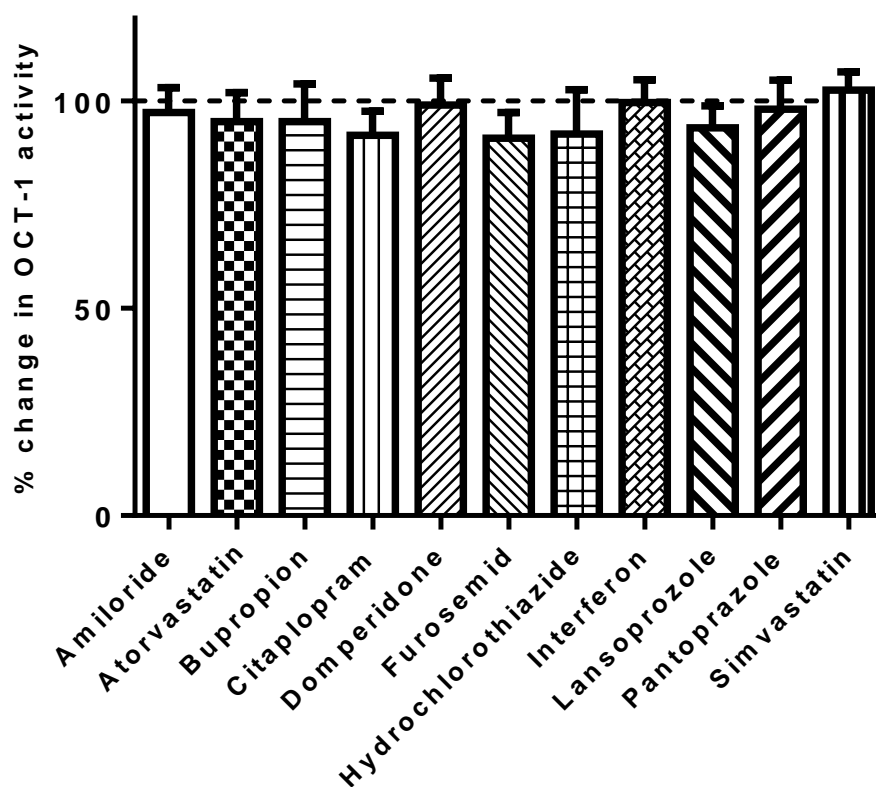
Figure 3.6   OCT-1 activity in K562 cells in the absence or presence of 11 clinically applicable drugs

OCT-1 activity in K562 cells was assessed with or without 11 commonly prescribed drugs over a 2-hour period. Results (mean±SEM) are expressed as percentage of own solvent control, which was set at a value of 100% (n≥3).
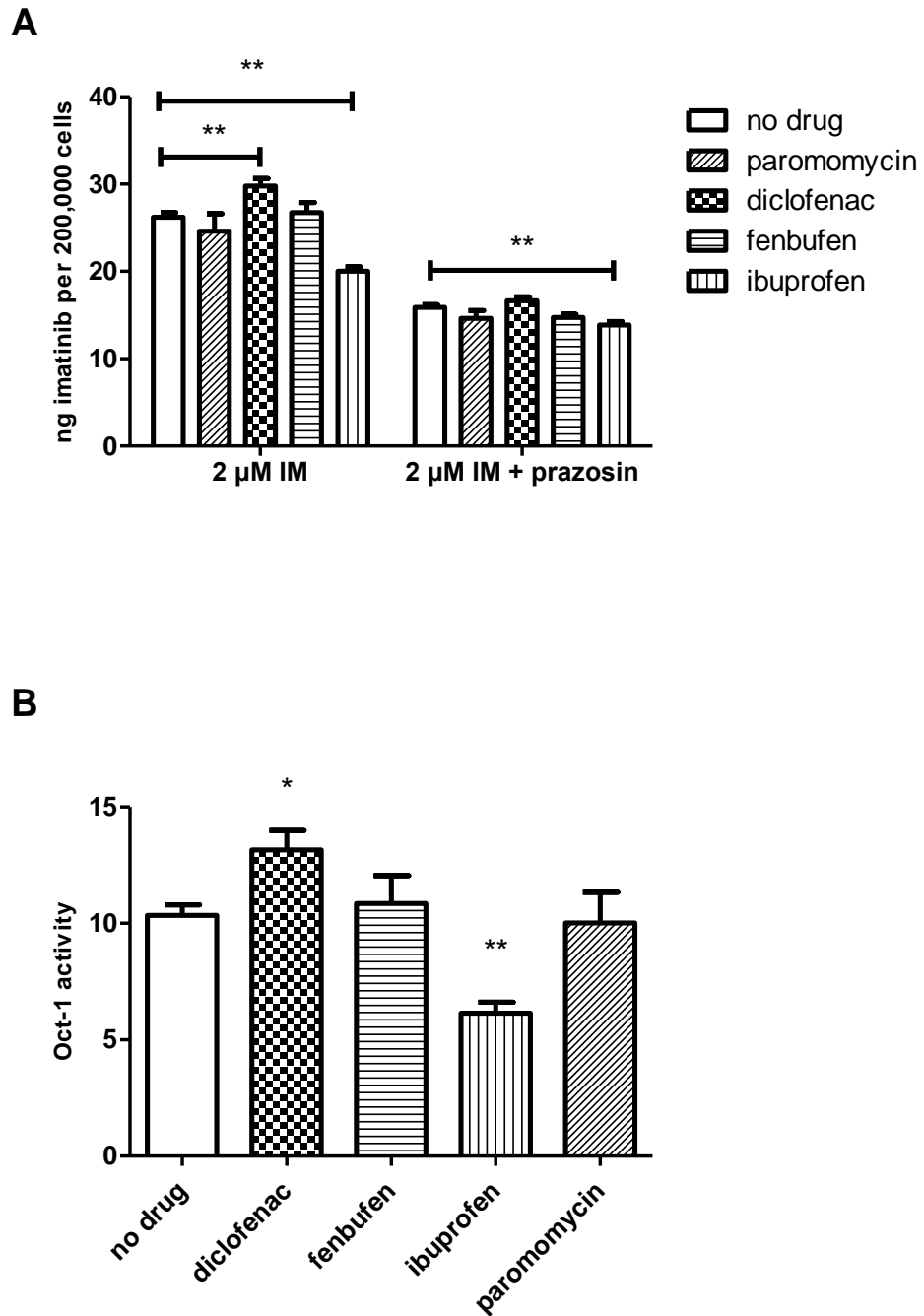
Figure 3.7   Intracellular uptake of imatinib and OCT-1 activity in KU812 cells in the absence or presence of diclofenac, fenbufen, ibuprofen and paromomycin

The IUR of 2 µM imatinib (**A**) and OCT-1 activity (**B**) in KU812 cells was performed with or without diclofenac, fenbufen, ibuprofen and paromomycin over a 2-hour period. The error bars represent the standard deviation of the mean (n≥3). *, $p < 0.05$; **, $p < 0.001$

The highest OA was observed in the presence of diclofenac (average 13.2, range 6.1-19.0, $p<0.0057$, Figure 3.7B) with the lowest after treatment with ibuprofen (average 6.1, range 2.6-13.2, $p<0.0001$). No significant change was observed in the presence of either paromomycin (10.0, range 7.3-13.6, $p=0.81$) or fenbufen (10.9, range 7.0-13.7, $p=0.70$). These data suggested that diclofenac is likely to be a potent OA enhancer while the other non-steroidal anti-inflammatory drug, ibuprofen significantly inhibits the active imatinib transport in CML cells.

3.3.7. Effects of temperature on the regulation of IUR by diclofenac and ibuprofen in KU812 cells

It has been reported that the uptake of imatinib is temperature dependent (130). To further investigate whether the modulation of IUR and OA by diclofenac and ibuprofen was affected by the temperature, the IUR and OA assays were then performed in KU812 cells at 4°C and the result were compared with that at 37°C. In keeping with previous study, a significant difference was found between the IUR for imatinib at the two temperatures (26.49 ng/200,000 cells at 37°C; 21.00 ng/200,000 cells at 4°C, $p=0.008$, Figure 3.8A). A difference in the IUR for imatinib in the presence of OCT-1 inhibitor, prazosin, was also observed at the two temperatures (13.93 ng/200,000 cells at 37°C; 19.49 ng/200,000 cells at 4°C, $p=0.001$). As ABCB1 and ABCG2 are both ATP-dependent, this increase of the IUR of imatinib in the presence of prazosin was most likely due to the decreased efflux transport of imatinib at 4°C. The suggestion that OCT-1 is a temperature-dependent transporter was also confirmed when the OA at 4°C was assessed. It was found that the OA was very low (median 1.75 ng/200,000 cells, range 0-4.31) and significantly lower compared with that of 37°C (median 12.57 ng/200,000 cells, $p=0.0002$).

On addition of diclofenac, the IUR of imatinib (with or without prazosin) remained unchanged compared with control KU812 cells at 4°C ($p=0.47$ and 0.86, respectively,

A

B
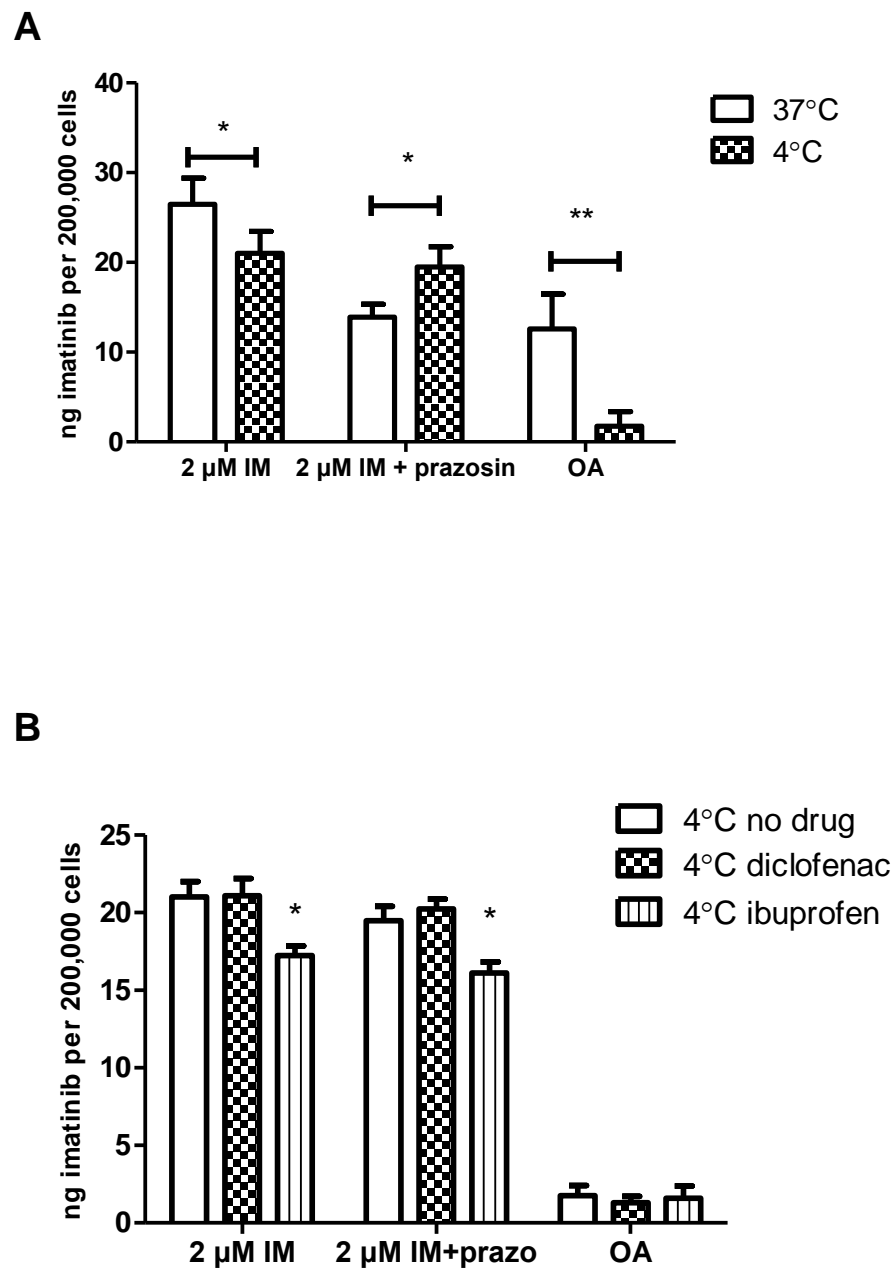
Figure 3.8   The effects of temperature on the IUR of imatinib in KU812 cells and the OA in the presence of diclofenac and ibuprofen

The IUR assays of 2 µM imatinib in KU812 (**A**) were performed at 37°C and at 4°C over a 2-hour period. The effect of diclofenac and ibuprofen on OA at 4°C were also assessed (**B**). The error bars represent the standard deviation of the mean (n≥3).

*, $p<0.05$; **, $p<0.001$

Figure 3.8B) and the OA at 4°C after the treatment with diclofenac remained at a similar low level as control (p=0.58). This is consistent with diclofenac acting through an effect on the OCT-1 transporter. Unlike diclofenac, treatment with ibuprofen further decreased IUR of imatinib at 4°C (from 21.00 to 17.23 ng/200,000 cells, p=0.006), suggesting an effect independent from OCT-1. In addition, the IUR in the presence of prazosin was also reduced by ibuprofen (from 19.49 to 16.12 ng/200,000 cells, p=0.011). Thus, no further decrease in OA was observed when ibuprofen was added (p=0.89).

3.3.8. Effects of diclofenac and ibuprofen on IC50^{imatinib} of BCR-ABL-positive cell lines

As diclofenac and ibuprofen demonstrated the most significant effect on OA in two different cell lines, and as both are commonly used in clinical practice, these two drugs were selected for further experimentation. To assess whether the observed divergent alterations in IUR of imatinib and OA translate into changes in tyrosine kinase inhibition, the IC50^{imatinib} was examined in K562 and KU812 cells with or without diclofenac or ibuprofen. It was hypothesised that increased intracellular imatinib concentration by an OA enhancer would lead to a greater tyrosine kinase inhibition which translates into a decreased IC50^{imatinib}. Also the cells with reduced OA would be predicted to display increased IC50^{imatinib}. In K562 cells, a significant decrease in the IC50^{imatinib} was observed when treated with diclofenac as hypothesized (5.7 to 3.7 µM, p=0.013, Figure 3.9A). The IC50^{imatinib} in KU812 (3.5 µM) was lower than in K562 cells (p=0.016). When treated with diclofenac, a similar decrease to 2.2 µM, was observed in the KU812 IC50^{imatinib} (p=0.007, Figure 3.9B). In contrast, ibuprofen significantly elevated the IC50^{imatinib} in K562 and KU812 cells, as expected (5.7 to 8.1 µM in K562 cells and 3.5 to 6.6 µM in KU812 cells, respectively; p<0.001). These data confirm that the contrasting effect of these two drugs on OA
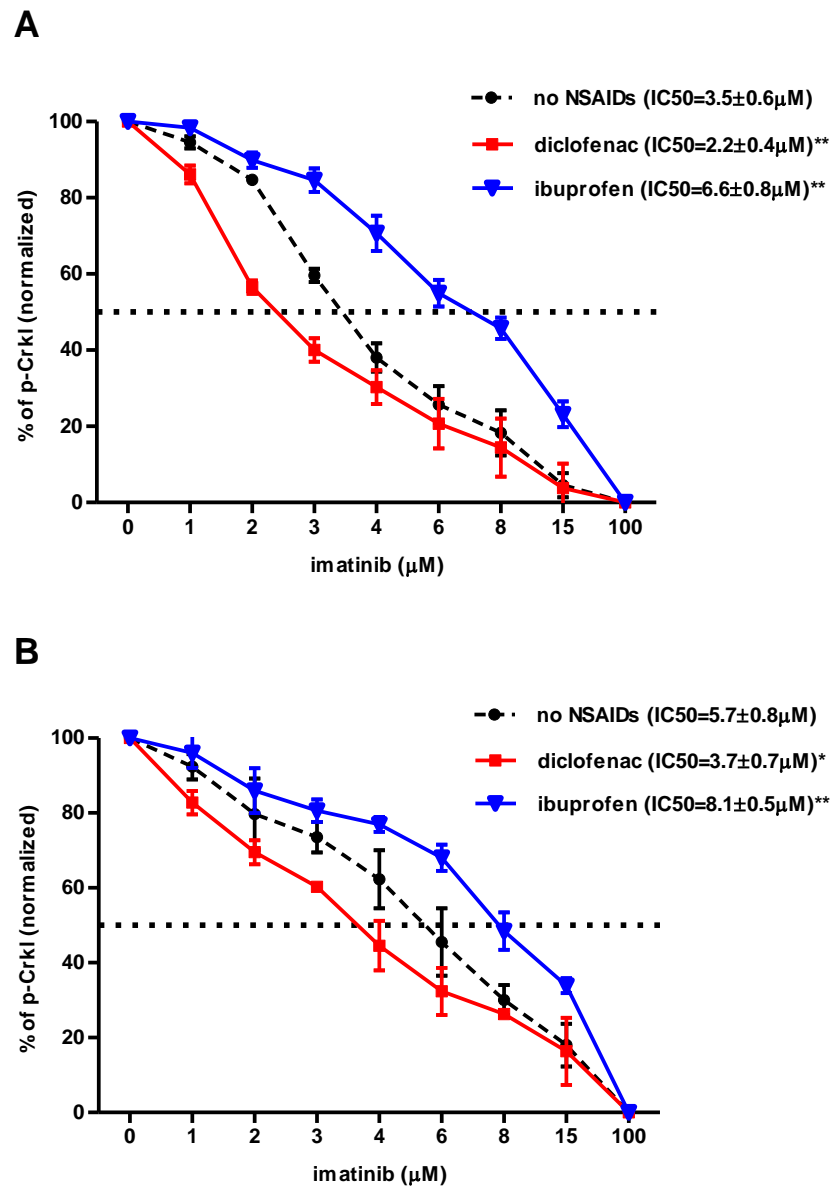
Figure 3.9 **The IC50^{imatinib} results in the presence or absence of diclofenac or ibuprofen**

The *in vitro* reduction in the level of p-CrkI by imatinib was detected using the IC50^{imatinib} assay. The cumulative results **A:** in K562 cells **B:** in KU812 cells. The error bars represent the standard deviation of the mean (n≥3). *, $p<0.05$; **, $p<0.001$

leads to corresponding alterations in tyrosine kinase inhibition in CML cells due to the different levels of intracellular imatinib levels.

3.3.9. Effects of diclofenac and ibuprofen on viable cell counts when co-administrated with imatinib in BCR-ABL-positive cells

To address whether the changes in imatinib intracellular concentration and IC50^{imatinib} mediated by diclofenac or ibuprofen translate to changes in viable cell number, the trypan blue cell exclusion assay was performed with K562 and KU812 cells in the presence or absence of diclofenac and ibuprofen. After 72 hours incubation as shown in Figure 3.10, dose-dependent reduction of live cell number in the presence of imatinib alone was observed. KU812 cells were more sensitive to the effects of imatinib than K562 cells. At 0.25 µM of imatinib, significantly fewer live KU812 cells were counted (0.64x10^5/mL) compared with K562 cells (10.95x10^5/mL, $p<0.001$). Thus, different doses of imatinib were applied to K562 and KU812 cells. For K562 cells, 0.25 µM of imatinib co-incubated diclofenac resulted in a significantly lower number of viable cells (7.82x10^5/mL) compared with imatinib alone (10.95x10^5/mL, $p=0.021$), which is consistent with the observed decrease in K562 IC50^{imatinib}. The KU812 cells displayed similar results when treated with 0.05 µM imatinib and diclofenac, where the viable cells decreased from 8.40x10^5/mL to 5.40x10^5/mL ($p=0.019$, Figure 3.10A and 3.10B). Interestingly, this effect is not due to diclofenac-induced cell death as there was no significant change observed in cell viability in the presence or absence of diclofenac alone.

In contrast, when K562 cells were co-incubated with 0.5 µM imatinib and ibuprofen for 72-hour there was a significant increase in viable cell number compared with cells treated with imatinib alone (from 4.88x10^5/mL to 8.16x10^5/mL, $p=0.004$). A similar result was also observed in KU812 cells treated with 0.1 µM of imatinib where the live
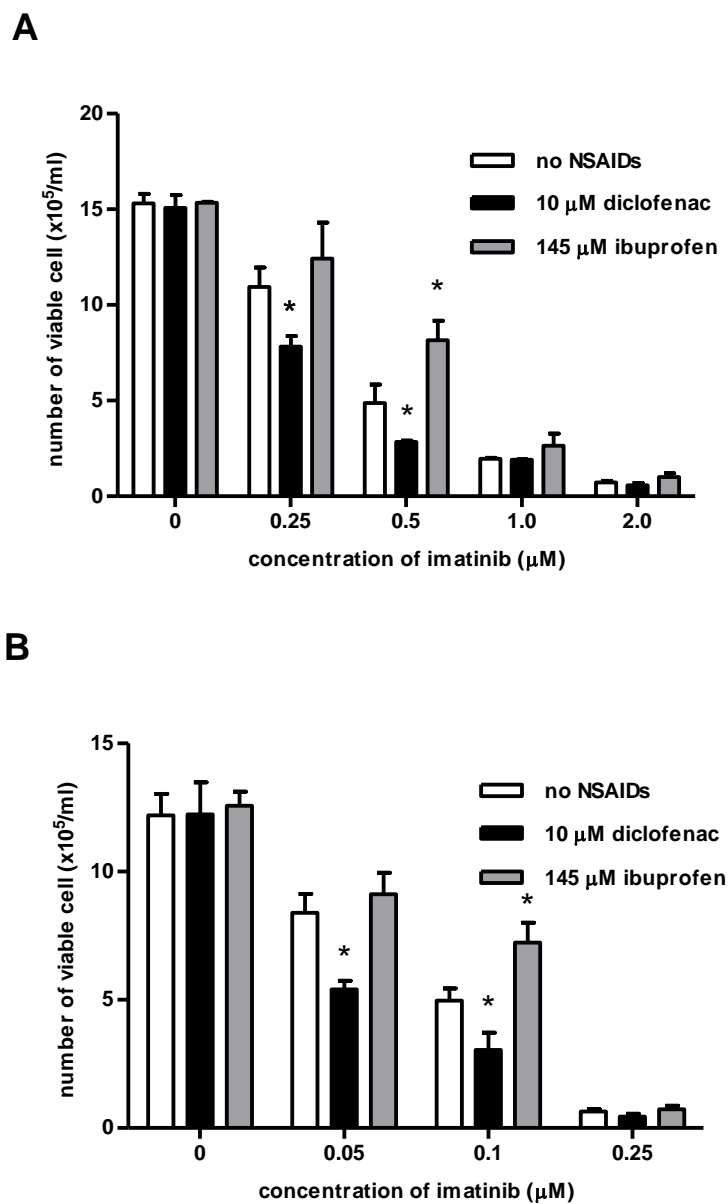
Figure 3.10   The effects of diclofenac and ibuprofen on the number of viable cells after 72 hours co-incubation with imatinib.

The number of viable cells was determined using the trypan blue exclusion method after treatment with NSAIDs and imatinib for 72 hours. **A:** in K562 cells **B:** in KU812 cells. The results (mean±SEM) are expressed as the viable cell number determined by trypan blue exclusion assay (n=3). *, $p < 0.05$.

cells number increased from 4.97×10^5/mL to 7.23×10^5/mL when treated with ibuprofen (p=0.002, Figure 3.10A and 3.10B).

3.3.10. Effects of diclofenac and ibuprofen on the OA of primary cells

To examine the effect of both drugs on OA in primary CML samples, OA of MNC isolated from CP-CML patients were assessed in the presence or absence of diclofenac or ibuprofen.

Patients' baseline OA result were divided into quartiles as previously defined (140). The effect of diclofenac on MNC was firstly investigated with the samples collected from patients with OA in the lowest quartile (Q1, OA<4 ng/200,000 cells). After treatment with diclofenac, the OA was enhanced in 93% of the Q1 patients' samples tested (n=29). The median OA in Q1 patients increased from 1.39 to 4.17 ng/200,000 cells (p<0.001, Figure 3.11A). Notably, as the result of this increase, 15 of 29 cases (51.7%) moved from Q1 to a higher OA quartile group. However, for patients with higher OA values (median OA 5.49 ng/200,000 cells, range 4.1-8.9, n=21), treatment with diclofenac did not lead to a significant increase in OA (median OA 5.92 ng/200,000 cells, range 2.3-13.9, p=0.714, Figure 3.11B).

In MNC treated with ibuprofen, a consistent inhibitory effect (41% reduction in OA) was observed in all 12 cases tested (Figure 3.11C). The average OA in these 12 samples (7.53±0.82 ng/200,000 cells, range 3.53-14.52) was significantly reduced (4.30±0.52 ng/200,000 cells, range 1.53-7.85, p<0.001) after the treatment with ibuprofen.

In addition, the effects of diclofenac or ibuprofen on MNC were also examined with samples collected from normal individuals (n=10). The overall OA in normal MNC were significantly lower than that in CML samples (3.70±0.45 ng/200,000 cells, range 2.21-4.89, p<0.001, Figure 3.11D). After treatment with diclofenac, no significant

Figure 3.11   The effects of diclofenac or ibuprofen on OCT-1 activity in primary MNCs

OA assays were performed with fresh or frozen MNCs isolated from the blood of newly diagnosed patients with CML. Box-plots display the median value, the minimum and maximum value of OA. **A**: patients with basal OA less than 4 ng/200,000 cells (n=29) **B**: patients with basal OA greater than 4 ng/200,000 cells (n=21) **C**: *de-novo* CP-CML patients (n=12) **D**: healthy donors (n=6)
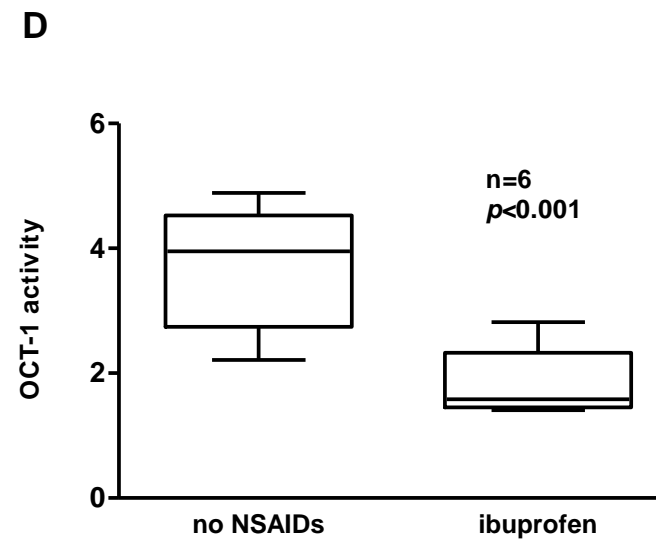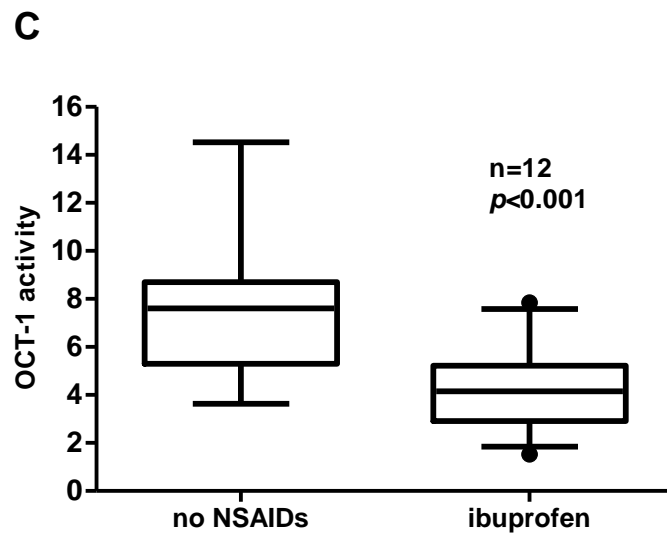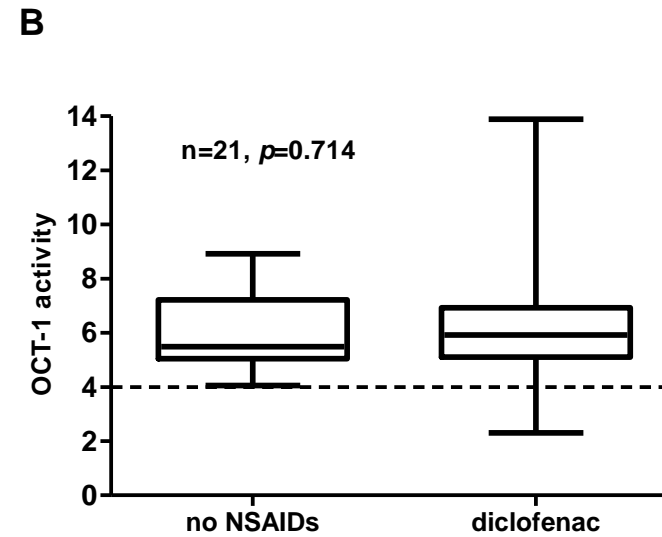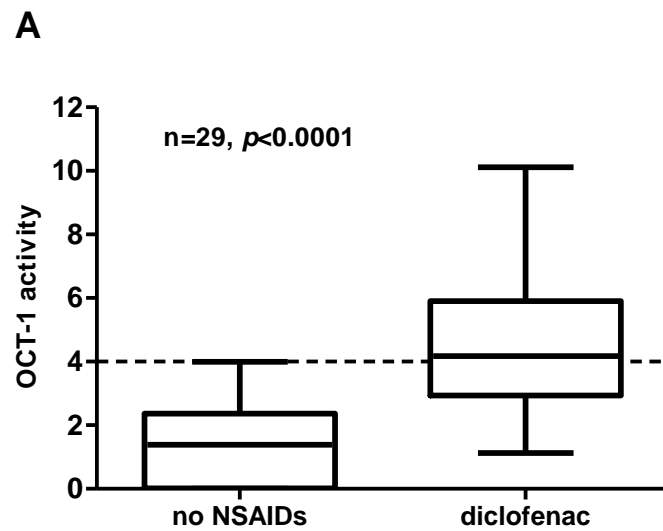
change in OA was observed (3.64±0.58 ng/200,000 cells, range 1.93-5.17, *p*=0.63). However, a 50% decrease in OA was observed in all normal MNC following incubation with ibuprofen for 2 hours (1.83±0.26 ng/200,000, range 1.41-2.82, *p*<0.001, Figure 3.11D).

3.4. Discussion

As OCT-1 is the major active influx transporter for imatinib, OA is a strong predictor of response to imatinib treatment in *de novo* CML patients (64, 65). Patients with OA in the lowest quartile (Q1, OA<4ng/200,000 cells) performed poorly on standard imatinib therapy due to the low intracellular imatinib concentration and inefficient kinase inhibition. Increasing the degree of kinase inhibition in these patients is a potential strategy to improving response. While escalating imatinib dosage may be of benefit in some patients, not all patients are able to tolerate imatinib at doses greater than 400mg (155). Furthermore, increasing the dosage of imatinib does not necessarily translate to higher levels of intracellular imatinib and kinase inhibition in the CML target cells. Enhancing transporter activity might serve as an alternate strategy to pharmacologically increase the efficiency of BCR-ABL kinase inhibition by imatinib.

The present chapter therefore focused on identification of drugs using connectivity map analysis (CMAP) and queried the drug expression profiles with an input signature weighted to OCT-1 as the primary up-regulated gene. Eight compounds with the highest ranking and lowest toxicity profile were chosen as potential OA enhancers. Their effects on imatinib uptake and kinase inhibition were extensively validated in CML cell lines and patient samples, together with 12 NSAIDs and 11 commonly CML cell lines and patient samples, together with 12 NSAIDs and 11 commonly prescribed drugs.

The findings from this chapter show that paromomycin selected from CMAP analysis

significantly increased the IUR of imatinib and OA in K562 cells but not in KU812 cells. However, none of the other 7 candidates achieved substantial changes in OA in either BCR-ABL cell line. This is, in part, explained by the difference in the experimental setting between this study and the CMAP database. CMAP uses a large reference database of genome-wide expression profiling from cultured human cancer cell lines (HL60, PC3, MCF7, and SKMEL5) under standard conditions (174, 175). In the present study, imatinib IUR and OA were examined in two BCR-ABL positive cell lines. This might explain why highly ranked compounds with OCT-1 as an up-regulated gene in BCR-ABL negative cells would not necessarily follow the same pattern in CML cells. Furthermore, K562 cells are of the erythroleukemia type (181, 182) while KU812 had been described as an immature prebasophilic cell line (150). It is possible that intrinsic differences between K562 and KU812 contribute to the different effects of paromomycin as well as that of fenbufen. In additional to these, it is also possible that the increased up-regulated *SLC22A1* gene expression would not necessarily lead to the functional change of OCT-1 transporter. Whether this suggestion could be the reason for the results with the OA enhancer by CMAP will be investigated in the next chapter.

When the effects of NSAIDs and commonly prescribed drugs on imatinib uptake were assessed, a consistent enhancement of IUR and OA was observed in both K562 and KU812 cells when treated with diclofenac. Importantly this increase in OA translated to a significant increase in BCR-ABL kinase inhibition as demonstrated by a reduction in the $IC50^{imatinib}$ in both cell lines. This finding also highlights, in line with the previous studies (62), the correlation between OA and $IC50^{imatinib}$. Additionally, trypan blue exclusion assays provided further evidence that by increasing functional OA and tyrosine kinase inhibition, diclofenac in combination with imatinib results in a significant reduction in viable cell numbers.

Importantly, the effect of diclofenac was also observed in CML patients' samples. In 93% of MNC samples from CML patients with basal OA less than 4 ng/200,000 cells (Q1), diclofenac at clinically relevant concentrations resulted in a significant increase in OA. Importantly, 51.7% of Q1 cases tested increased from Q1 to higher quartiles. From a clinical perspective, this increase is of greater significance for the Q1 patients who have a particularly poor outcome on standard imatinib therapy. Based on the TIDEL data this may significantly increase the probability of these patients achieving a major molecular response (MMR), and significantly reduce the risk of suboptimal response or imatinib failure (140). However, it is important to note that diclofenac did not significantly increase OA in cells from patients with higher OA. This differential effect of diclofenac in patients with higher OA suggested that this population may not be targeted as well as Q1 patients by diclofenac intervention. Thus, the mechanism of the OA regulation by diclofenac might represent the reason underlying the biological difference between patients with low and high OA.

When applied to MNC from healthy donors, diclofenac did not mediate the same effect as seen in CML patients, implicating a role for BCR-ABL or disease related processes in this interaction. These findings raise the possibility that combination therapy with imatinib plus diclofenac may be more effective than imatinib alone in Q1 patients without adding greatly to the toxicity of the therapy. Importantly from a clinical perspective, this may translate to an increase in the probability of patients with low OA achieving a MMR, and a significantly reduced risk of suboptimal response or imatinib failure. In addition, this strategy may also benefit patients with low OA by allowing for a lower/standard dosage of imatinib (400 mg/day) without adding greatly to the toxicity commonly observed when higher doses of imatinib are used (600 or 800 mg/day). However, these findings should however be interpreted cautiously. Extrapolations of *in vitro* effects to *in vivo* effects and clinical response will require careful validation.

Another interesting finding in this study is that NSAIDs can exhibit divergent effects on OA in CML cell lines. Although all NSAIDs have antipyretic, analgesic, and anti-inflammatory properties, there are several important differences in their activities which are mostly due to their affinity towards COX isoforms: COX-1 and COX-2. In CML, it was reported that expression of COX-2 was significantly higher in CML than in healthy volunteers and that increasing levels of COX-2 were significantly associated with shorter survival(183). Therefore several studies have been conducted to investigate the role of COX-2 in imatinib resistance and the use of COX-2 inhibitors as an alternative therapy. It has been reported that celecoxib, a COX-2 inhibitor, reduced cell growth by causing cell cycle arrest at G0/G1 phase and inducing apoptosis by inhibiting NF-κB activation in K562 cells(184). In imatinib-resistant K562 (IR-K562) cells, over-expression of COX-2 and ABCB1 were observed and in addition, celecoxib could induce cell apoptosis by inhibiting COX-2 and ABCB1 (185), probably through the PGE2-cAMP-PKC-mediated pathway(186). However, there is no universal effect on imatinib uptake among COX-2 inhibitors in the current study. Although sharing similar COX-2 selectivity with diclofenac(187), celecoxib, as well as another more potent selective COX-2 inhibitor, rofecoxib, had no significant impact on imatinib uptake via OCT-1 in K562 or KU812 cells. This finding suggests that COX-2 inhibition are unlikely to be the critical target of the interaction between OCT-1 and diclofenac observed in this study.

Unexpectedly, while diclofenac increased OA significantly, ibuprofen significantly decreased the OA in both K562 and KU812 cells. This inhibitory effect on OA of ibuprofen translated into an increase in $IC50^{imatinib}$ and cell growth in the presence of imatinib. Given the common administration and over-the-counter access of ibuprofen, this finding is likely to be of significant clinical relevance. Unlike diclofenac, ibuprofen reduced the IUR of imatinib in KU812 cells regardless of the addition of prazosin. As

the IUR of imatinib in the presence of prazosin represents the intracellular amount of imatinib that passively entered target cells, this phenomenon indicated that ibuprofen might also block the passive transporter of imatinib. This hypothesis was then confirmed by the result that the IUR of imatinib was further reduced by ibuprofen at 4°C when all the active transporters were inhibited. Furthermore, the effect of ibuprofen was also observed in normal cells to the same extent as leukemic cells, which again, suggested that the mechanisms of these two NSAIDs are different.

The various effects of NSAIDs on OCT-1 mediated drug-drug interactions is in contrast with a previous study reporting that diclofenac, ibuprofen, indomethacin and sulindac could all significantly inhibit OCT1-mediated TEA uptake (173). However, it should be noted that the concentration of NSAIDs used in that study (0.5 mM) was much higher than the concentrations used in our study. Given that the mean maximum plasma concentration (Cmax) of diclofenac after a single dose of 50 mg in healthy volunteers is 5 µM (188, 189), the dose used in the present study is more relevant to the clinical setting. Similarly, the concentration of ibuprofen used here (145 µM, equal to 30 µg/mL) was determined according to the clinically achievable level (Cmax=37 µg/mL, after 400 mg single administration in healthy volunteers) (190). Although this concentration is also lower than 0.5 mM, it is still much higher (up to 20-fold) than other NSAIDs selected in the current work. Since it has been shown that NSAIDs are not substrates of OCT transporters (173), it is unlikely that ibuprofen inhibits imatinib uptake by competing for OCT-1. Molecular structural analysis is necessary to further understand the interaction between ibuprofen and imatinib at the binding site of OCT-1, which is beyond the scope of the project in this chapter.

In conclusion, this study provides evidence that diclofenac and ibuprofen may modulate OA which directly impacts on leukaemic cell response, suggesting that these drugs have the potential to impact significantly on CML patient outcome. The

effect of NSAIDs on OA was highly selective suggesting the mechanism is not related to direct COX inhibition and further studies are required to establish the nature of the mechanism in leukemic cells. While drugs such as diclofenac may have a positive influence on imatinib efficacy, this is in contrast to the effect seen with ibuprofen, suggesting caution is required when administrating NSAIDs to CML patients on imatinib treatment.

CHAPTER IV
Diclofenac Regulates OCT-1 Activity at the Transcriptional Level

4.1.   Introduction

Data presented in Chapter 3 has shown that the treatment with two non-steroidal anti-inflammatory drugs (NSAIDs), diclofenac and ibuprofen, significantly changed the functional OCT-1 activity (OA) in BCR-ABL positive cells. Unlike ibuprofen, the effect of diclofenac was more specific on the active uptake of imatinib via OCT-1. However, the mechanism of this regulation by diclofenac is still unknown.

Previous studies have shown that functional regulation of imatinib transporters may occur at the transcriptional level. Overexpression of two recognized efflux transporters ABCB1 and ABCG2 has been shown to be associated with suboptimal intracellular imatinib concentrations, and to be partially involved in secondary resistance to imatinib therapy (74, 75). Using the human colon carcinoma cell line (Caco2 cells) as an *in vitro* model, it was found that the transcript expression of *ABCB1* and *ABCG2* significantly increased after continuous exposure (up to 100 days) to imatinib. This result was accompanied with a decrease of up to 50% in intracellular accumulation of imatinib (74). Furthermore, similar results have also been reported in K562 Dox cell lines cultured in gradually increasing concentrations of imatinib. The only detectable mechanism of resistance for those cells was overexpression of *ABCB1* (191). In a study conducted with 33 CML patients taking imatinib, RQ-PCR results showed that patients who failed to achieve complete or major cytogenetic response had 10-fold higher *ABCB1* expression in the bone marrow cells than those who did achieve a cytogenetic response. In addition, an increase in *ABCB1* expression was also detected in patients who later relapsed (192). Similar results were reported when assessing *ABCB1* transcript expression in 32 chronic phase chronic myeloid leukaemia (CP-CML) patients taking imatinib (193). The patients with higher pre-therapy expression of *ABCB1* all subsequently developed kinase domain

mutations and disease progression. These observations indicate a role for increased transcript expression *of ABCB1* in imatinib resistance in CML.

Compared with ABCB1 and ABCG2, the regulation of OCT-1 in CML has not been well defined. OCT-1 (also known as SLC22A1) is primarily expressed at the basolateral membranes of human hepatocytes and intestinal enterocytes (194). Therefore, the OCT-1 transporter activity can be measured by determining the liver uptake and intestinal secretion of various cationic drugs and endogenous substrates from portal blood. In an Oct1 −/− mouse model, the liver accumulation and the direct intestinal excretion of tetraethylammonium (TEA; an OCT-1 substrate) were significantly lower than that in wild-type mice (195). Several groups went on to investigate the transcriptional control of *SLC22A1* and whether the transport of OCT-1 substrates is influenced by changes in *SLC22A1* expression levels. In the *SLC22A1* promoter, two adjacent putative transcription factor-response elements were identified for the Hepatocyte Nuclear Factor-4α (HNF-4α) transcription factor (196). In transiently transfected Huh7 hepatocarcinoma cells, *SLC22A1* gene expression was suppressed when HNF-4α-mediated transactivation was inhibited (196). Whether the suppressed expression of *SLC22A1 OCT-1* transcript led to a further decrease in OA was not investigated. More recently, the effects of Peroxisome Proliferator Agonist Receptor (PPAR) agonists on the hepatic regulation and function of *Slc22a1* have been investigated in mouse models and rat hepatoma (H-35) cells (197). A PPAR-response element was identified in the promoter region of *Slc22a1,* and *Slc22a1* expression was elevated by treatment with PPAR-α and -γ agonist in both murine livers and H35 cells. Further *in vitro* functional assays confirmed that TEA cellular uptake was significantly increased by the treatment with PPAR-α and -γ agonist in H35 cells.

Since OCT-1 is the major transporter responsible for active imatinib uptake in CML cells (66, 130), the link between *SLC22A1* expression level and imatinib uptake was investigated by several groups. In the KCL22 CML cell line transfected with a pcDNA-OCT-1 plasmid or control plasmid (135), it was found that the uptake of the specific OCT-1 substrate 4-(4-(dimethylamino)styryl)-N-methylpyridinium (ASP) and imatinib was significantly increased when compared with the parental line. As mentioned in Chapter 1, subsequent results from several groups have shown that *SLC22A1* expression level is related to imatinib uptake and is associated with clinical response to imatinib in CML (135-138). However, contrary results have been reported, as other studies found no difference in the diagnosis *SLC22A1* transcript levels between newly diagnosed patients with different molecular response to imatinib therapy (62, 139, 140). Thus the significance of the gene expression level of *SLC22A1* alone and the relationship to OA and critical intracellular drug levels is still controversial.

Data presented in Chapter 3 has shown that diclofenac increased the OA significantly in CML cell lines and primary CML cells. To date, the detailed mechanism of how diclofenac alters OA is unknown. Further understanding the mechanism by which diclofenac increases OA and IUR will provide leads into the regulation of *SLC22A1* and OA in CML cells.

4.2. Methods

4.2.1. IUR and OA assessment in the presence and absence of Actinomycin D

To investigate whether diclofenac enhances OA through transcriptional regulation, a transcriptional inhibitor, Actinomycin D (ActD), was utilized. ActD inhibits cell transcription by binding DNA at the transcription initiation complex and preventing elongation by RNA polymerase (198). It has been found that approximately 90% of

RNA synthesis was inhibited after 6 hours exposure to 5 µg/mL ActD in many human cancer cells, including breast, prostate, and cervical epithelial cancer, nephroblastoma cells, acute T cell leukaemia, cutaneous, T lymphocytes, and acute lymphoblastic leukemic cells (199). The intracellular uptake and retention (IUR) of 2µM imatinib and OA were measured in ActD-treated KU812 cells using ^{14}C-labeled imatinib and the OCT-1 inhibitor prazosin, and values expressed as ng of imatinib per 200,000 cells (Section 2.6.1). The effects of diclofenac on OA were compared between KU812 cells in the presence or absence of ActD.

4.2.2. *Gene expression profiling analysis*

To better define the effects of diclofenac on gene expression, gene expression profiling analysis was conducted using the Affymetrix GeneChip® Human gene 1.0 ST array using RNA isolated from cells with a miRNeasy Mini kit from QIAGEN (Section 2.6.3.1) for the array analysis. The microarray data was analysed as described in Section 2.6.4. ChIP Enrichment Analysis (ChEA) was used to analyse the candidate genes that are potential direct targeted genes for transcriptional factors of interest. Selected genes were chosen for further analysis in independent RQ-PCR assays.

4.3. Results

4.3.1. *Effect of transcriptional inhibition on the ability of diclofenac to increase OA in KU812 cell line*

To investigate whether diclofenac affects IUR and OA through transcriptional regulation, Actinomycin D (ActD) was used to block transcription in KU812 cells. The cells were exposed to 5 µg/mL ActD for 6 hours prior to conducting the IUR assay. Trypan blue cell exclusion was used to assess cell viability after the incubation with ActD to ensure that at least 90% of cells remained alive. As shown in Figure 4.1A, the

incubation of 5 μg/mL ActD for 6 hours did not cause any significant difference in the IUR of imatinib in KU812 cells compared with untreated cells (22.98 vs. 22.33 ng/200,000 cells, p=0.77). The addition of prazosin reduced the imatinib IUR in untreated and ActD pre-treated KU812 cells to a similar level (14.04 vs. 13.52 ng/200,000 cells, p=0.82). Therefore, assessment of OA showed no difference between the control and ActD pre-treated KU812 cells (8.9 versus 8.81, p=0.83, Figure 4.1B).

To further investigate if the enhancement of OA by diclofenac is affected at the transcriptional level, the IUR and OA assay was then performed with KU812 cells pre-treated with ActD in the absence or presence of diclofenac. While diclofenac induced a significant increase in both imatinib IUR and OA in untreated KU812 cells ActD (previously described in Section 3.3.6.), there was no significant change in the IUR of imatinib (p=0.90) or OA (p=0.97) after incubation with diclofenac in ActD pre-treated cells (Figure 4.1), indicating that the effect of diclofenac on IUR and OA was removed by ActD.

4.3.2. *Identification of candidate gene for OA regulation by diclofenac using gene expression profiling with GeneChip Human gene 1.0ST Array*

The results in Figure 4.1 are consistent with the effect of diclofenac on OA in KU812 cells being mediated at the transcriptional level, as the enhancement of OA was sensitive to ActD treatment. To determine the underlying mechanism, KU812 cells treated with 4 different conditions: no treatment control, diclofenac only, imatinib only, and co-administration of diclofenac and imatinib. The RNA isolated from KU812 cells were subjected to microarray profiling using Affymetrix GeneChip® Human gene 1.0 ST array. Electronic gel electrophoresis and Bioanalyser were used to determine the RNA quality (Figure 4.2A). Two standardized assessments of RNA, the ratio of 28S:18S ribosomal RNA (rRNA) and RNA Integrity Number (RIN), were determined
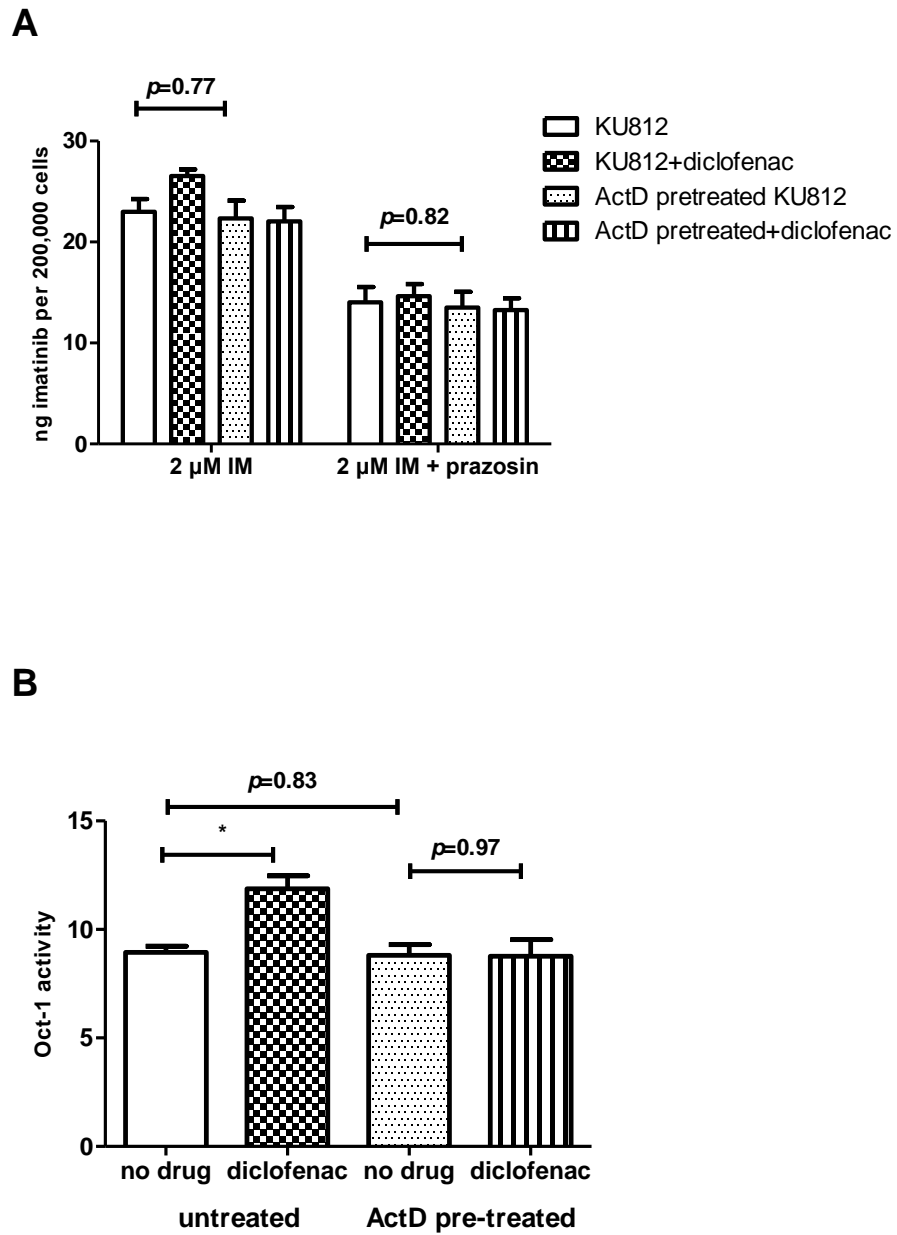
Figure 4.1   Intracellular uptake of imatinib and OCT-1 activity in untreated and ActD pre-treated KU812 cells in the absence or presence of diclofenac

KU812 cells were firstly exposed to 5 µg/mL ActD for 6 hours prior to the IUR assay. The IUR of 2 µM imatinib (**A**) and OCT-1 activity (**B**) in untreated and pre-treated KU812 cells were determined with or without diclofenac over a 2-hour period. The error bars represent the standard deviation of the mean (n≥3). *, $p < 0.05$

A

B
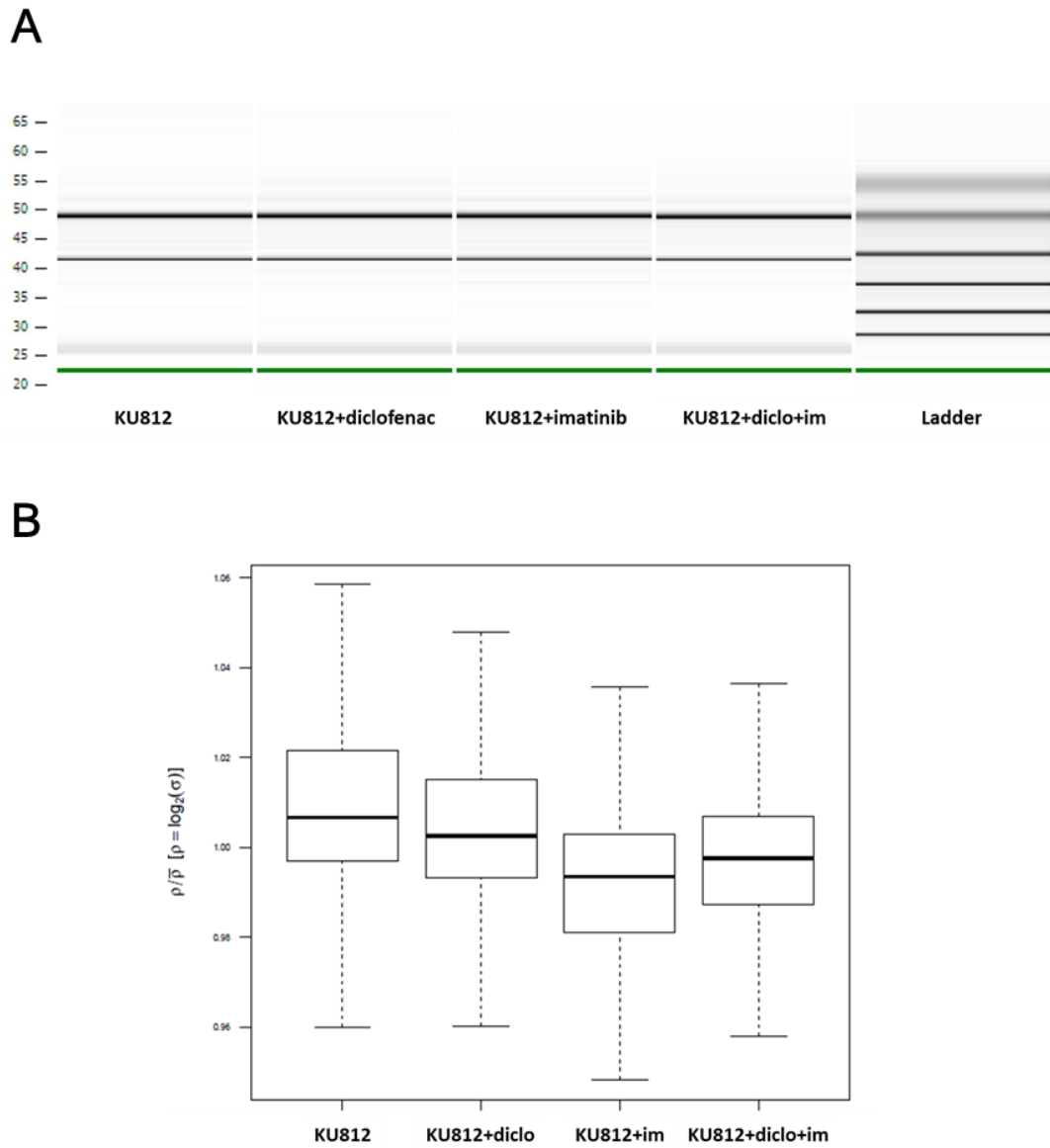
Figure 4.2   Quality control of RNA and microarray samples

A: The quality of RNA isolated from KU812 cells was checked with gel electrophoresis using Bioanalyser. **B:** The NUSE plot portrays the chip-wise distribution of standard error estimates for each sample, where a NUSE value lower than 1.5 is generally considered to be acceptable in regards to quality.

and listed in Table 4.1. While the rRNA ratio is theoretically 2:1, RIN indicates/quantifies the RNA quality based on a numbering system from 1 to 10, with 1 being the most degraded and 10 being the most intact. A Normalised Unscaled Standard Errors (NUSE) plot was also created (Figure 4.2B), where a NUSE value lower than 1.5 is generally considered to be acceptable.

To determine the global gene expression similarity between samples, unsupervised clustering of gene expression was performed after filtering based on median Interquartile Range (IQR) across samples using a Euclidean distance matrix with average linkage (Figure 4.3). There was a high level of gene expression similarity between the vehicle control and diclofenac treated cells, suggesting that diclofenac resulted in fewer effects after 2 hours incubation than treatment with imatinib alone.

To identify genes of interest, the cur-off criterion was set as a fold change (FC) between conditions greater than 1.5 (log2 difference of 0.59). For each treatment condition, the top 15 up-regulated and top 15 down-regulated genes with significant FC comparing with the control were listed in Table 4.2, Table 4.3 and Table 4.4, respectively. To better identify the gene that may critical for the OA regulation by diclofenac, the gene expression after treatment of imatinib alone was compared to that of dual treatment. The top 25 genes ranked on the FC between these two conditions were listed in Table 4.5. The effect of diclofenac on gene expression was also assessed by comparing the conditions without diclofenac (control and imatinib alone) to the other conditions with diclofenac (diclofenac and dual treatment of two drugs). Ranked by the *p*-value, the top 25 genes were shown in Table 4.6.

It is worthy of note that expression of *PTGS2* (encoding prostaglandin endoperoxide synthase-2, also known as cyclooxygenase-2, or simply COX-2) was significantly reduced by imatinib treatment alone. There was a 2.79 folds decrease in *PTGS2* expression level in the imatinib treated sample compared with control (Table 4.2).

Table 4.1   The ratio of 28S:18S rRNA and RNA integrity number (RIN) value of the samples for the Affymetrix GeneChip® Human gene 1.0 ST array

	control	imatinib	diclofenac	diclofenac +imatinib
rRNA Ratio [28s / 18s]	1.8	1.9	1.8	1.9
RNA Integrity Number	9.8	9.8	9.9	10

The quality of the RNA for the array analysis was assessed by two standardized methods of RNA. The rRNA ratio is theoretically 2:1. The RIN implicates the RNA quality based on a numbering system from 1 to 10, with 1 being the most degraded and 10 being the most intact.
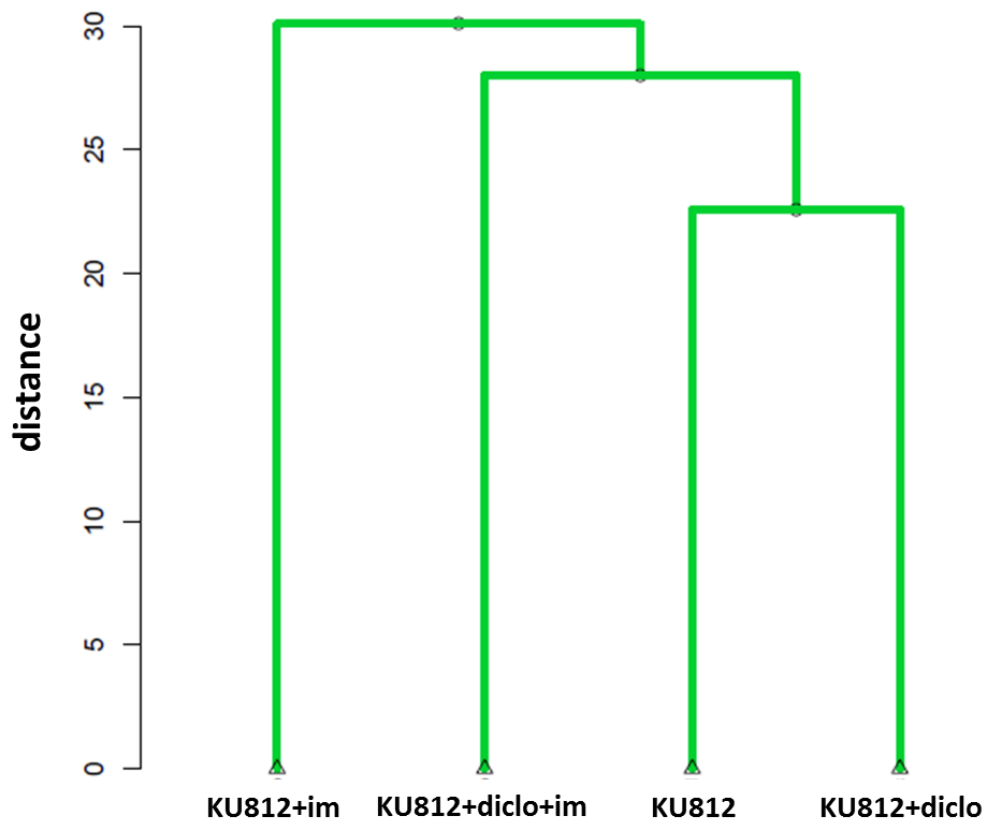
Figure 4.3   Unsupervised clustering for the KU812 cells treated with imatinib and/or diclofenac for 2 hours

Unsupervised clustering of gene expression was performed after filtering based on median Interquartile Range (IQR) across samples using a Euclidean distance matrix with average linkage.

Table 4.2   Top 15 up-regulated or down-regulated genes ranked based on the fold change between the control and imatinib alone in KU812 cells

Up-regulated		Down-regulated	
Gene Symbol	**Fold-Change (I vs. C)**	**Gene Symbol**	**Fold-Change (I vs. C)**
RAG2	3.20	LIF	4.65
SNAI2	2.67	PIM1	4.50
SNRPN	2.48	OSM	3.93
RNU5F	2.37	CD69	3.47
SNORD68	2.25	SPRED1	3.46
EIF4A2	2.18	CCL2	3.43
SNORD103A	2.16	APOL4	3.33
SLITRK6	2.14	DUSP6	3.19
HIST1H2BB	2.07	CISH	3.01
HIST1H3J	2.06	SLC2A3	2.99
SNORD58A	2.06	HHEX	2.97
LOC100133130	2.05	PTGS2	2.79
HIST1H2AJ	2.05	ID1	2.70
ARRDC3	2.01	CD80	2.61
ANKRD20B	1.99	SPRY4	2.56

I indicated KU812 cells treated with imatinib alone; C indicated KU812 control.

Table 4.3   Top 15 up-regulated or down-regulated genes ranked based on the fold change between the control and diclofenac alone in KU812 cells

Up-regulated		Down-regulated	
Gene Symbol	**Fold-Change (D vs. C)**	**Gene Symbol**	**Fold-Change (D vs. C)**
RBMY2EP	2.15	GOLGA6	2.11
LOC391532	1.98	SPRYD5	1.87
KIR2DL3	1.90	ND6	1.84
ADAM21	1.89	LOC729574	1.80
FCGR3A	1.82	ZNF285B	1.78
RBMY1E	1.75	OR1F2P	1.78
ZNF204	1.71	LYZL2	1.75
SNRPN	1.70	LOC644950	1.69
GAGE13	1.63	FLJ38894	1.69
ROCK1	1.62	BTBD11	1.68
IFITM3	1.62	GOLGA6	1.67
SNORA58	1.62	DPPA3	1.66
SNORD103A	1.61	SNRPN	1.65
LOC285908	1.60	FLJ16171	1.64
SNORD96B	1.60	ALDH1L2	1.64

D indicated KU812 cells treated with diclofenac alone; C indicated KU812 control.

Table 4.4   Top 15 up-regulated or down-regulated genes ranked based on the fold change between the control and co-administration of imatinib and diclofenac in KU812 cells

Up-regulated		Down-regulated	
Gene Symbol	Fold-Change (ID vs. C)	Gene Symbol	Fold-Change (ID vs. C)
RBMY2EP	2.57	LIF	4.85
SNAI2	2.48	PIM1	4.44
MGC23284	2.46	CD69	3.91
CST1	2.32	OSM	3.71
SNORD68	2.17	SPRED1	3.60
RAG2	2.04	CCL2	3.47
AK2P2	2.03	DUSP6	3.21
SNRPN	2.01	PTGS2	2.98
FLJ36116	1.91	CD80	2.88
HIST1H2AK	1.89	APOL4	2.88
TISP43	1.89	RAB11FIP1	2.76
HIST1H3J	1.84	HHEX	2.69
ADAM21	1.84	ID1	2.66
TRAF1	1.80	SLC2A3	2.58
KIR2DL3	1.79	CISH	2.57

ID indicated KU812 cells treated with imatinib and diclofenac; C indicated KU812 control.

Table 4.5   Top 15 up-regulated or down-regulated genes ranked based on the fold change between imatinib alone and co-administration of imatinib and diclofenac in KU812 cells

Up-regulated		Down-regulated	
Gene Symbol	Fold-Change (ID vs. I)	Gene Symbol	Fold-Change (ID vs. I)
TISP43	2.69	SCARNA9	2.19
LOC441233	2.37	SNRPN	2.17
PGK2	2.03	LOC100133130	2.10
FLJ25715	1.93	LOC100132728	2.07
LOC646870	1.90	PAGE2B	2.04
LYZL2	1.88	ANKRD20B	2.03
FLJ43093	1.85	RNU5B-1	2.02
C11orf41	1.85	GAGE13	2.02
CYP4Z2P	1.79	LOC730144	2.00
HLA-DPB1	1.79	C20orf69	1.96
C3orf53	1.78	SNORD58A	1.94
FAM90A1	1.76	SNORD42A	1.92
FLJ16171	1.76	ANKRD20B	1.91
KRTAP4-5	1.75	CCDC112	1.89
LOC646093	1.75	LOC100132418	1.89

ID indicated KU812 cells treated with imatinib and diclofenac; I indicated KU812 cells treated with imatinib alone.

Table 4.6   Top 25 genes ranked based on the *p*-value when comparing the conditions of control and imatinib alone to the conditions of diclofenac alone and dual treatment of two drugs

Gene symbol	Conditions without diclofenac		Conditions with diclofenac		*p*-value
	C	I	D	ID	
LOC391532	3.23	3.44	4.21	4.04	0.0005
LOC729574	5.72	5.62	4.87	5.07	0.0008
hsa-mir-15b	5.13	5.29	4.55	4.66	0.0016
MAGEL2	5.19	5.01	5.66	5.74	0.0018
HSPB3	4.34	4.38	4.84	5.02	0.0022
A3GALT2	4.99	4.90	5.44	5.50	0.0025
CAPN6	5.32	5.45	5.87	5.99	0.0029
LOC100133142	7.50	7.32	7.90	8.07	0.0029
PLAC2	6.17	6.12	6.65	6.63	0.0032
PSG3	3.63	3.71	4.13	4.23	0.0033
SLC17A1	4.22	4.23	4.78	4.67	0.0034
LOC729898	5.14	4.96	5.51	5.72	0.0038
MSL3L2	7.29	7.25	6.81	6.79	0.0039
CRISPLD2	4.80	4.85	5.27	5.34	0.0040
LOC613266	5.36	5.30	5.76	5.88	0.0041
GPRC5A	5.18	5.19	5.59	5.77	0.0046
ARG1	5.60	5.69	5.25	5.03	0.0053
ZBTB42	6.53	6.73	7.06	7.21	0.0060
hsa-mir-301a	4.07	4.13	3.44	3.72	0.0061
OR4D5	5.35	5.52	5.87	5.92	0.0068
C15orf5	5.16	5.36	4.83	4.74	0.0070
ELOVL4	4.51	4.42	4.88	4.90	0.0072
PHYHD1	6.18	6.05	6.52	6.60	0.0073
KIR2DL3	4.65	5.14	5.57	5.49	0.0076

The log2 expression in each condition was shown. C indicated KU812 control, I indicated KU812 cells treated with imatinib alone, D indicated KU812 cells treated with diclofenac alone and ID indicated KU812 cells treated with imatinib and diclofenac.

This result was then validated by RQ-PCR with an additional 2 independent biological replicates of KU812 cells treated similarly. As shown in Figure 4.4B, the baseline average expression of *PTGS2* expression level was significantly decreased from 10.70% to 2.07% (relative to the GUSB control gene) after imatinib treatment for 2 hours (p=0.0014). No change in *PTGS2* expression level was observed with the incubation with diclofenac only (p=0.86). A significant reduction also occurred in the co-administration condition when compared to the vehicle control (from 10.70% to 1.93%, p=0.01). However, this decrease in *PTGS2* expression level was most likely effected by imatinib itself rather than an additive effect of imatinib and diclofenac, as there was no difference between the imatinib only and dual treatment (p=0.73).

4.3.2.1. Changes in transporter gene expression levels

It was then determined whether there was any change in expression level for transporter genes involved in OA enhancement. Based on the microarray data, there was no significant change of the *SLC22A1* (*OCT-1*) expression level in either diclofenac alone or dual treatment relative to baseline.

To validate this result, *SLC22A1* mRNA expression was then assessed in KU812 cells after incubation with imatinib and/or diclofenac at the same time point (2 hours). Using human TATA-binding protein (*hTBP*) as the reference gene, the *SLC22A1* mRNA expression level in KU812 cells was 0.080±0.012% (Figure 4.5B). In cells treated with 2 µM imatinib or 10 µM diclofenac for 2 hours, there was no significant change in the expression level of *SLC22A1* compared with vehicle control (p=0.39 and 0.58, respectively). As increased imatinib IUR and OA in KU812 cells was observed in the setting of imatinib and diclofenac co-administration, it was therefore critical to determine the *SLC22A1* gene expression level in KU812 cells treated with both drugs for 2 hours. However, the *SLC22A1* mRNA expression level remained unchanged
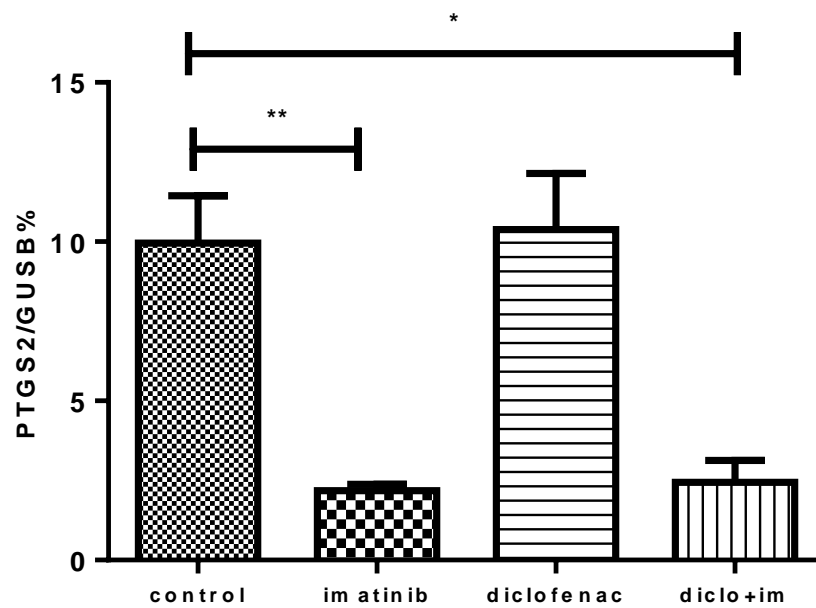
Figure 4.4 *PTGS2* **mRNA expression levels in KU812 after treatment with imatinib and/or diclofenac for 2 hours**

The *PTGS2* mRNA (assessed by RQ-PCR) was significantly decreased after treatment with imatinib. The error bars represent the standard deviation of the mean (n=3). *, $p<0.05$; **, $p<0.001$
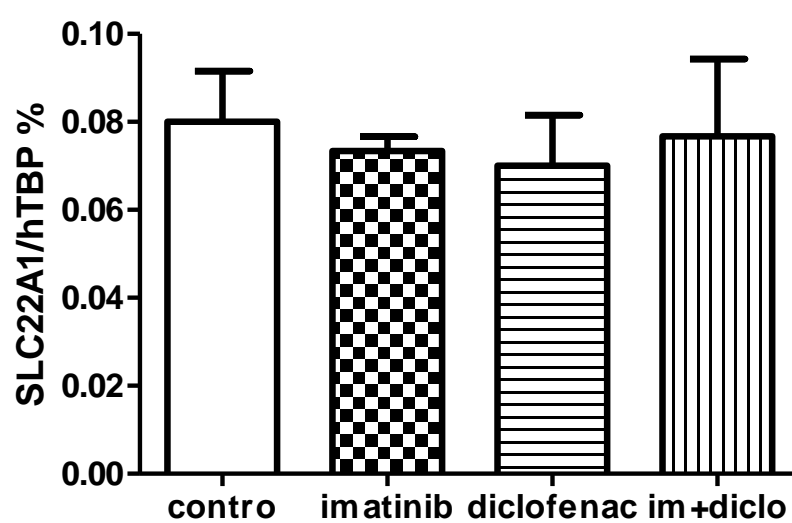
Figure 4.5 ***SLC22A1* expression levels in KU812 after treatment with imatinib and/or diclofenac for 2 hours**

The *SLC22A1* mRNA expression was assessed by RQ-PCR. The error bars represent the standard deviation of the mean (n=3).

when compared with control cells (*p*=0.19). Thus, the change in OA by diclofenac is not associated with change in level of transcriptions encoding OCT-1.

The expression levels of the other solute carrier transporters were also analysed to determine whether diclofenac affect transporter gene expression. The cut-off criteria were set as a FC greater than1.5 between imatinib alone and dual treatment and a *p*-value<0.05 (calculated as described in Section4.2). Among all 374 SLC superfamily transporters examined, only *SLC6A7* met these two criteria with a 1.55 folds increase in dual treatment comparing with the control. The heat map of SLC superfamily transporters was shown in Supplementary Figure 1. Further studies will be needed to validate this change and investigate the role of this transporter in increased OA.

The expression levels of two known efflux transporters of imatinib (122, 123), ABCB1 and ABCG2, were also analysed. Similar to *SLC22A1*, the expression levels of either *ABCB1* or *ABCG2* remained unchanged among each treatment. Of the other 51 ATP-binding cassette (ABC) transporter family members examined in the microarray, the range of the fold change compared to control is small as indicated by the heat map (Supplementary Figure 2). None of the ABC transporters met the 1.5 fold-change cut-off criterion.

4.3.2.2. Identification of candidate genes responsible for OA enhancement

Since no significant change was found in *SLC22A1* mRNA level in KU812 cells in the four conditions tested, the regulation of OA by diclofenac might be affected by altered expression of other genes. Similar criteria as described in section 4.3.2.1 (FC>1.5 and *p*-value<0.05) were applied to identify the genes that are associated with increased OA caused by diclofenac in KU812 cells. After removing unannotated genes from the microarray result, there were a total of 327 genes that met the 1.5 fold change criterion and a total of 375 genes that had the *p*-value less than 0.05 (heat map shown

in Supplementary Figure 3 and Figure 4). As a result, there were 53 genes meet these two criteria as shown in Figure 4.6. Five representative genes were selected from this list for validation of the findings (as highlighted in Figure 4.6 and Table 4.7).

Two additional independent biological replicates of KU812 cells were incubated with imatinib alone, diclofenac alone, or co-administration of both drugs for a 2-hour period and RQ-PCR assays were performed to determine the expression levels of the 5 genes selected. Due to the relatively low expression level, the amount of *HSP90AA6P* was determined as a percentage of *hTBP,* while *GUSB* was used as the reference gene for the other four candidates*.* As shown in Figure 4.7, no significant gene expression change was found when comparing dual treatment with imatinib only in *HSPB3* (*p*=0.85), *ARG1* (*p*=0.91), *TRAF1* (*p*=0.73), or *PAGE2B* (*p*=0.85). For *HSP90AA6P,* there was a 33.86% decrease in the mRNA expression level in dual treatment when compared to imatinib only. However, this decrease failed to achieve significance (*p*=0.16, Figure 4.7D).

4.3.2.3. Identification of direct target genes of PPARγ

There is evidence showing that diclofenac is a PPARγ ligand in COS cells (200), a fibroblast-like cell line derived from monkey kidney tissue. Therefore, the involvement of PPARγ might be of great importance in the regulation of OA by diclofenac. The direct target genes of this transcription factor were identified using Chip Enrichment Analysis (ChEA), which is a web-based interface for mining the binding of transcription factors to target genes based on ChIP-seq data (201). All327 genes with FC greater than 1.5 between imatinib alone and dual treatment were input into ChEA. The enquiry results showed that there were 28 genes containing potential binding sites for PPARγ (Table 4.8). RQ-PCR assays were performed to determine the expression levels of four representative genes selected (as highlighted in Table 4.8) with additional 2

Figure 4.6   Identification of candidate genes based on fold change greater than 1.5 and *p*-value less than 0.05 in KU812 cells

The Venn diagram shows the number of genes with the FC greater than 1.5 in dual treatment compared with imatinib only and the *p*-value less than 0.05 when the average values of diclofenac only and dual treatment was compared to that of KU812 control and imatinib only. 53 genes met both criteria and are demonstrated in heat map format. Red and green colour indicates up-regulated and down-regulated genes compared to control respectively. **indicates representative genes selected for validation with RQ-PCR assay.
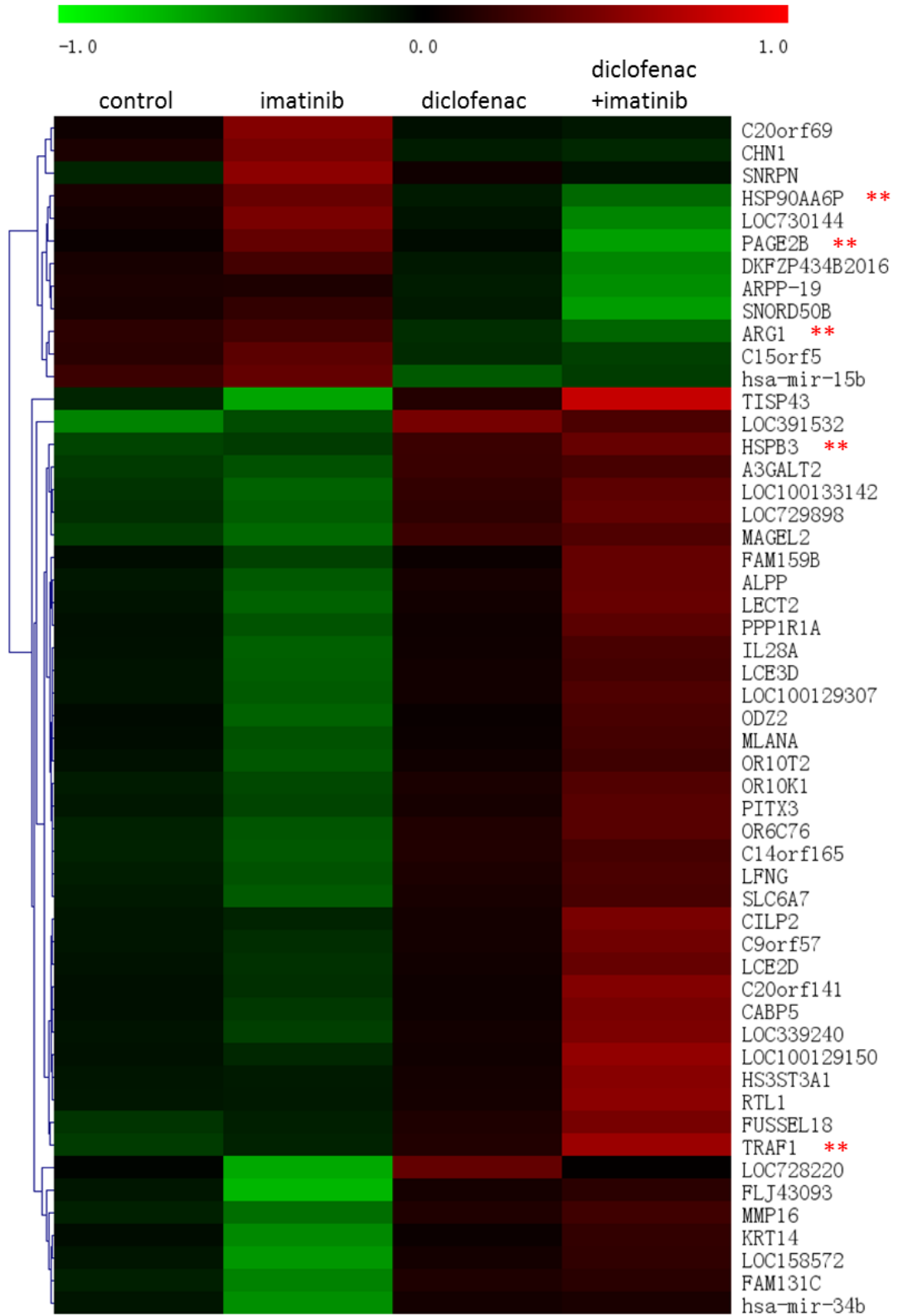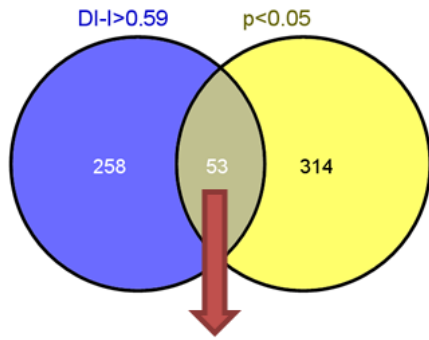
Table 4.7   List of candidate genes that meet the criteria of fold change >1.5 and

***p*-value<0.05**

Gene Symbol	Gene full name	Fold-Change (ID vs. I)	*p*-value
HSPB3	heat shock 27kDa protein 3	1.56	0.00
ARG1	arginase, liver	1.58	0.01
TRAF1	TNF receptor-associated factor 1	1.68	0.01
HSP90AA6P	heat shock protein 90kDa alpha (cytosolic), class A member 6 (pseudogene)	1.77	0.01
PAGE2B	P antigen family, member 2B	2.04	0.03

Five genes were selected based on two criteria described in the text. Firstly, a fold change greater than 1.5 when comparing dual treatment (DI) to imatinib only (I). The second selection criterion is for the *p*-value to be less than 0.05 when the conditions without diclofenac (control and imatinib alone) were compared to the conditions with diclofenac (diclofenac and dual treatment of two drugs). The genes were ranked by *p*-value.
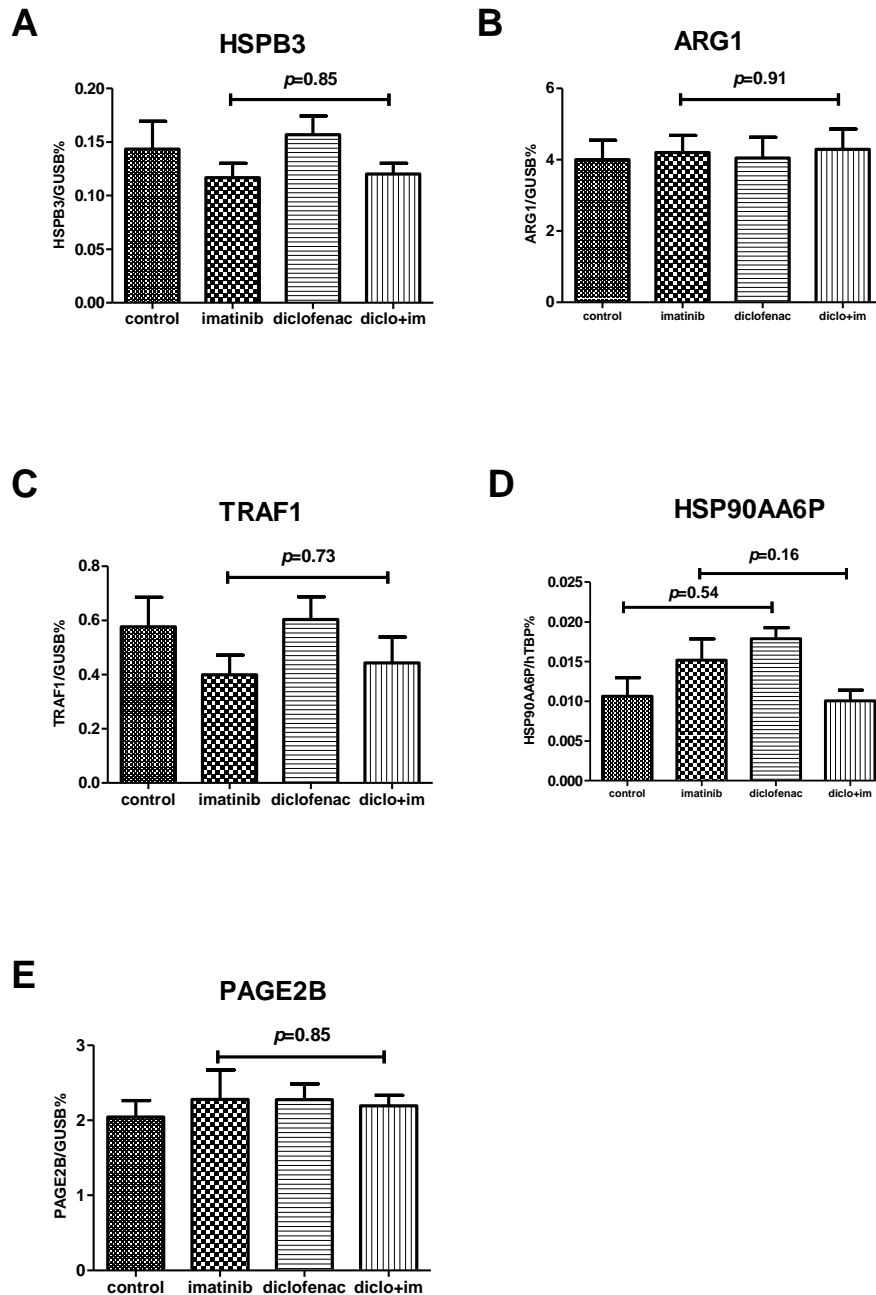
Figure 4.7   Gene expression levels of five candidate genes after the treatment with KU812 cells with imatinib and/or diclofenac for 2 hours

The mRNA expression level of 5 candidate genes was assessed by RQ-PCR and is expressed as a % of house-keeping gene. The error bars represent the standard deviation of the mean (n=3).

Table 4.8   Potential target genes of PPARγ identified using Chip Enrichment Analysis

Gene symbol	Fold-Change (ID vs. I)
MCART1	1.79
MRPS18C	1.79
LRRC39	1.72
PXDN	1.67
TMEM45B	1.66
CCDC104	1.66
SLC14A2	1.64
LYPD6B	1.64
LRRFIP1	1.64
HIST1H3E	1.64
NAT2	1.62
ODF2L	1.6
TGFBR3	1.59
KCNA2	1.59
GRK5	1.59
GRIN2B	1.58
ARG1	1.58
EEA1	1.56
ID3	1.55
RBMS1	1.55
CHRNE	1.54
CILP2	1.54
PPID	1.54
CAMP	1.52
BANF2	1.52
MLANA	1.52
XCL1	1.52
MKKS	1.52

Using Chip Enrichment Analysis (ChEA), 28 genes were identified as the direct target genes of PPARγ and ranked based on the fold change between the sample treated with imatinib only (I) and the sample treated with imatinib and diclofenac (DI). Four representative genes were selected for validation as highlighted.

independent biological replicates of mRNA from KU812 cells. The result of RQ-PCR showed that there was no significant gene expression change in *GRK5* (p=0.66), *EEA1* (p=0.91), or *ID3* (p=0.49) between dual treatment with imatinib only, as shown in Figure 4.13. Although not significant (p=0.16), there was a 15.97% decrease in the average expression level of *LRRFIP1* gene in dual treatment when compared with imatinib only (Figure 4.8A).

4.4. Discussion

OCT-1 activity (OA), measured in mononuclear cells (MNC) from CP-CML at diagnosis, is a strong predictor for the TKI failure and long-term outcome to imatinib therapy. In Chapter 3, a significant increase in OA was observed when CML cells were treated with the non-steroidal anti-inflammatory drug, diclofenac, at its therapeutic concentration. Understanding the mechanism leading to this enhancement of OA may make it possible not only to overcome the barrier of low OA, but also to provide new approaches identifying patients who are likely to experience poor response to imatinib. There have been some studies conducted to investigate the transcriptional and post-transcriptional regulation of OCT-1 in liver and kidney settings (196, 197). However, the critical role of OCT-1 in patients' response to imatinib has only been known for a few years, therefore limited data as yet exists in the field of OA regulation in CML cells (135).

The data presented in this chapter describes the negative effect of ActD, an inhibitor of transcription (198), on the enhancement of OA by diclofenac. The pre-treatment with ActD did not induce any change in the IUR of imatinib or OA in KU812 cells. However, diclofenac failed to enhance the IUR and OA in ActD pre-treated cells (Figure 4.1). This result indicates that the increase of OA caused by diclofenac is mostly likely mediated at the transcriptional level.
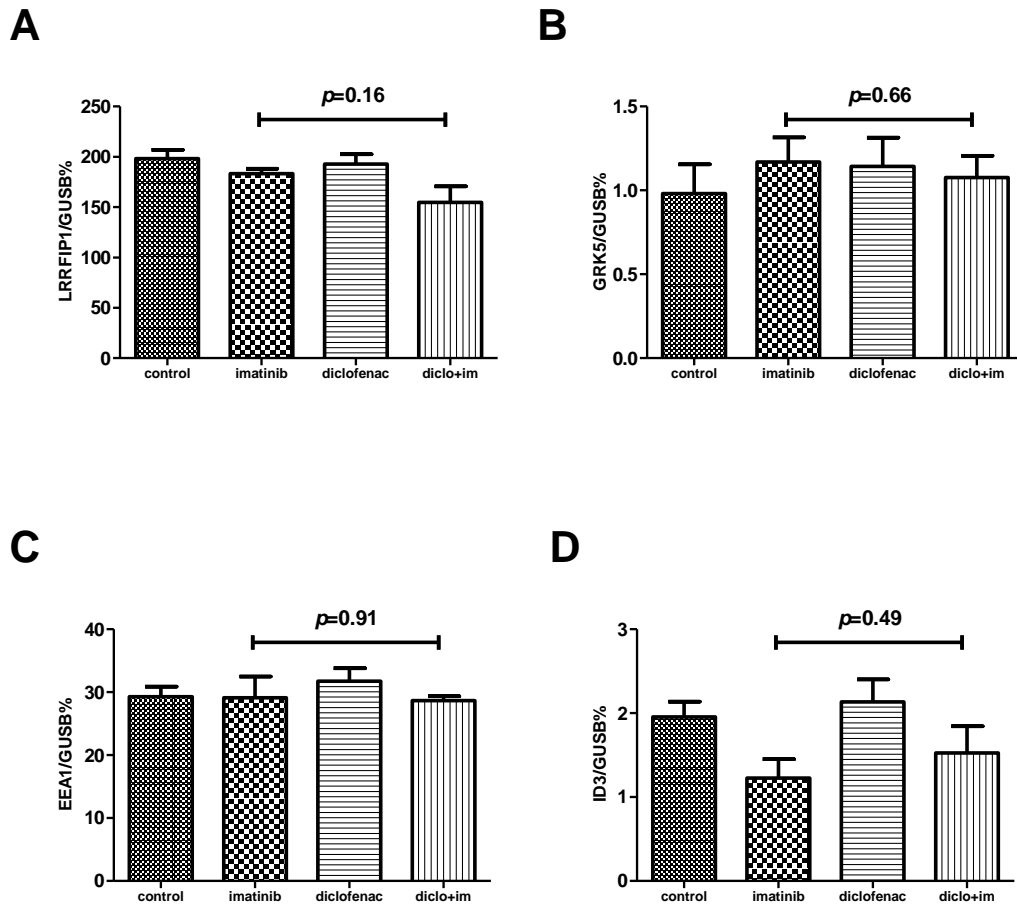
Figure 4.8   Gene expression levels of four candidate genes in KU812 after the treatment with imatinib and/or diclofenac for 2 hours

KU812 cells were treated with imatinib and/or diclofenac for 2 hours. The mRNA expression level of four candidate genes was assessed by RQ-PCR and is expressed as a % of house-keeping gene. The error bars represent the standard deviation of the mean (n=3).

Using liver and kidney cell lines as models, several groups have demonstrated that the expression level of OCT-1 encoding gene *SLC22A1* can be regulated at the transcriptional levels (196, 197) and that changes in transcript levels of *SLC22A1* can translate into altered substrate uptake mediated by the OCT-1 protein (195, 197). In this chapter, the expression level of *SLC22A1* was assessed by Affymetrix GeneChip® Human gene 1.0 ST array analysis and RQ-PCR assays indicating that the treatment with either diclofenac or imatinib had no effect on the *SLC22A1* mRNA levels. Therefore, the increase in imatinib IUR and OA by diclofenac is not likely to be due to an alteration in the expression of the *SLC22A1* gene itself in KU812 cells. As the experiments using ActD pre-treated cells illustrated, the expression of other target genes may be critical for OA modulation, resulting in increased imatinib IUR.

The Affymetrix GeneChip® Human gene 1.0 ST array makes it possible to identify candidate genes involved in *OCT-1* regulation using genomic profiling which utilises over 5.4 million probes representing about 1.4 million probe sets. These are designed based on the genomic regions of known genes and regions that harbor predicted genes. Similarly to OCT-1*,* transcripts for the imatinib efflux transporters ABCB1 and ABCG2 remained unchanged in all conditions. A previously published study using Caco2 cells has shown that the expression levels of *ABCB1* and *ABCG2* were up-regulated by continuous exposure (up to 100 days) to imatinib (74). *ABCB1* over-expression was also observed when inducing imatinib resistance in K562 Dox cells using a similar method (191). However, these escalated efflux transporter genes are most likely due to the selection of high expression clones after long term culture in the presence of imatinib. As the IUR and OA are all assessed after a 2-hour period, such short term treatment might not be enough to cause a significant change for either efflux transporter.

Another interesting observation is that *PTGS2* (COX-2) expression levels in KU812 cells were significantly reduced after incubation with imatinib. Since diclofenac treatment failed to induce any change to *PTGS2* expression levels and no additive effect was observed in the diclofenac and imatinib treated samples, there appears to be no direct association between *PTGS*2 expression levels and OA enhancement by diclofenac. However, cumulative evidence demonstrates that COX-2 is also involved in the biology of poor patient outcome on imatinib therapy (183, 185, 186, 202). The role of COX-2 and its metabolites will be investigated in the next chapter.

In this study, 3 selection criteria were used to identify candidate genes involved in the enhancement of OA by diclofenac. Five genes were selected by their fold change and *p*-value (as indicated in Figure 4.6). Four different genes were selected by ChEA analysis, which contain potential binding sites for PPARγ. RQ-PCR revealed that only 2 out of the 9 selected genes (*HSP90AA6P* and *LRRFIP1*) had an expression pattern consistent with the microarray results (Figure 4.11D and Figure 4.13A). However, none of the genes had significant changes in expression levels after imatinib and/or diclofenac treatment in the RQ-PCR assays based on triplicated. In this study, a basophilic leukemia cell line, KU812, was used for the microarray experiment, which might not reflect the genomic characteristics of primary CML cells. Furthermore, KU812 is established from a blast crisis (BC) CML patient (150). Given diclofenac exhibited the same enhancement effect on OA in CML cell lines and CP-CML samples, it will be important to identify candidate genes in samples collected from CP-CML patients treated with or without diclofenac given the significant difference in genomic profiling between BC and CP (203). However, due to the large number of the primary samples required for the microarray analysis, only CML cell line were included in this chapter.

In conclusion, the studies presented in this chapter indicated that the effect of diclofenac on imatinib uptake in KU812 cells is mediated by transcriptional regulation. There was no correlation between *SLC22A1* or *PTGS2* expression levels and elevated OA in KU812 induced by diclofenac. Therefore diclofenac regulates OA via changes at the transcriptional level, but not directly via up-regulated *SLC22A1* expression. Given that diclofenac is a duel COX-2 and PPARγ inhibitor, the roles of COX-2 and PPARγ in OA regulation were further investigated in the following chapters.

CHAPTER V
The Association between OCT-1 Activity and COX-2 in CP-CML Patients

5.1.   Introduction

Cyclooxygenase (COX), also known as Prostaglandin H synthase (PTGS), is the key enzyme responsible for the oxidation of arachidonic acid to prostaglandin and other eicosanoids (204, 205). So far, two isoforms of COX have been identified and are referred to as COX-1 (PTGS1) and COX-2 (*PTGS2*), which differ in many respects. COX-1 is expressed constitutively in most tissues and controls normal physiological functions such as regulation of renal blood flow and maintenance of the gastric mucosa (206). COX-2, on the other hand, is not expressed under normal conditions in most cells. It is induced by a variety of stimuli (i.e., tumour necrosis factor alpha, interleukin 1β), growth factors (i.e.m epidermal growth factor) or tumour promoters (i.e., bile acids) (207).

The COX enzymes are responsible for catalyzing the conversion of arachidonic acid to prostaglandins by a series of radical reactions. As shown in Figure 5.1, COX-2 firstly converts arachidonic acid into PGG2 which is rapidly reduced to PGH2 in the peroxidase active site. PGH2 is later converted into a variety of biologically active prostaglandins (PGD2, PGE2, $PGF_{2\alpha}$), prostacyclin (PGI2), or thromboxane A_2 by tissue-specific isomerases (205, 208). Notably, by the elimination of two molecules of water, PGD2 can be further dehydrated into 15-deoxy-Δ12,14-Prostaglandin J2 (15d-PGJ2), which is a potent endogenous PPARγ ligand (209, 210).

Over the past decade, COX has been shown to be a therapeutic target for preventing cancer in a series of studies. Epidemiologic and experimental studies have shown that aberrant induction of COX-2 and up-regulation of the prostaglandin cascade plays a significant role in carcinogenesis (211-217). This is most likely due to the accumulation of known COX-2 inducers (oncogenes, growth factors, and tumour promoters) in both pre-malignant tissues and malignant tumours (218-220). Moreover,

Figure 5.1   An overview of Cyclooxygenase pathway

Arachidonic acid is a polyunsaturated fatty acid that constitutes the phospholipid domain of most cell membranes and is liberated from the cellular membranes by cytoplasmic phospholipase A2 (PLA2). Free arachidonic acid can be metabolized through the cyclooxygenase (COX) pathways. In the COX pathway, the key step is the enzymatic conversion of arachidonic acid to the intermediate prostaglandin G2 (PGG2), which is then reduced to an intermediate PGH2 by the peroxidase activity of COX. PGH2 is sequentially metabolized to prostanoids, including prostaglandins (PGs) and thromboxanes (TXs) by specific prostaglandin and thromboxane synthases. Each of the prostaglandins exerts its biological effects by binding to its cognate G protein-coupled receptor. PGI2 can transactivate the nuclear peroxisome proliferator-activated receptor-δ (PPARδ), and a PGD2 dehydration product, 15d-PGJ2, is a natural ligand for PPARγ. (Figure modified from Wang et al. 2010)
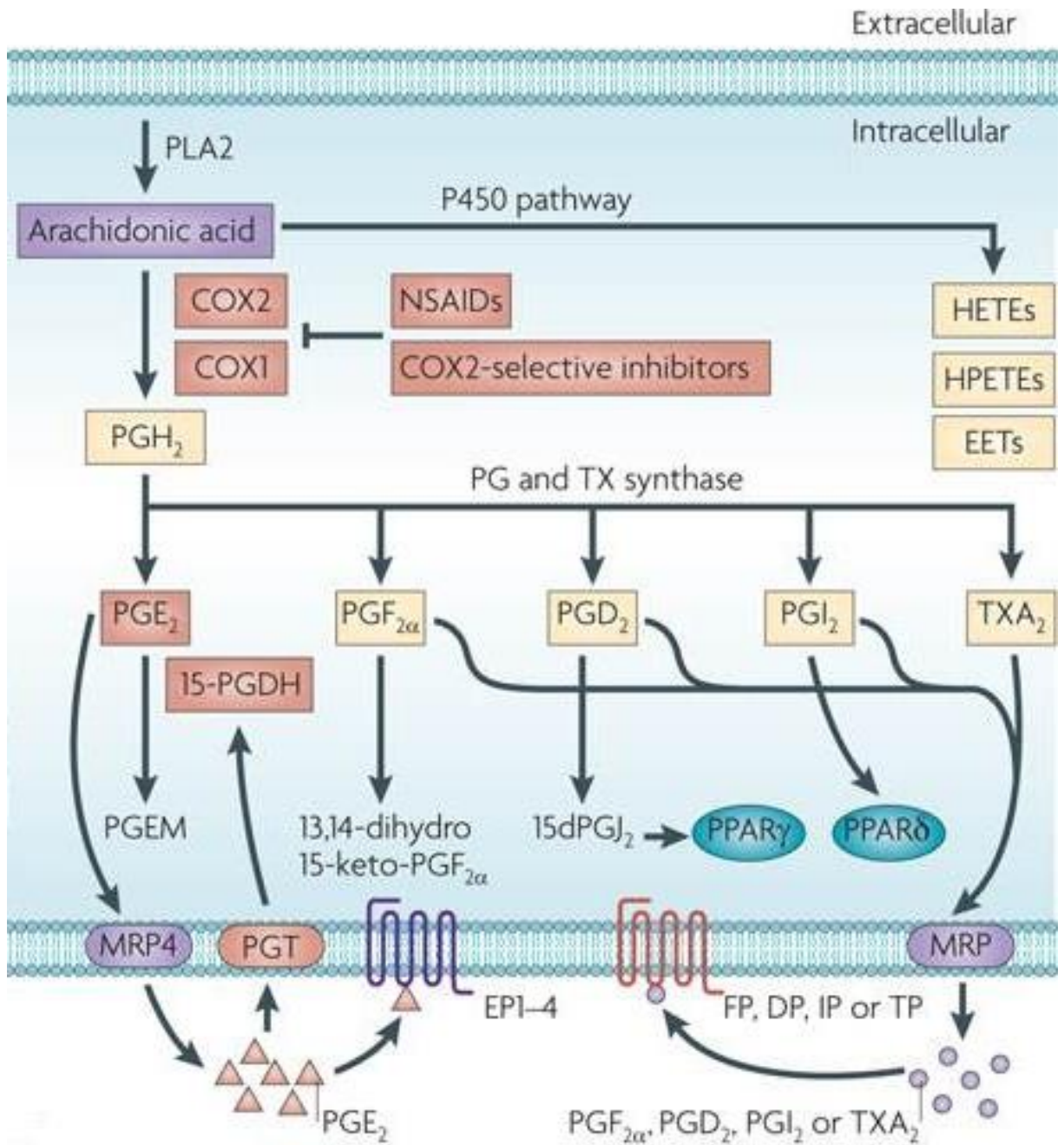
the status of the p53 tumour suppressor gene has also been suggested as a determinant of COX-2 expression(221, 222). Genetic studies have shown that overexpressing the human *PTGS2* gene in the mammary glands of transgenic mice is sufficient to induce tumour growth (223). In addition, knocking out the *PTGS2* gene in a mouse model reduced the tumour burden in a gene-dose dependent way (224, 225). Pharmacological evidence also implicates COX-2 in carcinogenesis. Either alone or in combination with other chemotherapeutic agents, selective COX-2 inhibitors such as celecoxib and rofecoxib reduced the formation of tumours (226) and suppressed the growth of a variety of established solid tumours (227-229).

The mechanism by which COX-2 contributes to cancer has been suggested to be mediated by its effect on many processes. The prostaglandins generated by COX-2 may induce expression of angiogenic factors including vascular endothelial growth factor (VEGF), basic fibroblast growth factor (bFGF), transforming growth factor-β (TGF-β) and interleukin 6 (230-233). Recent data suggests that the anti-tumor effects of COX-2 inhibitors are partially associated with the suppression of VEGF- or bFGF-induced angiogenesis (233-235). Overexpression of COX-2 has been shown to increase the migration of endothelial cells by reducing cellular attachment to the extracellular matrix (ECM) (236, 237). In addition, overexpression of COX-2 may reduce apoptosis by decreasing the amount of the pro-apoptotic proteins, Bcl-XL, and Bax, thereby increasing amounts of Bcl-2 (236, 238). COX-2 may also promote resistance to chemotherapeutic drugs by increasing the expression and function of one of the efflux pumps associated with the transport of chemotherapeutic drugs, ABCB1 (239). In human breast tumour specimens, immunohistochemical analyses revealed a strong correlation between gene expression levels of *PTGS2* and *ABCB1*. It was therefore postulated that increased prostaglandin production by Cox-2 induces PKC and the expression of transcriptional factor c-Jun, which in turn up-regulated the

expression of ABCB1 (240).

The vascularity of the bone marrow and plasma levels of angiogenic factors have been found to be significantly elevated in a number of haematological malignancies including CML (241). Increased bone marrow angiogenesis has been shown to be associated with an adverse prognosis in CML patients (242). Thus, COX-2 has been postulated to be an important protein in the pathophysiology of CML due to its involvement in angiogenesis as descried previously. Although the involvement of COX-2 in angiogenesis has been well studied in solid tumours, knowledge about the role of COX-2 in CML remains limited.

Several studies have also investigated the effect of COX-2 inhibitors on BCR-ABL positive cell lines. In K562 cells, treatment with the COX-2 inhibitor celecoxib reduced cell growth as a result of cell cycle arrest, caspase-3 activation and possibly inhibiting NF-kB (184). In imatinib-resistant K562 cells (IR-K562) with no detectable mutations in the Abl kinase domain, overexpression of COX-2 and ABCB1 was shown to play a role in the development of resistance to imatinib (185). Compared to the parental K562 cells, IR-K562 were more sensitive to treatment with celecoxib. Either alone or in combination with imatinib, celecoxib induced apoptosis by inhibition of COX-2 and ABCB1 through the Akt/p-Akt signaling pathway. Furthermore, celecoxib exhibited a synergistic effect with imatinib by causing apoptosis in CML bone marrow cells (202).

In addition, expression of *PTGS2* was found to be significantly higher in imatinib non-responders compared to responders in gene expression profiling of CD34^{+} cells from imatinib-naive chronic phase chronic myeloid leukaemia (CP-CML) patients (243). Giles *et al* also showed that the levels of COX-2 was significantly higher in CML BM cells compared with normal donor cells using western blot and solid-phase radioimmunoassay (183). Furthermore, increasing levels of COX-2 were also significantly associated with shorter survival.

While OCT-1 activity (OA) is a strong indicator of molecular responses in *de novo* CML patients, the association between COX-2 and OA in CML cells remains unclear. Our group has previously demonstrated that the OA in mononuclear cells is strongly related to cell lineage, and that the OA in monocytes is significantly lower than in neutrophils (244). Since COX-2 is enriched in monocytes/macrophage after stimulation (245), this suggests a potential role for COX-2 in OA regulation.

To understand whether COX-2 and its metabolite are involved in the variation of OA, this chapter investigates the relationship between COX-2 and OA in primary leukaemic cells by assessing the *PTGS2* expression and levels of PGE2. The patient plasma levels of 15d-PJG2 were also assessed and compared with OA in the present chapter. Since this prostaglandin share a common target (PPARγ) with the OA enhancer diclofenac, its correlation with OA might indicate the possible the involvement of PPARγ in OA regulation. Secondly, these studies sought to ascertain whether *PTGS2* expression level or prostaglandin levels are prognostic indicators. Due to limitations of the IUR and OA assay (predominantly the safety and availability of ^{14}C-labeled imatinib), these studies had the additional objective to provide transferable method for measurement of OA which can be easily adopted into other diagnostic laboratories.

5.2. Methods

5.2.1. Examination of PTGS2 gene expression in primary samples

As described previously in Section 2.6.1, the IUR and OA were measured in cryopreserved and subsequently thawed peripheral blood mononuclear cells (PB-MNC) collected from CML patients at diagnosis. To investigate the possibility of an alternative to OCT-1 activity measurement, total white cells (TWC) freshly isolated from the PB of CP-CML patients at diagnosis were used in these studies due to the

simple preparation procedure. The gene expression level of *PTGS2* in each TWC sample was assessed using RQ-PCR and expressed as a percentage of the reference gene, the human TATA box binding protein (hTBP). *PTGS2* expression in MNC of CP-CML patients at diagnosis was also evaluated using Affymetrix GeneChip® Human gene 1.0 ST array as described in Section 2.6.4. The levels of *PTGS2* expression in TWC by RQ-PCR and in MNC by microarray were compared with OA and molecular response where data was available.

5.2.2. Examination of plasma levels of PGE2 and 15d-PGJ2

Plasma samples were collected from the PB of CP-CML patients at diagnosis and stored at -70°C. The PGE2 and 15d-PGJ2 levels in plasma samples were detected by an immunoassay as described in Section 2.6.5 and Section 2.6.6. The PGE2 and 15d-PGJ2 plasma levels were then compared with OA and molecular response data where available.

5.3. Results

5.3.1. PTGS2 expression in CML patients

The *PTGS2* expression levels were first measured TWC collected from CML patients at the time of diagnosis. As shown in Figure 5.2A, there was substantial variation in *PTGS2* expression in CML patients (average 959.3%, range from 0 to 5196%). 3 out of 78 patients (4.1%) displayed no or extremely low level of *PTGS2* expression by RQ-PCR. The *PTGS2* expression level was also measured in 10 TWC samples from normal donors. Variation was also observed in normal donor samples (average 723.8%, range from 68.61 to 1786%). No significant difference was observed when comparing the *PTGS2* mRNA levels in CML samples to that of normal donors (p=0.46).

The gene expression of *PTGS2* was also analysed in CML MNC. However due to the

A

B
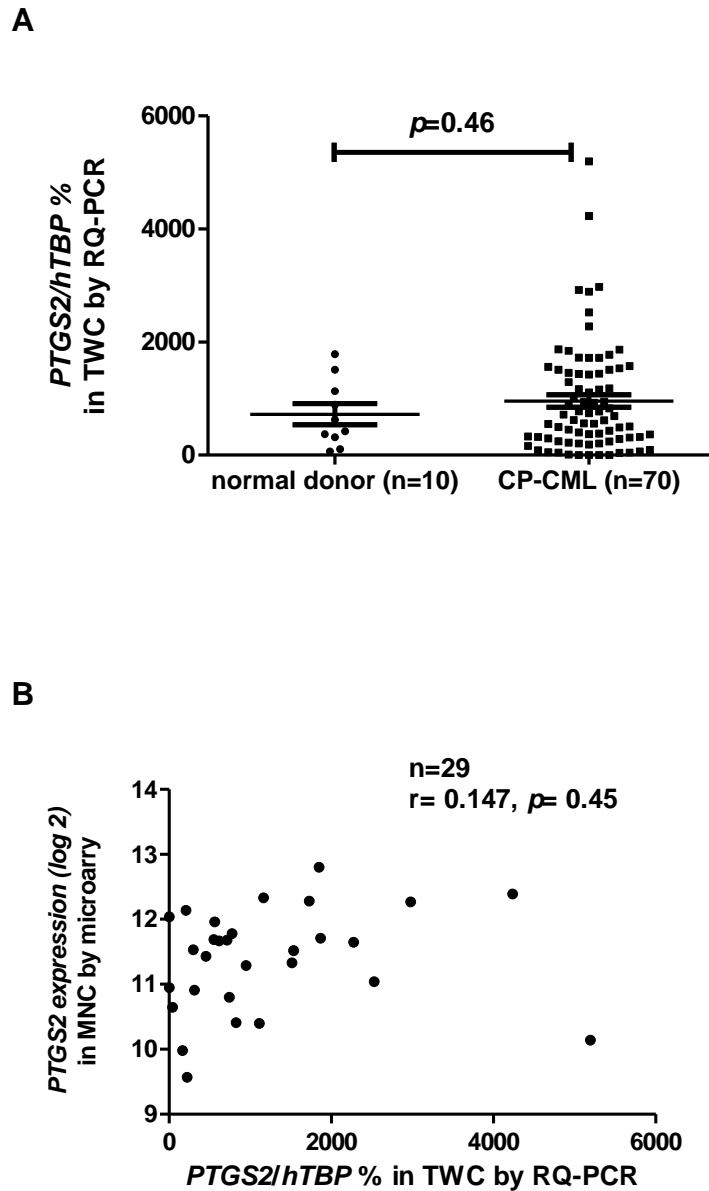
Figure 5.2 *PTGS2* **expressions in normal donors and CP-CML patients at diagnosis**

A: The *PTGS2* expression levels in 70 CML TWCs samples and 10 normal donor TWCs samples were assessed by RQ-PCR and expressed as a percentage of the reference gene hTBP. The error bars represent the mean ± the standard error of the mean. **B:** The *PTGS2* gene was also assessed in 80 CML MNCs samples by Affymetrix GeneChip® Human gene 1.0 ST array and presented as log2 expression. 29 out of 80 patients had matched RQ-PCR results for *PTGS2* expression.

limitation of the samples cells, available microarray data source from Gene Expression Profiling (GEP) of MNC from CP-CML patients (n=80) from our group were used instead of RQ-PCR assay. The relationship between *PTGS2* expression in TWC and in MNC was then determined. In 29 samples with matched data from both assays, no significant correlation was observed in *PTGS2* expression between the two cell populations (r= 0.147, *p*= 0.45, Figure 5.2B).

5.3.2. PGE2 and 15d-PGJ2 levels in CML patients

Since PGE2 is a prostaglandin product which is produced from the conversion of arachidonic acid by COX-2, PGE2 levels provide an indication of COX-2 activity (Figure 5.1). An ELISA assay was performed to determine the amount of PGE2 in plasma collected from CML patients at diagnosis. In 24.2% (36 out of 150) of CML samples, PGE2 was undetectable (with optical density equal to or lower than the zero standards wells). In normal donors, 6 out of 16 samples had undetectable PGE2 (37.5%). As shown in Figure 5.3A, CML plasma samples had significantly higher levels of PGE2 than normal samples (average 132.8 vs. 48.0 pg/mL, *p*=0.043), suggesting greater COX-2 enzyme activity in CML patients.

15d-PGJ2 is another prostaglandin product of COX-2 activity. Furthermore, 15d-PGJ2 is a potent endogenous PPARγ ligand which might share the same targets as diclofenac, which is a known COX-2 and PPARγ inhibitor, and play a role in OA regulation in CML cells (Figure 5.1). Therefore, 15d-PGJ2 was measured in plasma samples collected from 17 normal donors and 150 CML patients at diagnosis. As shown in Figure 5.3B, CML patients at diagnosis had significantly higher levels of plasma 15d-PGJ2 (average 2673 pg/mL) compared with the normal donors (average 878.7 pg/mL, *p*=0.0009). Unexpectedly, no significant association was observed between PGE2 and 15d-PGJ2 (r=0.103, *p*=0.21, Figure 5.3C), even though they are both products of COX-2 activity.
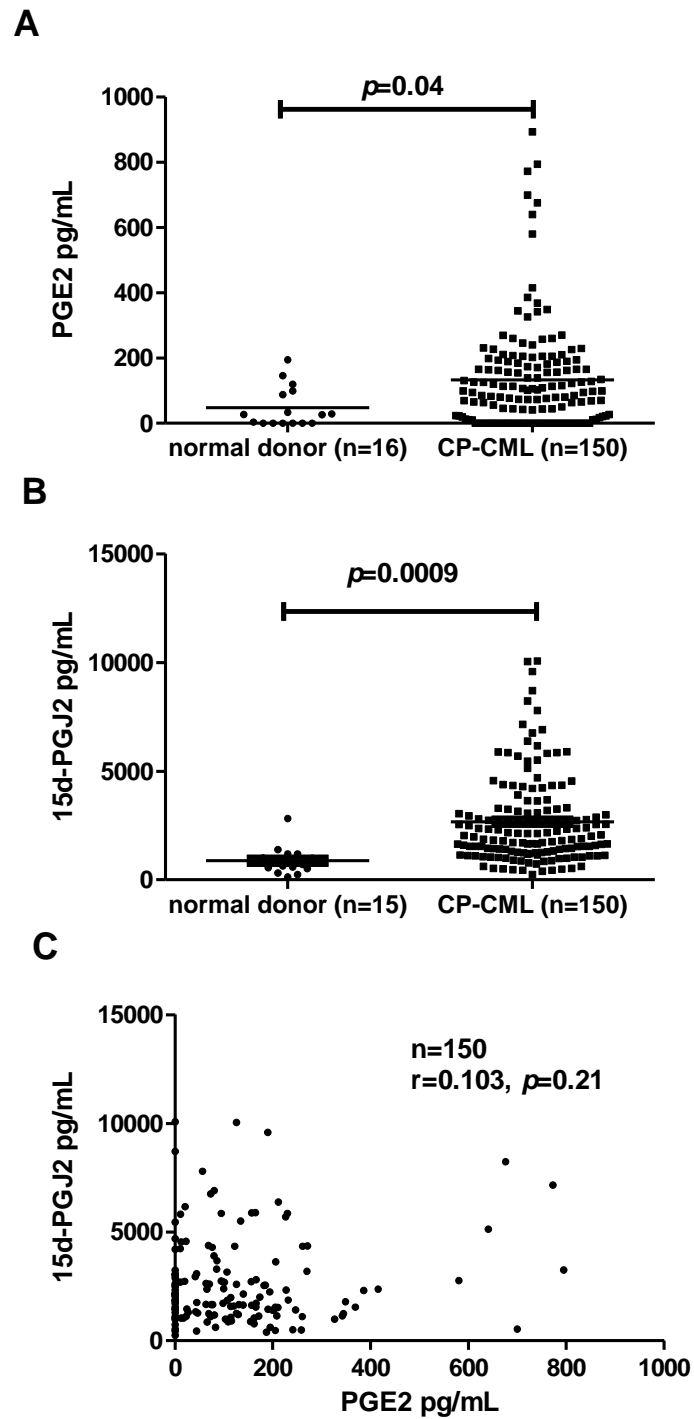
Figure 5.3   Plasma levels of PGE2 and 15d-PGJ2 in normal donors and CP-CML patients at diagnosis

The plasma levels of PGE2 **(A)** and 15d-PGJ2 **(B)** were assessed by ELISA assay in 150 CML samples compared with normal donor samples. The error bars represent the standard deviation of the mean. **C:** The association between the two COX-2 products were examined in CML samples.

5.3.3. Correlation of PTGS2 expression and PGE2/15d-PGJ2 plasma levels

Since PGE2 and 15d-PGJ2 are both converted from arachidonic acid by COX-2, the correlation between the expression of *PTGS2* (COX-2 encoding gene) and the two metabolic products of COX-2 was examined in CP-CML samples. No significant correlation was observed when comparing plasma levels of PGE2/15d-PGJ2 with *PTGS2* expression in either TWC samples (r=-0.132, *p*=0.39 and r=0.118, *p*=0.44, respectively, Figure 5.4A and B,) or MNC samples (r=0.006, *p*=0.97 and r=0.250, *p*=0.11, respectively, Figure 5.4C and D).

5.3.4. Correlation of OCT-1 Activity with PTGS2 expression, PGE2 and 15d-PGJ2 levels

As mentioned previously, OA is a significant predictor of response in CP-CML patients treated with imatinib (62). To determine whether the *PTGS2* expression levels can be used as a surrogate measurement for OA, *PTGS2* expression in CML patients at diagnosis was compared with the patients' OA. Using Pearson product-moment correlation, no significant correlation was observed between TWC *PTGS2* expression and OA (r=-0.010, *p*=0.93, Figure 5.5A). The CML patient data was then grouped into low and high OA groups by using the median OA of 7.2 ng/200,000 cells as previously defined (140). No significant difference in TWC *PTGS2* expression level was observed when comparing the low OA group (average 943.8%, n=68) to the high OA group (average 1141%, n=9, *p*=0.57, Figure 5.5B). Previous studies from our group have demonstrated that patients with lowest quartile of OA (Q1, defined as patients with OA lower than 4 ng/200,000 cells) achieve significantly poorer response than those in all other quartiles (140). Therefore, patient data were segregated into a Q1 only group, and a Q2-4 group, and the TWC *PTGS2* expression level was then compared between these two groups. As shown in Figure 5.5C, in the 78 CML TWC samples assessed, the average *PTGS2* expression level in Q1 patients was not

Figure 5.4   Correlation of *PTGS2* expression and plasma levels of PGE2/15d-PGJ2 in CP-CML patients at diagnosis

Pearson product-moment correlation was used to determine the relationship between TWC *PTGS2* expression and **(A)** plasma PGE2 levels **(B)** or 15d-PGJ2 levels in 45 CML samples. The association between MNC *PTGS2* expression and PGE2 **(C)** or 15d-PGJ2 **(D)** levels was also examined in 43 CML samples.

A

n=45
r=-0.132, *p*=0.39

B

n=45
r=0.118, *p*=0.44

C

n=43
r= 0.006, *p*=0.97

D

n=43
r=0.250, *p*=0.11

137

A

B

C
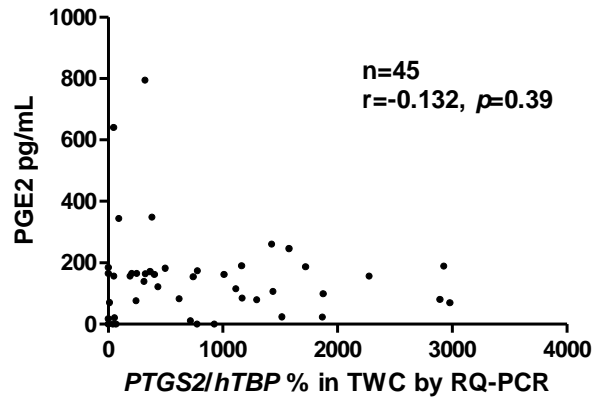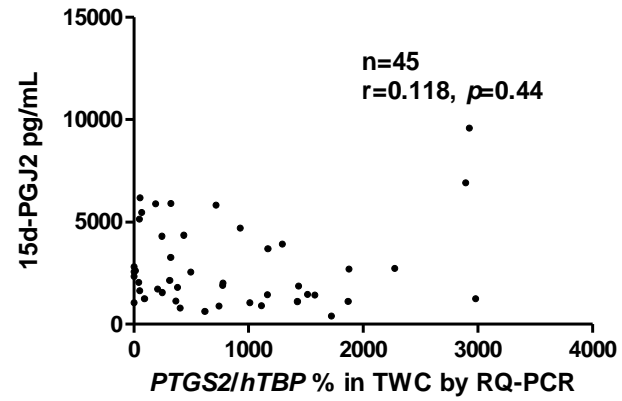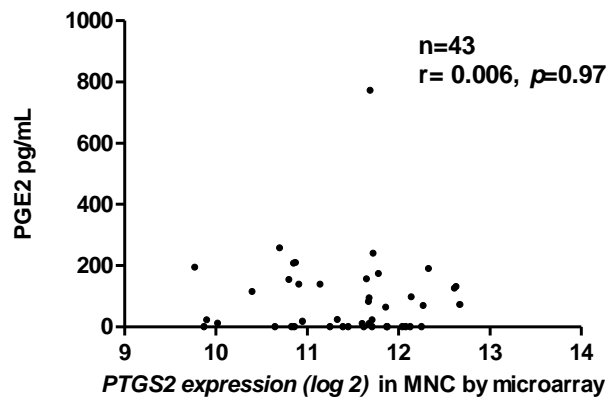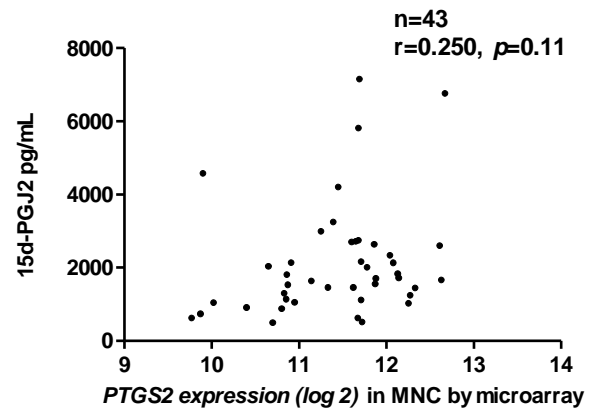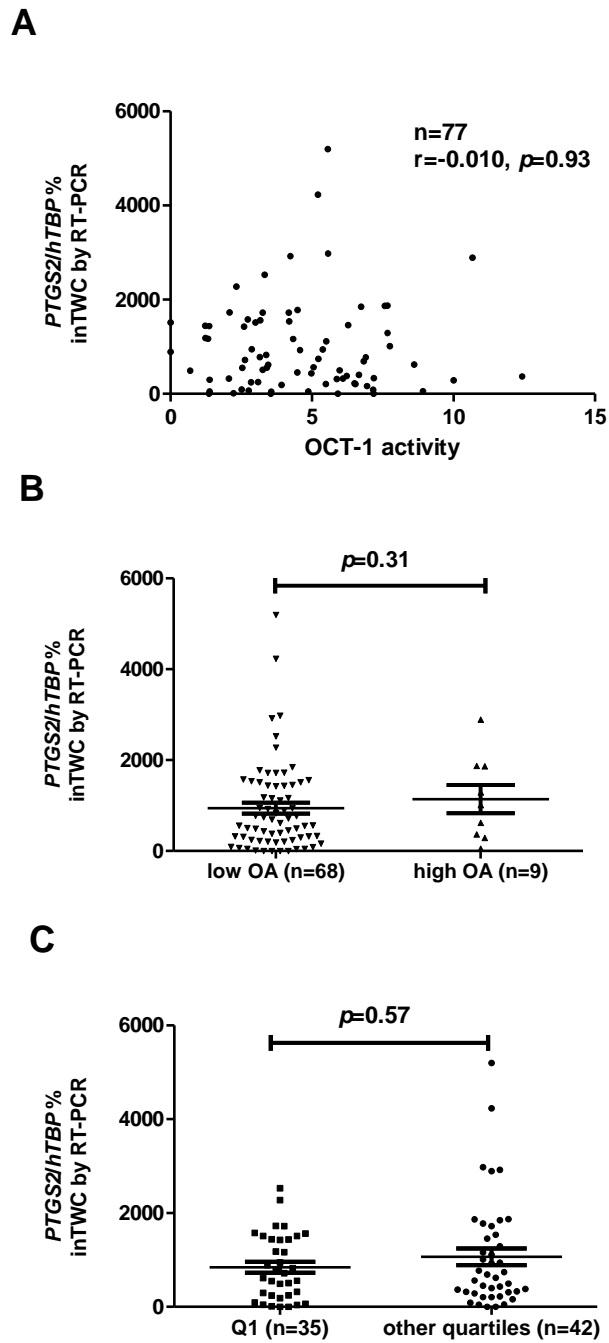
Figure 5.5   Relationship between OCT-1 activity and *PTGS2* expression levels in total white cells in CP-CML patients at diagnosis

A: The link between TWC *PTGS2* expression and OA was assessed in 77 CP-CML patients by Pearson product-moment correlation. **B:** The *PTGS2* expression levels in TWC were compared between high and low OA groups. **C:** The *PTGS2* expression levels in TWC were compared between Q1 patients and Q2-4 patients. The error bars represent the standard deviation of the mean.

significantly different from the other quartiles (1070% vs. 843.4%, *p*=0.31).

The OA was also compared with MNC *PTGS2* expression levels in microarray data in 80 CP-CML samples. Similarly to the previous results, there was no significant association between OA and MNC *PTGS2* expression (r=-0.205, *p*=0.07, Figure 5.6A). In addition, no significant difference was observed in *PTGS2* expression between high and low OA groups (*p*=0.11, Figure 5.6B) or between patients with Q1 OA and others (*p*=0.19, Figure 5.6C).

Although there was no obvious relationship between COX-2 transcript/protein levels and OA, it is possible that a measure of COX-2 activity may provide a better association between OA and COX-2. Therefore, the levels of two products of COX-2 enzyme, PGE2 and 15d-PGJ2, were correlated with OA.

A total of 150 plasma samples were assessed for PGE2 levels, however there was no correlation with the corresponding OA value (r=-0.095, *p*=0.25, Figure 5.7A). There was also no significant difference in the plasma PGE2 levels when comparing low and high OA groups (*p*=0.34, Figure 5.7B) or when comparing the OA of Q1 with the other quartiles (*p*=0.72, Figure 5.7C).

The relationship between OA and 15d-PGJ2 plasma levels was also examined. A weak but significant correlation between OA and plasma 15d-PGJ2 levels was observed in CML patients at diagnosis (r=-0.16, *p*=0.045, Figure 5.8A). When patient data was divided into high and low OA groups, there was no significant difference in 15d-PGJ2 levels between the two groups (low OA group average 2747 pg/mL; high OA groups average 2331 pg/mL; *p*=0.34, Figure 5.8B). However, the average 15d-PGJ2 level was significantly higher in Q1 patients when compared to patients from other quartiles (average 3094 pg/mL vs. 2323 pg/mL, *p*=0.02, Figure 5.8C).

A

B

C
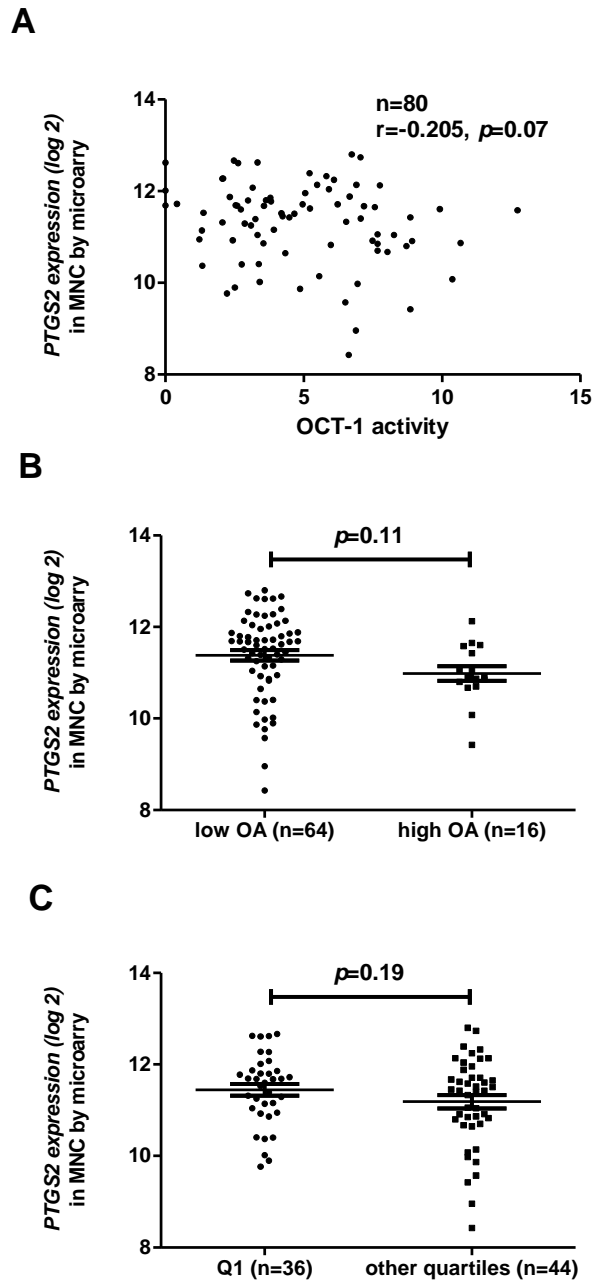
Figure 5.6   Relationship between OCT-1 activity and *PTGS2* expression levels in mononuclear cells in CP-CML patients at diagnosis

A: The link between MNCs *PTGS2* expression and OCT-1 activity was assessed in 80 CP-CML patients. **B:** The *PTGS2* expression levels in MNCs were compared between high and low OA groups. **C:** The *PTGS2* expression levels in MNCs were compared between Q1 patients (OA< 4 ng/200,000 cells) and others. The error bars represent the standard deviation of the mean
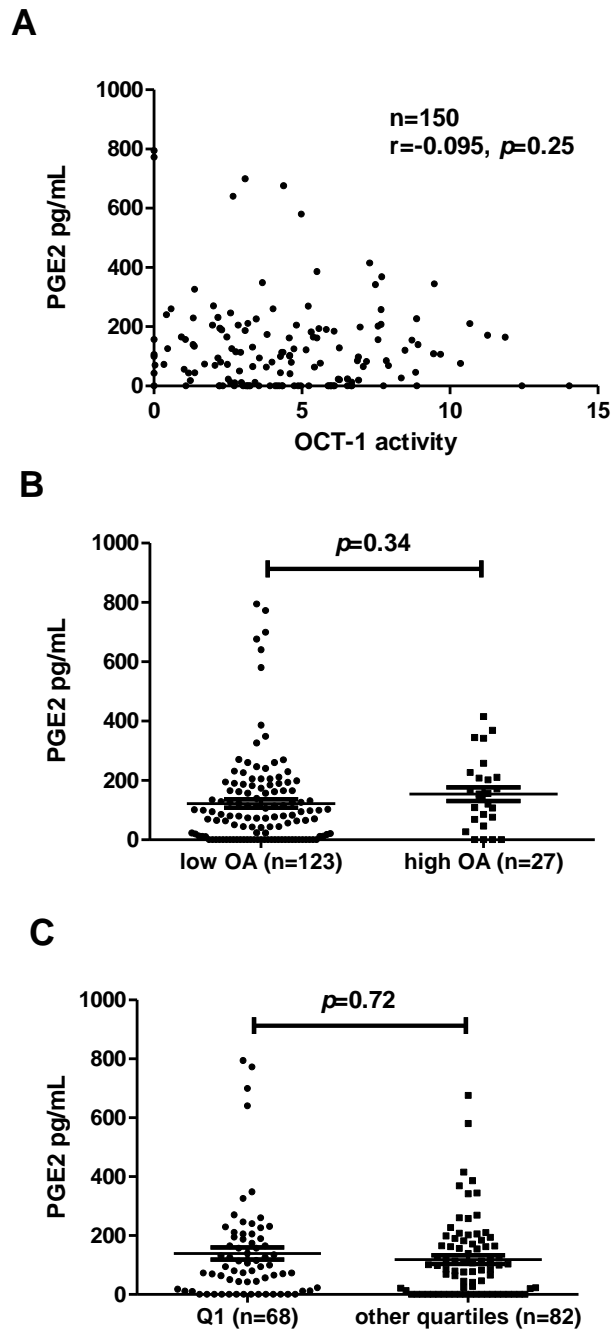
Figure 5.7 Relationship between PGE2 and OCT-1 activity in CP-CML patients at diagnosis

A: The link between PGE2 and OA was assessed in 150 CP-CML patients at diagnosis. **B:** The PGE2 levels were compared between low and high OA groups. **C:** The PGE2 levels were compared between Q1 patients (OA< 4 ng/200,000 cells) and others. The error bars represent the standard deviation of the mean.

A

B

C
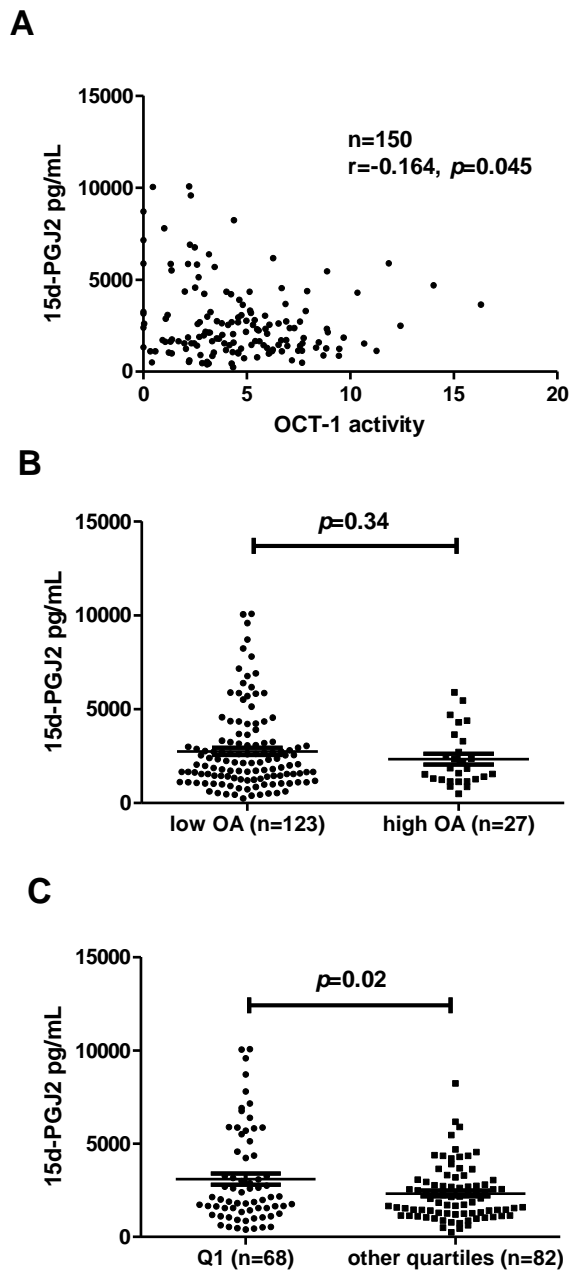
Figure 5.8 Relationship between 15d-PGJ2 and OCT-1 activity in CP-CML patients at diagnosis

A: The association between 15d-PGJ2 levels and OA were assessed in 150 CP-CML patients at diagnosis. **B:** The 15d-PGJ2 levels were compared between high and low OA groups. **C:** The 15d-PGJ2 levels were compared between Q1 patients (OA< 4 ng/200,000 cells) and others. The error bars represent the standard deviation of the mean.

5.3.5. Correlation of Molecular Response to imatinib and PTGS2 expression, PGE2 and 15d-PGJ2

Previous gene expression profiling data showed that the levels of *PTGS2* in CD34$^+$ cells was significantly higher in non-responders at diagnosis (failing to achieve partial cytogenetic response by 12 month imatinib therapy) compared with responders (243). Therefore, the correlation of expression levels of *PTGS2* in either TWC or MNC and patients' molecular response was analysed.

Among all 78 CML samples assessed for TWC *PTGS2* expression levels, 73 patients had been followed up to 12 months. Patient data was divided based on the major molecular response (MMR) achievement. As shown in Figure 5.9A, there was no difference in the *PTGS2* expression in TWC between two groups (*p*=0.10). Similar result was also observed in 52 patients with matched MNC *PTGS2* expression result and 12 months MMR data (*p*=0.08), indicating the gene expression of *PTGS2* was no likely a predictor for molecular response.

The association between PGE2 or 15d-PGJ2 levels and MMR was also analysed in 136 patients with matched plasma prostaglandin results and molecular response data. However, no difference was observed in PGE2 plasma levels (Figure 5.9C, *p*=0.56) between the patients who achieved MMR by 12 months imatinib therapy and those who did not. Similar result was also found when assessed the 15d-PGJ2 levels in two groups (Figure 5.9D, *p*=0.64).

5.4. Discussion

COX-2 has long been regarded as a potential therapeutic target in many solid tumours (211-220). Recently, the involvement of COX-2 in CML has been suggested in several studies, which have shown carcinogenesis effects using COX-2 specific

Figure 5.9   Relationship between the molecular response and *PTGS2* expression, PGE2 and 15d-PGJ2

The achievement of MMR by 12 month in CML patients was compared with the PTGS2 expression in TWC samples (**A**), PTGS2 expression in MNC samples (**B**), PGE2 (**C**) and 15d-PGJ2 (**D**) plasma levels when the follow up data was available. The error bars represent the standard deviation of the mean.

A
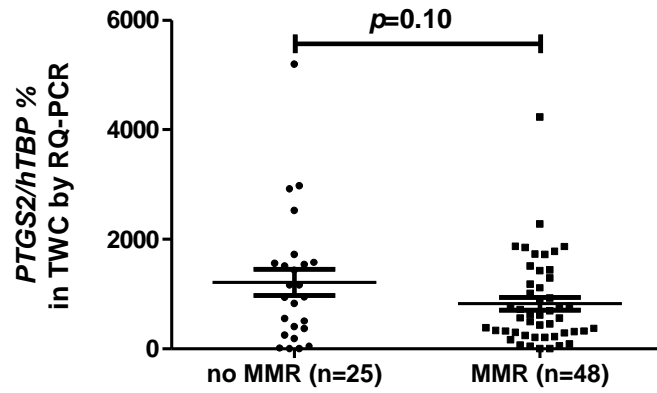
B
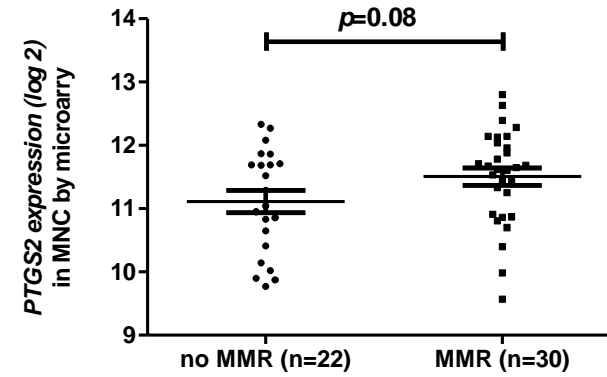
C
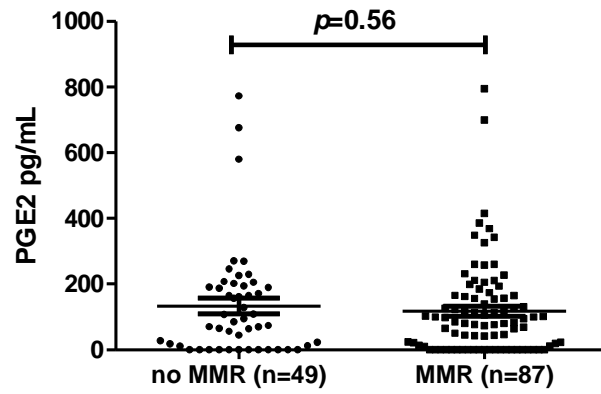
D
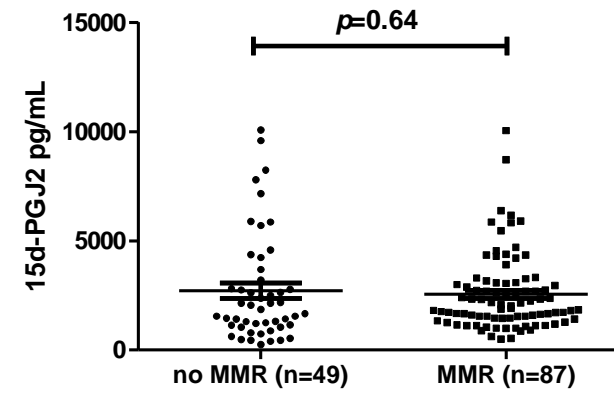
inhibitors (184, 185, 202). It has also been reported that over expression of COX-2 in bone marrow cells is linked with poor survival in CML patients (183). Given the importance of functional OA in predicting patient response to imatinib therapy, understanding the potential association between COX-2 and OA is crucial.

In this chapter *PTGS2* expression levels were first determined in normal donors and CML patients. In 78 CML samples, the *PTGS2* expression in TWC was highly variable and was not significantly different from that in normal samples. This result suggests that *PTGS2* expression in TWC is not important for the development or maintenance of CML. The fact that increased COX-2 protein levels have been detected in CML BM cells (183) does not contradict the results presented herein, as different material was used (BM vs. TWC from peripheral blood). In addition, the expression of mRNA does not necessarily reflect the presence or level of the corresponding protein. Using GEP data, *PTGS2* expression was also determined in MNC from CP-CML patients. Comparing *PTGS2* expression between TWC and MNC, no correlation was observed possibly due to the presence of a large proportion of granulocytes in the TWC. In addition, the composition of the cell population in MNC may also have changed after a freeze/thaw process, while the TWC used in the present chapter were freshly isolated. This conclusion should however be interpreted cautiously as the inter-assay reliability might need to assessed by comparing PCR and microarray results using same cell population.

The predictive value of *PTGS2* expression was also assessed in this study by comparing these results with the OA. No significant association was observed between TWC *PTGS2* expression and OA. Since OA is determined using MNC and is strongly associated with cell lineage (244), the MNC *PTGS2* expression level was then compared to OA, however, no significant correlation was observed. Therefore, it is unlikely that *PTGS2* expression can be used as a surrogate marker for OA.

Whether the *PTGS2* expression in either TWC or MNC can be used to predict response to imatinib treatment was also investigated retrospectively in this chapter. The comparison of MMR achievement by 12 months or 24 months showed no significant difference between high and low *PTGS2* expression groups. This result is in contrast with previous gene expression profiling data using CD34$^+$ cells, where elevated levels of *PTGS2* were found in non-responders (defined as those who failed to achieve at least a partial cytogenetic response within 12 months of imatinib therapy) (243). Again, the disagreement is most likely due to the different cell population (CD34$^+$ cells vs. TWC/MNC) and possibly the different response achievement (PCyR vs. MMR) used.

Due to the limitation of the available amount of primary CML cells, the protein level of COX-2 was not assessed in the present study. To directly investigate COX-2 enzyme activity in the setting of CML, the levels of the COX-2 metabolic product PGE2 were evaluated in plasma collected at diagnosis. In some plasma samples, PGE2 was undetectable and the frequency of this occurrence was higher in normal donors (24.2% in CML vs. 37.5% in normal). In addition, the CML samples had significantly higher plasma levels of PGEs when compared with normal, suggesting that COX-2 is more active in CML cells. Elevated PGE2 has been reported in many different tumours (230, 246-248), including acute myeloid leukaemia (249). Although the role of PGE2 in CML is unclear, some studies suggest that PGE2 contributes to the process of leukemogenesis. For example, a number of groups reported that long-term exposure to PGE2 inhibited progenitor cell differentiation *in vitro* (250, 251). In more recent studies using zebrafish embryos, knockdown of PGE2 synthase resulted in decreased numbers of hematopoietic stem cells. Furthermore, high concentrations of PGE2 had an inhibitory effect on differentiation in the murine embryonic stem cell (252, 253). Therefore, the observation of increased PGE2 levels in CP-CML samples in this

chapter is consistent with previous studies.

Despite the elevated PGE2 levels in CML, no significant correlation between PGE2 and OA was observed in CML patients, suggesting that PGE2 is not a determinant of OA. This result is in agreement with the results in Chapter 3, which showed that non-steroidal anti-inflammatory drugs (NSAIDs) including the COX-2 inhibitors celecoxib and rofecoxib had no significant effect on OA regulation. Furthermore, there was no significant difference in PGE2 plasma levels between patients who achieved MMR and those who failed to achieve MMR by 12 or 24 months. Similar to *PTSG2* expression levels, PGE2 plasma levels were not predictive of the achievement of MMR in CML patients treated with imaitnib.

One study has previously reported that PPARγ acting as a transcription factor is responsible for OCT-1 regulation (197). Furthermore, the OA enhancer diclofenac is a known PPARγ ligand (200). In a study conducted by our group, monocytes, in which PPARγ is abundantly expressed (254-256), were found to have significantly lower OA than neutrophils (244). Since the COX-2 protein is also enriched in monocytes/macrophage (245), and one of the COX-2 enzymatic products 15d-PGJ2 is a potent intrinsic PPARγ ligand, it was hypothesised that there might be an association between PPARγ and OA via 15d-PGJ2. Therefore, the plasma level of 15d-PGJ2 was examined in CML patients to further investigate the potential role of prostaglandins in CML.

Similar to PGE2, the 15d-PGJ2 plasma levels were significantly higher in CML cohorts compared to normal samples. It appears that CML patients may be characterised by increased plasma levels of PGE2 and 15d-PGJ2. Although the transcript level of *PTGS2* remains unchanged in CML compared to normal, the production of prostaglandins might be the result of increased COX-2 protein in CML patients as previously reported (183).

Of interest, a significant correlation between 15d-PJG2 and OA was observed. Although there was no significant difference in 15d-PGJ2 levels when comparing low and high OA groups, levels were significantly elevated in patients with the lowest OA (Q1, OA<4 ng/200,000 cells) when patient data was grouped based on quartiles of OA. Given the potent ability of 15d-PGJ2 to activate PPARγ, these results highlighted the possible negative effect on OA mediated by 15d-PGJ2 via the PPARγ pathway (Figure 5.1). The role of PPARγ in OA regulation will be further investigated in experiments described in Chapter 6.

Having discovered an association between 15d-PGJ2 and OA, the predictive value of 15d-PGJ2 for patient response was evaluated using 12 and 24 month MMR data. Similarly to PGE2, patients with low or high 15d-PGJ2 were equally likely to have achieved MMR at these time points. Therefore, while 15d-PGJ2 levels are weakly correlated with OA, these values are not likely to be used as an effective predictor of molecular response in CML patients treated with imatinib.

The relationship between *PTGS2* expression levels and plasma levels of the two prostaglandins were also investigated in this chapter, however no significant association was found between these three variables. Unexpectedly, there was no association between the levels of PGE2 and 15d-PGJ2. These findings indicate that a number of factors including different prostaglandin synthesis enzymes may contribute to the variation between CML patients. While PGE2 was undetectable in several normal and CML samples, 15d-PGJ2 was detectable in all the samples examined, suggesting a preferential enhancement of the 15d-PGJ2 pathway over the PGE2 pathway in CML cells or a selective down-regulation of PGE2 (Figure 5.1).

In conclusion, while the expression of *PTGS2* in CML TWC remained at a similar level to normal, the PGE2 and 15d-PGJs levels in plasma samples at diagnosis were significantly higher in CML patients. Although no significant correlation was found

149

between *PTGS2* expression or PGE2 levels and OA, a significant association was observed between 15d-PJG2 and OA. Furthermore, significantly higher levels of 15d-PGJ2 were detected in patients with the lowest OA, suggesting potential negative involvement of 15d-PGJ2 and its targets in OA regulation. Despite the increased levels of PGE2 and 15d-PGJ2 in CML plasma, neither of them was sufficient to identify patients who would respond poorly to imatinib. Nevertheless, further investigation of 15d-PGJ2 and its ligand, PPARγ, may reveal important aspects of the molecular mechanisms regulating OA.

CHAPTER VI
The Association between OCT-1 Activity and PPARγ in CP-CML Patients

6.1.   Introduction

Peroxisome Proliferator-Activated Receptors (PPARs) are a family of transcription factors that regulate several metabolic pathways in a tissue-selective manner (257). There are three PPAR family members encoded by distinct genes designated as PPARα, PPARδ, and PPARγ (258). All PPARs form heterodimers with another nuclear receptor, the 9-*cis*-retinoic acid receptor (RXR). The PPAR/RXR heterodimer regulates target genes transcription by binding to the peroxisome proliferator response element (PPRE) on the promoters of target genes (258, 259). DNA binding domains of PPARs are highly conserved, while the ligand-binding domains of PPARs have a slightly lower level of conservation across the subtypes. The N-terminal region of PPARs is responsible for the differences in the biological function of the PPAR family members.

Of the three PPAR subtypes, PPARγ has been studied most extensively in diverse biological pathways and disease conditions such as insulin sensitivity, type 2 diabetes, atherosclerosis, and cancer. Human PPARγ locates to chromosome 3p25 and contains at least 11 exons (260). Tissue distribution differs between the PPARγ isoforms in normal tissue. PPARγ1 shows almost ubiquitous expression at low levels. PPARγ2 is predominantly expressed in adipose tissue and PPARγ3 is restricted in the colon, adipose tissue and macrophages (261, 262). However, the functional significance of the multiple isoforms of PPARγ is complex and currently unclear.

The transcriptional activity of PPARγ is regulated primarily by ligand binding (263) which results in the expression level changes of PPARγ target genes (264). PPARγ can bind with a variety of ligands due to a spacious ligand binding pocket. Natural PPARγ ligands include long chain fatty acids (265), lysophosphatidic acid (266), nitrolinoleic acid (267), 9- and 13-hydroxyoctadecadienoic acids (9- and 13-HODE)

(263), and 15-deoxy-Δ12,14- prostaglandin J2 (15d-PGJ2) (209, 210). As previously described in Chapter 5, 15d-PGJ2 is a major prostaglandin product of cyclooxygenase after a series of dehydration reactions (as described in Figure 5.1). 15d-PGJ2 activates the PPARγ at low micromolar concentrations and therefore is thought to be the most potent endogenous PPARγ ligand. Synthetic PPARγ ligands include the thiazolidinedione (TZD) family (e.g., troglitazone, ciglitazone, rosiglitazone, and pioglitazone) (268, 269) and nonsteroidal anti-inflammatory drugs (NSAIDS) such as indomethacin, ibuprofen, flufenamic acid, and fenoprofen (270, 271). Binding of the ligands induces the three dimensional structure change of the PPARγ, the heterodimerization with RXR, DNA-binding, release of co-repressors, recruitment of co-activators and transactivation of promoters. Of note, PPARγ ligands can exert both PPARγ-dependent and -independent effects on inflammation, angiogenesis and tumor growth (272).

Similar to other nuclear receptors, PPARγ is tightly regulated by various mechanisms. The mitogen-activated protein kinase/extracellular signal-regulated kinase (MAPK/ERK) cascade has previously been demonstrated to suppress PPARγ by phosphorylation of serine residue 82 of PPARγ1 and serine residue 112 of PPARγ2 in prostate and colorectal cancer cells (273-275). PPARγ can also be phosphorylated and thereby inhibited by other molecules including platelet derived growth factor (PDGF) (276). The phosphorylation of PPARγ results in a conformational change that translates to a decrease in ligand-binding affinity and a decrease in the recruitment of co-activators (277). Notably, the transactivation of PPARγ can be also regulated by a S82/112-independent mechanism which modulates the subcellular localization. PPARγ resides mainly in the nucleus (278, 279) and can be exported out of the nucleus by the MAPK/ERK kinase 1/2 (MEK1/2). This MEK1/2-dependent export from

the nucleus to the cytoplasm reduces the transactivation ability driven by PPARγ (280).

In the past decades, there has been emerging evidence of the involvement of PPARγ in cancer formation. PPARγ ligands have also been shown to inhibit the proliferation of various malignant cells from different tissues, including liposarcoma, breast, prostate, colon, non–small-cell lung, pancreatic, bladder, and gastric origin (281, 282). Since PPARγ is expressed in monocytes/macrophages, dendritic cells, granulocytes, mast cells, T cells, and B cells, and platelets, PPARγ might play an important role in the development of immunological diseases and myelo-proliferative disorders (283-285). In the AML cell line HL-60, treatment with the PPARγ ligands such as troglitazone and 15d-PGJ2 resulted in inhibition of cell growth proliferation, possibly by a G1 cell cycle arrest, or the in induction of apoptosis (286-289). PPARγ ligands were also found to induce macrophage differentiation (290) and to inhibit cell growth (291) in acute myelomonocytic leukemia cell line, THP-1. PPARγ has been less intensively studied in CML. One study utilized a synthetic dual PPARα and PPARγ ligand, TZD18, which inhibited cell proliferation and induced apoptosis in the human CML erythroid blast crisis cell line K562(292). However, these effects were PPARα- and PPARγ-independent, as the cell proliferation and survival could not be rescued by either PPARα or PPARγ antagonists. Hirase et al. (293) also reported that TZDs inhibited both cell proliferation and suppresses the expression of erythroid phenotype of K562 cells. Another synthetic dual PPARα and PPARγ ligand, compound 48, induced a strong growth inhibition in imatinib-sensitive and -resistant K562 cell lines. These effects were associated with G0/G1 cell cycle arrest and interference of AKT and STATs signaling (294).

Despite the *in vitro* studies indicating PPARγ as a tumour suppressor, PPARγ-ligands failed to bring a clear benefit in several clinical studies with cancer patients (295, 296).

Moreover, PPARγ has been shown to promote tumour growth in rodent models in other independent studies. The PPARγ protein was constitutively active and served as a tumour promoter in mammary glands of transgenic mice (297). The pro-oncogenic effect of PPARγ causes epithelial to mesenchymal transformation in intestinal epithelial cells, through a mitogen-activated protein kinase cascade that involves phosphatidylinositol 3-kinases (PI3K), p21-activated kinase, MEK1, and ERK1/2 (298). In addition, there is evidence suggesting that PPARγ ligands induce tumour formation in mouse models of colon cancer (299-302) and in human (303), and rodent bladder cancer (304, 305).

At its therapeutic concentration, diclofenac is a partial PPARγ agonist and can competitively antagonize PPARγ trans-activation (200). The fact that the OCT-1 activity (OA) was significantly increased by diclofenac indicates the potential involvement of PPARγ in OA regulation. In a mouse model and the rat hepatoma (H-35) cells (197), a PPAR-response element was identified in the promoter region of *Slc22a1* (*Oct-1*) and the gene expression levels were elevated by treatment with PPARα and PPARγ agonists. Further *in vitro* functional studies confirmed that the rat Oct-1 transporter uptake was significantly increased by the treatment with PPARα and PPARγ agonists in H35 cells. It should be noted that all of these studies were performed using a mouse model or a rat hepatoma cell lines. In human BCR-ABL positive KU812 cells, gene expression profiling and RQ-PCR data could not demonstrate a significant association between *SLC22A1* gene expression level and the functional OA (as presented in Chapter 4). However, there was a significant negative correlation between OA and plasma levels of PPARγ ligand, 15d-PGJ2, in CML patients at diagnosis. This result suggests that PPARγ might be critical in OA regulation in CML cells, although not directly changing the transcription level of *SLC22A1* gene.

A study from our group previously demonstrated that the OA in patient MNCs was strongly related to cell lineage, as the OA was higher in neutrophils than in monocytes (244). This finding raised the possibility that the enrichment of PPARγ in monocytes/macrophages is at least in part responsible low OA in that population. This current chapter aims to investigate whether PPARγ plays a key role in OA regulation in CML cell lines. As cell lineage is a demonstrated determinant of OA, the enrichment or activation of PPARγ in certain cell types was also investigated in the control of OA.

6.2. Methods

6.2.1. PPARγ expression levels after treatment with ligands in CML cell line

BCR-ABL positive KU812 cells were treated with PPARγ ligands (GW1929, GW9662, troglitazone, and rosiglitazone) for one hour before the IUR assay. The IUR and OA were measured using ^{14}C-labelled imatinib and the OCT-1 inhibitor prazosin as described in Chapter 2. The expression level of *PPARγ* was examined by RQ-PCR using cervical cancer cell line HeLa as a positive control according to BioGPS (http://biogps.org/#goto=welcome), which is an on-line source for biologic information (Figure 6.1). The protein level of PPARγ was examined by western blotting using the whole cell lysate of KU812 cells (Section 2.6.7). Western blotting using lysates of the nuclear and cytoplasmic fraction (prepared as described in Section 2.6.8) were also performed to assess the subcellular localization of PPARγ. The protein levels were quantified using ImageQuant and expressed as a percentage of a loading control.

6.2.2. PPARγ transcriptional activity in CML MNC samples

Nuclear extractions from the MNC of chronic phase chronic myeloid leukaemia (CP-CML) patients at diagnosis were performed following the protocol (Section 2.6.8).
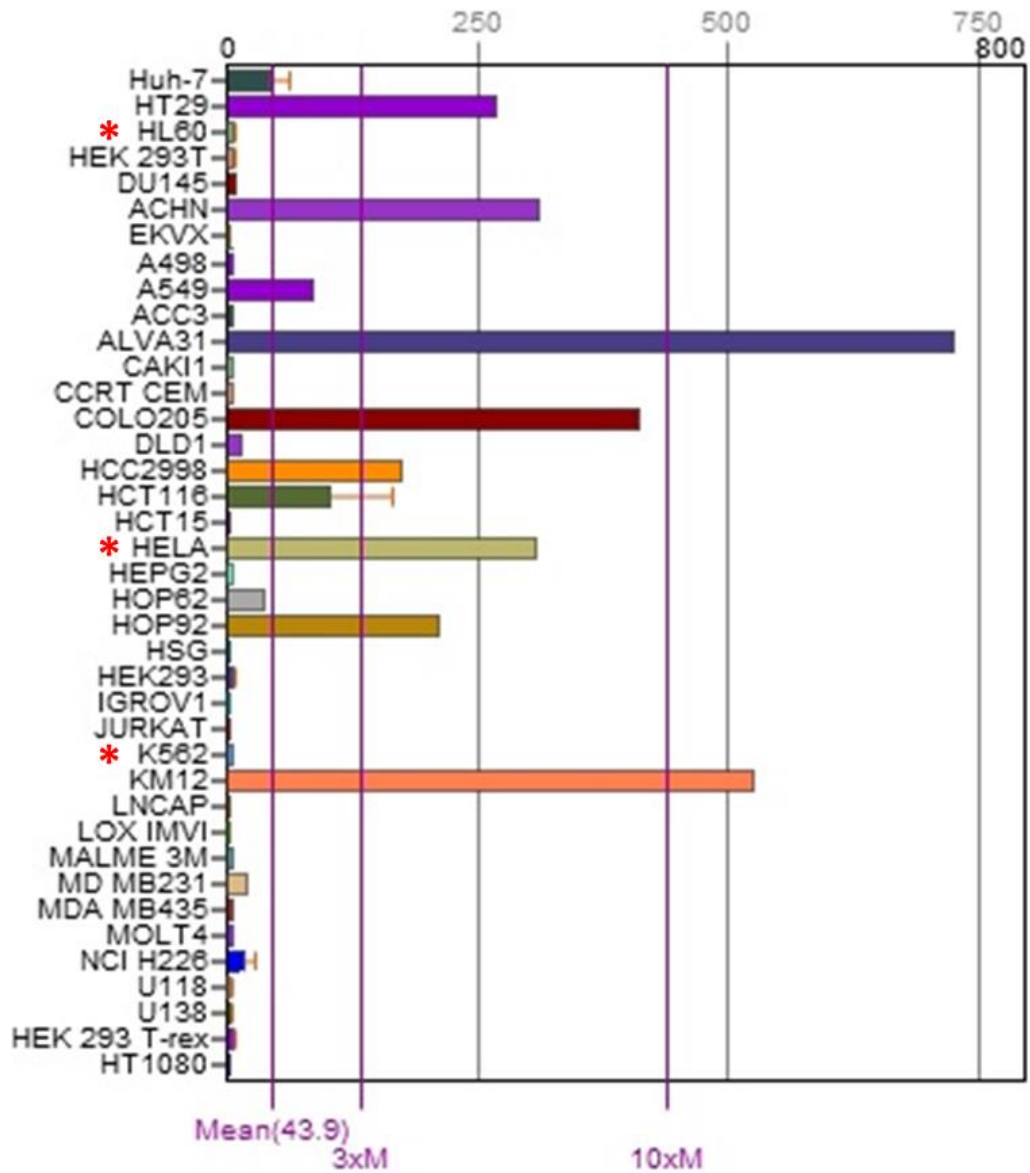
Figure 6.1   The *PPARG* gene expression in cancer cell lines

Comparing with leukemic cell lines HL60 and K562, solid tumour cell lines (such as human prostate tumour cell line ALVA-31, colon cancer cell lines KM12 and COLO205, and cervical cancer cell line HeLa) have much higher levels of *PPARG* gene expression. HeLa cell line was selected as a positive control for the RQ-PCR assay in this study. Figure adapted from BioGPS. *Indicates cell lines of interests

157

The transactivational activity of PPARγ was measured by an ELISA based assay (TransAM™ PPARγ kit). The 96-well plate provided in the kit was immobilized an oligonucleotide containing a PPRE (5'-AACTAGGTCAAAGGTCA-2'). When the same amount of nuclear extract was loaded into the plate, the activated PPARγ bound with the PPRE while the inactive PPARγ was removed by the following wash. The primary antibody recognized an accessible epitope on PPARγ protein upon DNA binding and the addition of the secondary conjugated antibody provided a sensitive colorimetric readout quantified by spectrophotometry. The results of the assay were expressed as the OD values. The IUR and OA were measured in all CP-CML samples and were compared with the level of transactivation of PPARγ.

6.2.3. PPARγ in isolated CD14$^+$ and CD15$^+$ cells from CML patients and healthy donors

The primary samples were collected from CP-CML patients at diagnosis or healthy donors as described in Section 2.4. MNC were isolated from the PB of patients at diagnosis using lymphoprep density gradient separation (Section 2.5.6). Cell isolation was performed using magnetic cell sorting (MACS; Section 2.6.10). Isolated populations were assessed for purity by morphology with Wrights stained cytospins and immunophenotyping for the expression of surface markers CD14$^+$ and CD15$^+$. The expression of PPARγ and the transcriptional activity of PPARγ were assessed in isolated CD14$^+$ and CD15$^+$ cells.

6.3. Result

6.3.1. The IUR assay in the presence of PPARγ ligands

To examine the effect of PPARγ antagonists on imatinib uptake, KU812 cells were first incubated with 40 µM GW9662 (a PPARγ antagonist) for one hour. The viability of

KU812 cells after the treatment was greater than 98% assessed by trypan blue exclusion assay (as described in Section 2.5.2). The IUR imatinib and OA in these pre-treated KU812 cells were determined in the presence or absence of GW9662 over a 2-hour period and compared with the vehicle control. As indicated in Figure 6.2A, the average IUR of KU812 cells in the vehicle control was 28.5 ng/200,000 cells (range 26.3 to 30.4 ng/200,000 cells). The presence of GW9662 significantly increased imatinib IUR (average 32.4 ng/200,000 cells, p=0.01). The addition of prazosin reduced the imatinib IUR to similar levels in the vehicle control and GW9662 pre-treated cells (p=0.75). Calculation of OA revealed a similar trend (Figure 6.2B). Treatment with GW9662 resulted in a significantly higher OA compared to the vehicle control (average OA increased from 12.7 to 15.4, p=0.011).

The effect of PPARγ agonists on imatinib IUR and OA were also examined in. KU812 cells following 1 hour treatment with either 40 μM GW1929, 40 μM rosiglitazone or 40 μM troglitazone. The viability of KU812 cells after the treatment was greater than 98%. Compared to the vehicle control (average 27.2 ng/200,000 cells, Figure 6.3A), there was a significant decrease in IUR when cells were pre-treated with PPARγ agonists (GW1929: 23.8 ng/200,000 cells, p=0.018; rosiglitazone: 21.7 ng/200,000 cells, p=0.034; troglitazone: 23.2 ng/200,000 cells, p=0.027). In the presence of prazosin, there was no significant difference with each condition. Compared with the OA in the vehicle control (average 10.50, Figure 6.3B), the treatment with all three PPARγ agonists significantly decreased the OA (GW1929: 7.50, p=0.020; rosiglitazone: 5.50, p=0.022; troglitazone: 6.78, p=0.037).
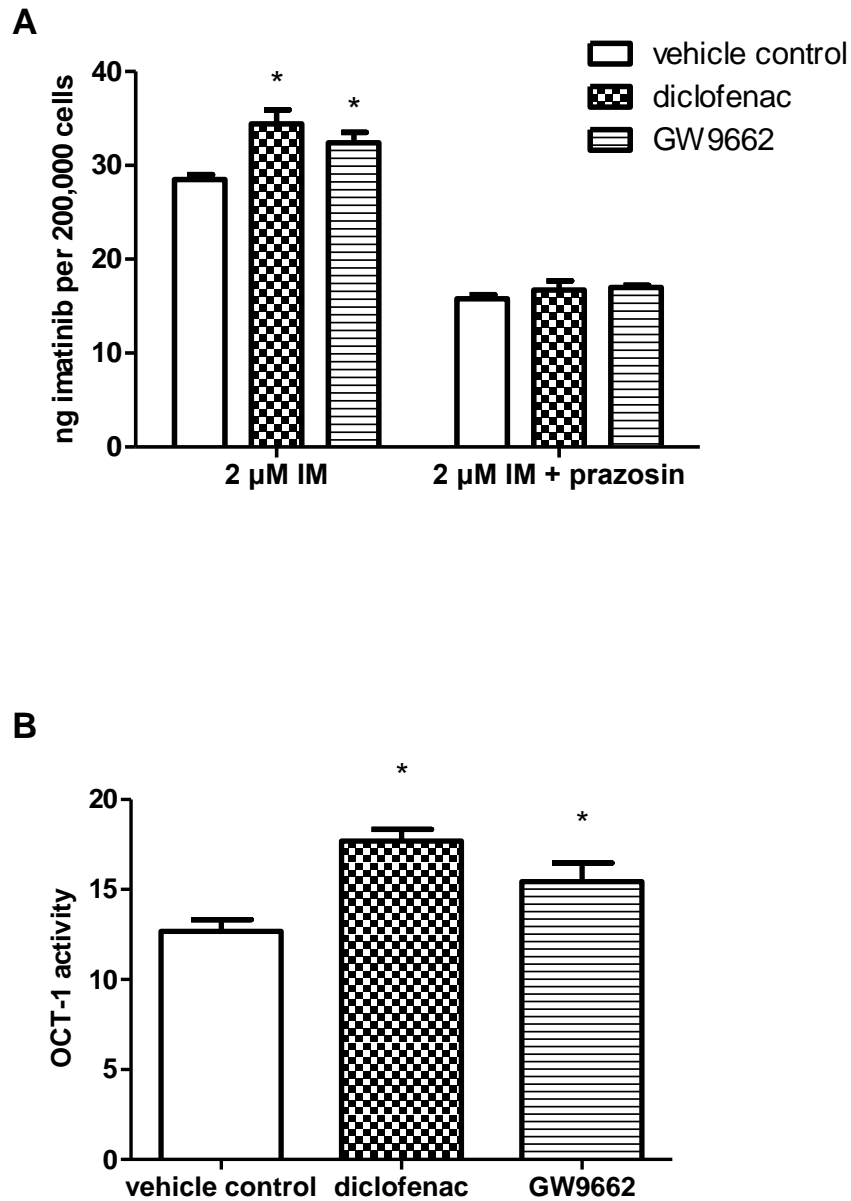
Figure 6.2   Pre-treatment with PPARγ antagonists diclofenac and GW9662 resulted in an increase in Imatinib IUR and OA in KU812 cells

Cells were firstly exposed to 40 µM GW9662 for 1 hour prior to the IUR assay. The IUR of 2 µM imatinib (**A**) and OCT-1 activity (**B**) were determined over a 2-hour period. The effect of GW9662 was compared with that of diclofenac. The error bars represent the standard deviation of the mean (n≥3). *, $p < 0.05$
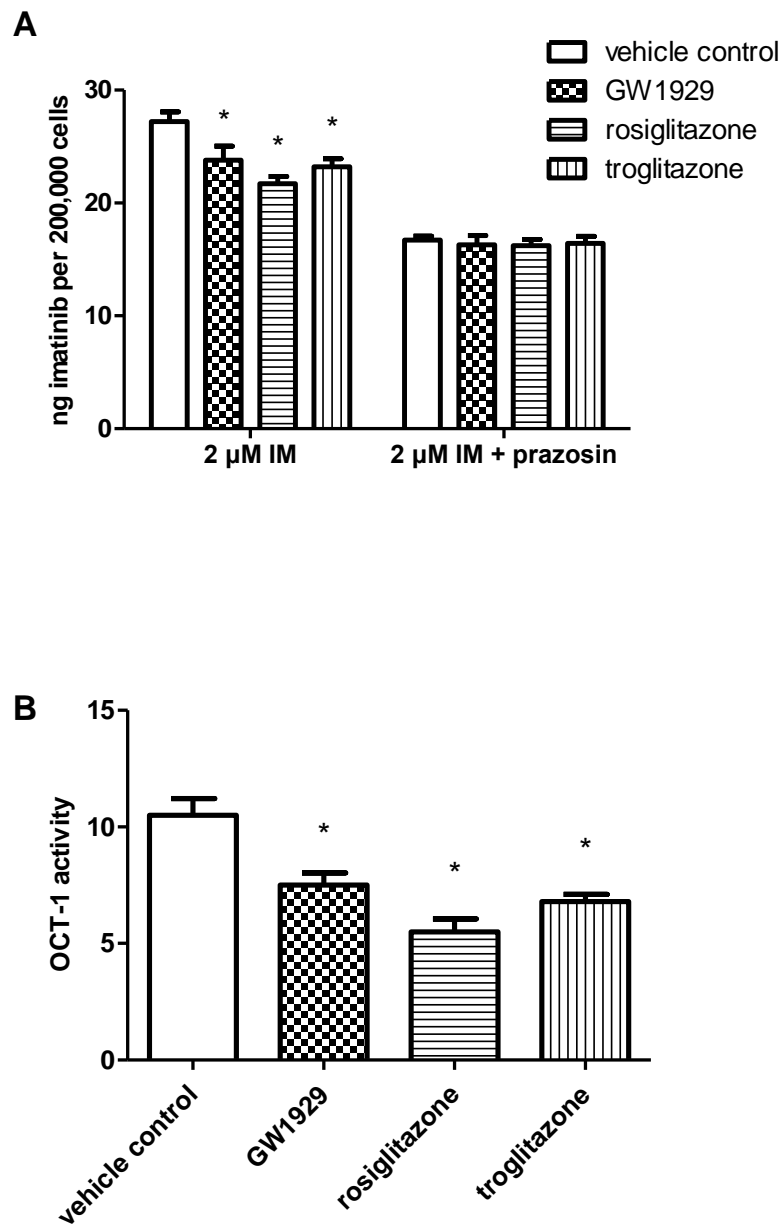
Figure 6.3   Pre-treatment with PPARγ agonists GW1929, rosiglitazone, or troglitazone resulted in a decrease in Imatinib IUR and OA in KU812 cells

Cells were firstly exposed to 40 µM GW1929, rosiglitazone or troglitazone for 1 hour prior to the IUR assay. The IUR of 2 µM imatinib (**A**) and OCT-1 activity (**B**) were determined over a 2-hour period. The error bars represent the standard deviation of the mean (n=3). *, $p<0.05$.

6.3.2. PPARγ expression and its subcellular localization in CML cells by Western Blotting

The effect of PPARγ ligands on imatinib IUR and OA further supported the involvement of PPARγ in OA regulation. Whether the treatment with PPARγ ligands caused any change in the gene expression level of PPARγ in CML cells was examined by RQ-PCR. The results were expressed as a percentage of the reference gene (*hTBP*). After 40 PCR cycles, the *PPARγ* gene is expressed at a lower level in CML cell lines KU812 (0.0013%) and K562 (0.0088%) compared with HeLa (average level 15.33%) and AML cell line HL60 (average level 1.14%) (Figure 6.4A). In addition, treatment with PPARγ antagonists (40 µM GW9662) or PPARγ agonists (40 µM GW1929, 40 µM rosiglitazone, or 40 µM troglitazone) for 3 hours had no significant effect on the *PPARγ* gene expression in KU812 cells ($p > 0.5$, Figure 6.4B).

The level of PPARγ protein was also assessed using whole cell lysates of KU812 cells. As shown in Figure 6.5A, PPARγ protein was detectable in KU812 cells treated with PPARγ antagonists (40 µM GW9662) or PPARγ agonists (40 µM GW1929, 40 µM rosiglitazone, 40 µM troglitazone) for 3 hours. However, no significant difference was observed when comparing the effects of PPARγ agonists and antagonists with vehicle control ($p > 0.5$, Figure 6.5B). Similarly, there was no significant change in PPARγ protein level when KU812 cells were incubated with 2 µM imatinib, 10 µM diclofenac or with a combination of both drugs ($p > 0.5$, Figure 6.5C and 6.5D).

While there was no change in PPARγ expression observed, the subcellular localization of PPARγ was also investigated in the presence of PPARγ ligands. Using Lamin B1 as a nuclear-specific loading control and β-actin as a cytoplasmic marker, western blotting for PPARγ was performed using either the nuclear extract or the plasma fraction isolated from KU812 cells. After the treatment with PPARγ agonists (40 µM rosiglitazone or troglitazone) for 3 hours, there was no significant change in

162

A

B
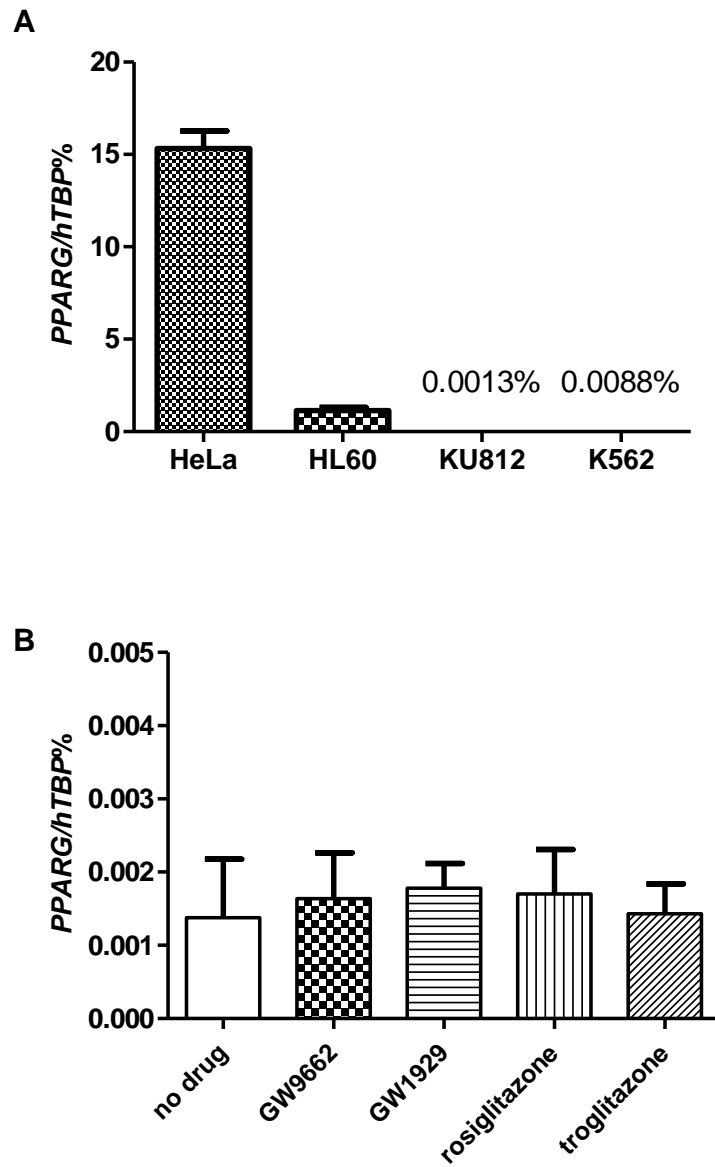
Figure 6.4 *PPARG* **expression levels remained unchanged after treatment with**

PPARγ ligands in CML cell lines

A: *PPARG* gene expression was assessed by RQ-PCR. **B:** *PPARG* gene expression levels in KU812 cells were assessed after a 3-hour treatment with PPARγ ligands. The error bars represent the standard deviation of the mean (n=3).

Figure 6.5 PPARγ ligands did not affect PPARγ protein expression in KU812 cells after a 3-hour incubation

A: One representative western blot is shown of PPARγ protein levels in KU812 cells after treatment with PPARγ ligands for 3 hours. **B:** The protein levels in Figure 6.4A were quantified using ImageQuant and expressed as a percentage to loading control (GAPDH). The error bars represent the standard deviation of the mean (n=3). **C:** One representative western blot is shown of PPARγ protein levels in KU812 cells after treatment with imatinib and/or diclofenac for 2 hours. **D:** The protein levels in Figure 6.4C were quantified using ImageQuant and expressed as a percentage of loading control (GAPDH). The error bars represent the standard deviation of the mean (n=3).

A

B

C

D
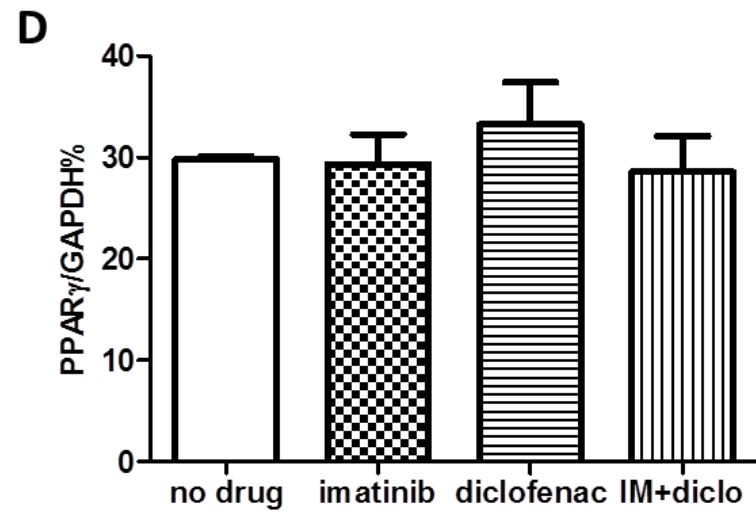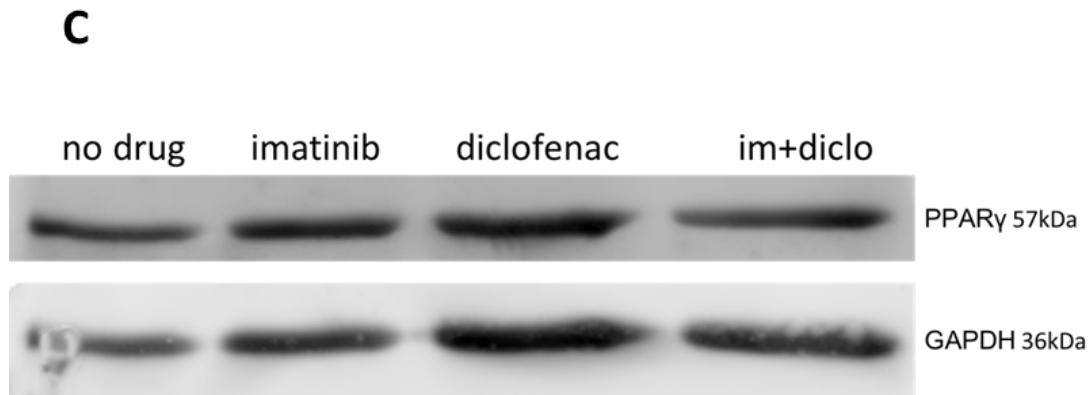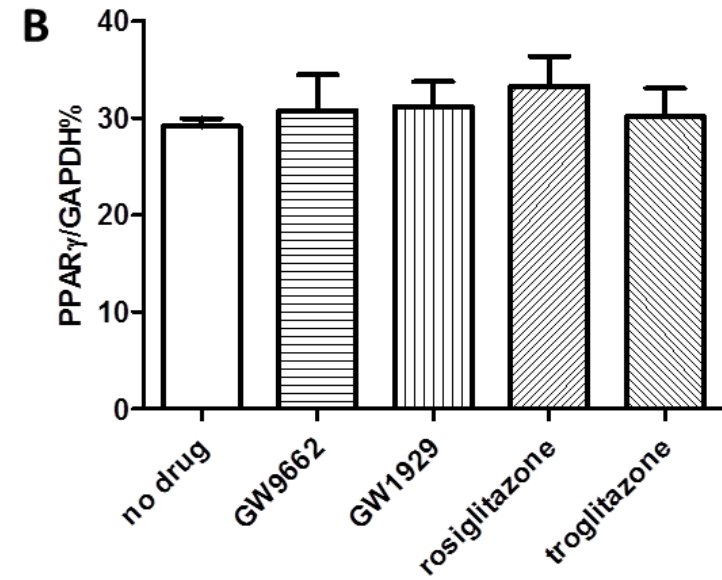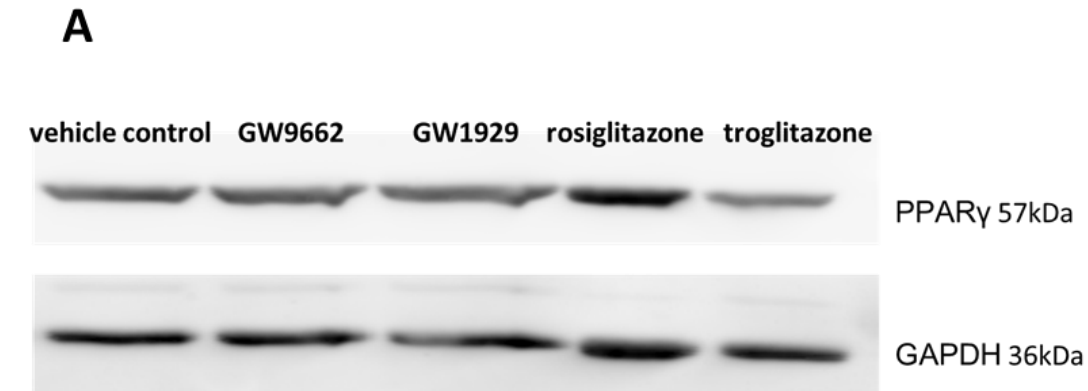
PPARγ protein levels in either the nuclear or cytoplasmic compartments when compared to the vehicle control (Figure 6.6A and 6.6B), indicating that treatment with ligands did not alter the subcellular localization of the PPARγ.

6.3.3. Correlation of OCT-1 activity with PPARγ transcriptional activity in CP-CML MNCs

Since the expression level of PPARγ and its subcellular location was unchanged upon the treatment with ligands, the transactivation of PPARγ was then measured using the nuclear extract from MNCs of CP-CML patients at diagnosis.

In forty CP-CML nuclear samples, the optical density varied from 0 to 0.057, with an average value of 0.0138. To determine whether the transactivation of PPARγ affects OA, the optical density results of the PPARγ assay were compared with the OA of the matched CP-CML samples. A significant negative correlation was observed between the transcriptional activity of PPARγ and OA (r=-0.676, p<0.0001, Figure 6.7A). To further investigate this relationship, CML patients' data was then grouped into low and high OA based on the median OA of 7.2 ng/200,000 cells as previously defined (140). A significantly higher level of PPARγ transcriptional activity was observed in the low OA group (average OD value 0.0167, n=32) when compared to high OA groups (average OD value 0.0042, n=8, *p*=0.013, Figure 6.7B). Patients' data was also grouped by previously defined quartiles (140) and PPARγ transcriptional activity was compared between patients with lowest OA (Q1, OA<4 ng/200,000 cells) and patients in other higher OA quartiles. The result confirmed that nuclear PPARγ transcriptional activity was significantly higher in Q1 patients (average OD value 0.0217, n=22) than in patients in other higher OA quartiles (average OD value 0.0048, n=18, *p*<0.0001, Figure 6.7C).

The ability of PPARγ transcriptional activity to predict the Q1 OA was then analysed

Figure 6.6   No significant change observed in the subcellular localization of PPARγ protein after the treatment with PPARγ ligands for 3 hours in KU812 cells

A: KU812 cells were treated with the indicated PPARγ ligands for 3 hours before a nuclear extraction was conducted. One representative western blot of PPARγ protein levels is shown. **B:** The protein levels were quantified using ImageQuant and expressed as a percentage of nuclear loading control Lamin B1. Columns represent the mean plus standard error of the mean, n=3. **C:** KU812 cells were treated with the indicated PPARγ ligands for 3 hours before the cytoplasmic fraction was isolated. One representative western blot of PPARγ protein levels is shown. **D:** The protein levels were quantified using ImageQuant and expressed as a percentage to cytoplasmic loading control, β-actin. The error bars represent the standard deviation of the mean (n=3).
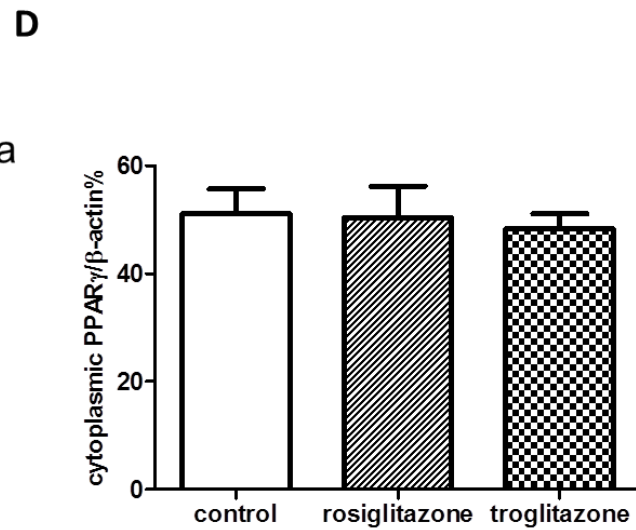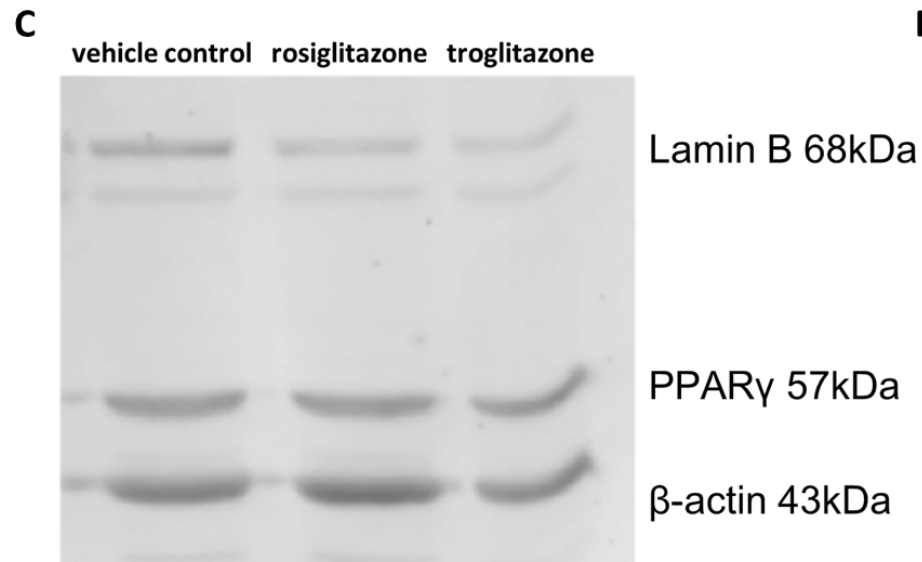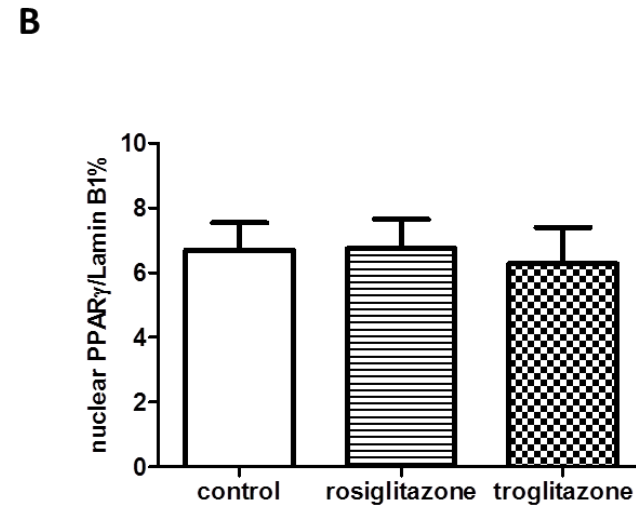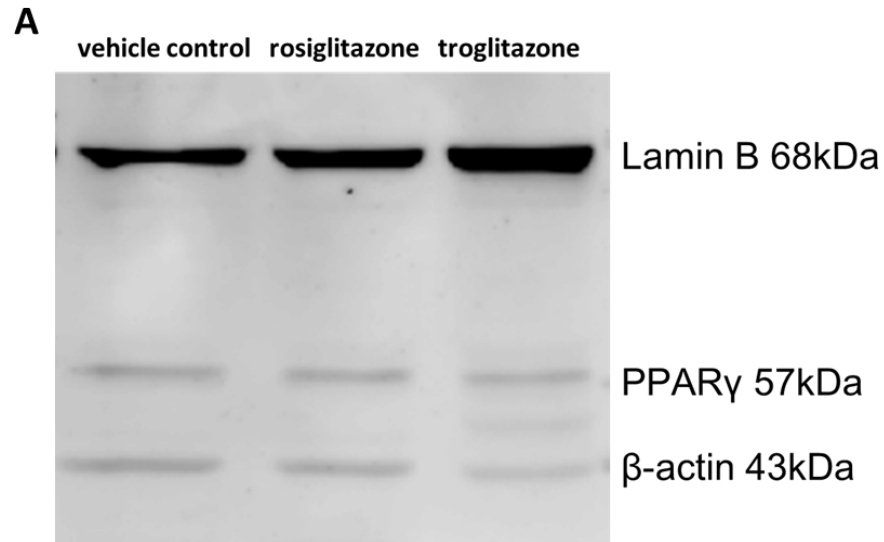
Figure 6.7   PPARγ transcriptional activity in mononuclear cells was negatively associated with OCT-1 activity in CP-CML patients at diagnosis

A: The correlation between PPARγ transcriptional activity and OA was investigated in 40 CP-CML patients by Pearson product-moment correlation. **B:** The levels of PPARγ transcriptional activity were compared between high and low OA groups. **C:** The levels of PPARγ transcriptional activity were compared between Q1 patients and patients in other OA quartiles. **D:** The accuracy of the PPARγ transcriptional activity assay for OA predicting was analysed by ROC curve. The error bars represent the standard deviation of the mean. *, $p<0.05$; **, $p<0.001$
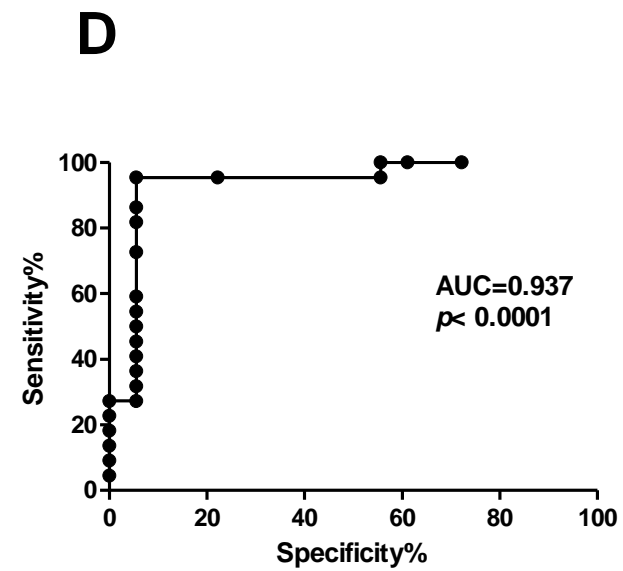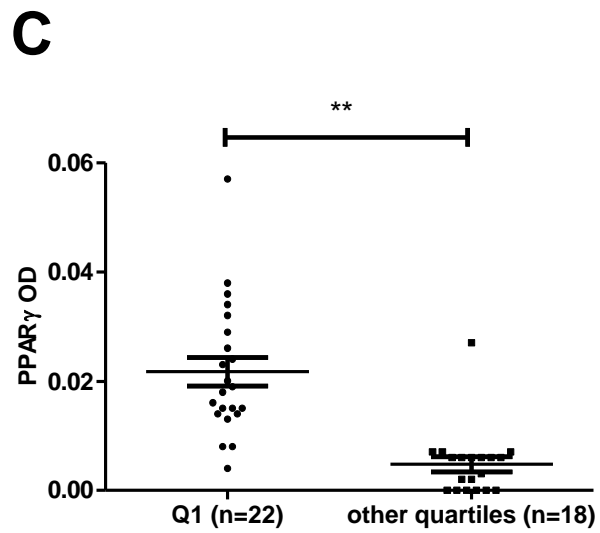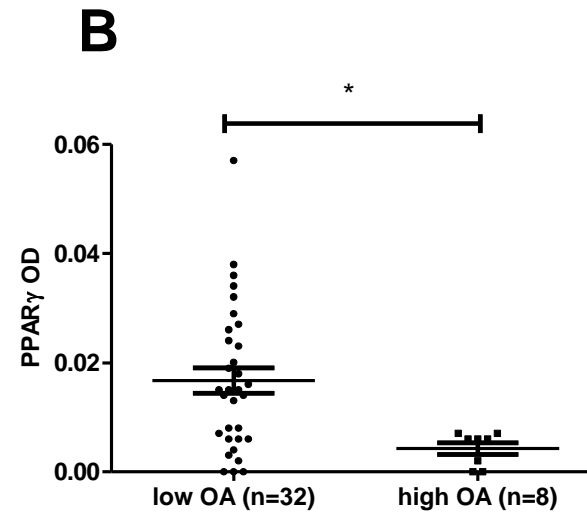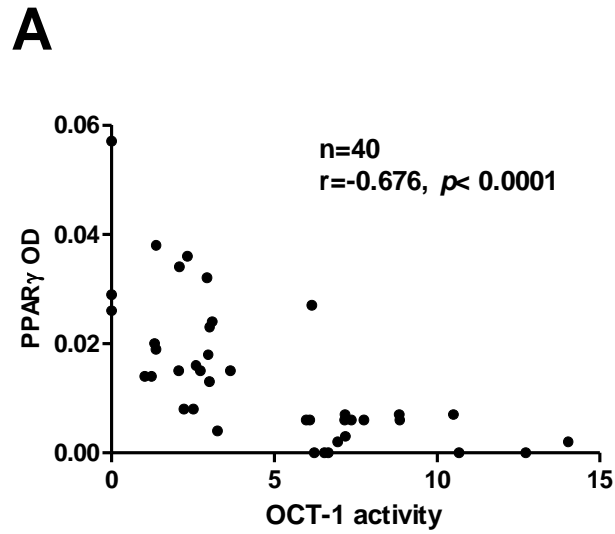
by Receiver Operating Characteristic (ROC) curve. The optimal cut-off value of PPARγ for Q1 OA predicting was determined where equal weight is given to the sensitivity and the specificity. As shown in Figure 6.7D, the accuracy of the assay was measured by the area under the ROC curve (AUC). While an area of 1 represents a perfect test and an area of 0.5 represents a worthless test, the AUC for the PPARγ transcriptional activity assay was 0.937 (p<0.0001). The ROC analysis also identified 0.0075 as the cut-off value. Patient with a PPARγ readout higher than 0.0075 would be predicted to have a Q1 OA, and vice versa. The predicting for Q1 OA using this cut-off achieved a sensitivity of 95.45% and a specificity of 94.44%, with an overall accuracy of 95% (38 out of 40).

6.3.4. Correlation between PPARγ transcriptional activity in MNCs and 15d-PGJ2 plasma levels in CP-CML samples

The data presented in Chapter 5 demonstrated that 15d-PGJ2, a potent endogenous PPARγ agonist, had a negative association with OA. This finding raises the possibility that 15d-PGJ2 is the key factor that activates the PPARγ and therefore leads to a low OA in CML MNC samples. However, in 30 samples with matched results, there was no significant correlation between the plasma 15d-PGJ2 concentration and PPARγ transcriptional activity in MNC (r=0.190, p=0.31, Figure 6.8A).

6.3.5. Isolation of CD14$^+$ cells and CD15$^+$ cells from CML patients and normal donors

Data from our previous study demonstrated a significant correlation between the cell lineage and OA, where a higher level of OA was observed in neutrophils compared with that in monocytes (244). Given that PPARγ is abundantly expressed in monocytes, it was next examined whether the PPARγ transcriptional activity levels also varied with the cell lineage. The CD14$^+$ cells and CD15$^+$ cells were isolated from
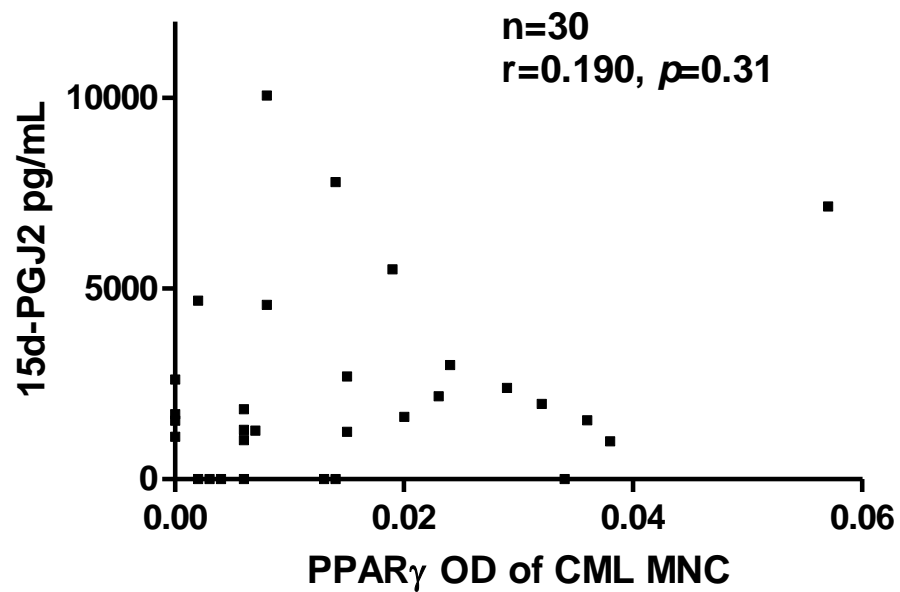
Figure 6.8   PPARγ activity in CP-CML MNCs had no correlation with the 15d-PGJ2 plasma levels

The association between PPARγ transcriptional activity in MNCs and plasma levels of 15d-PGJ2 was assessed in 30 CML samples.

peripheral blood samples of *de novo* CP-CML patients and normal donors (as described in Section 2.6.10 and summarized in Figure 6.9). The purity of the isolated populations was assessed using Wright staining to visualise morphology and immunophenotyping.
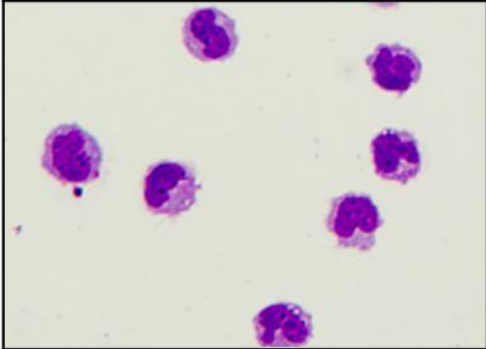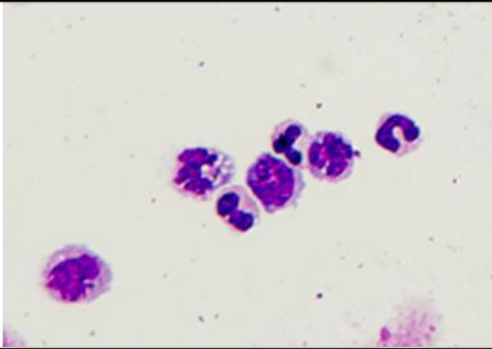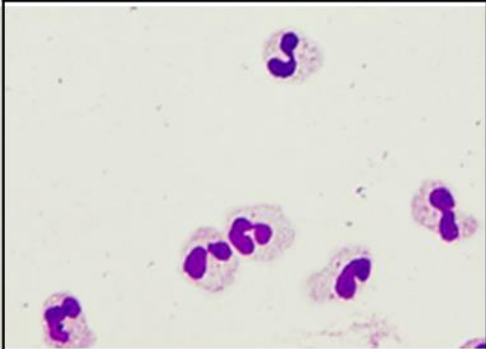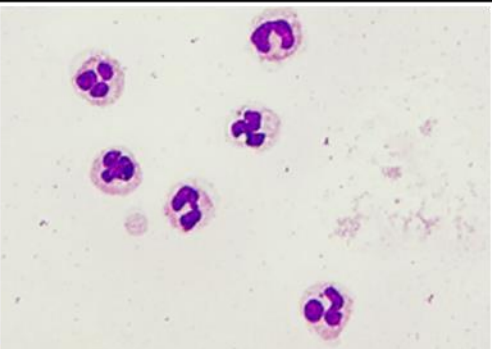
As shown in Figure 6.10, the CD14^{+} cells isolated from normal samples showed typical morphologic characters of monocytes, including the "C"-shaped nucleus and blue cytoplasm. The CD15^{+} cells isolated from normal PB had more cytoplasmic granules than CD14^{+} cells and their nucleus were frequently multi-lobed with lobes connected by thin strands of nuclear material, which are the typical morphologic characters of granulocytes. Immunophenotypic analysis also suggested that the CD14^{+} cells and CD15^{+} cells isolated from normal individuals were highly pure, with the average purity of 95.9% (CD14^{+}) and 92.3% (CD15^{+}), respectively.

In CML samples, typical granulocyte morphologic character (multi-lobed nucleus) and similar purity were observed in CD15^{+} isolated cells (the average purity 91.5%, Figure 6.10). The CML CD14^{+} cells exhibited a greater variation, in which some cells appeared to be more granulocytes with multi-lobed nucleus in appearance. In addition, these CP-CML CD14^{+} cells had a lower purity (the average purity 88.5%) when analysed using immunophenotyping. However, given the small proportion of monocyte populations (less than 10% of all leukocytes) in peripheral blood and the limited MNC cell number, it was difficult to isolate highly pure populations from CML samples at diagnosis.
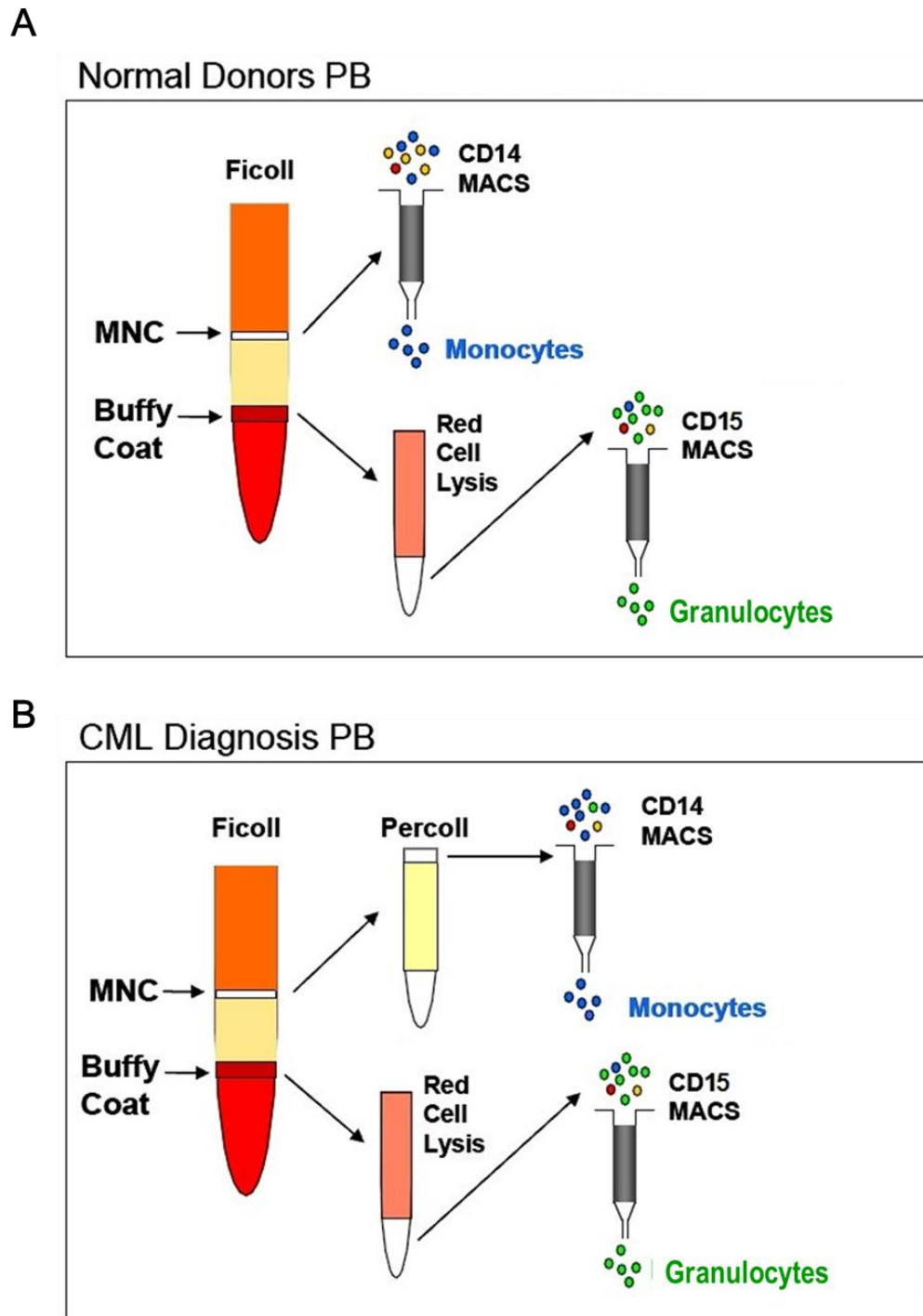
Figure 6.9 **Procedure for ilsolation procedures for of neutrophils and monocytes**

MNCs were isolated from peripheral blood by Ficoll density gradient centrifugation. Pure monocytes were isolated from the mononuclear layer using CD14 microbeads while neutrophils were isolated from the buffy coat using CD15 microbeads. **A:** Procedure for normal donors. **B:** Procedure for CP-CML at diagnosis.

Figure 6.10   Purity of isolated neutrophils, monocytes and lymphocytes

The purity of all sorted populations was assessed using immunophenotyping and morphological analysis. The average percentage of surface markers as assessed by flow cytometry are expressed for each isolated population. Representative pictures of Wright stained cells are shown.

6.3.6. *Protein and transcriptional activity levels of PPARγ in isolated CD14$^+$ and CD15$^+$ isolated cells*

Total PPARγ protein levels were then assessed in isolated granulocytes and monocytes and expressed as a percentage of the loading control. A significantly higher level of PPARγ protein was observed in CD14$^+$ cells compared with CD15$^+$ cells in both normal samples (p=0.0001) and CML samples (p=0.047, Figure 6.11A and 6.11B). A significant difference was also observed in PPARγ expression between the normal and CML CD14$^+$ cells (average 11.79% vs. 6.48%, p=0.043). However, there was no significant difference when comparing the PPARγ protein level between normal and CML CD15$^+$ cells (p=0.17).

PPARγ transcriptional activity levels were also measured in the nuclear extracts of isolated CD14$^+$ cells and CD15$^+$ cells. In normal samples, CD14$^+$ cells had significantly higher PPARγ transcriptional activity than CD15$^+$ cells (average optical density 0.098 vs. 0.021, n=7, p=0.033, Figure 6.11C). CML samples showed a similar trend, with higher PPARγ transcriptional activity in CD14$^+$ cells than in CD15$^+$ cells. However, this was not statistically significant (average optical density 0.029 vs. 0.0025, n=8, p=0.65). Additionally, a significant difference in PPARγ transcriptional activity was observed between normal and CML CD14$^+$ cells (0.098 vs. 0.029, p=0.002) but not in CD15$^+$ cells (0.021 vs. 0.0025, p =0.097).

It was then hypothesised that the PPARγ transcriptional activity of MNCs was possibly a reflection of the PPARγ activity of one population of cells. Therefore, the PPARγ activity of MNCs was correlated with that of isolated CD14$^+$ cells and CD15$^+$ cells, to observe any association. However, there was no significant association of PPARγ transcriptional activity between MNCs and CD14$^+$ cells (r=-0.093, p=0.83, Figure 6.12A) or between MNCs and CD15$^+$ cells (r=-0.427, p=0.29, Figure 6.12B).
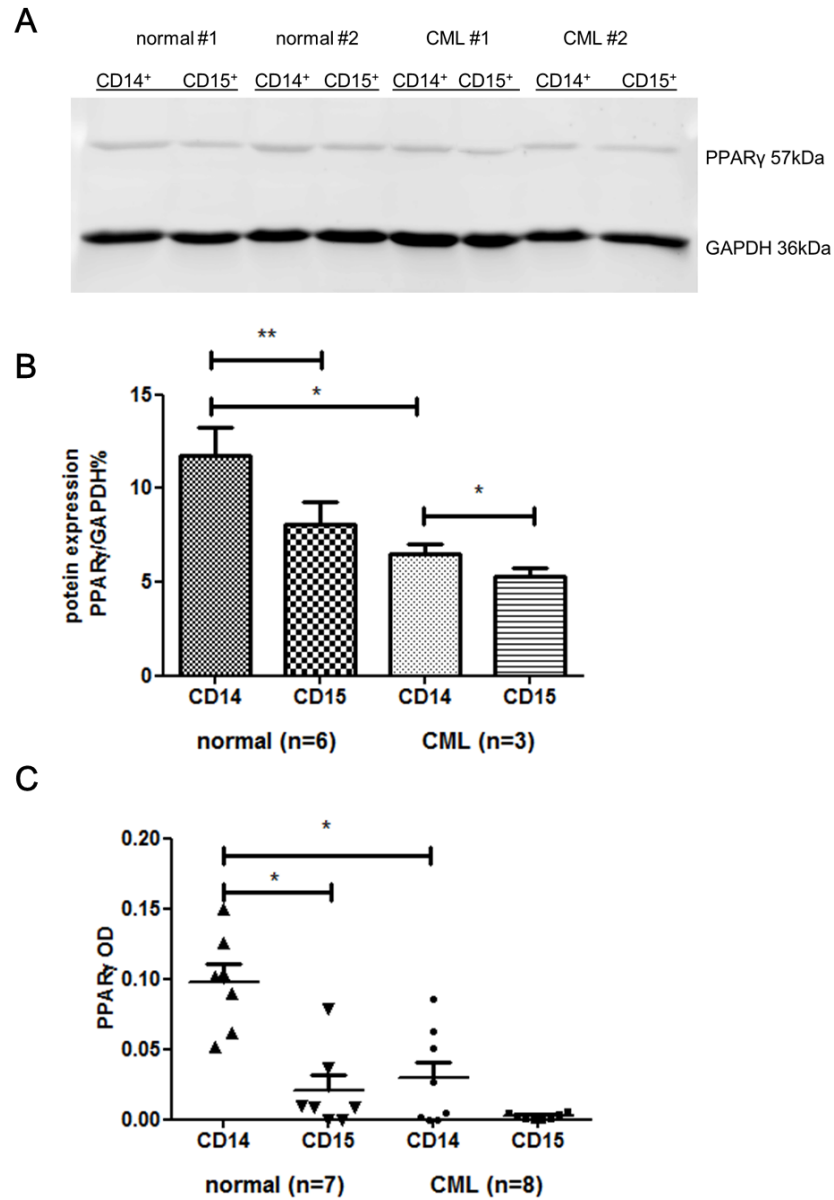
Figure 6.11   PPARγ protein expression and activity in CD14$^+$ cells and CD15$^+$ from normal donors and CP-CML patients at diagnosis

A: One representative western blot is shown for the PPARγ protein in CD14$^+$ and CD15$^+$ cells isolated from normal individuals and CP-CML patients at diagnosis. **B:** PPARγ protein levels were quantified using ImageQuant and expressed as a percentage to loading control (GAPDH). **C:** PPARγ transcriptional activity levels were measured in isolated CD14$^+$ cells and CD15$^+$ from normal individuals and CP-CML patients at diagnosis. The error bars represent the standard deviation of the mean.
*, $p<0.05$; **, $p<0.001$

A

B
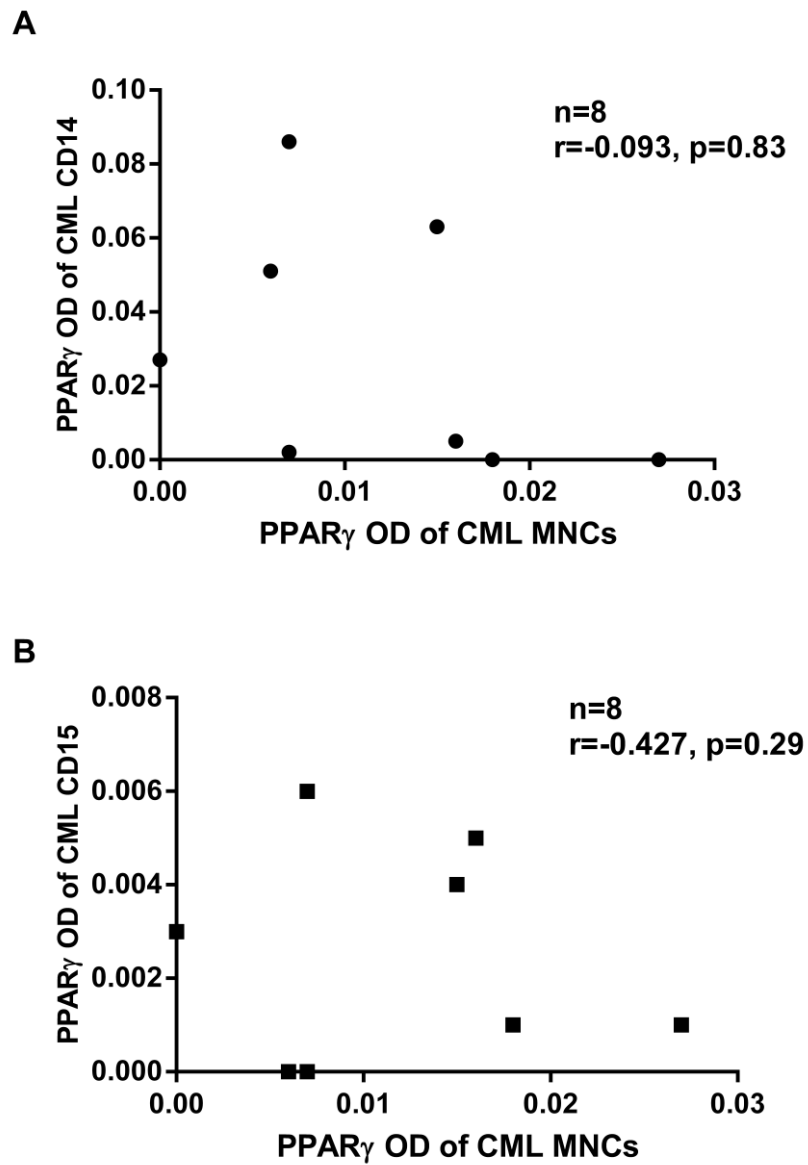
Figure 6.12 PPARγ activity in CP-CML MNCs had no correlation with the PPARγ activity of CD14$^+$ cells or CD15$^+$

Pearson product moment was used to determine the correlation of PPARγ transcriptional activity in MNCs and that of **(A)** isolated CD14$^+$ cells **(B)** or CD15$^+$ cells in 8 CML samples.

6.4. Discussion

PPARγ belongs to the nuclear receptor superfamily and is mainly expressed in adipose tissue, as well as immunocytes (especially in activated macrophages, lymphocytes and dendritic cells) (8–10). PPARγ alters the target genes expression and is therefore responsible for inhibiting activation of monocyte/macrophages, suppressing dendritic cell function (14) and promoting apoptosis of T cells (15).

The data presented in Chapter 3 demonstrated that diclofenac, a PPARγ ligand, significantly increased the imatinib uptake and retention mediated by OCT-1. Furthermore, the plasma level of 15d-PGJ2, a potent PPARγ endogenous ligand, was found to be significantly associated with OA in CML patients. To further investigate the role of PPARγ in OA regulation, the effect of various synthesised PPARγ ligands on OA were assessed using the BCR-ABL positive cell line, KU812. Similar to the effect of diclofenac, OA was significantly increased when PPARγ was repressed by the antagonist GW9662. Furthermore, OA in KU812 cells was reduced when PPARγ was stimulated by the agonists, GW1929, rosiglitazone and troglitazone. These opposite effects induced by PPARγ ligands provide evidence that PPARγ is involved in OA regulation in CML cells. This regulation is most likely through a PPARγ-dependent pathway as the different ligands used in this chapter (agonists or antagonists) exhibited consistent but opposing impacts on OA.

While our study demonstrated that PPARγ agonists significantly decreased the OA in KU812 cells, a recent study by Wang et al reported treatment with PPARα agonists increased imatinib uptake mediated by OCT-1 in CML KCL22 cells and primitive CML CD34^{+} cells (306). Although PPARα ligands were not examined in the current study, the opposite effects of PPARs (PPARα vs. PPARγ) in OA regulation however should

be interpreted cautiously. After treatment with PPARα agonists, Wang et al found significantly increased *PPARA* expression levels (306). However, ligand treatment had no effect in expression of PPARγ in the current study. Our observation is in keeping with the major regulatory mechanism of PPAR ligands by which the direct binding of ligands to PPARs causes conformational alterations and subsequent changes in transcriptional activity (258, 259). Whether the increased *PPARA* expression levels was due to PPAR-independent effects of the PPARα agonists, however, is beyond the scope of this project. In their study, Wang et al also found treatment with PPARα agonists induced the expression of *SLC22A1* (*OCT-1*) which subsequently led to increased OA (306). At the moment, the association between *SLC22A1* expression level and functional OA still remains controversial. More recent clinical studies have demonstrated no significant correlation between *SLC22A1* transcript levels in CML patients at diagnosis and the molecular response to imatinib therapy (62, 139, 140). Data in Chapter 4 showed that increased OA induced by diclofenac did not correspond with a significant change in *SLC22A1* expression (Figure 4.5). Of note, the treatment with PPARγ ligands lasted only 3 hours in the current study. Data in Chapter 3 has demonstrated that 2 hours incubation was sufficient for the regulation of OA by diclofenac. To mimic the effect of diclofenac, same treatment duration was applied for the PPARγ ligands. An extra hour pre-treatment with PPARγ ligands was designed to fully activate/inactivate PPARγ without causing any significant cytotoxic effect. However, in the study performed by Wang et al, cells were treated with PPARα agonists for 16 hours before the assessment of the *SLC22A1* gene expression and the OA (306). Hence different durations of treatment could also be contributing to the different results reported by the two studies. Wether prolonged exposure to PPARγ ligands may cause the mRNA changes in *PPARG* or *SLC22A1* expression need to be further investigated.

To further understand how PPARγ regulates OA, the total protein level of PPARγ and its subcellular location was then determined. After treatment with agonists and antagonists, there was no significant change in either expression of PPARγ or its nuclear-cytoplasmic shuttling, suggesting this might not be the key mechanism by which OA is regulated by PPARγ. An ELISA based assay was performed to measure the transcriptional activity of PPARγ in the cell nuclear extracts. In a cohort of 40 CP-CML patients at diagnosis, a significant negative association was observed between transcriptional activity of PPARγ in MNCs and their functional OA, as high level of PPARγ transcriptional activity correlated with low OA and vice versa. In addition, PPARγ was a strong predictor of lowest OA (Q1, OA<4 ng/200,000 cells) by ROC analysis. Together with previous data which demonstrated that OA was regulated by PPARγ ligand binding, these cumulative results provide strong evidence that activation of PPARγ negatively impacts OA and therefore reduces imatinib uptake and retention.

This correlation between PPARγ activity and OA also explains the variable effects of COX inhibitor NSAIDs on OA presented in Chapter 3. As described previously, PPARγ is known to interact with several ligands including COX-2 prostaglandin products such as PGD2 and 15d-PGJ2 (209, 210), and NSAIDs such as indomethacin, flufenamic acid, and fenoprofen (270, 271). Therefore, treatment with NSAIDs may reduce the amount of endogenous PPARγ ligands by inhibiting COX-2 activity. However, NSAIDs themselves might serve as extraneous ligands and simultaneously activate PPARγ. As indicated in Figure 6.13, the distinguishing characteristic of diclofenac as a dual inhibitor of COX-2 as well as PPARγ may explain why it is the only NSAID that significantly increases OA.

Since both PPARγ and its endogenous ligands 15d-PGJ2 were negatively correlated with OA in CP-CML patients, it was hypothesised that a high concentration of
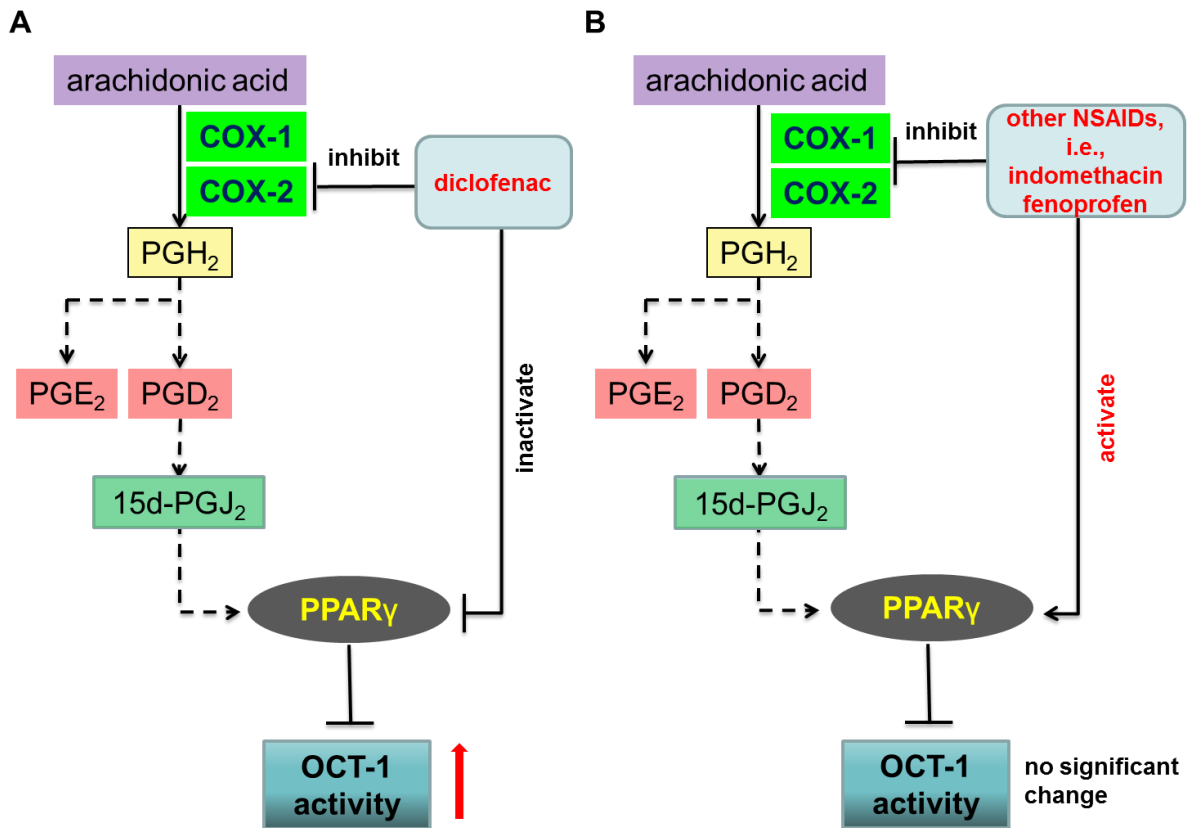
Figure 6.13 Postulated interactions between OCT-1 and diclofenac or other NSAIDs in CP-CML MNCs

(A) COX-2 prostaglandin product 15d-PGJ2 is a potent PPARγ agonist. COX-2 specific inhibitor diclofenac reduces the amount of PGD2 and 15d-PGJ2 by inhibiting COX-2 activity. Diclofenac is also a known antagonist for PPARγ. Therefore, treatment with diclofenac decreases PPARγ transcriptional activity by reducing the endogenous agonist and direct antagonizing, which leads to an increased OA in CML cells. (**B**) COX inhibitors such as indomethacin, flufenamic acid, and fenoprofen are also known agonists for PPARγ. Treatment with these NSAIDs may reduce the amount of endogenous agonist 15d-PGJ2 by inhibiting COX pathway. However, NSAIDs themselves may act as extraneous ligands and simultaneously activate PPARγ. This may be the reason that no significant change was observed in OA in the presence of the majority of NSAIDs.

15d-PGJ2 in plasma may be the key factor that contributes to high PPARγ transcriptional activity and results in a low OA in MNC. However, there was no significant association between these two values, suggesting ligand-binding is not the only reason underlying the variation of PPARγ transcriptional activity in CML. PPARγ is also known to interact with the MAPK/ERK cascade (273-275) which is involved in proliferation of BCR-ABL positive cells (307, 308). Whether the transcriptional activity of PPARγ is regulated by this pathway is the subject of ongoing investigation in our laboratory.

Previous studies from our group demonstrated that OA varies with the cell lineage and depends on the proportion of neutrophils in MNCs of CP-CML patients at diagnosis (244). The hypothesis that PPARγ negatively regulates OA was also validated by assessing PPARγ activity in different primary cell populations. CD14$^+$ cells and CD15$^+$ cells were isolated from normal individuals and newly diagnosed CML patients by MACS. A significantly higher level of PPARγ protein was detected in CD14$^+$ cells than in CD15$^+$ cells in both normal and CML samples, which is consistent with previous findings (309). In addition, CD14$^+$ cells exhibited significantly higher PPARγ transcriptional activity compared to granulocytes. Therefore, the different OA observed in different cell populations might due to the variant levels of PPARγ transcriptional activity.

To further identify the potential cell population that is responsible for the PPARγ transcriptional activity in MNC, the PPARγ activity of MNCs was correlated with that of CD14$^+$ cells and CD15$^+$ cells. No significant association was observed when the PPARγ transcriptional activity of MNC was compared to CD14$^+$ cells. Given the small proportion of monocytes in MNCs (less than 10%), it is likely that monocytes makes only a minors contribution to the PPARγ transcriptional activity in MNCs from CML patients. Although the percentage of neutrophils in MNC has been shown to be

strongly related to OA, there was no correlation of PPARγ transcriptional activity between MNCs and CD15^{+} cells. As described in Chapter 2, the CD15^{+} cells were isolated from the thin white cell layer above the red blood cell pellet following standard protocol (310). Therefore, this population might not reflect the true level of PPARγ transcriptional activity in the granulocytes from CML MNCs. Given the limited cell number of CP-CML MNC, granulocytes isolation from MNC and subsequent PPARγ transcriptional activity examination of this cell population were very difficult to perform. To identify the cell population that contributes to the PPARγ transcriptional activity of MNC, more pure cell isolation may be achieved with different combinations of CD markers (cluster of differentiation) that are more specific to the cell populations in question. It should be noted that the high PPARγ transcriptional activity observed in MNC from patients with low OA could also be the result of PPARγ transcriptional activity in several cell populations rather than one single cell population. Future work with a larger sample size will be required to identify the major contributor/contributors for the PPARγ transcriptional activity in MNC from CP-CML patients.

In conclusion, the findings presented in this chapter demonstrate that OA is strongly related to the PPARγ transcription factor. PPARγ antagonists significantly increased OA, while PPARγ agonists significantly decreased OA, implying that OA is regulated through a PPARγ-dependent pathway. RQ-PCR and western blotting indicated that PPARγ ligands had no effect on the gene or protein expression of PPARγ, nor did they regulate subcellular localization of PPARγ in CML cells after 3 hours treatment. The PPARγ transcriptional activity in MNCs had a significantly negative correlation with OA. The different levels of PPARγ transcriptional activity were also detected in isolated granulocyte and monocytes, which may cause the interpatient variability in OA in CP-CML patients that we have observed.

CHAPTER VII
Discussion

7.1. Introduction

Chronic myelogenous leukemia (CML) is a clonal myelo-proliferative disease characterized by the presence of a constitutively active BCR-ABL tyrosine kinase (1, 5). Imatinib mesylate is a rationally designed tyrosine kinase inhibitor (TKI) and currently used as front-line treatment for chronic phase CML (CP-CML) patients (57, 61, 154). Despite the impressive improvement in outcomes as result of imatinib, sub-optimal responses, primary or secondary resistance to imatinib is observed in approximately one third of patients (311, 312).

The organic cation transporter-1 (OCT-1) is the major transporter responsible for imatinib uptake into CML cells (130). The OCT-1 functional activity (OA), which is measured in mononuclear cells (MNC) from untreated *de novo* CP-CML patients (65), has been proven to be a powerful prognostic tool for the determination of short and longer-term patient responses on imatinib therapy (62, 140). Patients with a lower (below the median) OCT-1 activity (OA)   achieved a significantly lower rate of major molecular response (MMR) than those with high OA (above the median) by 24 months and 5 years of therapy (140). Patients in the lowest OA quartile (Q1, OA<4ng/200,000 cells) had poorer responses to standard imatinib therapy due to low intracellular imatinib concentration and inefficient kinase inhibition.

Although the negative impact of low OA may be partially overcome by escalating imatinib dose, this regimen is related to higher rates of adverse events (157) and only benefits approximately 60% of patients who are able to tolerate the dose increase without unacceptable toxicity (155). Second generation TKI's (nilotinib and dasatinib) are not substrates of OCT-1 (130, 158) and may provide a therapeutic alternative for patients with low OA. Given the excellent long-term safety profile and significant cost advantage of using imatinib especially after the expiration of current patent, it would

be of great clinical value to understand the factors that may affect imatinib uptake and develop a therapeutic intervention to allow those patients to continue imatinib treatment.

7.2. Major Findings

7.2.1. *Diclofenac and ibuprofen have opposite effects on OA in CML cells*

Given the determinant role of OCT-1 in imatinib influx, drug that affect OA have the potential to reduce or enhance OA and affect the efficiency of BCR-ABL kinase inhibition for patients. In CML patients, enhancer of OA may improve the outcome for those treated with imatinib. To identify drugs that may enhance the OA in CML cells, 31 compounds, including 8 drugs selected from Connectivity Map, 12 non-steroidal anti-inflammatory drugs (NSAIDs) and 11 commonly prescribed drugs, were extensively examined using CML cell lines and primary CML samples in Chapter 3. A significant enhancement of OA was observed when CML cell lines or primary CML cells were treated with diclofenac at clinically relevant concentrations. Critically, this increase in OA translated to a significant increase in BCR-ABL kinase inhibition and a significant reduction in viable CML cell numbers. Furthermore, when MNC samples from Q1 CML patients (poor responders, OA<4 ng/200,000 cells) were treated with diclofenac, 51.7% of those patients' samples demonstrated increased OA which resulted in a shift to a higher quartile. Based on experience gained in the TIDEL I study, if this translates to an *in vivo* response, it may significantly improve the likelihood of achieving MMR, and significantly reduce the risk of imatinib failure in this cohort of patients (140). Diclofenac had no effect on OA in normal MNC, which suggested that the effect of diclofenac was restricted to BCR-ABL positive cells. Whether the combination of imatinib and diclofenac will cause additional therapy toxicity or not will need further investigation on the off target effects in normal tissue

and *in vivo* studies. In contrast to diclofenac, another commonly used NSAID drug ibuprofen significantly decreased the OA in CML cells (cell lines and primary cells). This OA reduction translated into an increase in IC50^{imatinib} and an increase in cell growth in the presence of imatinib. Given the common administration and over-the-counter access of ibuprofen, this finding is likely to be of significant clinical relevance, as ibuprofen may interfere with imatinib uptake and ultimately may affect therapeutic efficacy. Ibuprofen also reduced imatinib IUR in the presence of OCT-1 inhibitor prazosin, suggesting an effect independent of OCT-1. In addition, ibuprofen further reduced it at 4°C when active (ATP-dependent) transporters are inactivated. Taken together, these results indicate that ibuprofen might also block the passive transport of imatinib across the plasma membrane. Furthermore, the inhibitory effect of ibuprofen was also observed in normal cells to the same extent as leukemic cells, which again, suggesting that the underlying mechanism by which ibuprofen mediates these changes is different to the mechanisms for diclofenac.

These findings provide important evidence that two commonly prescribed NSAIDs, diclofenac and ibuprofen, can modulate OA and have direct impact on leukemic cell response. While CML patients may benefit from the combination therapy of imatinib and diclofenac, caution may be required when administrating ibuprofen to CML patients on imatinib treatment.

7.2.2. Diclofenac regulates OA at the transcriptional level but not directly via SLC22A1 gene expression

Previous studies have suggested that HNF-4α and PPARs regulate OA at the transcriptional level in mouse models and hepatoma cells (196, 197). Several groups have also shown that *SLC22A1* expression is associated with clinical response to imatinib (135-138), however others have found that MMR may be achieved regardless of *SLC22A1* (*OCT-1*) transcript level at diagnosis (62, 139, 140). Therefore, the

transcription inhibitor Actinomycin D (ActD) was used in Chapter 4 to dissect the mechanism of OA regulation in CML cells. While pre-treatment with ActD did not influence baseline OA in KU812 cells, this transcriptional inhibitor prevented diclofenac from enhancing OA. This indicates that the increase of OA by diclofenac is mediated at the transcriptional level, as its effect is sensitive to the inhibition of transcription. However, no change in *SLC22A1* expression was detected by either gene expression profiling or RQ-PCR after diclofenac treatment. Therefore, the increase in OA by diclofenac is not due to altered expression of *SLC22A1* gene itself but by other genes associated with the control of OA. However, microarray and subsequent RQ-PCR validation failed to identify the genes altered by diclofenac treatment, possibly due to the limitation of the microarray analysis (discussed in Chapter 4).

7.2.3. *The role of the COX pathway in OA regulation*

COX-2 has long been regarded as a potential therapeutic target in many solid tumours (211-220). As overexpression of COX-2 has been found in the bone marrow of CML patients and has been linked to poor survival (183), the role of COX-2 in OA regulation was subsequently investigated. In a cohort of CP-CML patients at diagnosis, no correlation was observed between OA and *PTGS2* (*COX-2*) gene expression levels either in total white cells (TWC) or in MNC. In addition, there was no difference in *PTGS2* gene expression between patients who achieved MMR by 12 months and those who did not. Previous gene expression profiling data showed there was elevated *PTGS2* expression in CP-CML CD34^{+} cells from non-responders (243), however these contrasting results are likely due to the different cell populations that were used (CD34^{+} cells vs. TWC and MNC in the present study). As the mRNA level of *PTGS2* does not necessarily reflect COX-2 protein level or its function, the levels of PGE2 (a COX-2-pathway product) were assessed in plasma samples as a measure

of COX-2 enzymatic activity. In CML patients at diagnosis (n=150), PGE2 plasma levels were significantly higher than in normal samples. This observation was consistent with previous studies demonstrating the contribution of PGE2 to leukemogenesis (250-253). Another product of COX-2 activity is 15d-PGJ2, which can be measure in plasma. 15d-PGJ2 were also at significantly higher levels in CML patients compared to normal donors. The accumulation of these prostaglandins in CML plasma might be the result of increased COX-2 protein, which has been previously reported in bone marrow cells from in CML patients (183). Although PGE2 and 15d-PGJ2 are both downstream metabolites of COX-2, no significant association was found between these two prostaglandins, suggesting the possible involvement of other prostaglandin synthesis enzymes. Although PGE2 plasma levels were not predictive of OA, 15d-PGJ2 levels were significantly elevated in patients with the lowest OA (Q1, OA<4 ng/200,000 cells) when compared with patients with higher OA.

7.2.4. PPARγ negatively regulates OA in CML cells

As the increase in OA was restricted to diclofenac and not observed with other COX inhibitors, it is of interest to identify the mechanism by which diclofenac mediates this effect. In addition to being a COX-2 inhibitor, diclofenac also is a known PPARγ antagonist. Furthermore, the plasma level of a potent endogenous PPARγ agonist, 15d-PGJ2, was found to be significantly associated with OA in CML patients. As presented in Chapter 6, PPARγ agonists and antagonists regulated OA in CML cell lines through a PPARγ-dependent pathway. A significantly increased OA was observed when PPARγ was repressed by the antagonist GW9662, while OA was reduced by PPARγ agonists (GW1929, rosiglitazone and troglitazone). After treatment with PPARγ ligands, no significant change was observed in either expression of PPARγ (gene and total protein) or its subcellular localization. In a cohort of 40 CP-CML patients from whom the blood samples were collected at diagnosis, a

significant negative association was observed between MNC PPARγ transcriptional activity and OA. The level of PPARγ transcriptional activity was significantly higher in patients with low OA and vice versa, confirming a negative association of high PPARγ on OA in CP-CML cells. Since PPARγ protein is abundantly expressed in normal monocytes/macrophages (261, 262), it was not surprising that PPARγ protein level was significantly higher in CD14$^+$ cells than in CD15$^+$ cells in both normal and CML samples. In addition, CD14$^+$ cells also exhibited higher PPARγ transcriptional activity in comparison to that observed in CD15$^+$ cells. This may be the reason that different cell populations have different OA, as previously reported (244). However, there was no significant association between the PPARγ transcriptional activity levels of MNC and CD14$^+$ cells or CD15$^+$ cells. Further investigation of the PPARγ transcriptional activity in sub-populations of MNC may require a larger sample size and more specific cell isolation by different combinations of CD markers (cluster of differentiation).

7.3. Summary

Functional activity of the OCT-1 protein (OA) of CP-CML cells can be significantly increased by diclofenac. Patients with low OA may benefit from co-administration of diclofenac with imatinib, as its enhancement of OA translated into increased tyrosine kinase inhibition and reduced viable cell counts *in vitro*. This will need to be tested in a clinical trial setting to establish this translates to an *in vivo* response. A reduction of OA could be induced by another commonly prescribed NSAID, ibuprofen, which inhibits both active and passive uptake of imatinib into CML and normal cells. Therefore, based on this *in vitro* data, ibuprofen may not be recommended for CML patients on imatinib therapy. Although diclofenac is a COX-2 specific inhibitor, treatment with other COX-2 inhibitors such as celecoxib and rofecoxib had no significant effect on OA in CML cells. As a functional enhancer, diclofenac regulates

OA at the transcriptional level but does not increase the gene expression of *SLC22A1* (OCT-1) itself. In addition to a COX-2 inhibitor, diclofenac is also a known competitive antagonist for PPARγ, which negatively regulated OA. In CML cells, activation of PPARγ leads to a reduced OA, while PPARγ inhibition results in an increased OA. The activation/inhibition of PPARγ is reflected by its transcriptional activity, rather than its expression level (gene and total protein) or its subcellular localization. Although the PPARγ ligand 15d-PGJ2 is associated with OA, it is not the only factor that contributes to elevated PPARγ transcriptional activity in low OA patients. Other mechanisms of PPARγ regulation, including regulation through the MAPK/ERK1/2 pathway, need further investigation. PPARγ transcriptional activity is significantly higher in CD14$^+$ cells than in CD15$^+$ cells. However, the cell population/populations contributing to the high PPARγ transcriptional activity in low OA MNC still remains unclear. Identification of this population may provide better understanding of intrinsic OA interpatient variability, as well as the clinical and biological relevance of PPARγ in CML. Based on the findings presented in this thesis, Figure 7.1 presents a current working hypothesis of OA regulation in CP-CML MNC.

7.4.   Future Directions

As a result of the findings presented in this thesis, the following studies will be conducted to further our understanding of OA regulation:

● Increase the number of CP-CML MNC patient samples investigated to validate the power of PPARγ transcriptional activity at diagnosis for predicting OA.

● Isolation and characterization of CP-CML MNC subpopulations by flow cytometry using different combinations of markers. This will ensure purity of the populations isolated by flow cytometry. Each subpopulation will be examined for morphology to visually confirm cell type, and PPARγ transcriptional activity levels.
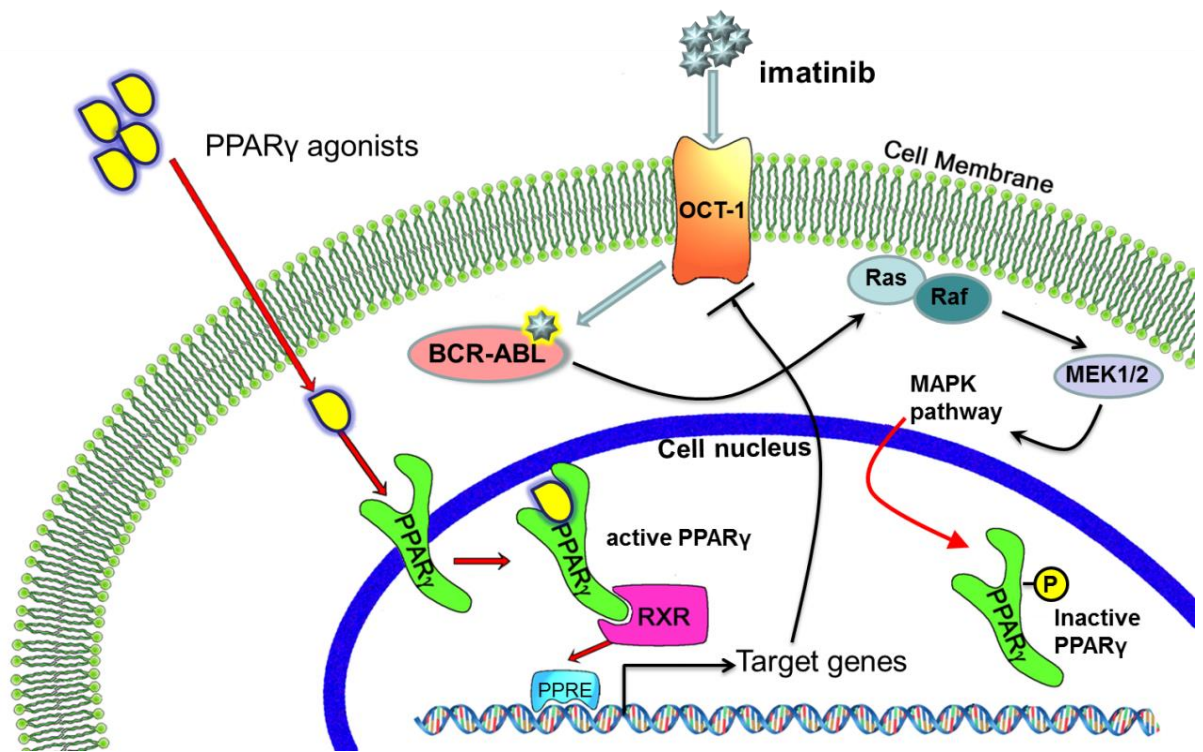
Figure 7.1   Working model of OCT-1 activity regulation by PPARγ in CP-CML patients

After binding with the ligands, PPARγ forms heterodimers with another nuclear receptor, the 9-cis-retinoic acid receptor (RXR). The PPAR/RXR heterodimer regulates target genes transcription by binding to the peroxisome proliferator response element (PPRE) on the promoters of target genes. The activation of PPARγ negatively regulates the functional activity of the OCT-1 protein in CP-CML cells. While ligand-binding is the major regulating mechanism for PPARγ, other pathways such as MAPK/ERK cascade may suppress PPARγ by phosphorylation of Serine 82/112 residues.

- Determine phospho-PPARγ levels in primary samples with low and high OA. Perform gene profiling and /or protein array analysis using primary samples with low and high OA to identify the possible mechanism by which PPARγ itself is regulated.

- Investigate the role of PPARγ in OA regulation by over-expression and knockdown of PPARγ in CML cell lines, CP-CML CD34$^+$ cells.

- Identify the mechanism by which PPARγ is regulating OA by performing microarray analysis with CML-CP samples treated with PPARγ ligands.

- Investigate whether the effects of PPARγ ligands on OA can be translate to the modulation on imatinib-mediated killing of CML cells.

- Investigate the activation status of the monocytes between the normal donors and the CML patients. Similar assay may also be performed to compare the activation status of monocytes between patients with high and low OA.

7.5.   Conclusion

In conclusion, the widely used NSAIDs, diclofenac and ibuprofen, exert opposite effects on OA in CML cells. These findings are important as they may affect the response of CP-CML patients treated with imatinib and hence overall treatment outcome. OA is regulated by diclofenac at the transcriptional level but the expression level of SLC22A1 remains unchanged. Importantly, PPARγ activity is highly predictive of OA in CP-CML patients at diagnosis. In CP-CML patients with low OA, PPARγ may provide a novel therapeutic target that leads to overall improvement of imatinib treatment outcome. Identification of the cell population/populations with high PPARγ activity may provide a novel marker for predicting outcome for patients treated with imatinib.

APPENDIX A
Publication Arising from this Thesis

npg

Full Paper

Contrasting effects of diclofenac and ibuprofen on active imatinib uptake into leukaemic cells

J Wang[1,2], TP Hughes[1,2,3], CH Kok[1,2], VA Saunders[1], A Frede[1], K Groot-Obbink[1], M Osborn[1,4], AA Somogyi[3,5], RJ D'Andrea[1,2,3,6] and DL White*[1,2,3]

[1]Department of Hematology, Centre for Cancer Biology/SA Pathology (RAH site), Adelaide, SA, Austarlia; [2]School of Medicine, University of Adelaide, Adelaide, SA, Austarlia; [3]Centre for Personalized Cancer Medicine, University of Adelaide, Adelaide, SA, Austarlia; [4]Women's and Children's Hospital, Adelaide, SA, Austarlia; [5]Discipline of Pharmacology, University of Adelaide, Adelaide, SA, Austarlia; [6]The Basil Hetzel Institute for Translational Health Research, Queen Elizabeth Hospital, Adelaide, SA, Austarlia

BACKGROUND: The human organic cation transporter-1 (OCT-1) is the primary active protein for imatinib uptake into target BCR-ABL-positive cells. Non-steroidal anti-inflammatory drugs (NSAIDs) are frequently used by chronic myeloid leukaemia (CML) patients on imatinib to manage musculoskeletal complaints.

METHODS: Here we investigated the impact of NSAIDs on functional activity of the OCT-1 (OCT-1 activity; OA) in CML cells.

RESULTS: Although ten of twelve NSAIDs tested had no significant impact on OA ($P > 0.05$), we observed increased OA (27% increase in K562; 22% increase in KU812 cells, $P < 0.05$) and reduced $IC50^{imatinib}$ when treated with diclofenac. Co-incubation with imatinib and diclofenac resulted in a significantly lower viable cell number compared with imatinib alone. In contrast, ibuprofen led to a significant decrease in OA, an increase in $IC50^{imatinib}$ and thus reduced the cytotoxicity of imatinib. In primary CML samples, diclofenac significantly increased OA, particularly in patients with low OA (< 4 ng per 200 000 cells), and significantly decreased $IC50^{imatinib}$. Ibuprofen induced significant decreases in OA in CML samples and healthy donors.

CONCLUSION: On the basis of the expected impact of these two drugs on OA, ibuprofen should be avoided in combination with imatinib. Further studies are warranted regarding the potential benefit of diclofenac to improve OA in a clinical setting.

British Journal of Cancer advance online publication, 24 April 2012; doi:10.1038/bjc.2012.173   www.bjcancer.com
© 2012 Cancer Research UK

Keywords: CML; OCT-1; drug–drug interaction; NSAIDs; imatinib

Imatinib mesylate is a rationally-designed inhibitor of BCR-ABL currently used as first-line treatment for chronic phase chronic myeloid leukaemia (CP-CML). According to the 7-year update of IRIS (International Randomized Study of Interferon and STI571), patients treated with imatinib (STI571) achieved an overall event-free survival of 81% and transformation-free survival (to accelerated phase/blast crisis) of 93% (Hughes *et al*, 2010). Despite these excellent outcomes, suboptimal response or resistance to imatinib was reported soon after the introduction of imatinib into clinical practice (Gorre *et al*, 2001; Shah *et al*, 2002).

Although the presence of mutations within the kinase domain of BCR-ABL is widely accepted as the most common reason for secondary imatinib resistance (Gorre *et al*, 2001; Hughes *et al*, 2006), the underlying cause of primary resistance is less well characterised. The human organic cation transporter-1 (OCT-1) has been identified as the major transporter responsible for imatinib uptake in CML cells (Thomas *et al*, 2004). We have demonstrated that low functional activity of the OCT-1 protein (OCT-1 activity; OA) measured at the time of diagnosis, results in reduced imatinib-mediated *in vitro* tyrosine kinase inhibition

(White *et al*, 2005) and is associated with a poor outcome in CP-CML patients receiving imatinib therapy (White *et al*, 2007b, 2010). In some patients the negative impact of a low OA may be partially overcome by escalating imatinib dosage where tolerated (Hughes *et al*, 2008; White and Hughes, 2012). However, clinical experience has demonstrated that increasing imatinib dose is related to higher rates of adverse events and may lead to dosage interruptions or cessation (Cortes *et al*, 2010).

Several commonly prescribed drugs have been identified as substrates or inhibitors of OCT-1, thus, the contribution of OCT-1 to drug–drug interactions (DDI) has been reported recently in several pharmacokinetic studies (Kindla *et al*, 2009; Fahrmayr *et al*, 2010). Most of these studies used cell lines stably expressing OCT-1, with 1-methyl-4-phenylpyridinium (MPP +) and metformin as test compounds. In MDCKII-OCT-1 cells, OCT-1 mediated MPP + and metformin uptake were inhibited by oral anti-diabetic drugs, rosiglitazone and repaglinide (Bachmakov *et al*, 2008). Antiretroviral drugs for HIV treatment and cardiovascular drugs have been found to inhibit OCT-1 mediated MPP + uptake in transformed HEK293 cells expressing OCT-1 and in primary hepatocytes (Jung *et al*, 2008; Umehara *et al*, 2008). Although there is accumulating evidence regarding OCT-1-mediated DDI, few studies have investigated the effect of DDI on OCT-1 mediated imatinib uptake. Minematsu and Giacomini (2011) reported the selective and potent inhibitory effect of imatinib on ^{14}C-metformin uptake using HEK293 cells stably expressing OCT-1. However, the

DDI involving imatinib and OCT-1 in CML cells has not been fully assessed to date.

Non-steroidal anti-inflammatory drugs (NSAIDs) are a class of structurally diverse drugs that effectively inhibit cyclooxygenases (COX-1 and COX-2) (Ulrich et al, 2006). Non-steroidal anti-inflammatory drugs are very commonly used for treatment of arthritic conditions and different types and severities of inflammation. There has been abundant evidence of DDI between NSAIDs and other co-administrated drugs, which may prolong the plasma elimination and lead to various side effects such as liver damage (Bjorkman, 1998), kidney dysfunction (Perneger et al, 1994), and aggravation of cardiovascular diseases (Farooq et al, 2008). Recently, several studies suggested that the transporter responsible for the renal uptake and secretion for NSAIDs is the human organic anion transporter-1 (OAT-1) (Apiwattanakul et al, 1999; Nozaki et al, 2004; Honjo et al, 2011). At clinically relevant concentrations, NSAIDs efficiently inhibit hOAT-1-mediated transport of adefovir in a cell line stably expressing hOAT-1 (Mulato et al, 2000). Although it has been reported that NSAIDs are not substrates of OCT transporters (Khamdang et al, 2002), NSAIDs such as diclofenac, ibuprofen, indomethacin and sulindac have been demonstrated to significantly inhibit OCT-1-mediated TEA uptake at the concentration of 0.5 mM in transfected S_2 cells expressing hOCT-1 (Khamdang et al, 2002). As about one-quarter to one-half of CML patients on imatinib develop musculoskeletal complaints (muscle cramps, myalgia, arthralgia), which may need to be managed with NSAIDs (Deininger et al, 2003), it is of particular relevance to investigate the effect on imatinib uptake of NSAIDs. An understanding of the effects that these drugs may have on imatinib influx in BCR-ABL-positive cells is of significant value for clinical practice.

In this study we performed a systematic functional analysis of the effects of 12 commonly used NSAIDs on imatinib uptake via OCT-1 in CML cell lines, and de novo CP-CML patients' cells. As previous studies have demonstrated that the influx of nilotinib and dasatinib are not mediated by OCT-1 (White et al, 2006; Giannoudis et al, 2008; Hiwase et al, 2008), imatinib was selected as the only relevant substrate for the OCT-1 transporter in the current study. Our data demonstrates that NSAIDs result in varying effects on OA. Among them two widely used NSAIDs, diclofenac and ibuprofen, resulted in significant change in the OA, kinase inhibition and imatinib efficacy in vitro at clinically achievable total plasma concentrations (10 μM for diclofenac and 130 μM for ibuprofen) (Siu et al, 2000; Juhlin et al, 2004; Bramlage and Goldis, 2008). Thus, their concomitant use with imatinib in CML patients warrants further experimental and clinical examination.

MATERIALS AND METHODS

Cell lines

Human BCR-ABL-positive K562 and KU812 CML cell lines were obtained from the American Type Culture Collection (ATCC, Manassas, VI, USA). All cell lines were cultured in a 37 °C humidified atmosphere of 5% CO_2 in RPMI-1640 media (Sigma-Aldrich, St. Louis, MO, USA) supplemented with 10% foetal bovine serum (JRH Biosciences, Lenexa, KS, USA), 2 mM L-glutamine (SAFC Biosciences, Lenexa, KS, USA) and 100 U ml^{-1} penicillin G/streptomycin (Sigma-Aldrich).

Patient samples

Blood was obtained from de novo CP-CML patients, before the commencement of imatinib therapy. Normal blood was obtained from healthy volunteers. All blood samples were collected with informed consent in accordance with the Declaration of Helsinki. Mononuclear cells (MNCs) were isolated from blood using Lymphoprep (Axis Shield, Oslo, Norway) density gradient centrifugation. Experiments were performed on fresh or frozen cells. Use of clinical trial patients' samples (TIDELI) was approved by the Royal Adelaide Hospital Research Ethics Committee (Novartis protocol No: CST15710106).

Drugs

Imatinib mesylate, together with labelled imatinib ([^{14}C]-STI571) were kindly provided by Novartis Pharmaceuticals (Basel, Switzerland). Celecoxib and rofecoxib were purchased from Toronto Research Chemicals (Ontario, CA, USA). Paracetamol was kindly provided by Professor Andrew A Somogyi, the University of Adelaide (Adelaide, Australia). Other NSAIDs were purchased from Sigma-Aldrich and dissolved as per manufacturer's instructions. For those drugs dissolved in DMSO or ethanol, the final concentration of the solvents ranged from 0.14–0.25% (v/v). The concentrations of NSAIDs used in this study were selected according to the concentrations reported to be the maximum plasma concentrations after therapeutic dosing. For those of which the optimal concentrations were unknown, the concentrations commonly chosen in high-throughput cell-based small-molecule screens were used (Supplementary Table 1). The OCT-1 inhibitor prazosin (Sigma-Aldrich) was dissolved in methanol and used at 100 μM. The final concentration of methanol was 1% (v/v).

Radio-labelled drug uptake (IUR) assay and OA assay: assessment of the effects of NSAIDs on OA modulation

As previously described (White et al, 2007b), the radio-labelled intracellular uptake and retention (IUR) assay measures the intracellular concentration of imatinib achieved and maintained in cells over a 2-hour period. Non-steroidal anti-inflammatory drugs and the potent inhibitor of OCT-1, prazosin were added to the IUR assay simultaneously with radio-labelled imatinib. After incubation, the cellular and aqueous phases were separated and incorporation was determined using a Topcount Microplate Beta Scintillation counter (Canberra Packard, Meriden, CO, USA) following the addition of Microscint20 scintillation fluid (Perkin Elmer, Boston, MA, USA). The OA was determined by calculating the difference of the IUR with or without 100 μM prazosin.

IC50^{imatinib} assay: assessment of the effects of NSAIDs on tyrosine kinase inhibition

The IC50 assay was performed as previously described (White et al, 2005), based on the in vitro reduction in the level of phosphorylated Crkl (p-Crkl) as a result of exposure to increasing concentrations of imatinib (ranged from 0 to 100 μM). The percentage of p-Crkl to non-p-Crkl at 0 μM imatinib was standardised to 100%, and all other data points were normalised to this value. The IC50 was defined as the concentration of imatinib producing a 50% decrease in the level of p-Crkl compared with untreated controls. The effects of NSAIDs were determined by comparing the IC50 in the presence and absence of NSAIDs in cell lines and primary patients' material.

Trypan blue exclusion assay: assessment of the effects of NSAIDs on the number of viable cells in the presence of imatinib

After treatment with NSAIDs and various concentrations of imatinib (indicated in the text) for 72 hours, cells were harvested and viable cell numbers were assessed using the trypan blue (Sigma-Aldrich) exclusion method. The number of viable cells was then compared with a control treatment in the absence of NSAIDs.

RQ-PCR assay: assessment of the effects of NSAIDs on OCT-1 mRNA levels

The RQ-PCR for transporter mRNA expression was performed as previously described (White *et al*, 2007b). The cells were harvested after 2-hour incubation with NSAIDs. RNA was then extracted using TRIzol Reagent (Invitrogen, Carlsbad, CA, USA). The sequences for the primers are as follows: OCT-1 forward 5′-CTGAGCTGTACCCCACATTCG-3′, OCT-1 reverse 5′-CCAACA CCGCAAACAAAATGA-3′.

Statistical analyses

All statistical analyses are indicated where applied and were performed using Sigma Stat Software 3.0 (Systat Software Asia Pacific Ltd, Richmond, CA, USA). The unpaired *t*-test was used to define differences between blank and NSAIDs-treated group, and correlation was performed using the Pearson Product Moment. Data are presented as mean ± s.e.m. for at least three biological replicates. Differences were considered to be statistically significant when the *P*-value was less than 0.05.

RESULTS

### Effects of NSAIDs on OA and IC50^{imatinib} of BCR-ABL-positive cell lines

Diverse effects on OA were observed in BCR-ABL positive cell lines (K562 and KU812) in the presence and absence of NSAIDs. Although the majority of NSAIDs selected (9 of 12) failed to induce any significant change in OA (Figure 1A), a significant increase in OA was observed in K562 cells treated with either 10 μM diclofenac (27%, $n = 4$, $P = 0.007$) or 16 μM fenbufen (33%, $n = 9$, $P = 0.006$), Similarly, a 22% increase was observed in OA when KU812 cells were treated with 10 μM diclofenac ($n = 6$, $P = 0.003$, Figure 1B). Although not significant, incubation with fenbufen resulted in a 21% increase in OA in KU812 cells ($n = 5$, $P = 0.328$). Surprisingly, and in contrast, the OA was reduced in the presence of ibuprofen (48% of vehicle control in K562, $n = 4$, $P < 0.001$, Figure 1A; 59% of vehicle control in KU812, $n = 6$, $P < 0.001$, Figure 1B). As diclofenac and ibuprofen demonstrated the most significant effect on OA, and as both are commonly used in clinical practice, these drugs were selected for further experimentation.

Effects of diclofenac and ibuprofen on IC50^{imatinib} of BCR-ABL-positive cell lines

To assess whether the observed divergent alterations in OA translate into changes in tyrosine kinase inhibition, the IC50^{imatinib} was examined in K562 and KU812 cells with or without diclofenac or ibuprofen. A significant decrease in the IC50^{imatinib} was observed in K562 cells when treated with diclofenac (5.7 ± 0.8 to 3.7 ± 0.7 μM, $P = 0.013$, $n = 3$, Figure 2A). In addition, a similar decrease in the KU812 IC50^{imatinib} in the presence of diclofenac (3.5 ± 0.6 to 2.2 ± 0.4 μM, $P = 0.007$, $n = 3$, Figure 2B). In contrast, ibuprofen significantly elevated the IC50^{imatinib} in K562 and KU812 cells (5.7 ± 0.8 to 8.1 ± 0.5 μM and 3.5 ± 0.6 to 6.6 ± 0.8 μM, respectively; $P < 0.001$, $n = 3$).

Effects of diclofenac and ibuprofen on viable cell counts when co-administrated with imatinib and OCT-1 mRNA levels in BCR-ABL-positive cells

To address whether the changes in imatinib intracellular concentration and IC50^{imatinib} mediated by diclofenac or ibuprofen translate to changes in viable cell number, the trypan blue cell exclusion assay was performed with K562 and KU812 cells in the presence or absence of diclofenac and ibuprofen. After 72 hours
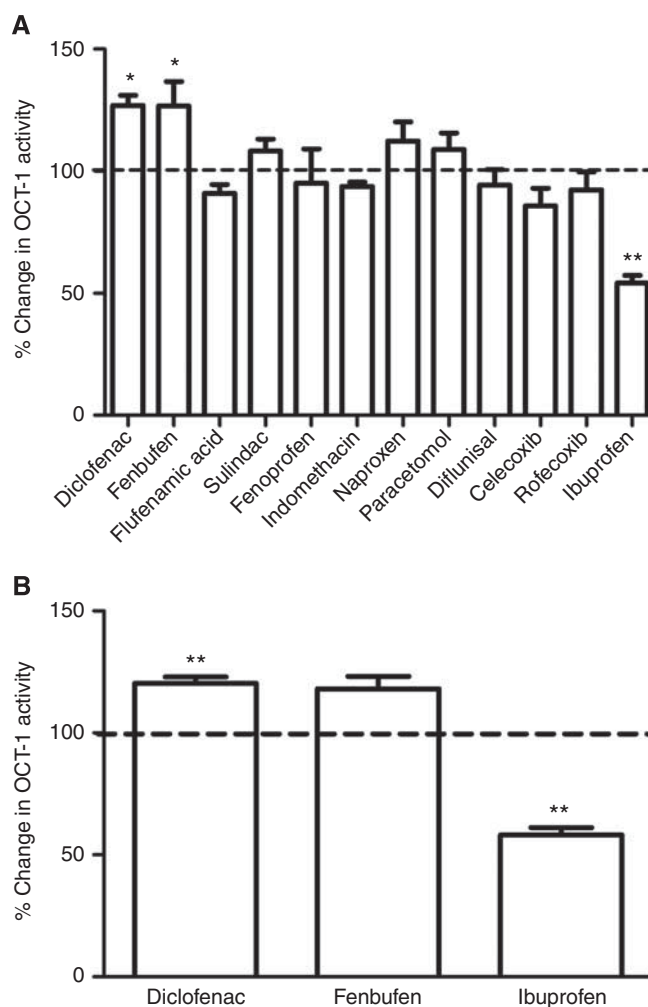
Figure 1 Non-steroidal anti-inflammatory drugs induce divergent effects on OCT-1 activity in BCR-ABL-positive cells. NSAIDs and the potent inhibitor of OCT-1, prazosin, were added to the OCT-1 activity assay simultaneously with ^{14}C-imatinib. After 2-hour incubation, the OA was determined by calculating the difference of the intracellular uptake and retention with or without prazosin. Results (mean ± s.e.m.) are expressed as percentage of own solvent control, which was set at a value of 100%, for at least three biological replicates. *$P < 0.05$ vs control; **$P < 0.001$ vs control. (**A**) OCT-1 activity in the presence of 12 NSAIDs in K562 cells. (**B**) OCT-1 activity in the presence of 10 μM diclofenac, 16 μM fenbufen and 145 μM ibuprofen in KU812 cells.

incubation with varying doses of imatinib as shown in Figure 3, KU812 cells are more sensitive to the effects of imatinib than K562 cells. Thus, different doses of imatinib were used in K562 and KU812 cells. At relatively low doses of imatinib (0.25 μM for K562 cells; 0.05 μM for KU812 cells), diclofenac resulted in a significantly lower number of viable cells after 72 hours compared with imatinib alone (7.82 ± 0.56 × 10^5 ml^{-1} vs 10.95 ± 1.01 × 10^5 ml^{-1} in K562 cells: $P = 0.021$, $n = 3$; 5.40 ± 0.34 × 10^5 ml^{-1} vs 8.40 ± 0.74 × 10^5 ml^{-1} in KU812 cells: $P = 0.019$, $n = 3$, Figures 3A and B), which is consistent with the observed decrease in IC50^{imatinib}. Interestingly, this effect is not due to diclofenac-induced cell death as there was no significant change observed in cell viability in the presence or absence of diclofenac alone.

In contrast, when K562 or KU812 cells were co-incubated with imatinib and ibuprofen there was a significant increase in viable cell number compared with cells treated with imatinib alone (8.16 ± 1.01 × 10^5 ml^{-1} vs 4.88 ± 0.96 × 10^5 ml^{-1} in K562 cells at 0.5 μM of imatinib, $P = 0.004$, $n = 3$; 7.23 ± 0.78 × 10^5 ml^{-1} vs
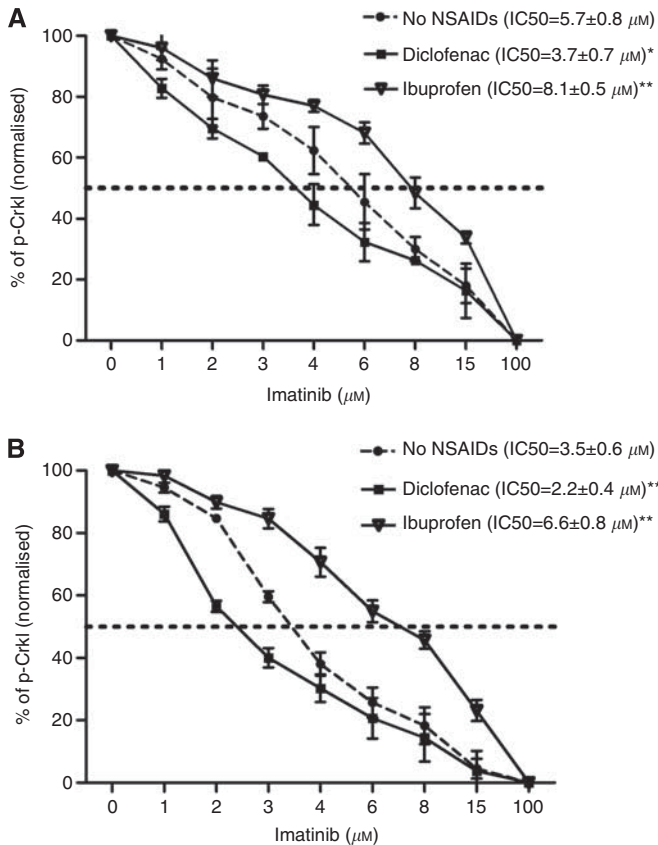
Figure 2 The IC50^{imatinib} results in the presence or absence of 10 μM diclofenac or 145 μM ibuprofen. The in vitro reduction in the level of p-Crkl by imatinib was detected using the IC50^{imatinib} assay. Cells were incubated with 10 μM diclofenac or 145 μM ibuprofen and increasing concentrations of imatinib for 2 hours. The percentage of p-Crkl to non-p-Crkl at 0 μM imatinib was standardised to 100%, and all other data points were normalised about this value. The IC50 was defined as the concentration of imatinib producing a 50% decrease in the level of p-Crkl compared with untreated controls. Error bars represent mean ± s.e.m. for three biological replicates. *$P < 0.05$ vs control; **$P < 0.001$ vs control. The cumulative results (**A**) in K562 cells (**B**) in KU812 cells.

$4.97 \pm 0.47 \times 10^5$ ml^{-1} in KU812 cells at 0.1 μM of imatinib, $P = 0.002$, $n = 3$, Figures 3A and B).

To determine whether the level of OCT-1 mRNA was affected by the presence of NSAIDs OCT1 transcript levels were analysed following a 2-hour incubation in the presence and absence of NSAIDs in both K562 and KU812 cells. There was no significant change in the level of OCT-1 mRNA with diclofenac or ibuprofen over the 2-hour period (data not shown), suggesting that these NSAIDs function via a post-transcriptional mechanism.

Effects of diclofenac and ibuprofen on the OA of primary cells

Our previous TIDEL study in newly diagnosed CML patients receiving imatinib at 600 mg per day has described the link between OA and achievement of optimal or sub-optimal molecular response. The percentage of patients with high OA achieving major molecular response (MMR) by 24 months was significantly greater than that of patients with low OA (85% vs 45%, $P = 0.004$) (White et al, 2007b). Dividing the OA groups further into quartiles, patients with OA in the lowest quartile (Q1, OA < 4 ng per 200 000 cells) have a significantly poorer response to imatinib treatment than those in higher quartiles (White et al, 2010). To examine the effect of both drugs on OA in primary CML samples, OA of MNCs
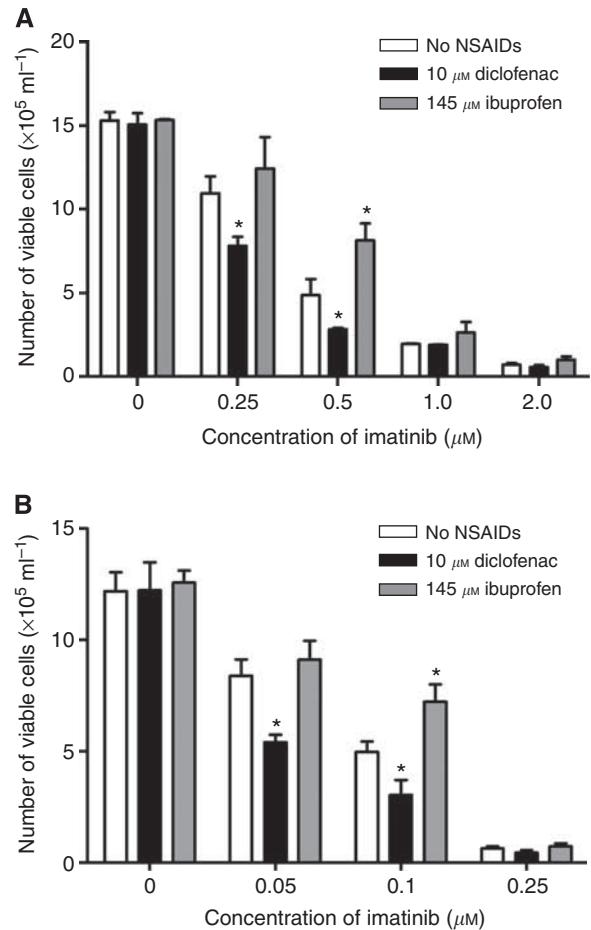
Figure 3 The effects of diclofenac and ibuprofen on the number of viable cells after 72 hours co-incubation with imatinib. The number of viable cells was determined using the trypan blue exclusion method after treatment with NSAIDs and imatinib for 72 hours. 10 μM diclofenac co-administered with imatinib induced a significantly lower viable cell number compared with imatinib alone. Conversely, the viable cell numbers were significantly increased by 145 μM ibuprofen with imatinib, especially at relatively higher concentration of imatinib. The results (mean ± s.e.m) are expressed as the viable cell number determined by trypan blue exclusion assay of three biological replicates. *$P < 0.05$ versus control. (**A**) in K562 cells ($n = 3$) (**B**) in KU812 cells ($n = 3$).

isolated from TIDEL patients were assessed in the presence or absence of 10 μM diclofenac or 145 μM ibuprofen.

We then compared the effect of diclofenac on MNCs from patients with OA in Q1 (OA less than 4 ng per 200 000 cells) with the effect observed in patients with OA greater than 4 ng per 200 000 cells. After treatment with diclofenac, the OA was increased in 93% of the Q1 patients' samples tested. The median OA in Q1 patients rose from 1.39 to 4.17 ng per 200 000 cells ($n = 29$, $P < 0.001$). Notably, as the result of this increase, 15 of 29 cases (51.7%) moved from Q1 to a higher OA quartile group (Figure 4A). However, for patients with higher basal OA value, treatment with diclofenac did not lead to a significant increase in OA (median OA in the absence or presence of diclofenac: 5.49 ng/200,000cells vs 5.92 ng per 200 000cells, $n = 21$, $P = 0.714$, Figure 4B). The different effect of diclofenac between quartiles indicated that the increase in OA mediated by diclofenac was largely confined to patients with low OA rather than in patients with higher OA.

In MNCs treated with ibuprofen, a consistent inhibitory effect (41% reduction in OA) was observed in all 12 cases tested (Figure 4C). The average OA in these 12 samples (7.53 ± 0.82 ng per
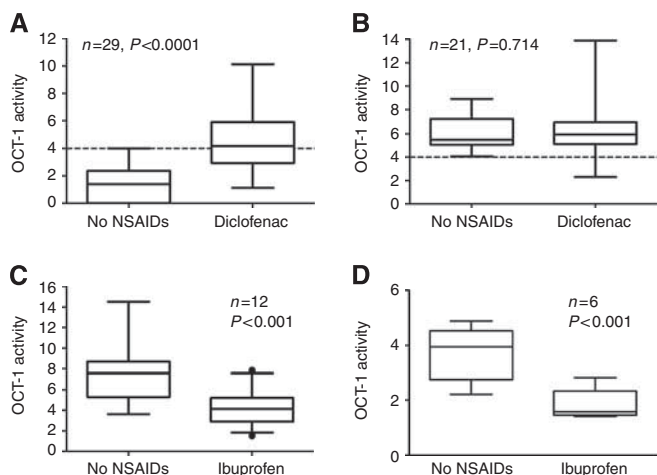
Figure 4 The effects of diclofenac or ibuprofen on OA in primary MNCs. OCT-1 activity assays were performed with fresh or frozen MNCs isolated from the blood of newly diagnosed patients with CML. Box-plots display the median value, the minimum and maximum value of OA. (**A**) 10 μM diclofenac increased OA in patients with basal OA less than 4 ng per 200 000 cells ($n = 29$). (**B**) No significant increase was observed in patients with basal OA greater than 4 ng per 200 000 cells ($n = 21$). (**C**) Decreased OA in MNCs from de-novo CP-CML patients were observed after treatment of 145 μM ibuprofen ($n = 12$). (**D**) Ibuprofen downregulated OA in healthy donors ($n = 6$).

Figure 5 The impact of diclofenac on the IC50^{imatinib} in primary MNCs from de-novo CP-CML patients. Mononuclear cells samples from 9 de-novo CP-CML patients were incubated with 10 μM diclofenac and increasing concentrations of imatinib for 2 hours. The percentage of p-Crkl to non-p-Crkl at 0 μM imatinib was standardised to 100%. All other data points were normalised about this value. The IC50 was defined as the concentration of imatinib achieving a 50% decrease of p-Crkl compared with no imatinib controls. When there were sufficient MNCs, analysis was performed in duplicate. Box-plots display the median value, the minimum and maximum value of OA.

200 000 cells, range 3.53–14.52) was significantly reduced (4.30 ± 0.52 ng per 200 000 cells, range 1.53–7.85, $P < 0.001$) after the treatment with ibuprofen.

In addition, we have examined the effect of diclofenac ($n = 10$) or ibuprofen ($n = 6$) on MNCs collected from normal individuals. Diclofenac did not result in a significant change in OA (data not shown), however, a 50% decrease in OA was observed following ibuprofen treatment (OA before treatment: 3.70 ± 0.45 ng per 200 000 cells, range 2.21–4.89; OA post treatment: 1.83 ± 0.26 ng per 200 000 cells, range 1.41–2.82, $P < 0.001$, Figure 4D).

The impact of diclofenac on the IC50^{imatinib} in primary cells

As diclofenac resulted in a significant increase in OA in MNCs of CP-CML patients, its impact on in vitro kinase inhibition was determined in 9 de novo CP-CML patients. Patients were chosen based on the availability of sufficient fresh blood cells for this analysis, not on the basis of OA. The median IC50^{imatinib} of this group was 1.2 μM (range 0.5–1.7 μM). A significant reduction was observed when diclofenac was added (median IC50^{imatinib} reduced to 0.75 μM, range 0.25–1.15 μM, $P = 0.018$, Figure 5).

DISCUSSION

The interaction between NSAIDs and OCT-1 remains unknown but has significant potential to impact response to imatinib. Here we investigate the potential involvement of NSAIDs in targeted cancer therapy where transport of the anti-leukaemic drug into leukaemic cells has a major role in patient response. Twelve NSAIDs were selected in this study; including the commonly used diclofenac, ibuprofen, naproxen, and celecoxib. Their effects on OCT-1 were first validated in assays of imatinib uptake (IUR). Two NSAIDs with the most significant effects on OA, diclofenac and ibuprofen, were then chosen for IC50^{imatinib} and cell proliferation assays using CML cell lines.

As OCT-1 is the major active influx transporter for imatinib, OA is a strong predictor of response to imatinib treatment in de novo

CML patients (White et al, 2005, 2007a). Here our data demonstrated that OA was increased in BCR-ABL-positive cell lines (K562 and KU812) by diclofenac. Importantly, this increase in OA translated to a significant increase in BCR-ABL kinase inhibition as demonstrated by a reduction in the IC50^{imatinib} in both cell lines. This finding also highlights, in line with our previous studies (White et al, 2007b), the correlation between OA and IC50^{imatinib}. In addition, trypan blue exclusion assays provided further evidence that by increasing functional OA and tyrosine kinase inhibition, diclofenac in combination with imatinib results in a significant reduction in viable cell numbers.

Interestingly, the effect of diclofenac was also observed in CML patients' samples. In 93% of MNCs samples from CML patients with basal OA less than 4 ng per 200 000 cells (Q1), we demonstrated a significant increase in OA in the presence of diclofenac at clinically relevant concentrations. Importantly, 51.7% of Q1 cases tested increased from Q1 to higher quartiles. From a clinical perspective, this increase is of greater significance for the Q1 patients who have a particularly poor outcome on standard imatinib therapy. On the basis of the TIDEL data this may significantly increase the probability of these patients achieving a MMR, and significantly reduce the risk of suboptimal response or imatinib failure (White et al, 2010). However, diclofenac did not significantly increase OA in cells from patients with higher OA. This differential effect of diclofenac in patients with higher OA suggested that this population may not be targeted as well as Q1 by diclofenac intervention.

When applied to MNCs from healthy donors, diclofenac did not mediate the same effect as seen in CML patients, implicating a role for BCR-ABL or disease-related processes in this interaction. These findings raise the possibility that combination therapy with imatinib plus diclofenac may be more effective than imatinib alone, although not adding greatly to the toxicity of the therapy. Importantly from a clinical perspective, this may translate to an increase in the probability of patients with low OA achieving a MMR, and a significantly reduced risk of suboptimal response or imatinib failure. In addition, this strategy may also benefit patients with low OA by allowing for a lower/standard dosage of imatinib (400 mg per day) without adding greatly to the toxicity commonly observed when higher doses of imatinib are used (600 or 800 mg per day). However, extrapolations of in vitro effects to in vivo effects and clinical response will require careful validation.

Another interesting finding in this study is that NSAIDs can exhibit divergent effects on OA in CML cell lines. Although all

NSAIDs have antipyretic, analgesic, and anti-inflammatory properties, there are several important differences in their activities that are mostly due to their affinity towards COX enzyme isoforms: COX-1 and COX-2. In CML, it was reported that expression of COX-2 was significantly higher in CML than in healthy volunteers and the increasing levels of COX-2 were significantly associated with shorter survival (Giles et al, 2002). Therefore several studies have been conducted to investigate the role of COX-2 in imatinib resistance and the use of COX-2 inhibitors as an alternative therapy. It has been reported that celecoxib, a COX-2 inhibitor, reduced cell growth with arrest of the cell cycle at G0/G1 phase and induction of apoptosis by inhibiting NF-κB activation in K562 cells (Subhashini et al, 2005). In imatinib-resistant K562 (IR-K562) cells, over-expression of COX-2 and MDR-1 were observed and in addition, celecoxib could induce cell apoptosis by inhibiting COX-2 and MDR-1 (Arunasree et al, 2008), probably through the PGE2-cAMP-PKC-mediated pathway (Kalle et al, 2010). However, we did not observe any universal effect among COX-2 inhibitors in this study. Although sharing similar COX-2 selectivity with diclofenac (Rich, 2001), celecoxib, as well as another more potent selective COX-2 inhibitor, rofecoxib, had no significant impact on imatinib uptake via OCT-1 in K562 or KU812 cells. This finding suggests that COX-2 inhibitors are unlikely to be the critical mediator of the interaction between OCT-1 and diclofenac observed in this study.

Unexpectedly, although diclofenac increased OA significantly, ibuprofen significantly decreased the OA in both K562 and KU812 cells. This effect on OA translated into an increase in $IC50^{imatinib}$ and cell growth in the presence of imatinib. Given the common administration and over-the-counter access of ibuprofen, this finding is likely to be of significant clinical relevance. Unlike diclofenac, the effect of ibuprofen is also observed in normal cells to the same extent as leukaemic cells, suggesting that the mechanisms of these two interactions are different.

The various effects of NSAIDs on OCT-1-mediated DDI is in contrast with a previous study reporting that diclofenac, ibuprofen, indomethacin and sulindac could all significantly inhibit OCT1-mediated TEA uptake (Khamdang et al, 2002). However, it should be noted that the concentration of NSAIDs used in that study (0.5 μM) was much higher than the concentrations used in our study. Given that the mean maximum plasma concentration (Cmax) of diclofenac after a single dose of 50 mg in healthy volunteers is 5 μM (Siu et al, 2000; Juhlin et al, 2004), the dose used in this study is more relevant to the clinical setting. Similarly, the concentration of ibuprofen used here (145 μM, equal to 30 μg ml^{-1}) is determined according to the clinically achievable level (Cmax = 37 μg ml^{-1}, after 400 mg single administration in healthy volunteers) (Bramlage and Goldis, 2008). Although this concentration is also lower than 0.5 μM, it is still much higher

(up to 20-fold) than other NSAIDs selected in the current work. As it has been shown that NSAIDs are not substrates of OCT transporters (Khamdang et al, 2002), it is unlikely that ibuprofen inhibits imatinib uptake by competing for OCT-1. Molecular structural analysis is necessary to further understand the interaction between ibuprofen and imatinib at the binding site of OCT-1.

We did not observe changes in OCT-1 mRNA that could explain the differences in imatinib uptake and intracellular level. Thus, the major cause of increased OA and kinase inhibition in these short-term assays may be from the effects of these drugs on the post-transcriptional regulation of OCT-1. So far a number of post-transcriptional mechanisms for OCT-1 modulation have been reported, including protein kinase A phosphorylation sites which can affect transporter regulation and substrate specificity (Ciarimboli et al, 2004; Ciarimboli et al, 2005; Holle et al, 2011). Other regulatory pathways identified in transfected Chinese hamster ovary cells include p56^{lck}, calmodulin and the calmodulin-dependent protein kinase II (Ciarimboli et al, 2004). However, the mechanisms underlining OCT-1 regulation in leukaemic cells remains unknown. Further studies are required to establish whether these drugs affect these pathways or impact on OCT-1 transcript or protein levels over longer time periods, or with constant in vivo exposure as would occur clinically. Better understanding of OCT-1 regulation and imatinib influx may lead to additional approaches and drug candidates to enhance imatinib efficacy in CML.

In conclusion, this study provides evidence for interactions between selected NSAIDs and imatinib that directly impact on leukaemic cell response, suggesting that these drugs have the potential to impact significantly on CML patient outcome. The effect of NSAIDs on OA was highly selective suggesting that the mechanism is not related to direct COX inhibition and further studies are required to establish the nature of the interaction in leukaemic cells. Although drugs such as diclofenac may have a positive influence on imatinib efficacy, this is in contrast to the effect seen with ibuprofen suggesting caution is required when administrating NSAIDs to CML patients on imatinib treatment.

ACKNOWLEDGEMENTS

Supplementary Information accompanies the paper on British Journal of Cancer website (http://www.nature.com/bjc)

REFERENCES

Apiwattanakul N, Sekine T, Chairoungdua A, Kanai Y, Nakajima N, Sophasan S, Endou H (1999) Transport properties of nonsteroidal anti-inflammatory drugs by organic anion transporter 1 expressed in Xenopus laevis oocytes. Mol Pharmacol 55(5): 847–854

Arunasree KM, Roy KR, Anilkumar K, Aparna A, Reddy GV, Reddanna P (2008) Imatinib-resistant K562 cells are more sensitive to celecoxib, a selective COX-2 inhibitor: Role of COX-2 and MDR-1. Leuk Res 32(6): 855–864

Bachmakov I, Glaeser H, Fromm MF, Konig J (2008) Interaction of oral antidiabetic drugs with hepatic uptake transporters: focus on organic anion transporting polypeptides and organic cation transporter 1. Diabetes 57(6): 1463–1469

Bjorkman D (1998) Nonsteroidal anti-inflammatory drug-associated toxicity of the liver, lower gastrointestinal tract, and esophagus. Am J Med 105(5 A): 17S–21S

Bramlage P, Goldis A (2008) Bioequivalence study of three ibuprofen formulations after single dose administration in healthy volunteers. BMC Pharmacol 8: 1471–1487

Ciarimboli G, Koepsell H, Iordanova M, Gorboulev V, Dürner B, Lang D, Edemir B, Schröter R, Van Le T, Schlatter E (2005) Individual PKC-phosphorylation sites in organic cation transporter 1 determine substrate selectivity and transport regulation. J Am Soc Nephrol 16(6): 1562–1570

Ciarimboli G, Struwe K, Arndt P, Gorboulev V, Koepsell H, Schlatter E, Hirsch JR (2004) Regulation of the human organic cation transporter hOCT1. J Cell Physiol 201(3): 420–428

Cortes JE, Baccarani M, Guilhot F, Druker BJ, Branford S, Kim DW, Pane F, Pasquini R, Goldberg SL, Kalaycio M, Moiraghi B, Rowe JM, Tothova E, De Souza C, Rudoltz M, Yu R, Krahnke T, Kantarjian HM, Radich JP, Hughes TP (2010) Phase III, randomized, open-label study of daily imatinib mesylate 400 mg versus 800 mg in patients with newly diagnosed, previously untreated chronic myeloid leukemia in chronic phase using molecular end points: tyrosine kinase inhibitor optimization and selectivity study. J Clin Oncol 28(3): 424–430

Deininger MWN, O'Brien SG, Ford JM, Druker BJ (2003) Practical management of patients with chronic myeloid leukemia receiving imatinib. *J Clin Oncol* 21(8): 1637–1647

Fahrmayr C, Fromm MF, König J (2010) Hepatic OATP and OCT uptake transporters: Their role for drug-drug interactions and pharmacogenetic aspects. *Drug Metab Rev* 42(3): 380–401

Farooq M, Haq I, Qureshi AS (2008) Cardiovascular risks of COX inhibition: Current perspectives. *Expert Opin Pharmacother* 9(8): 1311–1319

Giannoudis A, Davies A, Lucas CM, Harris RJ, Pirmohamed M, Clark RE (2008) Effective dasatinib uptake may occur without human organic cation transporter 1 (hOCT1): implications for the treatment of imatinib-resistant chronic myeloid leukemia. *Blood* 112(8): 3348–3354

Giles FJ, Kantarjian HM, Bekele BN, Cortes JE, Faderl S, Thomas DA, Manshouri T, Rogers A, Keating MJ, Talpaz M, O'Brien S, Albitar M (2002) Bone marrow cyclooxygenase-2 levels are elevated in chronic-phase chronic myeloid leukaemia and are associated with reduced survival. *Br J Haematol* 119(1): 38–45

Gorre ME, Mohammed M, Ellwood K, Hsu N, Paquette R, Nagesh Rao P, Sawyers CL (2001) Clinical resistance to STI-571 cancer therapy caused by BCR-ABL gene mutation or amplification. *Science* 293(5531): 876–880

Hiwase DK, Saunders V, Hewett D, Frede A, Zrim S, Dang P, Eadie L, To LB, Melo J, Kumar S, Hughes TP, White DL (2008) Dasatinib cellular uptake and efflux in chronic myeloid leukemia cells: therapeutic implications. *Clin Cancer Res* 14(12): 3881–3888

Holle SK, Ciarimboli G, Edemir B, Neugebauer U, Pavenstädt H, Schlatter E (2011) Properties and regulation of organic cation transport in freshly isolated mouse proximal tubules analyzed with a fluorescence reader-based method. *Pflugers Archiv Eur J Physiol* 462(2): 359–369

Honjo H, Uwai Y, Aoki Y, Iwamoto K (2011) Stereoselective inhibitory effect of flurbiprofen, ibuprofen and naproxen on human organic anion transporters hOAT1 and hOAT3. *Biopharm Drug Dispos* 32(9): 518–524

Hughes T, Deininger M, Hochhaus A, Branford S, Radich J, Kaeda J, Baccarani M, Cortes J, Cross NCP, Druker BJ, Gabert J, Grimwade D, Hehlmann R, Kamel-Reid S, Lipton JH, Longtine J, Martinelli G, Saglio G, Soverini S, Stock W, Goldman JM (2006) Monitoring CML patients responding to treatment with tyrosine kinase inhibitors: Review and recommendations for harmonizing current methodology for detecting BCR-ABL transcripts and kinase domain mutations and for expressing results. *Blood* 108(1): 28–37

Hughes TP, Branford S, White DL, Reynolds J, Koelmeyer R, Seymour JF, Taylor K, Arthur C, Schwarer A, Morton J, Cooney J, Leahy MF, Rowlings P, Catalano J, Hertzberg M, Filshie R, Mills AK, Fay K, Durrant S, Januszewicz H, Joske D, Underhill C, Dunkley S, Lynch K, Grigg A (2008) Impact of early dose intensity on cytogenetic and molecular responses in chronicphase CMLpatients receiving 600 mg/day of imatinib as initial therapy. *Blood* 112(10): 3965–3973

Hughes TP, Hochhaus A, Branford S, Müller MC, Kaeda JS, Foroni L, Druker BJ, Guilhot F, Larson RA, O'Brien SG, Rudoltz MS, Mone M, Wehrle E, Modur V, Goldman JM, Radich JP (2010) Long-term prognostic significance of early molecular response to imatinib in newly diagnosed chronic myeloid leukemia: An analysis from the International Randomized Study of Interferon and STI571 (IRIS). *Blood* 116(19): 3758–3765

Juhlin T, Björkman S, Gunnarsson B, Fyge A, Roth B, Höglund P (2004) Acute administration of diclofenac, but possibly not long term low dose aspirin, causes detrimental renal effects in heart failure patients treated with ACE-inhibitors. *Eur J Heart Fail* 6(7): 909–916

Jung N, Lehmann C, Rubbert A, Knispel M, Hartmann P, van Lunzen J, Stellbrink HJ, Faetkenheuer G, Taubert D (2008) Relevance of the organic cation transporters 1 and 2 for antiretroviral drug therapy in human immunodeficiency virus infection. *Drug Metab Dispos* 36(8): 1616–1623

Kalle AM, Sachchidanand S, Pallu R (2010) Bcr-Abl-independent mechanism of resistance to imatinib in K562 cells: Induction of cyclooxygenase-2 (COX-2) by histone deacetylases (HDACs). *Leuk Res* 34(9): 1132–1138

Khamdang S, Takeda M, Noshiro R, Narikawa S, Enomoto A, Anzai N, Piyachaturawat P, Endou H (2002) Interactions of human organic anion transporters and human organic cation transporters with nonsteroidal anti-inflammatory drugs. *J Pharmacol Exp Ther* 303(2): 534–539

Kindla J, Fromm MF, Konig J (2009) *In vitro* evidence for the role of OATP and OCT uptake transporters in drug-drug interactions. *Expert Opin Drug Metab Toxicol* 5(5): 489–500

Minematsu T, Giacomini KM (2011) Interactions of Tyrosine Kinase Inhibitors with Organic Cation Transporters, OCTs, and Multidrug and Toxic Compound Extrusion Proteins, MATEs. *Mol Cancer Ther* 10(3): 531–539

Mulato AS, Ho ES, Cihlar T (2000) Nonsteroidal anti-inflammatory drugs efficiently reduce the transport and cytotoxicity of adefovir mediated by the human renal organic anion transporter 1. *J Pharmacol Exp Ther* 295(1): 10–15

Nozaki Y, Kusuhara H, Endou H, Sugiyama Y (2004) Quantitative evaluation of the drug-drug interactions between methotrexate and nonsteroidal anti-inflammatory drugs in the renal uptake process based on the contribution of organic anion transporters and reduced folate carrier. *J Pharmacol Exp Ther* 309(1): 226–234

Perneger TV, Whelton PK, Klag MJ (1994) Risk of kidney failure associated with the use of acetaminophen, aspirin, and nonsteroidal antiinflammatory drugs. *N Engl J Med* 331(25): 1675–1679

Rich SA (2001) The coxibs, selective inhibitors of cyclooxygenase-2. *N Engl J Med* 345(23): 1709

Shah NP, Nicoll JM, Nagar B, Gorre ME, Paquette RL, Kuriyan J, Sawyers CL (2002) Multiple BCR-ABL kinase domain mutations confer polyclonal resistance to the tyrosine kinase inhibitor imatinib (STI571) in chronic phase and blast crisis chronic myeloid leukemia. *Cancer Cell* 2(2): 117–125

Siu SSN, Yeung JHK, Lau TK (2000) A study on placental transfer of diclofenac in first trimester of human pregnancy. *Hum Reprod* 15(11): 2423–2425

Subhashini J, Mahipal SVK, Reddanna P (2005) Anti-proliferative and apoptotic effects of celecoxib on human chronic myeloid leukemia *in vitro*. *Cancer Lett* 224(1): 31–43

Thomas J, Wang L, Clark RE, Pirmohamed M (2004) Active transport of imatinib into and out of cells: Implications for drug resistance. *Blood* 104(12): 3739–3745

Ulrich CM, Bigler J, Potter JD (2006) Non-steroidal anti-inflammatory drugs for cancer prevention: Promise, perils and pharmacogenetics. *Nat Rev Cancer* 6(2): 130–140

Umehara KI, Iwatsubo T, Noguchi K, Usui T, Kamimura H (2008) Effect of cationic drugs on the transporting activity of human and rat OCT/Oct 1-3 *in vitro* and implications for drug-drug interactions. *Xenobiotica* 38(9): 1203–1218

White D, Saunders V, Grigg A, Arthur C, Filshie R, Leahy MF, Lynch K, To LB, Hughes T (2007a) Measurement of *in vivo* BCR-ABL kinase inhibition to monitor imatinib-induced target blockade and predict response in chronic myeloid leukemia. *J Clin Oncol* 25(28): 4445–4451

White D, Saunders V, Lyons AB, Branford S, Grigg A, To LB, Hughes T (2005) *In vitro* sensitivity to imatinib-induced inhibition of ABL kinase activity is predictive of molecular response in patients with de novo CML. *Blood* 106(7): 2520–2526

White DL, Dang P, Engler J, Frede A, Zrim S, Osborn M, Saunders VA, Manley PW, Hughes TP (2010) Functional activity of the OCT-1 protein is predictive of long-term outcome in patients with chronic-phase chronic myeloid leukemia treated with imatinib. *J Clin Oncol* 28(16): 2761–2767

White DL, Hughes TP (2012) Classification of Patients With Chronic Myeloid Leukemia on Basis of BCR-ABL Transcript Level at 3 Months Fails to Identify Patients With Low Organic Cation Transporter-1 Activity Destined to Have Poor Imatinib Response. *J Clin Oncol* 30(10): 1144–1145

White DL, Saunders VA, Dang P, Engler J, Venables A, Zrim S, Zannettino A, Lynch K, Manley PW, Hughes T (2007b) Most CML patients who have a suboptimal response to imatinib have low OCT-1 activity: higher doses of imatinib may overcome the negative impact of low OCT-1 activity. *Blood* 110(12): 4064–4072

White DL, Saunders VA, Dang P, Engler J, Zannettino ACW, Cambareri AC, Quinn SR, Manley PW, Hughes TP (2006) OCT-1-mediated influx is a key determinant of the intracellular uptake of imatinib but not nilotinib (AMN107): Reduced OCT-1 activity is the cause of low *in vitro* sensitivity to imatinib. *Blood* 108(2): 697–704

APPENDIX B
Supplementary Figures and Tables

Supplementary Table 1   Primer sequences for RQ-PCR

	Primer Name	Sequence 5' to 3'
Standard	RANKL Forward:	TCA GCC TTT TGC TCA TCT CAC TAT
	RANKL Reverse:	CCA CCC CCG ATC ATG GT
Reference genes	GUSB Forward:	GAA AAA ATG AGG ACG GGT ACG T
	GUSB Reverse:	ATT TTG CCG ATT TCA TGA CTG A
	TBP forward	TAT AAT CCC AAG CGG TTT GC
	TBP reverse	GCT GGA AAA CCC AAC TTC TG
	BCR Forward:	CCT GCG ATG GCG TTC AC
	BCR Reverse:	CCT TCG ACG TCA ATA ACA AGG AT
Genes of interest	ARG1 Forward:	GAT TCC CGA TGT GCC AGG ATT
	ARG1 Reverse:	GCC AAT CCT AGT CTG TCA CTT
	COX-2 Forward:	GAA ACC CAC TCC AAA CAC A
	COX-2 Reverse:	GAG AAG GCT TCC AGC TTT TT
	EEA1 Forward:	CCC AAC TTG CTA CTG AAA TTG C
	EEA1 Reverse:	TGT CAG ACG TGT CAC TTT TTG T
	GRK5 Forward:	TGG CTG GAG TGT TAC ATT CA
	GRK5 Reverse:	GGG GTG AGG TAC TTG GTC ATA AT
	HSP90AA6P Forward:	CTG TTA AGA TCA GCC GCC AG
	HSP90AA6P Reverse:	CAG TAG GTT CCA CAA TAG GCT C
	HSPB3 Forward:	ATA GAG ATT CCA GTG CGT TAC CA
	HSPB3 Reverse:	CAG GCA GTG CAT ATA AAG CAT GA
	ID3 Forward:	CAT CGA CTA CAT TCT CGA CCT G
	ID3 Reverse:	TCC TTT TGT CGT TGG AGA TGA C
	LRRFIP1 Forward:	GCT ATG GTT CCA ATG CTC AGC
	LRRFIP1 Reverse:	GCC GCC TAG ATT CAG CCA G

OCT1 Forward:	CTG AGC TGT ACC CCA CAT TCG
OCT1 Reverse:	CCA CAC CGC AAA CAA AAT GA
PAGE2B Forward:	GAG CAT GTG AGA ACA AGA TCC C
PAGE2B Reverse:	CTC CTG GAC AAT CAC AGA TCC
PPARγ Forward:	TGA AGG ATG CAA GGG TTT CT
PPARγ Reverse:	CCA ACA GCT TCT CCT TCT CG
TRAF1 Forward:	TCC TGT GGA AGA TCA CCA ATG T
TRAF1 Reverse:	GCA GGC ACA ACT TGT AGC C
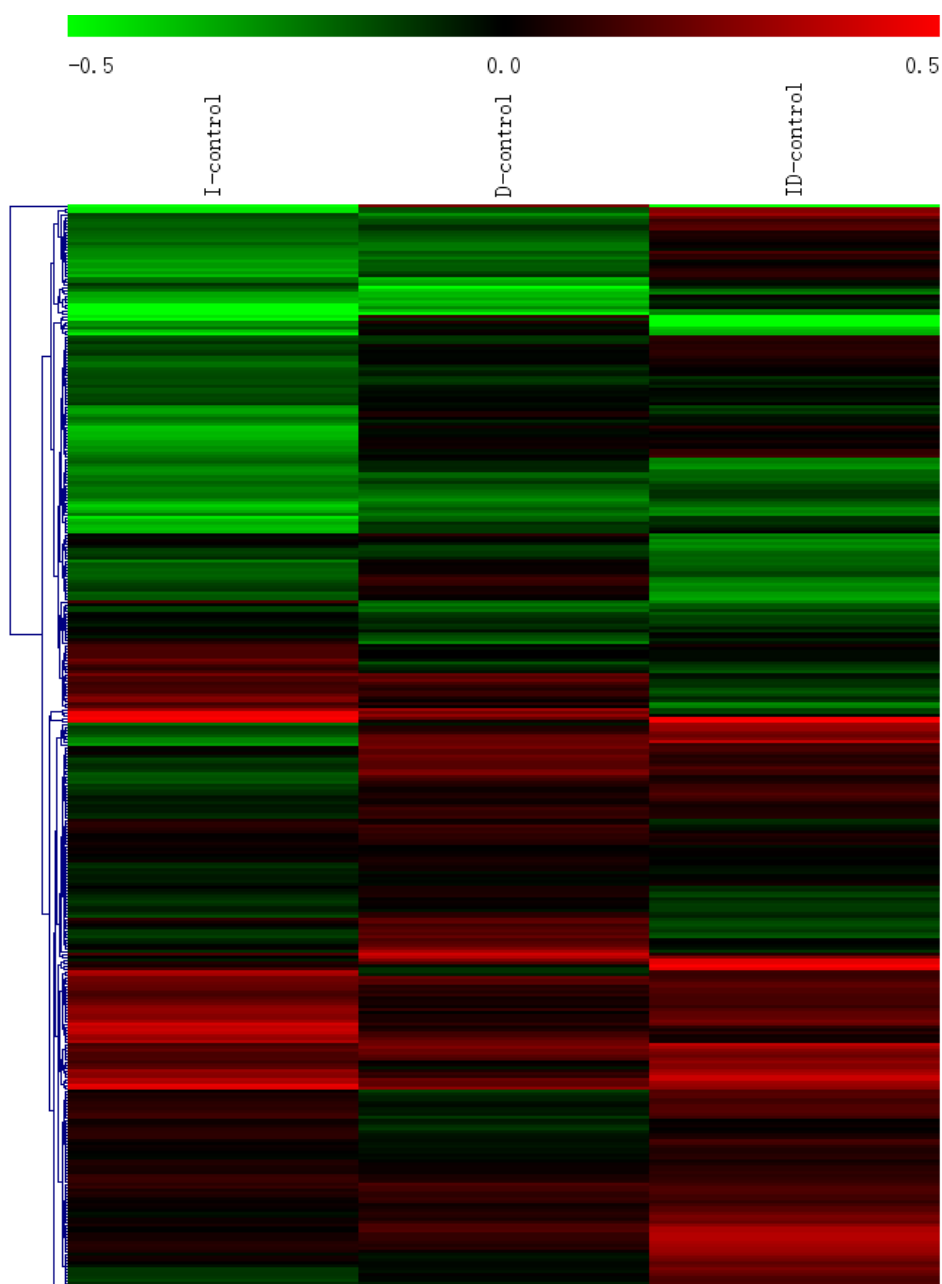
Supplementary Figure 1   The heat map of SLC superfamily transporters in KU812 after treatment with imatinib and/or diclofenac for 2 hours

The heat map indicates the fold change of SLC superfamily transporters gene expression compared with control of in the microarray. A total of 373 SLC transporter genes are shown. Red and green colour indicates up-regulated and down-regulated genes comparing with control respectively. As the scale of the expression is small (-0.5 to 0.5), the range of fold change compared to control in each condition is small.
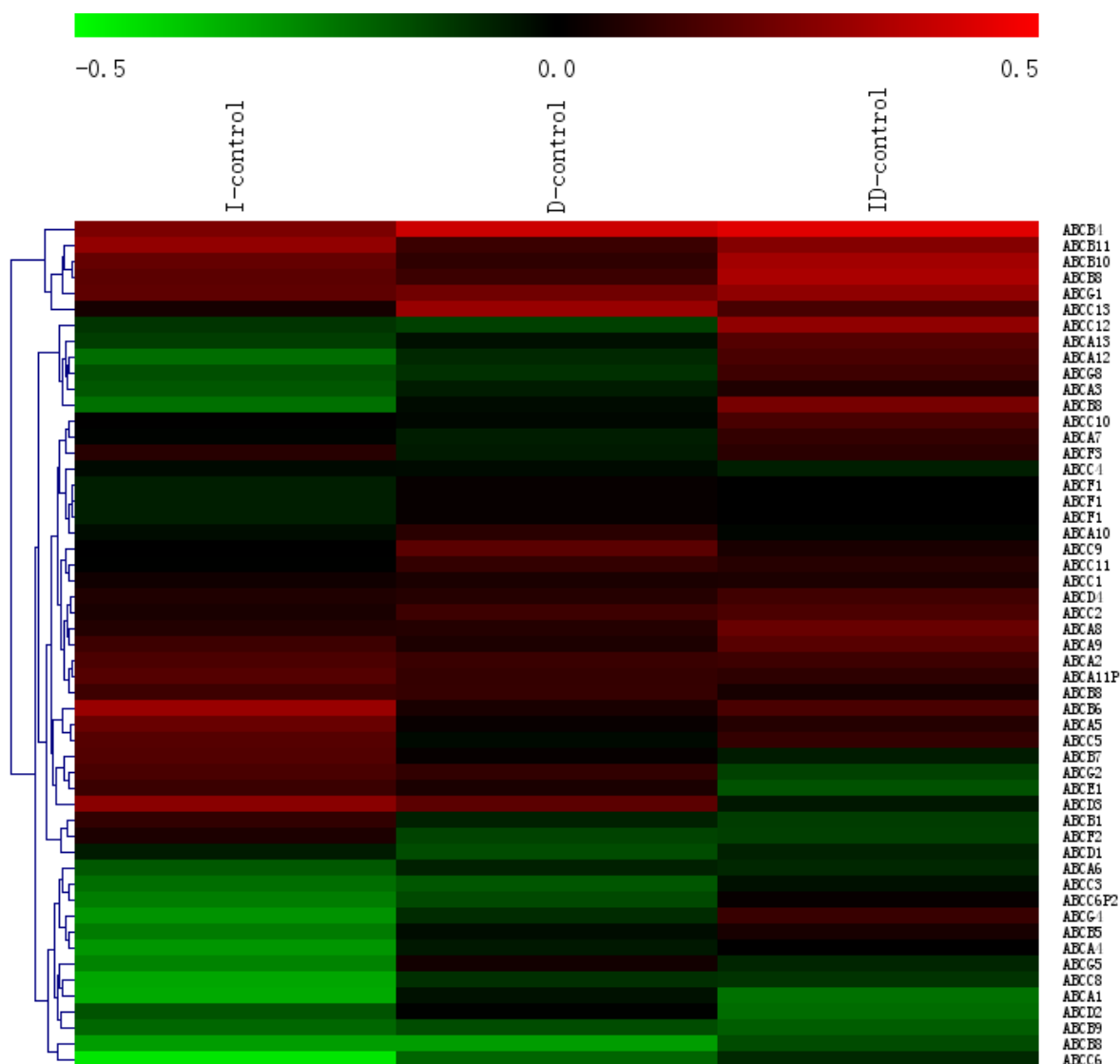
Supplementary Figure 2 The heat map of ABC superfamily transporters in KU812 after treatment with imatinib and/or diclofenac for 2 hours

The heat map indicates the fold change of ABC superfamily transporters gene expression compared with control of in the microarray. A total of 53 ABC transporters genes are shown. Red and green colour indicates up-regulated and down-regulated genes respectively. As the scale of the expression is small (-0.5 to 0.5), the range of fold change compared to control in each condition is small.
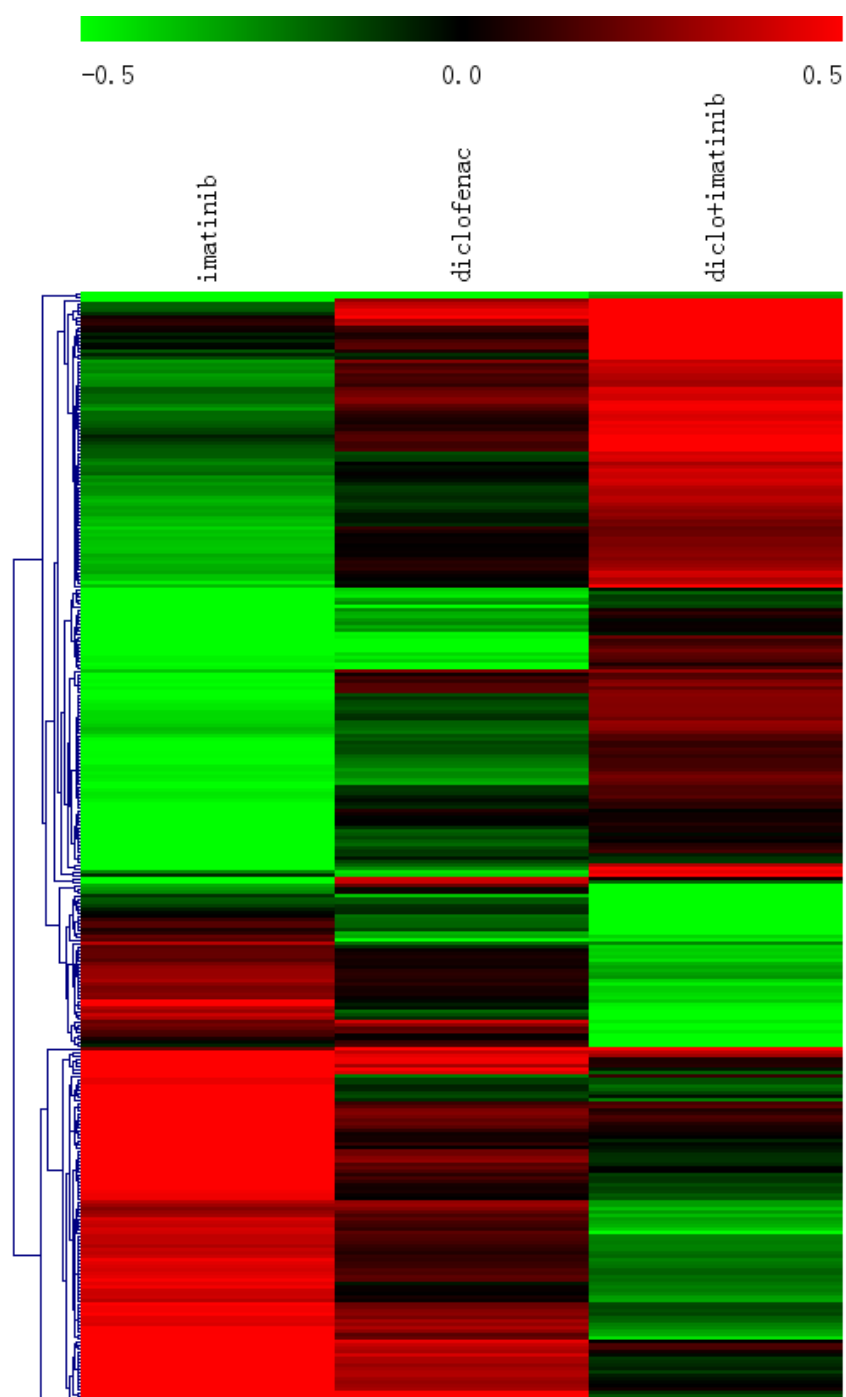
Supplementary Figure 3   The heat map showing genes with fold change greater than 1.5 in dual treatment compared with imatinib only in KU812 cells

Heat map showing 327 genes with the absolute value of the fold change greater than 1.5 when comparing dual treatment with diclofenac+imatinib to imatinib only. Red and green colour indicates up-regulated and down-regulated genes compared with control respectively.
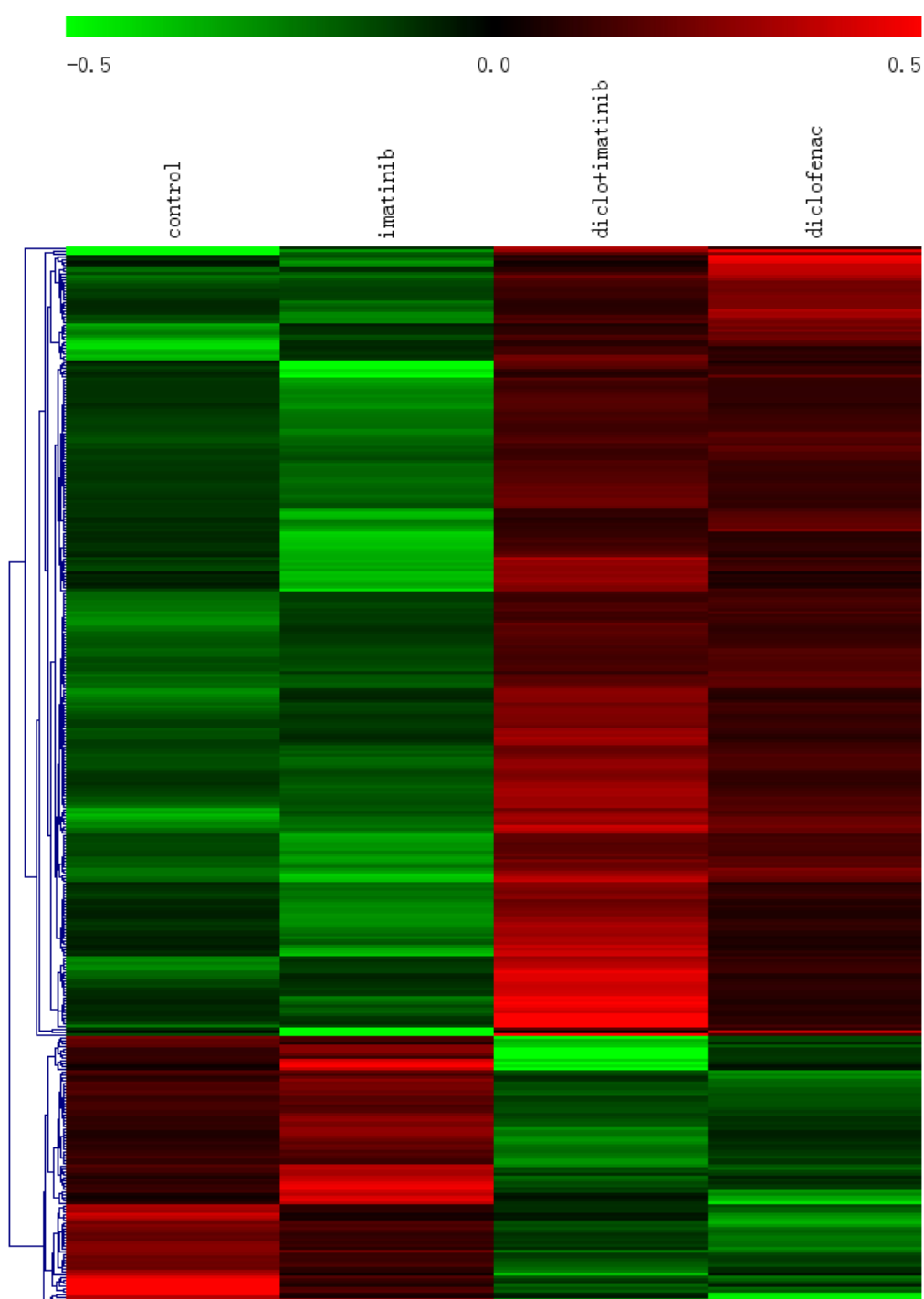
Supplementary Figure 4   The heat map showing genes with *p*-value<0.05 in KU812 cells

Heat map showing 375 genes with the *p*-value<0.05 when the average values of diclofenac only and dual treatment was compared to that of KU812 control and imatinib only by the moderated t statistic. Red and green colour indicates up-regulated and down-regulated genes compared to control respectively

REFERENCES

1. Faderl S, Talpaz M, Estrov Z, Kantarjian HM. Chronic myelogenous leukemia: biology and therapy. Annals of Internal Medicine. 1999 Aug 3;131(3):207-19.

2. Tefferi A. Classification, diagnosis and management of myeloproliferative disorders in the JAK2V617F era. Hematology / the Education Program of the American Society of Hematology American Society of Hematology Education Program. 2006:240-5.

3. Clarkson B, Strife A, Wisniewski D, Lambek C, Liu C. Chronic myelogenous leukemia as a paradigm of early cancer and possible curative strategies. Leukemia. 2003;17(7):1211-62.

4. Calabretta B, Perrotti D. The biology of CML blast crisis. Blood. 2004;103(11):4010-22.

5. National Academy of Sciences. Science. 1960 Nov 18;132(3438):1488-501.

6. Kurzrock R, Kantarjian HM, Druker BJ, Talpaz M. Philadelphia chromosome-positive leukemias: from basic mechanisms to molecular therapeutics. Annals of Internal Medicine. 2003 May 20;138(10):819-30.

7. Melo JV. The molecular biology of chronic myeloid leukaemia. Leukemia : official journal of the Leukemia Society of America, Leukemia Research Fund, UK. 1996 May;10(5):751-6.

8. Advani AS, Pendergast AM. Bcr-Abl variants: biological and clinical aspects. Leukemia Research. 2002 Aug;26(8):713-20.

9. Daley GQ, Van Etten RA, Baltimore D. Induction of chronic myelogenous leukemia in mice by the P210bcr/abl gene of the Philadelphia chromosome. Science. 1990 Feb 16;247(4944):824-30.

10. Zhao RC, Jiang Y, Verfaillie CM. A model of human p210(bcr/ABL)-mediated chronic myelogenous leukemia by transduction of primary normal human CD34(+) cells with a BCR/ABL-containing retroviral vector. Blood. 2001 Apr 15;97(8):2406-12.

11. Zhao RC, Jiang Y, Verfaillie CM. A model of human p210bcr/ABL-mediated chronic myelogenous leukemia by transduction of primary normal human CD34+ cells with a BCR/ABL-containing retroviral vector. Blood. 2001;97(8):2406-12.

12. Li S, Ilaria RL, Million RP, Daley GQ, Van Etten RA. The P190, P210, and P230 forms of the BCR/ABL oncogene induce a similar chronic myeloid leukemia–like syndrome in mice but have different lymphoid leukemogenic activity. The Journal of experimental medicine. 1999;189(9):1399.

13. Huettner CS, Koschmieder S, Iwasaki H, Iwasaki-Arai J, Radomska HS, Akashi K, et al. Inducible expression of BCR/ABL using human CD34 regulatory elements results in a megakaryocytic myeloproliferative syndrome. Blood. 2003;102(9):3363-70.

14. Sonoyama J, Matsumura I, Ezoe S, Satoh Y, Zhang X, Kataoka Y, et al. Functional cooperation among Ras, STAT5, and phosphatidylinositol 3-kinase is required for full oncogenic activities of BCR/ABL in K562 cells. Journal of Biological Chemistry. 2002;277(10):8076-82.

15. Vara JÁF, Casado E, de Castro J, Cejas P, Belda-Iniesta C, González-Barón M. PI3K/Akt signalling pathway and cancer. Cancer treatment reviews. 2004;30(2):193-204.

16. Baśkiewicz‐Masiuk M, Machaliński B. The role of the STAT5 proteins in the proliferation and apoptosis of the CML and AML cells. Eur J Haematol. 2004;72(6):420-9.

17. Bedi A, Zehnbauer BA, Barber JP, Sharkis SJ, Jones RJ. Inhibition of apoptosis by BCR-ABL in chronic myeloid leukemia. Blood. 1994 Apr 15;83(8):2038-44.

18. Steelman LS, Pohnert SC, Shelton JG, Franklin RA, Bertrand FE, McCubrey JA. JAK/STAT, Raf/MEK/ERK, PI3K/Akt and BCR-ABL in cell cycle progression and leukemogenesis. Leukemia : official journal of the Leukemia Society of America, Leukemia Research Fund, UK. 2004 Feb;18(2):189-218.

19. Van Etten RA. Mechanisms of transformation by the BCR-ABL oncogene: new perspectives in the post-imatinib era. Leukemia Research. 2004 May;28 Suppl 1:S21-8.

20. Skorski T, Kanakaraj P, Nieborowska-Skorska M, Ratajczak M, Wen SC, Zon G, et al. Phosphatidylinositol-3 kinase activity is regulated by BCR/ABL and is required for the growth of Philadelphia chromosome-positive cells. Blood. 1995;86(2):726-36.

21. Penserga ET, Skorski T. Fusion tyrosine kinases: a result and cause of genomic instability. Oncogene. 2007 Jan 4;26(1):11-20.

22. Calabretta B, Perrotti D. The biology of CML blast crisis. Blood. 2004 Jun 1;103(11):4010-22.

23. Shah NP, Sawyers CL. Mechanisms of resistance to STI571 in Philadelphia chromosome-associated leukemias. Oncogene. 2003 Oct 20;22(47):7389-95.

24. Chronic granulocytic leukaemia: comparison of radiotherapy and busulphan therapy. Report of the Medical Research Council's working party for therapeutic trials in leukaemia. Br Med J. 1968 Jan 27;1(5586):201-8.

25. Hehlmann R, Heimpel H, Hasford J, Kolb HJ, Pralle H, Hossfeld DK, et al. Randomized comparison of busulfan and hydroxyurea in chronic myelogenous leukemia: prolongation of survival by hydroxyurea. The German CML Study Group. Blood. 1993 Jul 15;82(2):398-407.

26. Hydroxyurea versus busulphan for chronic myeloid leukaemia: an individual patient data meta-analysis of three randomized trials. Chronic myeloid leukemia trialists' collaborative group. British Journal of Haematology. 2000 Sep;110(3):573-6.

27. Talpaz M, Kantarjian HM, McCredie K, Trujillo JM, Keating MJ, Gutterman JU. Hematologic remission and cytogenetic improvement induced by recombinant human interferon alpha A in chronic myelogenous leukemia. N Engl J Med. 1986 Apr 24;314(17):1065-9.

28. Ohnishi K, Ohno R, Tomonaga M, Kamada N, Onozawa K, Kuramoto A, et al. A randomized trial comparing interferon-alpha with busulfan for newly diagnosed chronic myelogenous leukemia in chronic phase. Blood. 1995 Aug 1;86(3):906-16.

29. Silver RT, Woolf SH, Hehlmann R, Appelbaum FR, Anderson J, Bennett C, et al. An evidence-based analysis of the effect of busulfan, hydroxyurea, interferon, and allogeneic bone marrow transplantation in treating the chronic phase of chronic myeloid leukemia: developed for the American Society of Hematology. Blood. 1999 Sep 1;94(5):1517-36.

30. Clarkson B, Strife A, Wisniewski D, Lambek CL, Liu C. Chronic myelogenous leukemia as a paradigm of early cancer and possible curative strategies. Leukemia. 2003;17(7):1211-62.

31. Fefer A, Buckner CD, Thomas ED, Cheever MA, Clift RA, Glucksberg H, et al. Cure of hematologic neoplasia with transplantation of marrow from identical twins. New England Journal of Medicine. 1977;297(3):146-8.

32. Clift RA, Buckner CD, Thomas ED. Treatment of chronic granulocytic leukaemia in chronic phase by allogeneic marrow transplantation. Lancet. 1982;2(8299):621-3.

33. Fefer A, Cheever MA, Greenberg PD. Treatment of chronic granulocytic leukemia with chemoradiotherapy and transplantation of marrow from identical twins. New England Journal of Medicine. 1982;306(2):63-8.

34. McGlave PB, Arthur DC, Kim TH. Successful allogeneic bone-marrow transplantation for patients in the accelerated phase of chronic granulocytic leukaemia. Lancet. 1982;2(8299):625-7.

35. Herve P, Cahn JY, Flesch M. Successful engraftment after three mismatched bone-marrow transplantations for chronic granulocytic leukemia. New England Journal of Medicine. 1985;312(4):242.

36. Savage DG, Goldman JM. Allografting for chronic myeloid leukemia. Current Opinion in Hematology. 1997;4(6):369-76.

37. Miyamura K, Tahara T, Tanimoto M, Morishita Y, Kawashima K, Morishima Y, et al. Long persistent bcr-abl positive transcript detected by polymerase chain reaction after marrow transplant for chronic myelogenous leukemia without clinical relapse: A study of 64 patients. Blood. 1993;81(4):1089-93.

38. Gratwohl A, Brand R, Apperley J, Crawley C, Ruutu T, Corradini P, et al. Allogeneic hematopoietic stem cell transplantation for chronic myeloid leukemia in Europe 2006: transplant activity, long-term data and current results. An analysis by the Chronic Leukemia Working Party of the European Group for Blood and Marrow Transplantation (EBMT). Haematologica. 2006 Apr;91(4):513-21.

39. Goldman JM, Gale RP, Horowitz MM, Biggs JC, Champlin RE, Gluckman E, et al. Bone marrow transplantation for chronic myelogenous leukemia in chronic phase. Increased risk for relapse associated with T-cell depletion. Annals of Internal Medicine. 1988;108(6):806-14.

40. Marmont AM, Horowitz MM, Gale RP, Sobocinski K, Ash RC, van Bekkum DW, et al. T-cell depletion of HLA-identical transplants in leukemia. Blood. 1991 Oct 15;78(8):2120-30.

41. Buckner CD, Stewart P, Clift RA, Fefer A, Neiman PE, Singer J, et al. Treatment of blastic transformation of chronic granulocytic leukemia by chemotherapy, total body irradiation and infusion of cryopreserved autologous marrow. Experimental hematology. 1978 Jan;6(1):96-109.

42. Goldman JM, Th'ng KH, Park DS, Spiers AS, Lowenthal RM, Ruutu T. Collection, cryopreservation and subsequent viability of haemopoietic stem cells intended for treatment of chronic granulocytic leukaemia in blast-cell transformation. British Journal of Haematology. 1978 Oct;40(2):185-95.

43. Reiffers J, Trouette R, Marit G, Montastruc M, Faberes C, Cony-Makhoul P, et al. Autologous blood stem cell transplantation for chronic granulocytic leukaemia in transformation: a report of 47 cases. British Journal of Haematology. 1991 Mar;77(3):339-45.

44. McGlave PB, De Fabritiis P, Deisseroth A, Goldman J, Barnett M, Reiffers J, et al. Autologous transplants for chronic myelogenous leukaemia: Results from eight transplant groups. Lancet. 1994;343(8911):1486-8.

45. Horowitz MM, Gale RP, Sondel PM, Goldman JM, Kersey J, Kolb HJ, et al. Graft-versus-leukemia reactions after bone marrow transplantation. Blood. 1990 Feb 1;75(3):555-62.

46. Slavin S, Naparstek E, Nagler A, Ackerstein A, Kapelushnik J, Or R. Allogeneic cell therapy for relapsed leukemia after bone marrow transplantation with donor peripheral blood lymphocytes. Experimental hematology. 1995 Dec;23(14):1553-62.

47. Druker BJ, Talpaz M, Resta DJ, Peng B, Buchdunger E, Ford JM, et al. Efficacy and safety of a specific inhibitor of the BCR-ABL tyrosine kinase in chronic myeloid leukemia. N Engl J Med. 2001 Apr 5;344(14):1031-7.

48. Druker BJ, Lydon NB. Lessons learned from the development of an abl tyrosine kinase inhibitor for chronic myelogenous leukemia. The Journal of clinical investigation. 2000 Jan;105(1):3-7.

49. Schindler T, Bornmann W, Pellicena P, Miller WT, Clarkson B, Kuriyan J. Structural mechanism for STI-571 inhibition of abelson tyrosine kinase. Science. 2000 Sep 15;289(5486):1938-42.

50. Okuda K, Weisberg E, Gilliland DG, Griffin JD. ARG tyrosine kinase activity is inhibited by STI571. Blood. 2001;97(8):2440-8.

51. Buchdunger E, Zimmermann J, Mett H, Meyer T, Muller M, Druker BJ, et al. Inhibition of the Abl protein-tyrosine kinase in vitro and in vivo by a 2-phenylaminopyrimidine derivative. Cancer Research. 1996 Jan 1;56(1):100-4.

52. Dewar AL, Cambareri AC, Zannettino ACW, Miller BL, Doherty KV, Hughes TP, et al. Macrophage colony-stimulating factor receptor c-fms is a novel target of imatinib. Blood. 2005;105(8):3127-32.

53. Druker BJ, Tamura S, Buchdunger E, Ohno S, Segal GM, Fanning S, et al. Effects of a selective inhibitor of the Abl tyrosine kinase on the growth of Bcr-Abl positive cells. Nat Med. 1996 May;2(5):561-6.

54. Talpaz M, Silver RT, Druker BJ, Goldman JM, Gambacorti-Passerini C, Guilhot F, et al. Imatinib induces durable hematologic and cytogenetic responses in patients with accelerated

phase chronic myeloid leukemia: results of a phase 2 study. Blood. 2002 Mar 15;99(6):1928-37.

55. Sawyers CL, Hochhaus A, Feldman E, Goldman JM, Miller CB, Ottmann OG, et al. Imatinib induces hematologic and cytogenetic responses in patients with chronic myelogenous leukemia in myeloid blast crisis: results of a phase II study. Blood. 2002 May 15;99(10):3530-9.

56. Kantarjian H, Sawyers C, Hochhaus A, Guilhot F, Schiffer C, Gambacorti-Passerini C, et al. Hematologic and cytogenetic responses to imatinib mesylate in chronic myelogenous leukemia. N Engl J Med. 2002 Feb 28;346(9):645-52.

57. O'Brien SG, Guilhot F, Larson RA, Gathmann I, Baccarani M, Cervantes F, et al. Imatinib compared with interferon and low-dose cytarabine for newly diagnosed chronic-phase chronic myeloid leukemia. New England Journal of Medicine. 2003;348(11):994-1004.

58. Druker BJ, Guilhot F, O'Brien SG, Gathmann I, Kantarjian H, Gattermann N, et al. Five-year follow-up of patients receiving imatinib for chronic myeloid leukemia. N Engl J Med. 2006 Dec 7;355(23):2408-17.

59. Deininger M, O'Brien S, Guilhot F, Goldman JM, Hochhaus A, Hughes TP, et al. International Randomized Study of Interferon Vs STI571 (IRIS) 8-Year Follow up: Sustained Survival and Low Risk for Progression or Events in Patients with Newly Diagnosed Chronic Myeloid Leukemia in Chronic Phase (CML-CP) Treated with Imatinib. ASH Annual Meeting2009. p. 1126.

60. Hughes TP, Kaeda J, Branford S, Rudzki Z, Hochhaus A, Hensley ML, et al. Frequency of major molecular responses to imatinib or interferon alfa plus cytarabine in newly diagnosed chronic myeloid leukemia. N Engl J Med. 2003 Oct 9;349(15):1423-32.

61. Hughes TP, Hochhaus A, Branford S, Müller MC, Kaeda JS, Foroni L, et al. Long-term prognostic significance of early molecular response to imatinib in newly diagnosed chronic myeloid leukemia: An analysis from the International Randomized Study of Interferon and STI571 (IRIS). Blood. 2010;116(19):3758-65.

62. White DL, Saunders VA, Dang P, Engler J, Venables A, Zrim S, et al. Most CML patients who have a suboptimal response to imatinib have low OCT-1 activity: Higher doses of imatinib may overcome the negative impact of low OCT-1 activity. Blood. 2007;110(12):4064-72.

63. Mauro MJ. Defining and managing imatinib resistance. Hematology / the Education Program of the American Society of Hematology American Society of Hematology Education Program. 2006:219-25.

64. White D, Saunders V, Lyons AB, Branford S, Grigg A, To LB, et al. In vitro sensitivity to imatinib-induced inhibition of ABL kinase activity is predictive of molecular response in patients with de novo CML. Blood. 2005;106(7):2520-6.

65. White D, Saunders V, Grigg A, Arthur C, Filshie R, Leahy MF, et al. Measurement of in vivo BCR-ABL kinase inhibition to monitor imatinib-induced target blockade and predict response in chronic myeloid leukemia. Journal of Clinical Oncology. 2007;25(28):4445-51.

66. White DL, Saunders VA, Dang P, Engler J, Zannettino ACW, Cambareri AC, et al. OCT-1-mediated influx is a key determinant of the intracellular uptake of imatinib but not nilotinib (AMN107): Reduced OCT-1 activity is the cause of low in vitro sensitivity to imatinib. Blood. 2006;108(2):697-704.

67. Gorre ME, Mohammed M, Ellwood K, Hsu N, Paquette R, Rao PN, et al. Clinical resistance to STI-571 cancer therapy caused by BCR-ABL gene mutation or amplification. Science. 2001 Aug 3;293(5531):876-80.

68. Branford S, Rudzki Z, Walsh S, Parkinson I, Grigg A, Szer J, et al. Detection of BCR-ABL mutations in patients with CML treated with imatinib is virtually always accompanied by clinical resistance, and mutations in the ATP phosphate-binding loop (P-loop) are associated with a poor prognosis. Blood. 2003 Jul 1;102(1):276-83.

69. Hochhaus A, Kreil S, Corbin AS, La Rosee P, Muller MC, Lahaye T, et al. Molecular and chromosomal mechanisms of resistance to imatinib (STI571) therapy. Leukemia : official journal of the Leukemia Society of America, Leukemia Research Fund, UK. 2002 Nov;16(11):2190-6.

70. Corbin AS, La Rosee P, Stoffregen EP, Druker BJ, Deininger MW. Several Bcr-Abl kinase domain mutants associated with imatinib mesylate resistance remain sensitive to imatinib. Blood. 2003 Jun 1;101(11):4611-4.

71. Keeshan K, Mills KI, Cotter TG, McKenna SL. Elevated Bcr-Abl expression levels are sufficient for a haematopoietic cell line to acquire a drug-resistant phenotype. Leukemia : official journal of the Leukemia Society of America, Leukemia Research Fund, UK. 2001 Dec;15(12):1823-33.

72. le Coutre P, Tassi E, Varella-Garcia M, Barni R, Mologni L, Cabrita G, et al. Induction of resistance to the Abelson inhibitor STI571 in human leukemic cells through gene amplification. Blood. 2000;95(5):1758-66.

73. Mohamed AN, Pemberton P, Zonder J, Schiffer CA. The effect of imatinib mesylate on patients with Philadelphia chromosome-positive chronic myeloid leukemia with secondary chromosomal aberrations. Clinical Cancer Research. 2003;9(4):1333-7.

74. Burger H, van Tol H, Brok M, Wiemer EA, de Bruijn EA, Guetens G, et al. Chronic imatinib mesylate exposure leads to reduced intracellular drug accumulation by induction of the ABCG2 (BCRP) and ABCB1 (MDR1) drug transport pumps. Cancer Biol Ther. 2005 Jul;4(7):747-52.

75. Burger H, Van Tol H, Boersma AWM, Brok M, Wiemer EAC, Stoter G, et al. Imatinib mesylate (STI571) is a substrate for the breast cancer resistance protein (BCRP)/ABCG2 drug pump. Blood. 2004;104(9):2940-2.

76. Quentmeier H, Eberth S, Romani J, Zaborski M, Drexler HG. BCR-ABL1-independent PI3Kinase activation causing imatinib-resistance. J Hematol Oncol. 2011;4:6.

77. Dai Y, Rahmani M, Corey SJ, Dent P, Grant S. A Bcr/Abl-independent, Lyn-dependent form of imatinib mesylate (STI-571) resistance is associated with altered expression of Bcl-2. Journal of Biological Chemistry. 2004;279(33):34227-39.

78. Donato NJ, Wu JY, Stapley J, Gallick G, Lin H, Arlinghaus R, et al. BCR-ABL independence and LYN kinase overexpression in chronic myelogenous leukemia cells selected for resistance to STI571. Blood. 2003;101(2):690-8.

79. O'Hare T, Walters DK, Stoffregen EP, Jia T, Manley PW, Mestan J, et al. In vitro activity of Bcr-Abl inhibitors AMN107 and BMS-354825 against clinically relevant imatinib-resistant Abl kinase domain mutants. Cancer Research. 2005;65(11):4500-5.

80. Weisberg E, Manley PW, Breitenstein W, Bruggen J, Cowan-Jacob SW, Ray A, et al. Characterization of AMN107, a selective inhibitor of native and mutant Bcr-Abl. Cancer Cell. 2005 Feb;7(2):129-41.

81. Hughes T, Saglio G, Branford S, Soverini S, Kim DW, Müller MC, et al. Impact of baseline BCR-ABL mutations on response to nilotinib in patients with chronic myeloid leukemia in chronic phase. Journal of Clinical Oncology. 2009;27(25):4204-10.

82. Weisberg E, Manley P, Mestan J, Cowan-Jacob S, Ray A, Griffin JD. AMN107 (nilotinib): a novel and selective inhibitor of BCR-ABL. British Journal of Cancer. 2006 Jun 19;94(12):1765-9.

83. Kantarjian H, Giles F, Wunderle L, Bhalla K, O'Brien S, Wassmann B, et al. Nilotinib in imatinib-resistant CML and Philadelphia chromosome–positive ALL. New England Journal of Medicine. 2006;354(24):2542-51.

84. le Coutre P, Ottmann OG, Giles F, Kim DW, Cortes J, Gattermann N, et al. Nilotinib (formerly AMN107), a highly selective BCR-ABL tyrosine kinase inhibitor, is active in patients with imatinib-resistant or-intolerant accelerated-phase chronic myelogenous leukemia. Blood. 2008;111(4):1834-9.

85. Kantarjian HM, Giles F, Gattermann N, Bhalla K, Alimena G, Palandri F, et al. Nilotinib (formerly AMN107), a highly selective BCR-ABL tyrosine kinase inhibitor, is effective in patients with Philadelphia chromosome-positive chronic myelogenous leukemia in chronic phase following imatinib resistance and intolerance. Blood. 2007 Nov 15;110(10):3540-6.

86. Koren-Michowitz M, le Coutre P, Duyster J, Scheid C, Panayiotidis P, Prejzner W, et al. Activity and tolerability of nilotinib: a retrospective multicenter analysis of chronic myeloid leukemia patients who are imatinib resistant or intolerant. Cancer. 2010 Oct 1;116(19):4564-72.

87. Giles FJ, Abruzzese E, Rosti G, Kim DW, Bhatia R, Bosly A, et al. Nilotinib is active in chronic and accelerated phase chronic myeloid leukemia following failure of imatinib and dasatinib therapy. Leukemia. 2010;24(7):1299-301.

88. Saglio G, Kim DW, Issaragrisil S, Le Coutre P, Etienne G, Lobo C, et al. Nilotinib versus imatinib for newly diagnosed chronic myeloid leukemia. New England Journal of Medicine. 2010;362(24):2251-9.

89. Giles FJ, Rosti G, Beris P, Clark RE, le Coutre P, Mahon FX, et al. Nilotinib is superior to imatinib as first-line therapy of chronic myeloid leukemia: the ENESTnd study. Expert Rev Hematol. 2010 Dec;3(6):665-73.

90. Lombardo LJ, Lee FY, Chen P, Norris D, Barrish JC, Behnia K, et al. Discovery of N-(2-chloro-6-methyl-   phenyl)-2-(6-(4-(2-hydroxyethyl)-piperazin-1-yl)-2-methylpyrimidin-4- ylamino)thiazole-5-carboxamide (BMS-354825), a dual Src/Abl kinase inhibitor with potent antitumor activity in preclinical assays. Journal of Medicinal Chemistry. 2004 Dec 30;47(27):6658-61.

91. Lindauer M, Hochhaus A. Dasatinib. Recent Results Cancer Res. 2010;184:83-102.

92. O'Hare T, Walters DK, Stoffregen EP, Jia T, Manley PW, Mestan J, et al. In vitro activity of Bcr-Abl inhibitors AMN107 and BMS-354825 against clinically relevant imatinib-resistant Abl kinase domain mutants. Cancer Research. 2005 Jun 1;65(11):4500-5.

93. Shah NP, Tran C, Lee FY, Chen P, Norris D, Sawyers CL. Overriding imatinib resistance with a novel ABL kinase inhibitor. Science. 2004 Jul 16;305(5682):399-401.

94. Hochhaus A, Kantarjian HM, Baccarani M, Lipton JH, Apperley JF, Druker BJ, et al. Dasatinib induces notable hematologic and cytogenetic responses in chronic-phase chronic myeloid leukemia after failure of imatinib therapy. Blood. 2007 Mar 15;109(6):2303-9.

95. Cortes J, Rousselot P, Kim DW, Ritchie E, Hamerschlak N, Coutre S, et al. Dasatinib induces complete hematologic and cytogenetic responses in patients with imatinib-resistant or -intolerant chronic myeloid leukemia in blast crisis. Blood. 2007 Apr 15;109(8):3207-13.

96. Huang WS, Metcalf CA, Sundaramoorthi R, Wang Y, Zou D, Thomas RM, et al. Discovery of 3-[2-(imidazo[1,2-b]pyridazin-3-yl)ethynyl]-4-methyl-N-{4-[(4-methylpiperazin-1-yl)methyl]-3-(trifluoromethyl)phenyl}benzamide (AP24534), a potent, orally active pan-inhibitor of breakpoint cluster region-abelson (BCR-ABL) kinase including the T315I gatekeeper mutant. Journal of Medicinal Chemistry. 2010 Jun 24;53(12):4701-19.

97. Burke AC, Swords RT, Kelly K, Giles FJ. Current status of agents active against the T315I chronic myeloid leukemia phenotype. Expert Opin Emerg Drugs. 2011 Mar;16(1):85-103.

98. O'Hare T, Shakespeare WC, Zhu X, Eide CA, Rivera VM, Wang F, et al. AP24534, a pan-BCR-ABL inhibitor for chronic myeloid leukemia, potently inhibits the T315I mutant and overcomes mutation-based resistance. Cancer Cell. 2009 Nov 6;16(5):401-12.

99. Gozgit JM, Wong MJ, Wardwell S, Tyner JW, Loriaux MM, Mohemmad QK, et al. Potent activity of ponatinib (AP24534) in models of FLT3-driven acute myeloid leukemia and other hematologic malignancies. Molecular Cancer Therapeutics. 2011 Jun;10(6):1028-35.

100. Talpaz M, Cortes J, Deininger M, Shah N, Flinn I, Mauro M, et al. Phase I trial of AP24534 in patients with refractory chronic myeloid leukemia (CML) and hematologic malignancies. J Clin Oncol. 2010;28(15S):6511.

101. Gratwohl A, Heim D. Current role of stem cell transplantation in chronic myeloid leukaemia. Best Pract Res Clin Haematol. 2009 Sep;22(3):431-43.

102.   Giralt SA, Arora M, Goldman JM, Lee SJ, Maziarz RT, McCarthy PL, et al. Impact of imatinib therapy on the use of allogeneic haematopoietic progenitor cell transplantation for the treatment of chronic myeloid leukaemia. British Journal of Haematology. 2007 Jun;137(5):461-7.

103.   Baccarani M, Cortes J, Pane F, Niederwieser D, Saglio G, Apperley J, et al. Chronic myeloid leukemia: an update of concepts and management recommendations of European LeukemiaNet. Journal of Clinical Oncology. 2009;27(35):6041-51.

104.   Sanchez-Guijo FM, Lopez-Jimenez J, Gonzalez T, Santamaria C, Gonzalez M, Del Canizo MC. Multitargeted sequential therapy with MK-0457 and dasatinib followed by stem cell transplantation for T315I mutated chronic myeloid leukemia. Leukemia Research. 2009 Jun;33(6):e20-2.

105.   Basak G, Torosian T, Snarski E, Niesiobedzka J, Majewski M, Gronkowska A, et al. Hematopoietic stem cell transplantation for T315I-mutated chronic myelogenous leukemia. Ann Transplant. 2010 Apr-Jun;15(2):68-70.

106.   Deininger M, Schleuning M, Greinix H, Sayer HG, Fischer T, Martinez J, et al. The effect of prior exposure to imatinib on transplant-related mortality. Haematologica. 2006 Apr;91(4):452-9.

107.   Lee SJ, Kukreja M, Wang T, Giralt SA, Szer J, Arora M, et al. Impact of prior imatinib mesylate on the outcome of hematopoietic cell transplantation for chronic myeloid leukemia. Blood. 2008 Oct 15;112(8):3500-7.

108.   Oehler VG, Gooley T, Snyder DS, Johnston L, Lin A, Cummings CC, et al. The effects of imatinib mesylate treatment before allogeneic transplantation for chronic myeloid leukemia. Blood. 2007 Feb 15;109(4):1782-9.

109.   Zaucha JM, Prejzner W, Giebel S, Gooley TA, Szatkowski D, Kalwak K, et al. Imatinib therapy prior to myeloablative allogeneic stem cell transplantation. Bone marrow transplantation. 2005 Sep;36(5):417-24.

110.   Jabbour E, Cortes J, Kantarjian H, Giralt S, Andersson BS, Giles F, et al. Novel tyrosine kinase inhibitor therapy before allogeneic stem cell transplantation in patients with chronic myeloid leukemia: no evidence for increased transplant-related toxicity. Cancer. 2007 Jul 15;110(2):340-4.

111.   Shimoni A, Leiba M, Schleuning M, Martineau G, Renaud M, Koren-Michowitz M, et al. Prior treatment with the tyrosine kinase inhibitors dasatinib and nilotinib allows stem

cell transplantation (SCT) in a less advanced disease phase and does not increase SCT Toxicity in patients with chronic myelogenous leukemia and philadelphia positive acute lymphoblastic leukemia. Leukemia : official journal of the Leukemia Society of America, Leukemia Research Fund, UK. 2009 Jan;23(1):190-4.

112.   Cortes J, Talpaz M, Bixby D, Deininger M, Shah N, Flinn I, et al. A phase 1 trial of oral ponatinib (AP24534) in patients with refractory chronic myelogenous leukemia (CML) and other hematologic malignancies: emerging safety and clinical response findings. Blood. 2010;116(21):210.

113.   Hegedus T, Orfi L, Seprodi A, Varadi A, Sarkadi B, Keri G. Interaction of tyrosine kinase inhibitors with the human multidrug transporter proteins, MDR1 and MRP1. Biochim Biophys Acta. 2002 Jul 18;1587(2-3):318-25.

114.   Oostendorp RL, Buckle T, Beijnen JH, van Tellingen O, Schellens JH. The effect of P-gp (Mdr1a/1b), BCRP (Bcrp1) and P-gp/BCRP inhibitors on the in vivo absorption, distribution, metabolism and excretion of imatinib. Invest New Drugs. 2009 Feb;27(1):31-40.

115.   Widmer N, Colombo S, Buclin T, Decosterd LA. Functional consequence of MDR1 expression on imatinib intracellular concentrations. Blood. 2003 Aug 1;102(3):1142.

116.   Dohse M, Scharenberg C, Shukla S, Robey RW, Volkmann T, Deeken JF, et al. Comparison of ATP-binding cassette transporter interactions with the tyrosine kinase inhibitors imatinib, nilotinib, and dasatinib. Drug metabolism and disposition: the biological fate of chemicals. 2010 Aug;38(8):1371-80.

117.   Shukla S, Sauna ZE, Ambudkar SV. Evidence for the interaction of imatinib at the transport-substrate site(s) of the multidrug-resistance-linked ABC drug transporters ABCB1 (P-glycoprotein) and ABCG2. Leukemia : official journal of the Leukemia Society of America, Leukemia Research Fund, UK. 2008 Feb;22(2):445-7.

118.   Thiebaut F, Tsuruo T, Hamada H, Gottesman MM, Pastan I, Willingham MC. Cellular localization of the multidrug-resistance gene product P-glycoprotein in normal human tissues. Proceedings of the National Academy of Sciences of the United States of America. 1987 Nov;84(21):7735-8.

119.   Maliepaard M, Scheffer GL, Faneyte IF, van Gastelen MA, Pijnenborg AC, Schinkel AH, et al. Subcellular localization and distribution of the breast cancer resistance protein transporter in normal human tissues. Cancer Research. 2001 Apr 15;61(8):3458-64.

120. Nagashige M, Ushigome F, Koyabu N, Hirata K, Kawabuchi M, Hirakawa T, et al. Basal membrane localization of MRP1 in human placental trophoblast. Placenta. 2003 Nov;24(10):951-8.

121. Cooray HC, Blackmore CG, Maskell L, Barrand MA. Localisation of breast cancer resistance protein in microvessel endothelium of human brain. Neuroreport. 2002 Nov 15;13(16):2059-63.

122. Burger H, van Tol H, Boersma AW, Brok M, Wiemer EA, Stoter G, et al. Imatinib mesylate (STI571) is a substrate for the breast cancer resistance protein (BCRP)/ABCG2 drug pump. Blood. 2004 Nov 1;104(9):2940-2.

123. Hamada A, Miyano H, Watanabe H, Saito H. Interaction of imatinib mesilate with human P-glycoprotein. The Journal of pharmacology and experimental therapeutics. 2003 Nov;307(2):824-8.

124. Illmer T, Schaich M, Platzbecker U, Freiberg-Richter J, Oelschlägel U, Von Bonin M, et al. P-glycoprotein-mediated drug efflux is a resistance mechanism of chronic myelogenous leukemia cells to treatment with imatinib mesylate. Leukemia. 2004;18(3):401-8.

125. Jordanides NE, Jorgensen HG, Holyoake TL, Mountford JC. Functional ABCG2 is overexpressed on primary CML CD34+ cells and is inhibited by imatinib mesylate. Blood. 2006;108(4):1370-3.

126. Houghton PJ, Germain GS, Harwood FC, Schuetz JD, Stewart CF, Buchdunger E, et al. Imatinib mesylate is a potent inhibitor of the ABCG2 (BCRP) transporter and reverses resistance to topotecan and SN-38 in vitro. Cancer Research. 2004;64(7):2333.

127. Ferrao PT, Frost MJ, Siah SP, Ashman LK. Overexpression of P-glycoprotein in K562 cells does not confer resistance to the growth inhibitory effects of imatinib (STI571) in vitro. Blood. 2003;102(13):4499-503.

128. Ciarimboli G, Schlatter E. Regulation of organic cation transport. Pflugers Archiv European Journal of Physiology. 2005;449(5):423-41.

129. Koepsell H, Lips K, Volk C. Polyspecific organic cation transporters: structure, function, physiological roles, and biopharmaceutical implications. Pharm Res. 2007 Jul;24(7):1227-51.

130. Thomas J, Wang L, Clark RE, Pirmohamed M. Active transport of imatinib into and out of cells: Implications for drug resistance. Blood. 2004;104(12):3739-45.

131.   Gründemann D, Gorboulev V, Gambaryan S, Veyhl M, Koepsell H. Drug excretion mediated by a new prototype of polyspecific transporter. Nature. 1994;372(6506):549-52.

132.   Koepsell H, Endou H. The SLC22 drug transporter family. Pflugers Archiv European Journal of Physiology. 2004;447(5):666-76.

133.   Giannoudis A, Davies A, Lucas CM, Harris RJ, Pirmohamed M, Clark RE. Effective dasatinib uptake may occur without human organic cation transporter 1 (hOCT1): implications for the treatment of imatinib-resistant chronic myeloid leukemia. Blood. 2008 Oct 15;112(8):3348-54.

134.   Hiwase DK, Saunders V, Hewett D, Frede A, Zrim S, Dang P, et al. Dasatinib cellular uptake and efflux in chronic myeloid leukemia cells: therapeutic implications. Clinical Cancer Research. 2008;14(12):3881-8.

135.   Wang L, Giannoudis A, Lane S, Williamson P, Pirmohamed M, Clark R. Expression of the uptake drug transporter hOCT1 is an important clinical determinant of the response to imatinib in chronic myeloid leukemia. Clinical Pharmacology & Therapeutics. 2007;83(2):258-64.

136.   Crossman LC, Druker BJ, Deininger MW, Pirmohamed M, Wang L, Clark RE. hOCT 1 and resistance to imatinib. Blood. 2005 Aug 1;106(3):1133-4; author reply 4.

137.   Labussiere H, Hayette S, Chabane K. Pharmacogenomic Factors Such as the Expression of Imatinib Transporters (OCT-1, ABCB-1 and ABCG-2) at Diagnosis, OCT-1 SNPs, and Steady-State Imatinib and Desmethyl-Imatinib Trough Plasma Levels in De Novo Chronic Phase Chronic Myelogenous Leukemia, May Influence Disease Response to Imatinib. Blood. 2008;112.

138.   Marin D, Bazeos A, Mahon FX, Eliasson L, Milojkovic D, Bua M, et al. Adherence is the critical factor for achieving molecular responses in patients with chronic myeloid leukemia who achieve complete cytogenetic responses on imatinib. Journal of Clinical Oncology. 2010;28(14):2381-8.

139.   Zhang WW, Cortes JE, Yao H, Zhang L, Reddy NG, Jabbour E, et al. Predictors of primary imatinib resistance in chronic myelogenous leukemia are distinct from those in secondary imatinib resistance. Journal of Clinical Oncology. 2009;27(22):3642-9.

140.   White DL, Dang P, Engler J, Frede A, Zrim S, Osborn M, et al. Functional activity of the OCT-1 protein is predictive of long-term outcome in patients with chronic-phase chronic myeloid leukemia treated with imatinib. Journal of Clinical Oncology. 2010;28(16):2761-7.

141.	Bazeos A, Marin D, Reid AG, Gerrard G, Milojkovic D, May PC, et al. HOCT1 transcript levels and single nucleotide polymorphisms as predictive factors for response to imatinib in chronic myeloid leukemia. Leukemia. 2010;24(6):1243-5.

142.	White D, Saunders V, Dang P, Engler J, Hughes T. OCT-1 activity measurement provides a superior imatinib response predictor than screening for single-nucleotide polymorphisms of OCT-1. Leukemia. 2010;24(11):1962-5.

143.	Cortes JE, Egorin MJ, Guilhot F, Molimard M, Mahon FX. Pharmacokinetic/pharmacodynamic correlation and blood-level testing in imatinib therapy for chronic myeloid leukemia. Leukemia : official journal of the Leukemia Society of America, Leukemia Research Fund, UK. 2009 Sep;23(9):1537-44.

144.	Widmer N, Gotta V, Haouala A, Decosterd LA. Tyrosine kinase inhibitors concentration monitoring in chronic myeloid leukemia. Leukemia Research. 2010 Jun;34(6):698-9.

145.	Breedveld P, Pluim D, Cipriani G, Wielinga P, van Tellingen O, Schinkel AH, et al. The effect of Bcrp1 (Abcg2) on the in vivo pharmacokinetics and brain penetration of imatinib mesylate (Gleevec): implications for the use of breast cancer resistance protein and P-glycoprotein inhibitors to enable the brain penetration of imatinib in patients. Cancer Research. 2005 Apr 1;65(7):2577-82.

146.	Haouala A, Widmer N, Duchosal MA, Montemurro M, Buclin T, Decosterd LA. Drug interactions with the tyrosine kinase inhibitors imatinib, dasatinib, and nilotinib. Blood. 2011 Feb 24;117(8):e75-87.

147.	Azuma M, Nishioka Y, Aono Y, Inayama M, Makino H, Kishi J, et al. Role of alpha1-acid glycoprotein in therapeutic antifibrotic effects of imatinib with macrolides in mice. Am J Respir Crit Care Med. 2007 Dec 15;176(12):1243-50.

148.	Kajita T, Higashi Y, Imamura M, Maida C, Fujii Y, Yamamoto I, et al. Effect of imatinib mesilate on the disposition kinetics of ciclosporin in rats. J Pharm Pharmacol. 2006 Jul;58(7):997-1000.

149.	Lozzio CB, Lozzio BB. Human chronic myelogenous leukemia cell-line with positive Philadelphia chromosome. Blood. 1975 Mar;45(3):321-34.

150.	Kishi K. A new leukemia cell line with Philadelphia chromosome characterized as basophil precursors. Leukemia Research. 1985;9(3):381-90.

151. Gallagher R, Collins S, Trujillo J, McCredie K, Ahearn M, Tsai S, et al. Characterization of the continuous, differentiating myeloid cell line (HL-60) from a patient with acute promyelocytic leukemia. Blood. 1979 Sep;54(3):713-33.

152. Scherer WF, Syverton JT, Gey GO. Studies on the propagation in vitro of poliomyelitis viruses. IV. Viral multiplication in a stable strain of human malignant epithelial cells (strain HeLa) derived from an epidermoid carcinoma of the cervix. The Journal of experimental medicine. 1953 May;97(5):695-710.

153. Lachmann A, Xu H, Krishnan J, Berger SI, Mazloom AR, Ma'ayan A. ChEA: transcription factor regulation inferred from integrating genome-wide ChIP-X experiments. Bioinformatics. 2010;26(19):2438-44.

154. Deininger MWN, O'Brien SG, Ford JM, Druker BJ. Practical management of patients with chronic myeloid leukemia receiving imatinib. Journal of Clinical Oncology. 2003;21(8):1637-47.

155. Hughes TP, Branford S, White DL, Reynolds J, Koelmeyer R, Seymour JF, et al. Impact of early dose intensity on cytogenetic and molecular responses in chronicphase CMLpatients receiving 600 mg/day of imatinib as initial therapy. Blood. 2008;112(10):3965-73.

156. White DL, Hughes TP. Classification of Patients With Chronic Myeloid Leukemia on Basis of BCR-ABL Transcript Level at 3 Months Fails to Identify Patients With Low Organic Cation Transporter-1 Activity Destined to Have Poor Imatinib Response. J Clin Oncol. 2012 Mar 5.

157. Cortes JE, Baccarani M, Guilhot F, Druker BJ, Branford S, Kim DW, et al. Phase III, randomized, open-label study of daily imatinib mesylate 400 mg versus 800 mg in patients with newly diagnosed, previously untreated chronic myeloid leukemia in chronic phase using molecular end points: tyrosine kinase inhibitor optimization and selectivity study. J Clin Oncol. 2010 Jan 20;28(3):424-30.

158. Hiwase DK, Saunders V, Hewett D, Frede A, Zrim S, Dang P, et al. Dasatinib cellular uptake and efflux in chronic myeloid leukemia cells: therapeutic implications. Clinical cancer research : an official journal of the American Association for Cancer Research. 2008 Jun 15;14(12):3881-8.

159.   Fahrmayr C, Fromm MF, König J. Hepatic OATP and OCT uptake transporters: Their role for drug-drug interactions and pharmacogenetic aspects. Drug Metabolism Reviews. 2010;42(3):380-401.

160.   Kindla J, Fromm MF, Konig J. In vitro evidence for the role of OATP and OCT uptake transporters in drug-drug interactions. Expert Opin Drug Metab Toxicol. 2009 May;5(5):489-500.

161.   Bachmakov I, Glaeser H, Fromm MF, Konig J. Interaction of oral antidiabetic drugs with hepatic uptake transporters: focus on organic anion transporting polypeptides and organic cation transporter 1. Diabetes. 2008 Jun;57(6):1463-9.

162.   Jung N, Lehmann C, Rubbert A, Knispel M, Hartmann P, van Lunzen J, et al. Relevance of the organic cation transporters 1 and 2 for antiretroviral drug therapy in human immunodeficiency virus infection. Drug Metab Dispos. 2008 Aug;36(8):1616-23.

163.   Umehara KI, Iwatsubo T, Noguchi K, Usui T, Kamimura H. Effect of cationic drugs on the transporting activity of human and rat OCT/Oct 1-3 in vitro and implications for drug-drug interactions. Xenobiotica. 2008 Sep;38(9):1203-18.

164.   Minematsu T, Giacomini KM. Interactions of Tyrosine Kinase Inhibitors with Organic Cation Transporters, OCTs, and Multidrug and Toxic Compound Extrusion Proteins, MATEs. Molecular Cancer Therapeutics. 2011;10(3):531-9.

165.   Ulrich CM, Bigler J, Potter JD. Non-steroidal anti-inflammatory drugs for cancer prevention: Promise, perils and pharmacogenetics. Nature Reviews Cancer. 2006;6(2):130-40.

166.   Bjorkman D. Nonsteroidal anti-inflammatory drug-associated toxicity of the liver, lower gastrointestinal tract, and esophagus. American Journal of Medicine. 1998;105(5 A):17S-21S.

167.   Perneger TV, Whelton PK, Klag MJ. Risk of kidney failure associated with the use of acetaminophen, aspirin, and nonsteroidal antiinflammatory drugs. New England Journal of Medicine. 1994;331(25):1675-9.

168.   Farooq M, Haq I, Qureshi AS. Cardiovascular risks of COX inhibition: Current perspectives. Expert Opinion on Pharmacotherapy. 2008;9(8):1311-9.

169.   Apiwattanakul N, Sekine T, Chairoungdua A, Kanai Y, Nakajima N, Sophasan S, et al. Transport properties of nonsteroidal anti-inflammatory drugs by organic anion transporter 1 expressed in Xenopus laevis oocytes. Mol Pharmacol. 1999 May;55(5):847-54.

170.   Nozaki Y, Kusuhara H, Endou H, Sugiyama Y. Quantitative evaluation of the drug-drug interactions between methotrexate and nonsteroidal anti-inflammatory drugs in the renal uptake process based on the contribution of organic anion transporters and reduced folate carrier. J Pharmacol Exp Ther. 2004 Apr;309(1):226-34.

171.   Honjo H, Uwai Y, Aoki Y, Iwamoto K. Stereoselective inhibitory effect of flurbiprofen, ibuprofen and naproxen on human organic anion transporters hOAT1 and hOAT3. Biopharmaceutics & Drug Disposition. 2011;32(9):518-24.

172.   Mulato AS, Ho ES, Cihlar T. Nonsteroidal anti-inflammatory drugs efficiently reduce the transport and cytotoxicity of adefovir mediated by the human renal organic anion transporter 1. J Pharmacol Exp Ther. 2000 Oct;295(1):10-5.

173.   Khamdang S, Takeda M, Noshiro R, Narikawa S, Enomoto A, Anzai N, et al. Interactions of human organic anion transporters and human organic cation transporters with nonsteroidal anti-inflammatory drugs. Journal of Pharmacology and Experimental Therapeutics. 2002;303(2):534-9.

174.   Lamb J. The Connectivity Map: A new tool for biomedical research. Nature Reviews Cancer. 2007;7(1):54-60.

175.   Lamb J, Crawford ED, Peck D, Modell JW, Blat IC, Wrobel MJ, et al. The connectivity map: Using gene-expression signatures to connect small molecules, genes, and disease. Science. 2006;313(5795):1929-35.

176.   Sanda T, Li X, Gutierrez A, Ahn Y, Neuberg DS, O'Neil J, et al. Interconnecting molecular pathways in the pathogenesis and drug sensitivity of T-cell acute lymphoblastic leukemia. Blood. 2009 Mar 4;115(9):1735-45.

177.   Vilar E, Mukherjee B, Kuick R, Raskin L, Misek DE, Taylor JM, et al. Gene expression patterns in mismatch repair-deficient colorectal cancers highlight the potential therapeutic role of inhibitors of the phosphatidylinositol 3-kinase-AKT-mammalian target of rapamycin pathway. Clin Cancer Res. 2009 Apr 15;15(8):2829-39.

178.   Rosenbluth JM, Mays DJ, Pino MF, Tang LJ, Pietenpol JA. A gene signature-based approach identifies mTOR as a regulator of p73. Mol Cell Biol. 2008 Oct;28(19):5951-64.

179.   Stegmaier K. Genomic approaches to small molecule discovery. Leukemia. 2009 Jul;23(7):1226-35.

180. Wang J, Hughes TP, Kok CH, Saunders VA, Frede A, Groot-Obbink K, et al. Contrasting effects of diclofenac and ibuprofen on active imatinib uptake into leukaemic cells. British Journal of Cancer. 2012;106(11):1772-8.

181. Klein E, Ben-Bassat H, Neumann H, Ralph P, Zeuthen J, Polliack A, et al. Properties of the K562 cell line, derived from a patient with chronic myeloid leukemia. Int J Cancer. 1976 Oct 15;18(4):421-31.

182. Andersson LC, Nilsson K, Gahmberg CG. K562--a human erythroleukemic cell line. Int J Cancer. 1979 Feb;23(2):143-7.

183. Giles FJ, Kantarjian HM, Bekele BN, Cortes JE, Faderl S, Thomas DA, et al. Bone marrow cyclooxygenase-2 levels are elevated in chronic-phase chronic myeloid leukaemia and are associated with reduced survival. British Journal of Haematology. 2002;119(1):38-45.

184. Subhashini J, Mahipal SVK, Reddanna P. Anti-proliferative and apoptotic effects of celecoxib on human chronic myeloid leukemia in vitro. Cancer Letters. 2005;224(1):31-43.

185. Arunasree KM, Roy KR, Anilkumar K, Aparna A, Reddy GV, Reddanna P. Imatinib-resistant K562 cells are more sensitive to celecoxib, a selective COX-2 inhibitor: Role of COX-2 and MDR-1. Leukemia Research. 2008;32(6):855-64.

186. Kalle AM, Sachchidanand S, Pallu R. Bcr-Abl-independent mechanism of resistance to imatinib in K562 cells: Induction of cyclooxygenase-2 (COX-2) by histone deacetylases (HDACs). Leukemia Research. 2010;34(9):1132-8.

187. Rich SA. The coxibs, selective inhibitors of cyclooxygenase-2. New England Journal of Medicine. 2001;345(23):1709.

188. Juhlin T, Björkman S, Gunnarsson B, Fyge A, Roth B, Höglund P. Acute administration of diclofenac, but possibly not long term low dose aspirin, causes detrimental renal effects in heart failure patients treated with ACE-inhibitors. European Journal of Heart Failure. 2004;6(7):909-16.

189. Siu SSN, Yeung JHK, Lau TK. A study on placental transfer of diclofenac in first trimester of human pregnancy. Human Reproduction. 2000;15(11):2423-5.

190. Bramlage P, Goldis A. Bioequivalence study of three ibuprofen formulations after single dose administration in healthy volunteers. BMC Pharmacology. 2008;8.

191. Tang C, Schafranek L, Watkins DB, Parker WT, Moore S, Prime JA, et al. Tyrosine kinase inhibitor resistance in chronic myeloid leukemia cell lines: investigating resistance pathways. Leuk Lymphoma. 2011 Nov;52(11):2139-47.

192.   Galimberti S, Cervetti G, Guerrini F, Testi R, Pacini S, Fazzi R, et al. Quantitative molecular monitoring of BCR-ABL and MDR1 transcripts in patients with chronic myeloid leukemia during Imatinib treatment. Cancer Genet Cytogenet. 2005 Oct 1;162(1):57-62.

193.   White D, Dang P, Venables A. ABCB1 overexpression may predispose imatinib treated CML patients to the development of Abl kinase domain mutations, and may be an important contributor to acquired resistance. Blood. 2006;108:608a.

194.   Jonker JW, Schinkel AH. Pharmacological and physiological functions of the polyspecific organic cation transporters: OCT1, 2, and 3 (SLC22A1-3). The Journal of pharmacology and experimental therapeutics. 2004 Jan;308(1):2-9.

195.   Jonker JW, Wagenaar E, Mol CA, Buitelaar M, Koepsell H, Smit JW, et al. Reduced hepatic uptake and intestinal excretion of organic cations in mice with a targeted disruption of the organic cation transporter 1 (Oct1 [Slc22a1]) gene. Mol Cell Biol. 2001 Aug;21(16):5471-7.

196.   Saborowski M, Kullak-Ublick GA, Eloranta JJ. The human organic cation transporter-1 gene is transactivated by hepatocyte nuclear factor-4alpha. J Pharmacol Exp Ther. 2006 May;317(2):778-85.

197.   Nie W, Sweetser S, Rinella M, Green RM. Transcriptional regulation of murine Slc22a1 (Oct1) by peroxisome proliferator agonist receptor-α and-γ. American Journal of Physiology-Gastrointestinal and Liver Physiology. 2005;288(2):G207-G12.

198.   Sobell HM. Actinomycin and DNA transcription. Proceedings of the National Academy of Sciences of the United States of America. 1985 Aug;82(16):5328-31.

199.   Hovanessian AG, Soundaramourty C, El Khoury D, Nondier I, Svab J, Krust B. Surface expressed nucleolin is constantly induced in tumor cells to mediate calcium-dependent ligand internalization. PLoS One. 2010;5(12):e15787.

200.   Adamson DJ, Frew D, Tatoud R, Wolf CR, Palmer CN. Diclofenac antagonizes peroxisome proliferator-activated receptor-gamma signaling. Mol Pharmacol. 2002 Jan;61(1):7-12.

201.   Lachmann A, Xu H, Krishnan J, Berger SI, Mazloom AR, Ma'ayan A. ChEA: transcription factor regulation inferred from integrating genome-wide ChIP-X experiments. Bioinformatics. 2010 Oct 1;26(19):2438-44.

202.   Zhang GS, Liu DS, Dai CW, Li RJ. Antitumor effects of celecoxib on K562 leukemia cells are mediated by cell-cycle arrest, caspase-3 activation, and downregulation of

Cox-2 expression and are synergistic with hydroxyurea or imatinib. Am J Hematol. 2006 Apr;81(4):242-55.

203.   Radich JP, Dai H, Mao M, Oehler V, Schelter J, Druker B, et al. Gene expression changes associated with progression and response in chronic myeloid leukemia. Proceedings of the National Academy of Sciences of the United States of America. 2006 Feb 21;103(8):2794-9.

204.   Kulkarni S, Jain N, Singh A. Cyclooxygenase isoenzymes and newer therapeutic potential for selective COX-2 inhibitors. Methods Find Exp Clin Pharmacol. 2000;22(5):291-8.

205.   O'Banion MK. Cyclooxygenase-2: molecular biology, pharmacology, and neurobiology. Crit Rev Neurobiol. 1999;13(1):45-82.

206.   Smith WL, DeWitt DL, Garavito RM. Cyclooxygenases: structural, cellular, and molecular biology. Annual review of biochemistry. 2000;69(1):145-82.

207.   Herschman HR. Prostaglandin synthase 2. Biochim Biophys Acta. 1996;1299(1):125.

208.   Park JY, Pillinger MH, Abramson SB. Prostaglandin E2 synthesis and secretion: the role of PGE2 synthases. Clin Immunol. 2006 Jun;119(3):229-40.

209.   Forman BM, Tontonoz P, Chen J, Brun RP, Spiegelman BM, Evans RM. 15-Deoxy-delta 12, 14-prostaglandin J2 is a ligand for the adipocyte determination factor PPAR gamma. Cell. 1995 Dec 1;83(5):803-12.

210.   Kliewer SA, Lenhard JM, Willson TM, Patel I, Morris DC, Lehmann JM. A prostaglandin J2 metabolite binds peroxisome proliferator-activated receptor gamma and promotes adipocyte differentiation. Cell. 1995 Dec 1;83(5):813-9.

211.   Ristimäki A, Sivula A, Lundin J, Lundin M, Salminen T, Haglund C, et al. Prognostic significance of elevated cyclooxygenase-2 expression in breast cancer. Cancer Research. 2002;62(3):632-5.

212.   Kirkpatrick K, Ogunkolade W, Elkak A, Bustin S, Jenkins P, Ghilchik M, et al. The mRNA expression of cyclo-oxygenase-2 (COX-2) and vascular endothelial growth factor (VEGF) in human breast cancer. Current Medical Research and Opinion®. 2002;18(4):237-41.

213.   Brown JR, DuBois RN. COX-2: a molecular target for colorectal cancer prevention. Journal of Clinical Oncology. 2005;23(12):2840-55.

214.   Marnett LJ, DuBois RN. COX-2: a target for colon cancer prevention. Annual review of pharmacology and toxicology. 2002;42(1):55-80.

215.   Kim HS, Youm HR, Lee JS, Min KW, Chung JH, Park CS. Correlation between cyclooxygenase-2 and tumor angiogenesis in non-small cell lung cancer. Lung cancer (Amsterdam, Netherlands). 2003;42(2):163.

216.   Sandler AB, Dubinett SM, editors. COX-2 inhibition and lung cancer2004: Elsevier.

217.   Khuri FR, Wu H, Lee JJ, Kemp BL, Lotan R, Lippman SM, et al. Cyclooxygenase-2 overexpression is a marker of poor prognosis in stage I non-small cell lung cancer. Clinical Cancer Research. 2001;7(4):861-7.

218.   Inoue H, Yokoyama C, Hara S, Tone Y, Tanabe T. Transcriptional Regulation of Human Prostaglandin-endoperoxide Synthase-2 Gene by Lipopolysaccharide and Phorbol Ester in Vascular Endothelial Cells INVOLVEMENT OF BOTH NUCLEAR FACTOR FOR INTERLEUKIN-6 EXPRESSION SITE AND cAMP RESPONSE ELEMENT. Journal of Biological Chemistry. 1995;270(42):24965-71.

219.   Sheng H, Shao J, Morrow JD, Beauchamp RD, DuBois RN. Modulation of apoptosis and Bcl-2 expression by prostaglandin E2 in human colon cancer cells. Cancer Research. 1998;58(2):362-6.

220.   Zhang F, Subbaramaiah K, Altorki N, Dannenberg AJ. Dihydroxy bile acids activate the transcription of cyclooxygenase-2. Journal of Biological Chemistry. 1998;273(4):2424-8.

221.   Subbaramaiah K, Altorki N, Chung WJ, Mestre JR, Sampat A, Dannenberg AJ. Inhibition of cyclooxygenase-2 gene expression by p53. Journal of Biological Chemistry. 1999;274(16):10911-5.

222.   Leung W, To K, Ng Y, Lee TL, Lau J, Chan F, et al. Association between cyclo-oxygenase-2 overexpression and missense p53 mutations in gastric cancer. British Journal of Cancer. 2001;84(3):335.

223.   Dannenberg AJ, Altorki NK, Boyle JO, Dang C, Howe LR, Weksler BB, et al. Cyclo-oxygenase 2: a pharmacological target for the prevention of cancer. The lancet oncology. 2001;2(9):544-51.

224.   Oshima M, Dinchuk JE, Kargman SL, Oshima H, Hancock B, Kwong E, et al. Suppression of intestinal polyposis in ApcD716 knockout mice by inhibition of cyclooxygenase 2 (COX-2). Cell. 1996;87(5):803-10.

225. Tiano H, Chulada P, Spalding J, Lee C, Loftin C, Mahler J, et al., editors. Effects of cyclooxygenase deficiency on inflammation and papilloma development in mouse skin1997.

226. Choy H, Milas L. Enhancing radiotherapy with cyclooxygenase-2 enzyme inhibitors: a rational advance? Journal of the National Cancer Institute. 2003;95(19):1440-52.

227. Nishimura G, Yanoma S, Mizuno H, Kawakami K, Tsukuda M. A selective cyclooxygenase‐2 inhibitor suppresses tumor growth in nude mouse xenografted with human head and neck squamous carcinoma cells. Cancer Science. 1999;90(10):1152-62.

228. Okajima E, Denda A, Ozono S, Takahama M, Akai H, Sasaki Y, et al. Chemopreventive effects of nimesulide, a selective cyclooxygenase-2 inhibitor, on the development of rat urinary bladder carcinomas initiated by N-butyl-N-(4-hydroxybutyl) nitrosamine. Cancer Research. 1998;58(14):3028-31.

229. Pentland AP, Schoggins JW, Scott GA, Khan KNM, Han R. Reduction of UV-induced skin tumors in hairless mice by selective COX-2 inhibition. Carcinogenesis. 1999;20(10):1939-44.

230. Liu XH, Kirschenbaum A, Yao S, Stearns ME, Holland JF, Claffey K, et al. Upregulation of vascular endothelial growth factor by cobalt chloride-simulated hypoxia is mediated by persistent induction of cyclooxygenase-2 in a metastatic human prostate cancer cell line. Clinical and Experimental Metastasis. 1999;17(8):687-94.

231. Bamba H, Ota S, Kato A, Kawamoto C, Fujiwara K. Prostaglandins up-regulate vascular endothelial growth factor production through distinct pathways in differentiated U937 cells. Biochemical and Biophysical Research Communications. 2000;273(2):485-91.

232. Ghosh AK, Hirasawa N, Niki H, Ohuchi K. Cyclooxygenase-2-mediated angiogenesis in carrageenin-induced granulation tissue in rats. Journal of Pharmacology and Experimental Therapeutics. 2000;295(2):802-9.

233. Williams CS, Tsujii M, Reese J, Dey SK, DuBois RN. Host cyclooxygenase-2 modulates carcinoma growth. Journal of Clinical Investigation. 2000;105(11):1589-622.

234. Daniel TO, Liu H, Morrow JD, Crews BC, Marnett LJ. Thromboxane A2 is a mediator of cyclooxygenase-2-dependent endothelial migration and angiogenesis. Cancer Research. 1999;59(18):4574-7.

235. Masferrer JL, Leahy KM, Koki AT, Zweifel BS, Settle SL, Woerner BM, et al. Antiangiogenic and antitumor activities of cyclooxygenase-2 inhibitors. Cancer Research. 2000;60(5):1306-11.

236.   Tsujii M, DuBois RN. Alterations in cellular adhesion and apoptosis in epithelial cells overexpressing prostaglandin endoperoxide synthase 2. Cell. 1995;83(3):493-501.

237.   Attiga FA, Fernandez PM, Weeraratna AT, Manyak MJ, Patierno SR. Inhibitors of prostaglandin synthesis inhibit human prostate tumor cell invasiveness and reduce the release of matrix metalloproteinases. Cancer Research. 2000;60(16):4629-37.

238.   Liu CH, Chang SH, Narko K, Trifan OC, Wu MT, Smith E, et al. Overexpression of cyclooxygenase-2 is sufficient to induce tumorigenesis in transgenic mice. Journal of Biological Chemistry. 2001;276(21):18563-9.

239.   Patel VA, Dunn MJ, Sorokin A. Regulation of MDR-1 (P-glycoprotein) by cyclooxygenase-2. Journal of Biological Chemistry. 2002;277(41):38915-20.

240.   Ratnasinghe D, DASCHNER PJ, Anver MR, KASPRZAK BH, TAYLOR PR, YEH GC, et al. Cyclooxygenase-2, P-glycoprotein-170 and drug resistance; is chemoprevention against multidrug resistance possible? Anticancer research. 2001;21(3C):2141-7.

241.   Aguayo A, Kantarjian H, Manshouri T, Gidel C, Estey E, Thomas D, et al. Angiogenesis in acute and chronic leukemias and myelodysplastic syndromes. Blood. 2000;96(6):2240-5.

242.   Thomas DA, Giles FJ, Cortes J, Albitar M, Kantarjian HM. Antiangiogenic therapy in leukemia. Acta haematologica. 2001;106(4):190-207.

243.   McWeeney SK, Pemberton LC, Loriaux MM, Vartanian K, Willis SG, Yochum G, et al. A gene expression signature of CD34+ cells to predict major cytogenetic response in chronic-phase chronic myeloid leukemia patients treated with imatinib. Blood. 2010;115(2):315-25.

244.   Engler JR, Zannettino ACW, Bailey CG, Rasko JEJ, Hughes TP, White DL. OCT-1 function varies with cell lineage but is not influenced by BCR-ABL. Haematologica. 2011;96(2):213-20.

245.   Crofford L. COX-1 and COX-2 tissue expression: implications and predictions. The Journal of rheumatology Supplement. 1997;49:15.

246.   Rigas B, Goldman I, Levine L. Altered eicosanoid levels in human colon cancer. The Journal of laboratory and clinical medicine. 1993;122(5):518.

247.   Huang M, Stolina M, Sharma S, Mao JT, Zhu L, Miller PW, et al. Non-small cell lung cancer cyclooxygenase-2-dependent regulation of cytokine balance in lymphocytes and

macrophages: up-regulation of interleukin 10 and down-regulation of interleukin 12 production. Cancer Research. 1998;58(6):1208-16.

248.   Schrey M, Patel K. Prostaglandin E2 production and metabolism in human breast cancer cells and breast fibroblasts. Regulation by inflammatory mediators. British Journal of Cancer. 1995;72(6):1412.

249.   Truffinet V, Donnard M, Vincent C, Faucher JL, Bordessoule D, Turlure P, et al. Cyclooxygenase‐1, but not‐2, in blast cells of patients with acute leukemia. International Journal of Cancer. 2007;121(4):924-7.

250.   Williams N. Preferential inhibition of murine macrophage colony formation by prostaglandin E. Blood. 1979;53(6):1089-94.

251.   Pelus LM, Broxmeyer H, Kurland J, Moore M. Regulation of macrophage and granulocyte proliferation. Specificities of prostaglandin E and lactoferrin. The Journal of experimental medicine. 1979;150(2):277-92.

252.   North TE, Goessling W, Walkley CR, Lengerke C, Kopani KR, Lord AM, et al. Prostaglandin E2 regulates vertebrate haematopoietic stem cell homeostasis. Nature. 2007;447(7147):1007-11.

253.   Grosser T, Yusuff S, Cheskis E, Pack MA, FitzGerald GA. Developmental expression of functional cyclooxygenases in zebrafish. Proceedings of the National Academy of Sciences. 2002;99(12):8418-23.

254.   Chinetti G, Fruchart JC, Staels B. Peroxisome proliferator-activated receptors (PPARs): nuclear receptors with functions in the vascular wall. Z Kardiol. 2001;90 Suppl 3:125-32.

255.   Chinetti G, Griglio S, Antonucci M, Torra IP, Delerive P, Majd Z, et al. Activation of proliferator-activated receptors alpha and gamma induces apoptosis of human monocyte-derived macrophages. J Biol Chem. 1998 Oct 2;273(40):25573-80.

256.   Chinetti G, Lestavel S, Bocher V, Remaley AT, Neve B, Torra IP, et al. PPAR-alpha and PPAR-gamma activators induce cholesterol removal from human macrophage foam cells through stimulation of the ABCA1 pathway. Nat Med. 2001 Jan;7(1):53-8.

257.   Braissant O, Foufelle F, Scotto C, Dauca M, Wahli W. Differential expression of peroxisome proliferator-activated receptors (PPARs): tissue distribution of PPAR-alpha,-beta, and-gamma in the adult rat. Endocrinology. 1996;137(1):354-66.

258. Committee NRN. A unified nomenclature system for the nuclear receptor superfamily. Cell. 1999;97(2):161-3.

259. Kliewer SA, Umesono K, Noonan DJ, Heyman RA, Evans RM. Convergence of 9-cis retinoic acid and peroxisome proliferator signalling pathways through heterodimer formation of their receptors. Nature. 1992;358(6389):771-4.

260. Beamer BA, Negri C, Yen CJ, Gavrilova O, Rumberger JM, Durcan MJ, et al. Chromosomal localization and partial genomic structure of the human peroxisome proliferator activated receptor-gamma (hPPARγ) gene. Biochemical and Biophysical Research Communications. 1997;233(3):756-9.

261. Fajas L, Auboeuf D, Raspé E, Schoonjans K, Lefebvre AM, Saladin R, et al. The organization, promoter analysis, and expression of the human PPARγ gene. Journal of Biological Chemistry. 1997;272(30):18779-89.

262. Mukherjee R, Jow L, Croston GE, Paterniti Jr JR. Identification, characterization, and tissue distribution of human peroxisome proliferator-activated receptor (PPAR) isoforms PPARγ2 versus PPARγ1 and activation with retinoid X receptor agonists and antagonists. Journal of Biological Chemistry. 1997;272(12):8071-6.

263. Willson TM, Brown PJ, Sternbach DD, Henke BR. The PPARs: From orphan receptors to drug discovery. Journal of Medicinal Chemistry. 2000;43(4):527-50.

264. Issemann I, Green S. Activation of a member of the steroid hormone receptor superfamily by peroxisome proliferators. Nature. 1990 Oct 18;347(6294):645-50.

265. Kliewer SA, Sundseth SS, Jones SA, Brown PJ, Wisely GB, Koble CS, et al. Fatty acids and eicosanoids regulate gene expression through direct interactions with peroxisome proliferator-activated receptors alpha and gamma. Proceedings of the National Academy of Sciences of the United States of America. 1997 Apr 29;94(9):4318-23.

266. McIntyre TM, Pontsler AV, Silva AR, St Hilaire A, Xu Y, Hinshaw JC, et al. Identification of an intracellular receptor for lysophosphatidic acid (LPA): LPA is a transcellular PPARgamma agonist. Proceedings of the National Academy of Sciences of the United States of America. 2003 Jan 7;100(1):131-6.

267. Schopfer FJ, Lin Y, Baker PR, Cui T, Garcia-Barrio M, Zhang J, et al. Nitrolinoleic acid: an endogenous peroxisome proliferator-activated receptor gamma ligand. Proceedings of the National Academy of Sciences of the United States of America. 2005 Feb 15;102(7):2340-5.

268.   Gelman L, Feige JN, Desvergne B. Molecular basis of selective PPARgamma modulation for the treatment of Type 2 diabetes. Biochim Biophys Acta. 2007 Aug;1771(8):1094-107.

269.   Lehmann JM, Moore LB, Smith-Oliver TA, Wilkison WO, Willson TM, Kliewer SA. An antidiabetic thiazolidinedione is a high affinity ligand for peroxisome proliferator-activated receptor gamma (PPAR gamma). The Journal of biological chemistry. 1995 Jun 2;270(22):12953-6.

270.   Lehmann JM, Lenhard JM, Oliver BB, Ringold GM, Kliewer SA. Peroxisome proliferator-activated receptors alpha and gamma are activated by indomethacin and other non-steroidal anti-inflammatory drugs. J Biol Chem. 1997 Feb 7;272(6):3406-10.

271.   Houseknecht KL, Cole BM, Steele PJ. Peroxisome proliferator-activated receptor gamma (PPARgamma) and its ligands: a review. Domest Anim Endocrinol. 2002 Mar;22(1):1-23.

272.   Sharma AM, Staels B. Review: Peroxisome proliferator-activated receptor gamma and adipose tissue--understanding obesity-related changes in regulation of lipid and glucose metabolism. The Journal of clinical endocrinology and metabolism. 2007 Feb;92(2):386-95.

273.   Hedvat M, Jain A, Carson DA, Leoni LM, Huang G, Holden S, et al. Inhibition of HER-kinase activation prevents ERK-mediated degradation of PPARγ. Cancer Cell. 2004;5(6):565-74.

274.   Chang AJ, Song DH, Wolfe MM. Attenuation of peroxisome proliferator-activated receptor gamma (PPARgamma) mediates gastrin-stimulated colorectal cancer cell proliferation. The Journal of biological chemistry. 2006 May 26;281(21):14700-10.

275.   Diradourian C, Girard J, Pegorier JP. Phosphorylation of PPARs: from molecular characterization to physiological relevance. Biochimie. 2005 Jan;87(1):33-8.

276.   Camp HS, Tafuri SR. Regulation of peroxisome proliferator-activated receptor gamma activity by mitogen-activated protein kinase. J Biol Chem. 1997 Apr 18;272(16):10811-6.

277.   Shao D, Rangwala SM, Bailey ST, Krakow SL, Reginato MJ, Lazar MA. Interdomain communication regulating ligand binding by PPAR-γ. Nature. 1998;396(6709):377-80.

278. Berger J, Patel HV, Woods J, Hayes NS, Parent SA, Clemas J, et al. A PPARgamma mutant serves as a dominant negative inhibitor of PPAR signaling and is localized in the nucleus. Mol Cell Endocrinol. 2000 Apr 25;162(1-2):57-67.

279. Gurnell M, Wentworth JM, Agostini M, Adams M, Collingwood TN, Provenzano C, et al. A dominant-negative peroxisome proliferator-activated receptor gamma (PPARgamma) mutant is a constitutive repressor and inhibits PPARgamma-mediated adipogenesis. The Journal of biological chemistry. 2000 Feb 25;275(8):5754-9.

280. Burgermeister E, Chuderland D, Hanoch T, Meyer M, Liscovitch M, Seger R. Interaction with MEK causes nuclear export and downregulation of peroxisome proliferator-activated receptor gamma. Molecular and cellular biology. 2007 Feb;27(3):803-17.

281. Grommes C, Landreth GE, Heneka MT. Antineoplastic effects of peroxisome proliferator-activated receptor gamma agonists. The lancet oncology. 2004 Jul;5(7):419-29.

282. Peters JM, Shah YM, Gonzalez FJ. The role of peroxisome proliferator-activated receptors in carcinogenesis and chemoprevention. Nature Reviews Cancer. 2012;12(3):181-95.

283. Padilla J, Leung E, Phipps RP. Human B lymphocytes and B lymphomas express PPAR-gamma and are killed by PPAR-gamma agonists. Clinical Immunology. 2002 Apr;103(1):22-33.

284. Akbiyik F, Ray DM, Gettings KF, Blumberg N, Francis CW, Phipps RP. Human bone marrow megakaryocytes and platelets express PPARgamma, and PPARgamma agonists blunt platelet release of CD40 ligand and thromboxanes. Blood. 2004 Sep 1;104(5):1361-8.

285. Ricote M, Li AC, Willson TM, Kelly CJ, Glass CK. The peroxisome proliferator-activated receptor-gamma is a negative regulator of macrophage activation. Nature. 1998 Jan 1;391(6662):79-82.

286. Fujimura S, Suzumiya J, Nakamura K, Ono J. Effects of troglitazone on the growth and differentiation of hematopoietic cell lines. International journal of oncology. 1998 Dec;13(6):1263-7.

287. Yamakawa-Karakida N, Sugita K, Inukai T, Goi K, Nakamura M, Uno K, et al. Ligand activation of peroxisome proliferator-activated receptor gamma induces apoptosis of leukemia cells by down-regulating the c-myc gene expression via blockade of the Tcf-4 activity. Cell Death and Differentiation. 2002 May;9(5):513-26.

288.   Liu JJ, Huang RW, Lin DJ, Peng J, Wu XY, Lin Q, et al. Expression of survivin and bax/bcl-2 in peroxisome proliferator activated receptor-gamma ligands induces apoptosis on human myeloid leukemia cells in vitro. Ann Oncol. 2005 Mar;16(3):455-9.

289.   Hirase N, Yanase T, Mu Y, Muta K, Umemura T, Takayanagi R, et al. Thiazolidinedione induces apoptosis and monocytic differentiation in the promyelocytic leukemia cell line HL60. Oncology. 1999 Oct;57 Suppl 2:17-26.

290.   Tontonoz P, Nagy L, Alvarez JGA, Thomazy VA, Evans RM. PPARγ promotes monocyte/macrophage differentiation and uptake of oxidized LDL. Cell. 1998;93(2):241-52.

291.   Zhu L, Gong B, Bisgaier CL, Aviram M, Newton RS. Induction of PPARgamma1 expression in human THP-1 monocytic leukemia cells by 9-cis-retinoic acid is associated with cellular growth suppression. Biochemical and Biophysical Research Communications. 1998 Oct 29;251(3):842-8.

292.   Zang C, Liu H, Waechter M, Eucker J, Bertz J, Possinger K, et al. Dual PPARalpha/gamma ligand TZD18 either alone or in combination with imatinib inhibits proliferation and induces apoptosis of human CML cell lines. Cell Cycle. 2006 Oct;5(19):2237-43.

293.   Hirase N, Yanase T, Mu Y, Muta K, Umemura T, Takayanagi R, et al. Thiazolidinedione suppresses the expression of erythroid phenotype in erythroleukemia cell line K562. Leukemia Research. 2000 May;24(5):393-400.

294.   Bertz J, Zang C, Liu H, Wachter M, Possinger K, Koeffler HP, et al. Compound 48, a novel dual PPAR alpha/gamma ligand, inhibits the growth of human CML cell lines and enhances the anticancer-effects of imatinib. Leuk Res. 2009 May;33(5):686-92.

295.   Michalik L, Desvergne B, Wahli W. Peroxisome-proliferator-activated receptors and cancers: complex stories. Nat Rev Cancer. 2004 Jan;4(1):61-70.

296.   Kebebew E, Peng M, Reiff E, Treseler P, Woeber KA, Clark OH, et al. A phase II trial of rosiglitazone in patients with thyroglobulin-positive and radioiodine-negative differentiated thyroid cancer. Surgery. 2006 Dec;140(6):960-6; discussion 6-7.

297.   Saez E, Rosenfeld J, Livolsi A, Olson P, Lombardo E, Nelson M, et al. PPAR gamma signaling exacerbates mammary gland tumor development. Genes Dev. 2004 Mar 1;18(5):528-40.

298.   Chen L, Necela BM, Su W, Yanagisawa M, Anastasiadis PZ, Fields AP, et al. Peroxisome proliferator-activated receptor gamma promotes epithelial to mesenchymal

transformation by Rho GTPase-dependent activation of ERK1/2. The Journal of biological chemistry. 2006 Aug 25;281(34):24575-87.

299.	Lefebvre AM, Chen I, Desreumaux P, Najib J, Fruchart JC, Geboes K, et al. Activation of the peroxisome proliferator-activated receptor gamma promotes the development of colon tumors in C57BL/6J-APCMin/+ mice. Nat Med. 1998 Sep;4(9):1053-7.

300.	Saez E, Tontonoz P, Nelson MC, Alvarez JG, Ming UT, Baird SM, et al. Activators of the nuclear receptor PPARgamma enhance colon polyp formation. Nat Med. 1998 Sep;4(9):1058-61.

301.	Pino MV, Kelley MF, Jayyosi Z. Promotion of colon tumors in C57BL/6J-APC(min)/+ mice by thiazolidinedione PPARgamma agonists and a structurally unrelated PPARgamma agonist. Toxicologic pathology. 2004 Jan-Feb;32(1):58-63.

302.	Yang K, Fan KH, Lamprecht SA, Edelmann W, Kopelovich L, Kucherlapati R, et al. Peroxisome proliferator-activated receptor gamma agonist troglitazone induces colon tumors in normal C57BL/6J mice and enhances colonic carcinogenesis in Apc1638 N/+ Mlh1+/- double mutant mice. Int J Cancer. 2005 Sep 10;116(4):495-9.

303.	Dormandy JA, Charbonnel B, Eckland DJ, Erdmann E, Massi-Benedetti M, Moules IK, et al. Secondary prevention of macrovascular events in patients with type 2 diabetes in the PROactive Study (PROspective pioglitAzone Clinical Trial In macroVascular Events): a randomised controlled trial. Lancet. 2005 Oct 8;366(9493):1279-89.

304.	Egerod FL, Nielsen HS, Iversen L, Thorup I, Storgaard T, Oleksiewicz MB. Biomarkers for early effects of carcinogenic dual-acting PPAR agonists in rat urinary bladder urothelium in vivo. Biomarkers. 2005 Jul-Aug;10(4):295-309.

305.	Oleksiewicz MB, Thorup I, Nielsen HS, Andersen HV, Hegelund AC, Iversen L, et al. Generalized cellular hypertrophy is induced by a dual-acting PPAR agonist in rat urinary bladder urothelium in vivo. Toxicologic pathology. 2005;33(5):552-60.

306.	Wang L, Giannoudis A, Austin G, Clark RE. Peroxisome proliferator-activated receptors (PPAR) activation increases imatinib uptake and killing of chronic myeloid leukaemia cells. Experimental Hematology. 2012.

307.	Marais R, Light Y, Paterson HF, Marshall CJ. Ras recruits Raf-1 to the plasma membrane for activation by tyrosine phosphorylation. Embo J. 1995 Jul 3;14(13):3136-45.

308.	Morgan MA, Dolp O, Reuter CW. Cell-cycle-dependent activation of mitogen-activated protein kinase kinase (MEK-1/2) in myeloid leukemia cell lines and

induction of growth inhibition and apoptosis by inhibitors of RAS signaling. Blood. 2001 Mar 15;97(6):1823-34.

309.   Greene ME, Pitts J, McCarville MA, Wang XS, Newport JA, Edelstein C, et al. PPAR[gamma]: observations in the hematopoietic system[star, open]. Prostaglandins & Other Lipid Mediators. 2000;62(1):45-73.

310.   BØYum A. Isolation of Lymphocytes, Granulocytes and Macrophages. Scandinavian Journal of Immunology. 1976;5:9-15.

311.   Shah NP, Nicoll JM, Nagar B, Gorre ME, Paquette RL, Kuriyan J, et al. Multiple BCR-ABL kinase domain mutations confer polyclonal resistance to the tyrosine kinase inhibitor imatinib (STI571) in chronic phase and blast crisis chronic myeloid leukemia. Cancer Cell. 2002;2(2):117-25.

312.   Gorre ME, Mohammed M, Ellwood K, Hsu N, Paquette R, Nagesh Rao P, et al. Clinical resistance to STI-571 cancer therapy caused by BCR-ABL gene mutation or amplification. Science. 2001;293(5531):876-80.